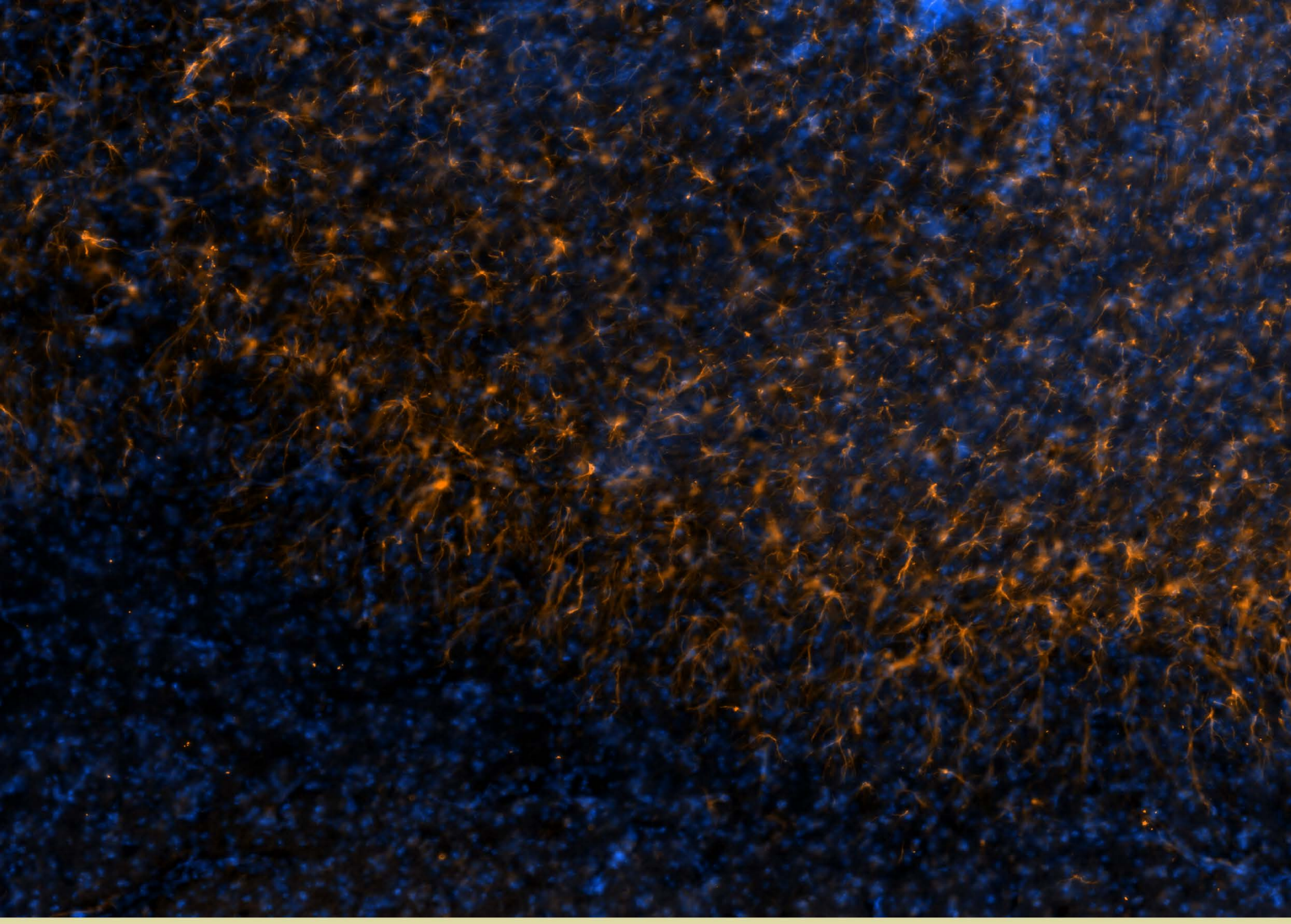

Sara Raquel Reis de Oliveira

Carbon Monoxide Modulation of Astrocytic Viability Following an Ischemic Injury – Metabolic Targets Disclosure

Tese de doutoramento em Biologia Experimental e Biomedicina, no ramo de Neurociências e Doença, orientada pelo Professor Doutor Carlos Bandeira Duarte e pela Doutora Helena Luísa de Araújo Vieira, apresentada ao Instituto de Investigação Interdisciplinar da Universidade de Coimbra.

Agosto 2017

· U C ·

Universidade de Coimbra

Carbon Monoxide Modulation of Astrocytic Viability Following an Ischemic Injury

–

Metabolic Targets Disclosure

Sara Raquel Reis de Oliveira

Universidade de Coimbra

2017

Dissertação apresentada ao Instituto de Investigação Interdisciplinar da Universidade de Coimbra para prestação de provas de Doutoramento em Biologia Experimental e Biomedicina, no ramo de Neurociências e Doença.

Este trabalho foi realizado em parte no Centro de Neurociências e Biologia Celular da Universidade de Coimbra e em parte no Centro de Estudos de Doenças Crónicas da Universidade Nova de Lisboa. A sua realização foi suportada pela bolsa de doutoramento SFRH / BD / 51969 / 2012 atribuída pela Fundação para a Ciência e a Tecnologia.

Cover note:

The image presented in the cover of this thesis represents an ischemic mouse brain slice labeled with anti-GFAP antibody (orange, astrocytes marker) and DAPI (blue, nucleus marker). Astrocytes are delimiting the injured tissue.

Table of Contents

AGRADECIMENTOS/ACKNOWLEDGMENTS

Sem o apoio e a companhia dos amigos, colegas, família e de todas as pessoas que me rodeiam no dia-a-dia, o percurso para chegar ao fim desta etapa tão desejada não teria sido tão agradável, é por isso com imenso carinho que quero agradecer:

Ao Professor Doutor Carlos Duarte, um grande e sincero obrigado! Primeiro por me ter aceite como aluna de Doutoramento no seu grupo de investigação e por me ter dado a possibilidade de chegar até aqui. Agradeço o apoio e incentivo constantes durante estes anos e sobretudo por ser um exemplo de dedicação à ciência e ao trabalho. Senti sempre liberdade para propor ideias e, mesmo em áreas em que ambos estávamos a "partir pedra", recebi sempre voto de confiança para seguir em frente.

À Doutora Helena Vieira, coorientadora no doutoramento, mas mentora e exemplo na vida científica. Com boa disposição constante e sempre um conselho a dar, foi uma sorte ter-me estreado em neurociência no seu grupo. O meu grande obrigado por tudo!

Ao Doutor João Peça, pela disponibilidade, simpatia, apoio e pelas críticas sempre construtivas que em muito ajudaram no desenvolver da tese.

À Miri pela grande ajuda e apoio que me deu desde o princípio da minha entrada no grupo CBD, tornando muito mais fácil a minha integração no laboratório, por todas as coisas que me ensinou, mas sobretudo pela disponibilidade e amizade demostrada ao longo destes anos. O meu mais sincero obrigado!

Aos meus colegas de grupo, nomeadamente: à Guidinha pelo carinho, a disponibilidade e o apoio que tem sempre demonstrado; ao Grace, ao Ivan e ao Pedro Afonso pela amizade, simpatia, partilhas cientificas, pelas conversas agradáveis com um toque de comédia que tornaram especiais todos os dias de trabalho. A todos muito, muito obrigado por terem feito parte deste percurso, sem vocês não teria sido tão bom!

À Marta Vieira e Joana Fernandes, muito obrigada pela partilha da vossa vasta experiência com o OGD e análise de RNA.

Ao João Gomes, um tutor exemplar e paciente que me ensinou tudo o que sabia sobre cirurgias e isquémia, confiando a 100% nas minhas capacidades. A distância não foi razão para que a troca de conselhos e experiências não fluísse.

Uma peça crucial durante grande parte do trabalho foi a boa colaboração estabelecida com a equipa de MRI. Obrigada ao Professor Doutor Miguel Castelo Branco pela prontidão em aceitar a colaboração e mesmo com esforço encontrar tempo para as reuniões. Um grande grande obrigado ao José Sereno, um exemplo de dedicação, profissionalismo, empenho, boa disposição e paciência. Um agradecimento também ao João Castelhano, Lorena Petrella e Sónia Gonçalves.

A todos os do IBILI que cederam o seu tempo e espaço para me ajudar e melhor fazer o meu trabalho: Professora Doutora Ana Paula Silva e Ricardo Leitão.

Aos LA's: Rui Nobre, Catarina Miranda e Mariana Mendonça. Sempre responderam às minhas dúvidas e não hesitaram em partilhar o seu conhecimento dos in vivo. Foram uma ajuda muito relevante.

Não posso deixar de referir o Mário Laço, alguém que me ajudou no "troubleshooting" do MRI e deu várias dicas para melhorar a análise.

A todos do grupo ALC pela simpatia e os conselhos preciosos: à Sandra Santos, à inigualável Tatiana, à Dominique e à Mariline pela companhia no Aquário e muito mais!

Aos RDAs: ao Luís Martins, Maria Joana e Rui Costa, mas em especial ao Pedro Alves sempre pronto a ajudar e à Joana Pedro pelas degustações de jantares e conversas que acabaram por se converter numa sincera amizade.

À D. Céu, pela ternura e o carinho tão maternal e pela ajuda que todos os dias dá no laboratório!

Não menos importantes, quero deixar um profundo obrigada aos meus colegas do BEB! Em especial à Gladys, Lara, Sofias, Mo! Tornámo-nos mais próximos, não por os nossos laboratórios serem vizinhos, mas porque efetivamente a entreajuda foi uma constante e se não havia razão para nos juntarmos, nós inventávamos.

Em Lisboa, mesmo durante a estadia em Coimbra, pude sempre contar com a ajuda dos meus colegas do grupo de citoproteção do CEDOC! A Queiroga desde o início e mais tarde a Sofia e a Pereira. Um grande obrigado também às recentes aquisições: a Daniela e o Nuno foram os colegas perfeitos de secretária e pausas para o café.

Fazer um doutoramento partilhado entre duas geografias não foi fácil, mas pude sempre contar com ajudas de ambos os grupos. Uma ajuda essencial foi a da Sara Amaral! Sem dúvida alguma facilitou grandemente as estadias intermitentes em Coimbra na fase final. Sempre disponível para oferecer estadia! Não menos importante é a sua paixão contagiante pela ciência, pela comunicação e pelos amigos. Foi quem me deu a descobrir o gosto por mostrar aos mais pequenos a ciência!

Ao Instituto de Investigação Interdisciplinar da Universidade de Coimbra, ao Centro de Neurociências e Biologia Celular de Coimbra e ao Centro de Estudos de Doenças Crónicas de Lisboa pelas condições facultadas para a realização deste trabalho.

À Fundação para a Ciência e Tecnologia que financiou o meu trabalho (Bolsa: SFRH/BD/51969/2012). Ao PDBEB e Professor João Ramalho pelas oportunidades de aprendizagem proporcionadas.

O contexto profissional é de extrema importância, mas nada se compara à família! Fica tudo mais fácil quando se é feliz e para isso várias pessoas foram indispensáveis para que esse sentimento fosse uma constante! As metas a alcançar na vida são facilmente atingidas quando se tem uma rede de segurança em que se pode sempre confiar:

Aos meus pais, a quem um simples obrigado está longe de ser suficiente! Foram os primeiros a dar-me asas para sonhar mais longe e mais alto, por me darem a oportunidade de construir a minha carreira e apoiado as minhas decisões. A liberdade e confiança que sempre depositaram em mim tornaram-me uma pessoa independente, e definitivamente moldaram quem sou hoje. Sem vocês, o hoje não seria possível.

Minha irmã Catarina, por estar sempre lá em tudo na minha vida, por ser extrovertida e na sua maioria o oposto de mim. Neste caso, é uma mais valia pois pude aprender muito com ela.

Ao Pedro, pela ajuda prática na realização desta tese, mas principalmente por ser o meu melhor amigo, estar comigo todos os dias e pelo equilíbrio que traz à minha vida. Completa-me em todos os aspetos, apoiar-me nos meus esforços e incentiva-me quando estou a esmorecer. Estou profundamente agradecida pelos momentos que passámos juntos e imensamente entusiasmada com os projetos futuros em conjunto. Obrigada!

Aos pais do pedro, que sempre me acarinharam e me receberam de braços abertos, ajudando em tudo.

Meus amigos de faculdade, que sem dúvida alguma são amigos para a vida! Marcaram positivamente meu percurso e continuam a fazê-lo, mesmo estando longe.

A toda a minha família, pela confiança, estima e afeto que sempre mostraram.

À minha família alargada do CNE, que sempre me apoiou e foi uma peça importante na minha formação.

Apesar de curta, a temporada dos quizzes foram importantes momentos de descontração que ajudaram à integração numa cidade desconhecida. Obrigada a todos os “quizzers”.

Por último agradeço a todos os que se cruzaram no meu caminho em vários momentos durante a minha vida, com quem compartilhei experiências e emoções. Por mais passageira que tenha sido a nossa convivência, contribuiu de certa forma para a formação da minha personalidade e identidade.

SUMMARY

Brain injury is a serious clinical problem, in particular in ischemic stroke, and is among the major causes of adult death and disability in developed countries. Therefore, there is an urgent need for investigation of novel therapies against ischemic injuries. A building body of evidence shows that carbon monoxide (CO) activates endogenous protective mechanisms and prevents tissue and cellular damage. CO is an endogenously produced molecule that induces the protection in several tissues.

The aim of this PhD project was to identify some of the key effectors of CO in the induction of cytoprotection in astrocytes. Moreover, the effects of CO were evaluated on the vasculature of healthy female and male mice, as well as in a mouse model of ischemic stroke.

Chapter I introduces general concepts concerning ischemic stroke and the importance of astrocytes in healthy and diseased brain. Ischemia-induced cell death is discussed, with particular attention given to the key role of immediate early genes. FosB was a major focus of the gathered information. Additionally, a detailed list of the models available to study ischemic stroke is also described. Finally, this chapter presents the biology of CO and its therapeutic potential, as well as the available routes to safe delivery of the gasotransmitter.

Chapter II.I reports the effects of CO in the transcriptome of primary cultures of astrocytes, as determined by RNA sequencing. Incubation of cultured astrocytes with CORM-A1 induced changes in the expression of 162 genes, and analysis of the results with different bioinformatic tools showed that the AP-1 transcription factor is an important regulator of several genes identified. Cytoskeleton related genes is a group identified in various interactome clusters, and several genes belong to this category were found to be differentially expressed in cultured astrocytes exposed to CO.

The results obtained in the RNA sequencing studies have to be validated using a different approach, typically qRT-PCR, and requires the identification of appropriate reference genes. In the work presented in **Chapter II.II**, a group of 8 genes was subjected to analysis regarding their expression stability after incubation of cultured astrocytes with CO. Four different algorithms were applied, resulting in the validation of *Gapdh* and *Ppia* as the best gene pair for internal control in the analysis of transcriptome alterations. To better understand the importance of the transcriptome alteration upon CO exposure, 7 genes were selected to further study the astrocytic response to CO.

Chapter II.III describes the validation of the selected genes by qRT-PCR and reports studies with the aim of analyzing how FosB (the gene with highest induction) influenced the protective effects of CO in an oxidative stress context. Two pathways of

FosB induction were addressed: (i) P2X7R activation and (ii) ROS production. The results showed that CO-induced FosB expression depends on P2X7R activation.

Chapter II.IV describes the work aiming at exploring the differential effects of CO in the cerebral vasculature of live healthy male and female mice, using a MRI technique. It is demonstrated that systemic injection of CO results in a regional and gender-dependent response. Female brain vasculature was found to be more responsive to CO and this gasotransmitter induced a general vasodilation and increase in BBB permeability.

After exploring the vascular functions of CO in healthy animals, we evaluated the effects of CO treatment in an animal model of ischemic stroke (**Chapter II.V**). The putative effect of CO as therapeutic agent to promote tissue protection and recovery was tested in the transient middle cerebral artery occlusion (tMCAo) model of focal brain ischemia. A 3-day treatment regimen based on a single daily dosage of CORM-A1 after the injury in mice, led to the following conclusions: (i) CO partly improved the recovery of motor function, (ii) minimized the BBB impairment, (iii) transiently limited the infarct size, (iv) reduced the metabolites load loss and (iv) ameliorated survival.

Finally, a general and integrative discussion is presented in **Chapter III**, for framing this thesis work in the current state of the art of the respective scientific field. The impact of the study is discussed as well as future perspectives to engage. In conclusion, this thesis contributed to better understand CO's cellular and molecular effectors, its cytoprotective role in astrocytes and its therapeutic potential as a treatment for ischemic stroke at clinically relevant timings.

Keywords

Carbon monoxide, Astrocytes, Cytoprotection, Transcriptome, Oxidative stress, Cerebral ischemia

SUMÁRIO

O acidente vascular cerebral (AVC) isquémico é uma das maiores causas de mortalidade e incapacidade em adultos em países desenvolvidos, sendo premente a investigação de novas terapias contra lesões deste tipo. Um crescente número de evidências mostra que o monóxido de carbono (CO), uma molécula produzida endogenamente, ativa mecanismos protetores e previne danos ao nível dos tecidos afetados.

O objetivo deste projeto de doutoramento consistiu na identificação de alguns efetores-chave do CO na indução de citoproteção em astrócitos. Foram também avaliados os efeitos do CO na vasculatura em murganhos fêmeas e machos saudáveis, assim como num modelo de AVC isquémico em roedores.

O **Capítulo I** introduz conceitos gerais sobre o AVC isquémico e a importância dos astrócitos no cérebros em condições fisiológicas normais e em contexto de doença. Os processos de morte celular induzida por isquémia são igualmente explorados, com particular atenção ao papel chave dos genes de expressão rápida, nomeadamente FosB. Neste capítulo são também descritos os modelos disponíveis para estudar o AVC isquémico. Por fim, este capítulo apresenta a biologia do CO e o seu potencial terapêutico, bem como as vias disponíveis para a administração segura do gasotransmissor.

No **Capítulo II.I** são reportados os efeitos do CO no transcritoma de culturas primárias de astrócitos, determinados através de sequenciação de RNA. A incubação de astrócitos com CORM-A1 induziu alterações na expressão de 162 genes, e análises bioinformáticas mostraram que o fator de transcrição AP-1 é um importante regulador de vários dos genes identificados. Os genes relacionados com o citoesqueleto estão envolvidos em diversos grupos do interatoma, e vários genes pertencentes a esta categoria foram identificados como sendo expressos de forma diferencial em astrócitos expostos a CO.

Os resultados obtidos no estudo da sequenciação de RNA necessitam de ser validados através de outra abordagem, tipicamente qRT-PCR, o que necessita da identificação de genes de referência apropriados. No trabalho apresentado no **Capítulo II.II**, foi analisado um grupo de 8 genes relativamente à estabilidade da sua expressão em astrócitos após exposição ao CO. Foram usados quatro algoritmos diferentes, resultando na validação dos genes *Gapdh* e *Ppia* como o melhor par para controlo interno de alterações transcricionais. Para melhor entender a importância das alterações ao nível do transcritoma após exposição a CO, foram selecionados 7 genes para aprofundar o estudo das respostas astrocíticas a este gasotransmissor.

O **Capítulo II.III** descreve a validação por qRT-PCR dos genes selecionados com base nos ensaios realizados no capítulo anterior, assim como os estudos com o objectivo de analisar de que forma o FosB (o gene com maior indução) atua como mediador da citoproteção pelo CO em contexto de stress oxidativo. Foram investigadas duas vias de sinalização envolvidas na indução da expressão de FosB: (i) ativação do P2X7R e (ii) produção de espécies reativas de oxigénio. Os resultados obtidos mostram que a expressão de FosB induzida por CO é dependente da activação do recetor P2X7.

No **Capítulo II.IV** está descrito o trabalho efetuado com o objetivo de explorar os efeitos *in vivo* do CO na vasculatura cerebral em murganhos fêmeas e machos saudáveis, usando uma técnica de imagiologia de ressonância magnética. É demonstrado que o efeito do CO administrado sistemicamente é dependente da região cerebral e do sexo. A vasculatura de cérebro de fêmeas é mais suscetível ao CO e verificou-se também que este gasotransmissor induz uma vasodilatação generalizada e o aumento da permeabilidade da barreira hematoencefálica.

Depois de explorar as funções vasculares do CO em animais saudáveis, avaliou-se os efeitos do tratamento de CO num modelo animal de AVC isquémico (**Capítulo II.V**). O potencial efeito do CO como agente terapêutico que promove a proteção e recuperação do tecido cerebral foi testado num modelo de isquémia cerebral transitória que consiste na oclusão transiente da artéria cerebral média (tMCAo) em murganhos. A administração diária de CORM-A1 durante três dias após o enfarte teve os seguintes efeitos: (i) melhoria parcial na recuperação de funções motoras, (ii) minimização do enfraquecimento da barreira hematoencefálica, (iii) limitação temporária do tamanho do enfarte, (iv) redução da perda de carga de metabolitos e (iv) aumento da taxa de sobrevivência.

Por fim, uma discussão geral e integrativa é apresentada no **Capítulo III** desta dissertação, com o objectivo de enquadrar este trabalho de tese no atual estado da arte da respetiva área científica. O impacto do estudo é discutido, bem como as perspetivas futuras para dar continuidade à investigação realizada. Concluindo, esta tese contribui para melhor perceber os efetores celulares e moleculares do CO, o seu papel citoprotector em astrócitos, e o seu potencial terapêutico como tratamento clinicamente relevante para o AVC isquémico.

Palavras-chave

Monóxido de carbono, Astrócitos, Citoproteção, Transcritoma, Stress oxidativo, Isquémia cerebral

THESIS PUBLICATIONS

Oliveira, S.R., Vieira, H.L.A. & Duarte, C.B., 2015. Effect of carbon monoxide on gene expression in cerebrocortical astrocytes: Validation of reference genes for quantitative real-time PCR. *Nitric Oxide*, 49, pp.80–89. DOI: 10.1016/j.niox.2015.07.003.

Available at: http://linkinghub.elsevier.com/retrieve/pii/S1089860315300045.

Oliveira, S.R., Queiroga, C.S.F. & Vieira, H.L.A., 2016. Mitochondria and carbon monoxide: cytoprotection and control of cell metabolism - a role for Ca^{2+}? *The Journal of Physiology*, 594(15), pp.4131–4138. DOI: 10.1113/JP270955.

Available at: http://www.ncbi.nlm.nih.gov/pubmed/26377343.

Chapter I

INTRODUCTION

INDEX

ABBREVIATIONS

AIF, apoptosis inducing factor
AMP, adenosine monophosphate
AMPA, α-amino-3-hydroxy-5-methyl-4-isoxazolepropionic acid
AMPAR, AMPA receptor
ANOVA, analysis of variance
ATP, adenosine-5'-triphosphate
BCA, bicinchoninic acid
Bcl-2, B-cell lymphoma 2 protein
Bim, Bcl2-interacting mediator of cell death
BZ, benzodiazepines
CA1, *cornu ammonis* 1 region of the hippocampus
$[Ca^{2+}]_i$, cytosolic calcium concentration
CaM, Ca2+/calmodulin
CBP, CREB binding protein
CCVs, clathrin-coated vesicles
CD95, cluster of differentiation 95
cDNA, complementary DNA
ClC-2, voltage-gated Cl- channel
CNS, central nervous system
CO, carbon monoxide
CORM, CO releasing molecule
CREB, cyclic-AMP response element binding protein
Ct, threshold cycle
DAPK, death-associated protein kinase
DG, dentate gyrus
DIV, days in vitro
DMEM, Dulbecco's Modified Eagle Medium
DNA, deoxyribonucleic acid
dNTP, deoxyribonucleotide triphosphate
DOC, sodium deoxycholate
DTT, dithiothreitol
ECF, enhanced chemifluorescence
ECl-, chloride equilibrium potential
EDTA, ethylenediaminetetraacetic acid
EGTA, ethylene glycol tetraacetic acid
ER, endoplasmic reticulum
ERK, extracellular signal-regulated kinase
F-actin, filamentous actin
FasL, Fas ligand
FBS, fetal bovine serum
FRAP, fluorescence recovery after photobleaching
GAPDH, glyceraldehyde 3-phosphate dehydrogenase
GDP, guanosine diphosphate
GODZ, Golgi-specific DHHC zinc finger protein
GTP, guanosine triphosphate
HBSS, Hank’s balanced salt solution
HEPES, hydroxyethyl piperazineethanesulfonic acid
HIF-1, hypoxia-inducible factor-1
i.p., intraperitoneal

i.v., intravenous
IC, infarct core
IL-1, interleukin 1
InsP3, inositol 1,4,5-trisphosphate
IP, immunoprecipitation
IPSPs, inhibitory postsynaptic potentials
IκB, inhibitor of NF-κB
MAP2, microtubule-associated protein 2
MCA, middle cerebral artery
MCAO, MCA occlusion
mGluR, metabotropic glutamate receptors
mRNA, messenger RNA
N.S., not significant
NBQX, 1,2,3,4-tetrahydro-6-nitro-2, 3-dioxo[f]quinoxaline-7-sulfonamide disodium
NF-kB, nuclear factor-kappa B
NMDA, N-methyl-D-aspartate
NMDAR, NMDA receptor
nNOS, neuronal NO synthase
NO, nitric oxide
NRSF, neuron-restrictive silencer factor
NSF, N-ethylmaleimide-sensitive factor
O2-, superoxide anion
OGD, oxygen and glucose deprivation
p53, protein 53
PBS, phosphate buffered saline
PCR, polymerase chain reaction
PGG2, prostaglandin G2
PGH, prostaglandin H
Pi, inorganic phosphate
PI3K, phosphoinositide 3-kinase
PKA, cAMP-dependent protein kinase
PKC, calcium/phospholipid-dependent protein kinase C
PLIC, proteins linking integrin-assocated protein with cytoskeleton
PMSF, phenylmethylsulfonyl fluoride
PTEN, phosphatase and tensin homolog on chromosome ten
PVDF, polyvinylidene difluoride
qPCR, quantitative PCR
rCBF, regional cerebral blood flow
REST, RE1-silencing transcription factor
RIPA, radioimmunoprecipitation assay lysis buffer
RNA, ribonucleic acidB
RT, room temperature
SDS, sodium dodecyl sulfate
SEM, standard error of the mean
Ser, serine
STATs, signal transducers and activators of transcription
STEP, striatal enriched tyrosine phosphatase
TE, tris-EDTA
Thr, threonine
TM, transmembrane domains
TNF, tumor necrosis factor

TORC, transducer of regulated CREB activity
TTC, triphenyltetrazolium chloride
WT, wild type
Ψm, mitochondrial membrane potential

1. Ischemic stroke

Hypoxia-ischemia and reperfusion (HIR) may result from a transient reduction in the blood supply to a given tissue, and it is particularly damaging to the brain, heart and retina. When HIR takes place in the brain, it can be a global (in the case of cardiac arrest) or focal event (in the case of a blood vessel occlusion). The former type of HIR, more commonly known as ischemic stroke, is the third cause of death worldwide, presenting high mortality and morbidity [1]. In Portugal, cardiovascular diseases are the main cause of death, with stroke contributing to almost twice as much deaths in 2012 (13 020) when compared with ischemic heart disease (6 605 deaths). In the same year, stroke caused 61.4 deaths *per* 100 000 persons [2]. In addition to its high incidence, stroke carries an enormous social and economic burden, since a great fraction of stroke patients suffer from permanent disabilities [3].

There are two types of stroke: hemorrhagic (a cerebral vessel bursts) and ischemic (a cerebral vessel gets clothed), being the latter about 4 times more frequent. The origin of the cloth discriminates the type of ischemic stroke: embolic or thrombotic [4].

Stroke presents a complex pathophysiology, since it involves multiple players (Figure 1A) which participate in consecutive events (Figure 1B) [5,6]. These entities may come from within the brain and from the periphery, and affect each other responses. Thus, signaling range from local to systemic level, and the response involves a cross-talk between different pathways.

At the cellular level, during the hypoxic period, brain tissue suffers immediately from the lack of blood flow due to its high demand for oxygen and nutrients. Cells that were fed by the occluded vessel die in few minutes *via* necrosis, forming the ischemic core of the lesion. Meanwhile, the neighboring cells take longer to die. In close proximity to the necrotic area cells die *via* apoptosis, forming the penumbra region of the lesion [7]. Death of the penumbra tissue that survived the acute hypoxic phase can take days to occur, indicating that cellular dysfunction is reversible if intervention is done timely. Therefore, the penumbra region comprises the therapeutic opportunity, where cytoprotective agents can act as cell fate modulators. The tissue within this region can be rescued, ultimately resulting in lesion size reduction [8]. When the blood flow is restored, cells sense another alteration of environment, since reperfusion itself gives rise to a very damaging environment, being oxidative stress a major killer [9].

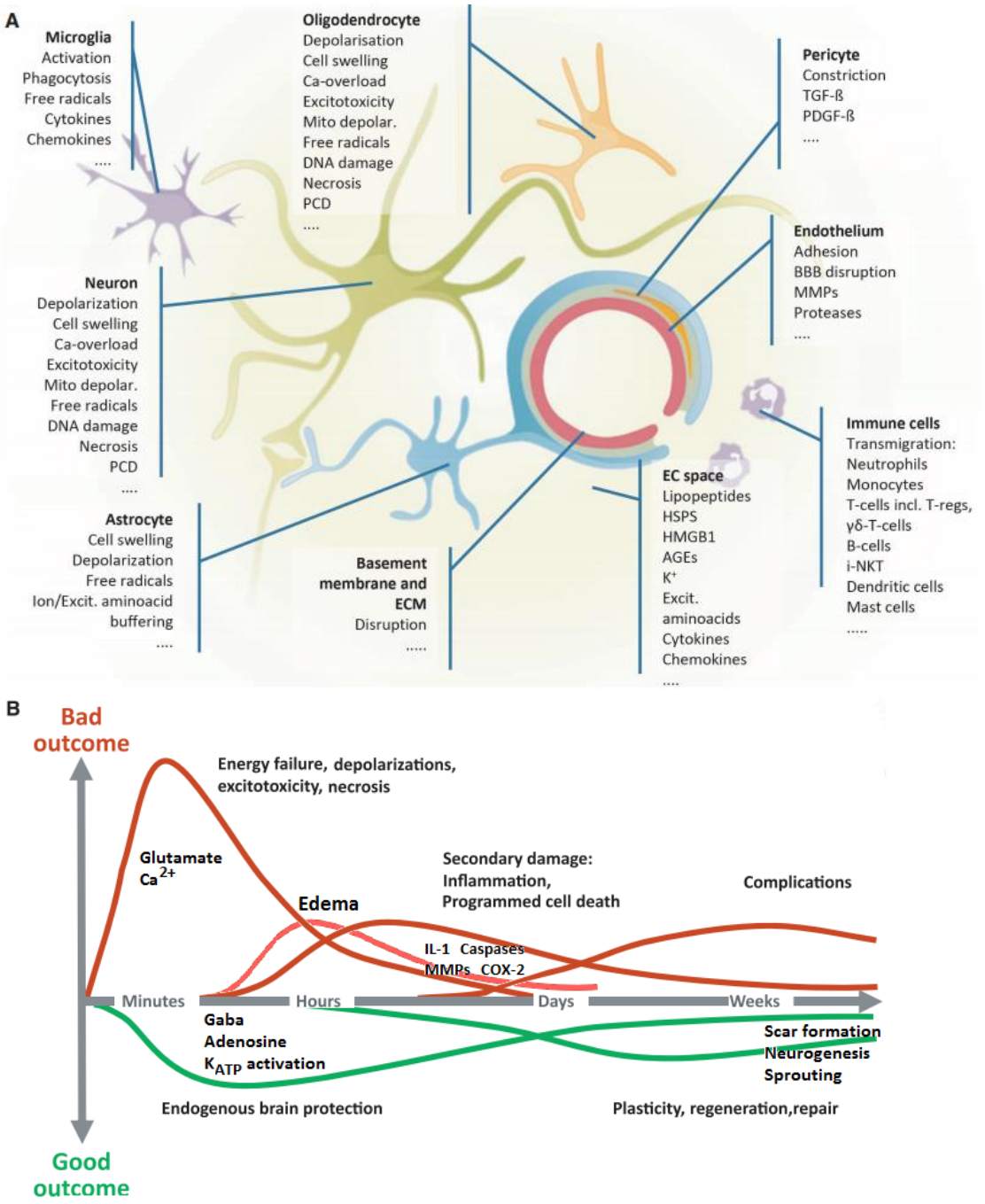

Figure 1 - Complexity of stroke pathophysiology. **A**, cellular and molecular mechanisms of ischemic cell death in the brain; **B**, simplified chronology after stroke onset of detrimental and protective mechanisms in stroke. Adapted from [5] and [230]. AGE, advanced glycosylation products; BBB, blood-brain barrier; EC, extracellular; ECM, extracellular matrix; HMGB, high mobility group box protein; HSP, heat shock protein; MMP, matrix metalloproteinase; PCD, programmed cell death; PDGF, platelet-derived growth factor; TGF, transforming growth factor.

Delayed cell death can occur by two general apoptotic pathways: intrinsic and extrinsic [10]. Besides the plethora of molecules, mitochondria are a key source of cell fate determinants belonging to the intrinsic pathway. In addition to the dysregulation in metabolic control, mitochondria release or expose effectors that may shift the equilibrium towards survival or ischemic-induced cell death, namely the Bcl-2 family of proteins, cytochrome c, reactive nitrogen species (RNS) and reactive oxygen species (ROS) (Figure 2) [11,12].

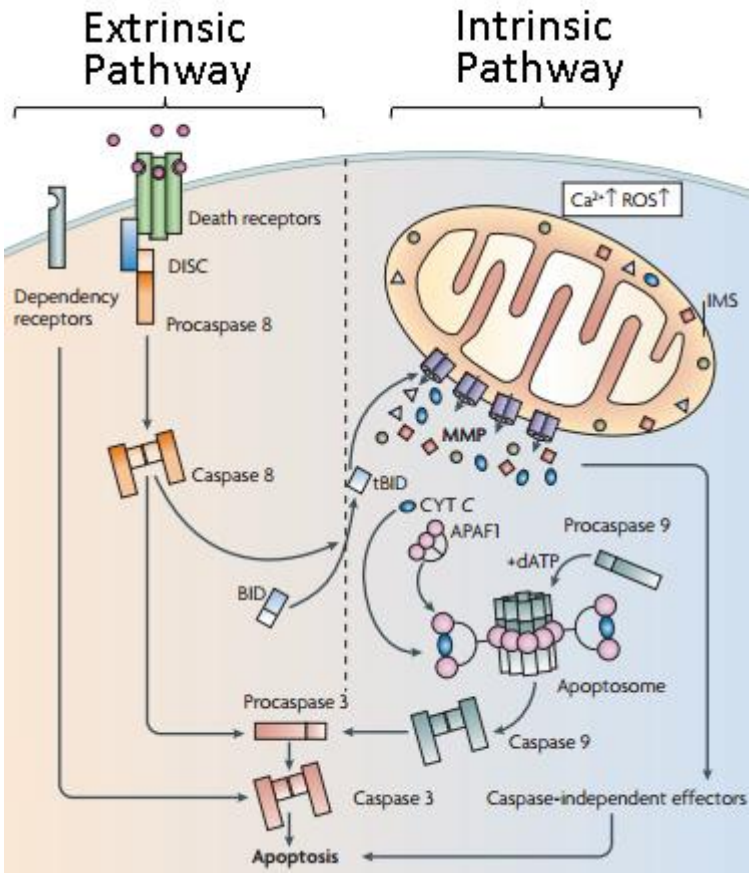

Figure 2 - Molecular events triggered by brain ischemia resulting in neuronal cell death. The extrinsic pathway includes the death signals initiated at the receptor level. The intrinsic apoptotic pathway is triggered by several stress conditions converging on mitochondria (adapted from [13]).

1.1. Astrocyte biology

For a proper brain function, a multitude of cell types, specific tissue architecture and cell signaling needs to be well orchestrated. This is essential both in physiologic and pathologic conditions. Despite the neurocentric perspective of brain research, astrocytes also play a crucial role in maintaining a fine-tuned cerebral function [14]. In addition to being the most abundant cell in brain tissue, astrocytes modulate all the other brain cells, including neurons and cerebral vasculature [15–17]. Astrocytes support neurons metabolically and structurally, being a key constituent of the tripartite synapse.

To modulate the surrounding environment, astrocytes communicate with neighboring cells either by contact or by releasing molecules. In particular, astrocyte-neuron communications require a complex network: on average an astrocyte is able to enwrap numerous neurons and one neuron interacts with 4 to 8 astrocytes [18]. Furthermore, astrocytic modulation of neurons includes: (i) uptake of neurotransmitters such as glutamate, (ii) restricting diffusion of neuroactive substances within the extracellular space, (iii) extracellular ionic homeostasis, and (iv) release of gliotransmitters able to modulate synaptic transmission, excitability and amino acid recycling. Moreover, astrocytes regulate water transport in the CNS by aquaporin 4 water channels, maintain the BBB function and act as the major buffering system for reactive oxygen species *via* glutathione and ascorbic acid metabolism [18–20]. Astrocytes are

also important for neurogenesis, neuronal migration, survival, and differentiation, axonal growth, normal dendritic maturation, spine formation and elimination, as well as functional integration of adult-born neurons [17,21]. All these processes depend on a variety of communication routes, which comprise plasma membrane channels, receptors, transporters, and mechanisms that mediate the exchange of molecules by exo- and endocytotic processes [22]. More and more the scientific community realizes the importance and relevance of astroglial cells, rising the awareness that there is still a lot to be discovered about these cells.

1.1.1. Importance of astrocytes in disease

Communication between neurons and astrocytes is bidirectional, thus any dysfunction can affect both cell populations. Astrocytic functions are even more pivotal in circumstances of injury and disease, where the efficacy of their support can dictate the neuronal fate [16,19]. Compelling evidence show that astrocytes play important biological roles in neuroinflammation and neuroprotection, namely in Alzheimer's disease, Parkinson's disease, Huntington's disease, amyotrophic lateral disease, epilepsy and cerebral ischemia [23,24]. Besides promoting neuroprotection, astrocytes can mediate microglia response and limit their activation preventing excessive inflammation [25]. The present awareness concerning the importance of these cells in brain health and disease, and the idea that these could be considered as therapeutic targets to indirectly - and more physiologically - protect neurons, is a major step forward. After the failure of numerous attempts to develop neuroprotective strategies effective in brain ischemia, it is crucial and urgent to investigate the neuronal cell injury with novel conceptual and methodological approaches that may eventually lead to novel therapies. In this work, we investigate strategies for neuronal protection through an indirect mechanism *via* astrocytes.

1.2. Ischemia-induced cell death

The common feature of most events, leading to cerebral dysfunction, is the loss of neurons along with other cell types by diverse cell death mechanisms. Ischemic events also result in neuronal loss, which occurs very promptly and restricted to the lesion site. After the ischemic insult, brain cells start immediately to alter their status at the transcriptional, cytoplasmic and membrane level in a way to avoid functional breakdown. However, when all the pro-survival strategies fail, cell death pathways take over. This can take place days after HIR [26,27].

1.2.1. Immediate Early Genes (IEGs)

Activation of the transcription machinery contributes to the survival of brain cells that do not die within the first instants after HIR [28]. The neuronal genomic response after HIR is very complex and involves activation of both protective and detrimental signaling pathways [29]. Immediate early genes (IEGs) represent the first wave of gene expression in response to ischemia and are induced in extensive regions, even in non-injured tissue [30]. In the early phase, IEG activation following ischemic insults occurs at the ischemic zone; however, it can extend to the entire hemisphere in the case of

prolonged occlusions. The fast induction of IEGs happens in the absence of *de novo* protein synthesis due to pre-existing transcription factors [30]. Therefore, IEG induction does not rely on ATP consumption, which is a great advantage since ischemia-induced cell death is accompanied by ATP depletion.

The type of IEGs that are expressed following HIR encode not only transcription factors but also effector proteins that can directly affect cellular function. The genes expressed upon ischemia range from trophic factors, synaptic proteins, and metabolic and signaling enzymes, to genes coding for proteins involved in cytoskeleton rearrangement and redox response, among others [31].

1.2.1.1. FosB

One of the IEG families whose expression is triggered by HIR is the FBJ murine osteosarcoma viral oncogene homolog (FOS) protein family. FOS transcripts were found to be upregulated in stroke patients and belong to a gene cluster able to discriminate ischemic stroke [32]. This family of leucine zipper proteins is constituted by four main elements: c-Fos, FosB, Fra1 and Fra2. Together with the Jun protein family members, they constitute the Activator Protein 1 (AP-1) transcription factor [33]. FOS family members were described to participate in adaptation processes, but their expression was correlated with beneficial and detrimental effects. For example, mitochondrial c-Fos expression is associated with increased vulnerability to neuronal death due to oxidative stress [34]. On the other hand, FosB complexed with Nrf2 promotes neuronal survival against kainate[1] administration [35]. Therefore, it is important to understand the action of FOS family members in each context and how do these contribute to the cell fate.

Several studies have addressed the role of c-Fos in the stroke context [34,36,37], while FosB (FBJ Murine Osteosarcoma Viral Oncogene Homolog B) is still fairly understudied in ischemic conditions. FosB presents 72% homology to c-Fos [38] and together with its truncated isoform, ΔFosB, was first studied in a cancer context [39] and in response to drugs of abuse [40]. Their function in seizures was also characterized [41]. As its siblings, FosB expression has a bidirectional result in cell fate. It remains to be determined what decides whether FosB is going to act in a pro- or anti-survival manner.

1.2.1.1.1. Gene transcription and alternative splicing

FosB exists in two main isoforms: a full-length with 338 amino acid residues and a truncated version with 237 residues (ΔFosB). A third isoform was also reported, known as Δ2ΔFosB, which derives from ΔFosB by an extra truncation (Figure 3A and B). Under physiological conditions FosB is generally expressed at low levels, but it is fast and transiently induced by different types of stimuli in a cell-type specific mode. Its mRNA is extremely unstable, as the transcripts half-life is only of 10-15 minutes [42]. The full-length protein was described to present a half-life of approximately 90 min *in vitro*. These FosB isoforms differ from each other in many aspects and sometimes their activation

[1] Kainic acid (kainate) is a potent neuroexcitatory amino acid agonist that acts by activating receptors for glutamate, the principal excitatory neurotransmitter in the central nervous system. Large doses of concentrated solutions produce immediate neuronal death by overstimulating neurons to death [229].

even results in opposite outcomes. First, the expression of FosB occurs in a very fast and transient manner, while ΔFosB presents a prolonged existence after induction due to the premature termination of the protein (Figure 3D). The lost portion of the transcript, which the full-length FosB still contains, codes for degrons (sequences of amino acids recognized by protein degradation machinery); therefore, ΔFosB is not polyubiquitylated and escapes degradation [43].

The FosB splicing phenomenon is associated to the saturation of polypirimidine tract binding protein (PTB1) with transcripts. Under non-stimulated conditions, PTB1 binds the intronic sequence on the FosB pre-mRNA avoiding access to the splicing machinery. Thus, under resting conditions, full-length FosB mRNA is preferentially produced. Following abundant transcription of FosB pre-mRNA, PTB1 is saturated, releasing FosB pre-mRNA to the splicing machinery [44]. The FosB/ΔFosB ratio is not only dependent on the stimuli sensed by the cell, but also depends on the cell type. For example, HeLa and HEK-293 cells produce much more ΔFosB than FosB mRNAs when compared with PC12 cells or neurons [45].

Since ΔFosB remains in the cells for longer periods, chronic stimulation may lead to a cumulative expression of this isoform. Indeed, accumulation of ΔFosB was observed in response to administration of drugs of abuse, being one of the mechanisms underlying addiction [40]. FosB and ΔFosB act in opposition to regulate Jun transactivity [46]. Moreover, ΔFosB modulates AP-1 transcriptional activity [47].

FosB expression induction was reported in a multitude of events: oxidative stress, amphetamine, nicotine, stress, growth factor exposure, ischemia, recurrent hypoglycemia seizures and neurogenesis [45,46,48–50]. The Serum Response Element (SRE) site of FosB is essential for serum-, platelet-derived growth factor- and phorbol 12-myristate 13-acetate (PMA)-induction of its expression [38]. FosB is a strong repressor of its own promoter by indirect interactions with the SRE [51]. FosB has a crucial role in conferring tolerance against methamphetamine [52], resilience to stress and depressive behavior [53], nurturing [54], among others.

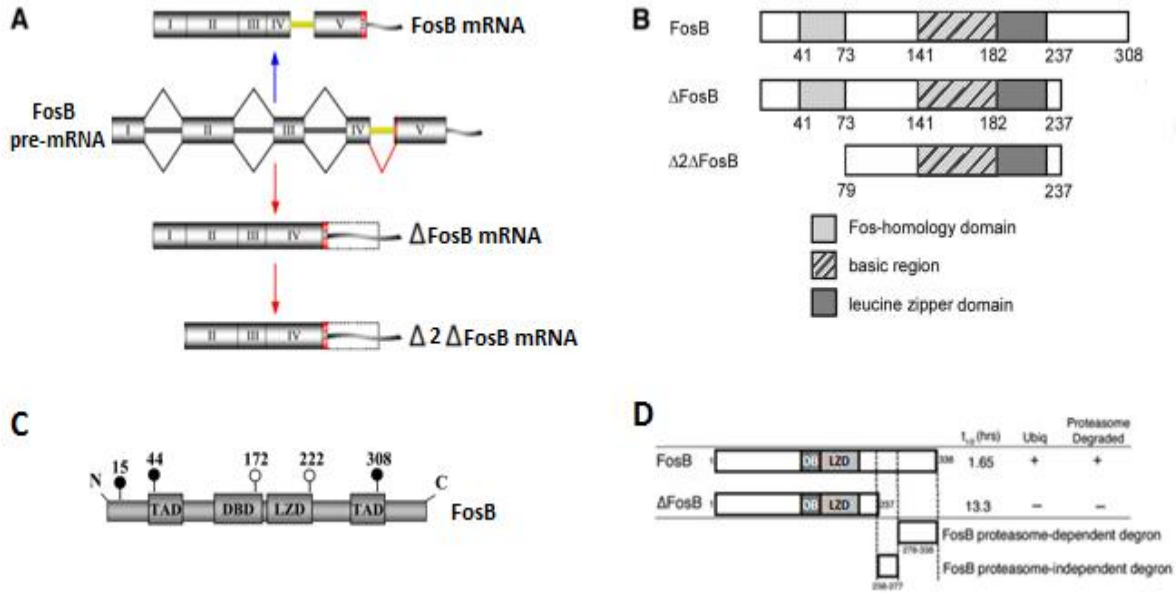

Figure 3 - Alternative splicing of *FosB* and structure domains of the protein. (A) ΔFosB is generated by a 140-nucleotide excision of an "intronic" sequence found in the open reading frame of exon 4 of full length *FosB*. This splice event results in a one nucleotide frameshift which creates a stop codon (TGA, colored red) [44]; *Δ2ΔFosB* is generated from *ΔFosB* by the use of an alternative translation initiation codon. (B) Representation of the domains in each isoform of FosB. (C) Schematic representation of the FosB protein domains and possible sites sensitive to alterations in the redox status. Circles indicate the cysteine residues that might participate in the redox regulation. Open circles represent the cysteine residues located in DBD and LZD of FosB protein. TAD, transcription-activating domain; LZD, leucine-zipper domain; DBD, DNA binding domain; N, amino terminus; C, carboxyl terminus (adapted from [55]). (D) Identification of *FosB* degron domains and their impact on protein half-life, ubiquitylation capacity and sensitivity to proteasome degradation [43].

1.2.1.1.2. Protein expression in the brain

The brain is the most studied organ regarding FosB research, but researchers have also gathered data from lung, heart, bone and several cancers [39,56,57]. From all brain cells, astrocytes, followed by microglia, are the cells with the highest expression of FosB [58]. Determination of FosB expression in neurons is a widely used tool to assess neuronal activity [59,60] and its cerebral expression is strongly induced in mood and reward regulatory neuronal circuits (Table 1). Other regions, such as the hippocampus, also present increased FosB levels after ischemia, chemoconvulsant administration or electroconvulsive seizures [46]. FosB expression was also identified in cerebellar granule cells under excitotoxic conditions [61]. The few studies of FosB expression at basal conditions localize it in neuronal populations scattered throughout layers II, IV, V and VI of the rat cortex, and in the dorsal portion of the dentate gyrus [38].

Concerning the time course of FosB expression in rodent brains, it is known that FosB protein levels peak at 1h after an acute amphetamine dosage, returning to basal levels after 12h. Chronic amphetamine administration produces a similar expression pattern, but with reduced levels of induction [44]. In the case of transient global cerebral ischemia, FosB protein was detected in the DG at 1h, and in CA2-4 and CA1 at 6h after reperfusion. Cohorts treated with hypothermia presented FosB protein expression in DG, CA2-4 and CA1 at 1h *post* reperfusion [62].

Table 1 – Induction of FosB expression in different brain regions under several contexts.

Brain regions	Chronic variable mild stree	Chronic fluoxetine	Methamphatamine	Stereotypic behaviour	Morphine withdrawal
Central & medial amygdala	↑	805%			↑↑
Dorsomedial bed nucleus of *stria terminalis*	↑	767%			
Ventral bed nucleus of *stria terminalis*	↑	1013%			
Oval bed nucleus of *stria terminalis*	↑↑				
Hippocampus, ca1	↑	146%			↑
Hippocampus, ca3		408%			↑
Hippocampus, dentate gyrus	↑	468%			↑↑
Ventral lateral septum	↑				
Parvo- and magnocellular paraventricular nucleus	↑↑				
Lateral periaqueductal gray	↑	322%			
Centrally projecting Edinger-Westphal nucleus	↑				
Dorsal raphe	↑↑	821%			
Ventral part of the lateral septal nucleus	↑↑				
Cortex		1590%	↑↑		↑
Orbital frontal cortex, ventrolateral		1298%			
Nucleus accumbens		297%		↑	↑
Caudate putamen		420%			
Lateral septal nucleus, ventral		390%			
Hypothalamus, dorsomedial		3041%			
Hypothalamus, lateral		3445%			
Substantia nigra, *pars compacta*		717%			
Ventral tegmental area		495%			↑
Periventricular nucleus		555%			
Locus coeruleus		406%			
References	[63]	[60]	[52]	[64]	[65]

1.2.1.1.3. Interactors

FOS family members do not form homodimers as Jun proteins do, but instead they form stable heterodimers with all Jun family members, constituting the AP-1 transcription complex. Together with Jun and c-Fos, FosB is a strong transactivator [66]. After association with the Jun protein, FosB undergoes extensive phosphorylation, being able to bind to CRE, AP-1 and CRE/AP-1-like elements with high affinity [67]. FosB binds stably to the TATA box binding protein (TBP) and the multiprotein general transcription complex TFIID via its C-terminus. Depending on the cell type and stimulus, the FosB binding partner may change (Table 2). For example, in the rat visual cortex, basal AP-1 consists mostly of FosB and JunD [68]. Carle and co-workers performed an immune-precipitation of FosB candidate binding partners, which were identified by mass spectrometry. The results of their study revealed 8 FosB binding candidates: Dynamin, Drebrin 1, Heat shock protein 70, Actin beta, Tropomodulin 2, JunD, Protein phosphatase 2a and DJ-1 protein [45].

Table 2 - Binding partners of FosB.

c-Jun	JunB	JunD	c-Fos	FosB	Fra-1	Fra-2
+↑	+↑	+↑	-	-	-	-
ATF-4	Nrf1	Nrf2	Hsp70	TBP	Hif-1α	
+	+	+↑	+	+	+↑	

+ : Formation of dimers has been observed.
- : Dimerization not yet observed.
↑: Dimerization leads to an increase in DNA-binding affinity.
↓: A decrease in DNA-binding affinity

1.2.1.1.4. Signaling pathways

As mentioned above, the consequences of FosB induction and the upstream events that result in FosB expression vary between cell type and stimulus. cAMP response element binding (CREB) and CREB-binding protein (CBP) are the most common upstream players described in FosB induction (Table 3). In general, in mammalian cells, Fos family members are triggered in response to extracellular stimuli *via* MEK1/2 pathway, which activates ERK1/2 [69].

Table 3 - Compilation of pathways described to induce FosB expression.

Cell type	Pathway/stimulus	Upstream		Downstream	Reference
Rat adrenal zona glomerulosa and *zona fasciculata*	Adrenocorticotropic hormone treatment		FosB mRNA		[70]
Mammalian cells	12-*O*-tetradecanoylphorbol-13-acetate (TPA) activation of ERK	CBP	JunD/ FosB	-	[71]
Osteoblasts	fluid shear stress	CREB	FosB/ ΔFosB	bone formation	[72]
Human Breast Cancer Cells	CD99 type II	ERK1/2	FosB	MMP-9 and motility-related genes	[73]
H295R human adrenocortical cells	Angiotensin II and Forskolin		FosB	11β-hydroxylase	[74]
Primary cultures of mouse astrocytes	serotonin 5-HT2B receptor-mediated EGF receptor	ERK1/2	FosB		[75]
Human retinal pigment epithelium (ARPE-19)	H_2O_2		FosB		[76]
RAW 264.7 cells and primary human monocytes	P2X7 receptor production of ROS	CREB	FosB	immune response	[77]
MC3T3-E1 cells	P2X7 ligand-mediated	CREB	FosB	COX-2	[57]
Human monocytes	E496A polymorphism of P2X7R	CREB	FosB/ ΔFosB	IL-1β and IL-18	[78]
Primary human bladder smooth muscle	Cyclic Stretch-Relaxation		c-Jun/ FosB	Tenascin C and Connective tissue growth factor	[79]
Kidney	GDNF-independent Wolffian duct budding	JNK	Jun/ FosB	Ureteric bud outgrowth	[80]
HEK293 cells	BzATP activated P2X7R	ERK1/2	FosB		[81]

Table 3 (continued) - Compilation of pathways described to induce FosB expression.

Cell type	Pathway/stimulus	Upstream		Downstream	Reference
Rat *substancia nigra*	NO/sGC	ERK1/2	FosB/ ΔFosB	L-DOPA-induced dyskinesia	[82]
Dominant-active DREAM transgenic mice striatum	L-DOPA	CREM or Ca^{2+}	FosB		[83]
Human perihilar cholangiocarcinoma (SK-ChA-1) cells	500 mW Photodynamic therapy regimen	NFE2L2	FosB	survival genes	[84]
6-OHDA-lesioned rats striatum	L-DOPA	ERK1/2	FosB/ ΔFosB	dyskinesia	[85]

1.2.1.1.5. FosB cytoprotective effect

There is evidence supporting both detrimental and cytoprotective effects of FosB. Nevertheless, since this work addresses cytoprotection, we will focus on the FosB beneficial pathways. FosB-containing AP-1 was previously reported to be implicated in protective adaptation in several contexts. Brains of FosB-null mice when exposed to methamphetamines present increased neurodegeneration, Blood-Brain Barrier (BBB) leakiness and self-injury, and reduced levels of small neutral amino acids [52]. Kuroda and colleagues proposed two mechanisms for this thermoregulation-independent protective functions of FosB against methamphetamine neurotoxicity in postsynaptic neurons: (I) activation of negative feedback regulation within postsynaptic neurons *via* Sprouty and RGK; (II) supporting astroglial function by BBB maintenance and metabolism of serine and glycine [52]. Furthermore, the antidepressant result of fluoxetine treatment was correlated with FosB expression [60]. Furthermore, FosB was also described to be crucial in adult neurogenesis and its absence results in epilepsy and depressive behavior [46]. In endothelial cells, hyperbaric oxygen treatment (HBOT) activated the expression of cytoprotective and growth-promoting genes, among which was FosB, presenting the highest induction immediately after the treatment [86]. Noteworthy, pituitary adenylate cyclase-activating polypeptide (PACAP) and other neuroprotective molecules promote FosB expression [87–89]. In addition to the building body of evidence describing cytoprotective effects of FosB, additional pathways need to be disclosed, to allow a deeper understanding of the regulatory entities involved in the control of FosB expression within each context.

1.2.2. Relevance of treatment time

Time is critical in stroke treatment and the only two therapies approved against acute ischemic stroke are intravenous tPA (tissue plasminogen activator) and thrombectomy (mechanical retrieval and recanalization), if given within the recommended time window (< 4.5h and < 8h respectively) [90]. Given later the efficacy is strongly reduced. Therefore, another potential strategy is conditioning. The concept of conditioning refers to brief subtoxic stimuli that trigger endogenous protective mechanisms, which can protect against a later damaging challenge. To act therapeutically in ischemic stroke, the intervention can be done in three time periods:

before injury (pre), between occlusion and reperfusion (per) and after reperfusion (post). Each treatment time targets different populations of patients. For example, prophylactic stroke therapy, due to its unpredictable nature, can be only performed in a restricted cohort of patients, namely in surgical interventions with high-risk for ischemia, patients with transient ischemic attacks (TIA) or patients with multiple vascular risk factors [91]. Ischemic preconditioning is an emerging neuroprotective strategy [92,93], which is also being evaluated as *per*- and *post*-conditioning therapy [94]. Although the majority of stroke patients arrive at the hospital with a considerable delay after the occurrence of stroke [95], a small fraction gets medical assistance before reperfusion. Under the latter conditions, remote ischemic preconditioning may become more relevant as an easy translational neuroprotective strategy that does not require direct intervention in the brain [96]. These time-dependent therapeutic strategies share some common pathways, but further studies are required to accurately understand the mechanisms behind these interventions and what distinguish them apart.

1.3. Experimental models for ischemic stroke

As mentioned above, stroke presents an extremely intricate pathophysiology, thus it is crucial to study it at different degrees of complexity. Therefore, researchers in the stroke field resort to several models, ranging from *in vitro* cell cultures [97] to *in vivo* models. The latter approaches can vary from small rodents to large mammals or even non-human primates [98]. Each model has its own advantages and limitations; the choice of the model to be used in stroke research should consider the scientific question to be addressed and the clinical relevance. Appropriate model choice contributes to overcome the difficulties in stroke translation from research to bedside [5].

1.3.1. *In vitro*

In order to investigate the biology of ischemic stroke, several events known to occur during this kind of injury are mimicked *in vitro*, using cell or tissue slice cultures. The strategy of using simplified model systems is usually followed to address the molecular mechanisms associated with stroke. *In vitro* models allow high-throughput screening, are cost effective and are easy to implement and manipulate. Furthermore, these stroke models present the great advantage of allowing the usage of human samples [99]. Nevertheless, the difficulties in mimicking key players in stroke pathology, such as BBB and inflammation, are still a major disadvantage [100]. *In vitro* models may represent tissue architecture by culturing dissociated cells in 3D structures or by culturing organotypic slices, which resemble to a larger extent the physiologic conditions and were shown to present different responses when compared to the 2D counterparts or monolayer cell cultures, respectively [101,102]. Table 4 represents the types of *in vitro* models used so far in HIR research.

Table 4 - Comparison of suitability of cellular platforms for *in vitro* neurological research [97].

Cellular Platform	HT Ready	Availability of Human Cells	Physiological Relevance	Structural Complexity Modeled	Possible Application to Stroke Research	Comments
Brain slice	No	Extremely limited	High	To a high degree	OGD, chemical ischemia, excitotoxicity	Tissue damage during preparation may induce abnormal functioning
Organotypic cell culture	No	Limited	High	To a high degree	OGD, chemical ischemia, excitotoxicity	Tissue damage during preparation may induce abnormal functioning
Primary cells	No	Limited	High	Artificial arrangement required	OGD, chemical ischemia, excitotoxicity, BBB models, thrombosis and leukocyte response	Limited proliferation capacity
Cell lines	Yes	Unlimited	Low	Artificial arrangement required	OGD, chemical ischemia, excitotoxicity, BBB models	Oncogenes present ad high passage may limit physiological relevance
Embryonic stem cells	Partial	Extremely limited	Potentially high	Artificial arrangement required	OGD, chemical ischemia, excitotoxicity, BBB models	Limited due to ethical issues
iPSCs	Yes	Potentially unlimited	Potentially high	Artificial arrangement required	OGD, chemical ischemia, excitotoxicity, BBB models	Single donor models of the relevant at-risk populations are possible

1.3.1.1. Oxidative stress inducers

One of the major consequences of HIR is the oxidative stress sensed by brain tissue, in particular during reperfusion phase. From the experimental point of view, this can be mimicked by adding pro-oxidant molecules to cell and brain slice cultures, or indirectly by activating endogenous mechanisms coupled to the induction of oxidative stress.

Stimulation of *in vitro* models with pro-oxidant molecules, such as hydrogen peroxide or *tert*-butyl hydroperoxide (*t*-BHP), is a common strategy to evaluate the effect of oxidative stress. *t*-BHP, in particular, induces apoptosis through molecular pathways shared with ischemia, such as caspase-3 activation and cytochrome c release into the cytosol [103,104]. Another strategy is the usage of electron transport chain blockers to induce high levels of ROS production [105].

Indirectly, oxidative stress can also be achieved by promoting excitotoxicity, a classical *in vitro* model of cerebral ischemia. Excessive stimulation of nerve cells by agonists of excitatory receptors triggers a pathological process named excitotoxicity, which results in neurodegeneration. This can be accomplished *in vitro* by adding glutamate receptor agonists to neuronal cultures [106].

1.3.1.2. Oxygen-glucose deprivation (OGD)

Oxygen-glucose deprivation (OGD) mimics the environmental changes that occur in stroke. To reach HIR conditions, the cells are incubated in a medium equilibrated with N_2/CO_2 and lacking glucose, in replacement of the culture medium containing glucose and equilibrated with O_2/CO_2, and the cells or slices are placed in hypoxic chambers. After a transient incubation under OGD, the cells show a classical ischemic injury, characterized by excessive glutamate release and intracellular calcium overload [107]. A multitude of OGD periods followed by reperfusion time combinations are used. The

experimental setting depends on the cell type and the percentage of cell death that is aimed to achieve [97].

1.3.2. ***In vivo***

Since *in vitro* models present several limitations, *in vivo* studies are crucial for stroke preclinical research. First, global, focal and multifocal forms of ischemic stroke should be discriminated. The global ischemic stroke is generally a result of a major reduction of blood flow throughout the entire brain, which may be a consequence of cardiac arrest in humans [108]. On the other hand, focal ischemic stroke is confined to the area where blockage of blood flow occurred [109]. Multifocal ischemic stroke occurs in the case of several cerebral vessels being occluded [110]. Second, it is relevant to distinguish the *in vivo* permanent models of stroke from those allowing reperfusion of the tissue. Permanent occlusions, which do not feature the reperfusion phase, can be attained by electrocoagulation or microaneurysm clips [111]. Conversely, transient occlusions reproduce the temporary blockage of blood flow, either *via* an intraluminal suture [112] or external clamp [98]. Noteworthy, models of focal ischemic stroke have been tailored to induce injury within the middle cerebral artery (MCA) area to mirror the clinical situation [113], since approximately 70% of all first strokes occur in this region [114]. Two other main categories in *in vivo* stroke models can be based on the fact that these require or not craniectomy, a procedure that alters intracranial pressure among other possible damaging consequences [115].

In conclusion, in order to build clinically relevant models to study the complexity of stroke, a plethora of animal models emerged, which are summarized in Figure 4. Nevertheless, the stroke models currently used present some key features that may explain the difficulty in translation, namely the fact that the animals used for these procedures are healthy young adults, conversely to the diseased elderly human population that suffers stroke.

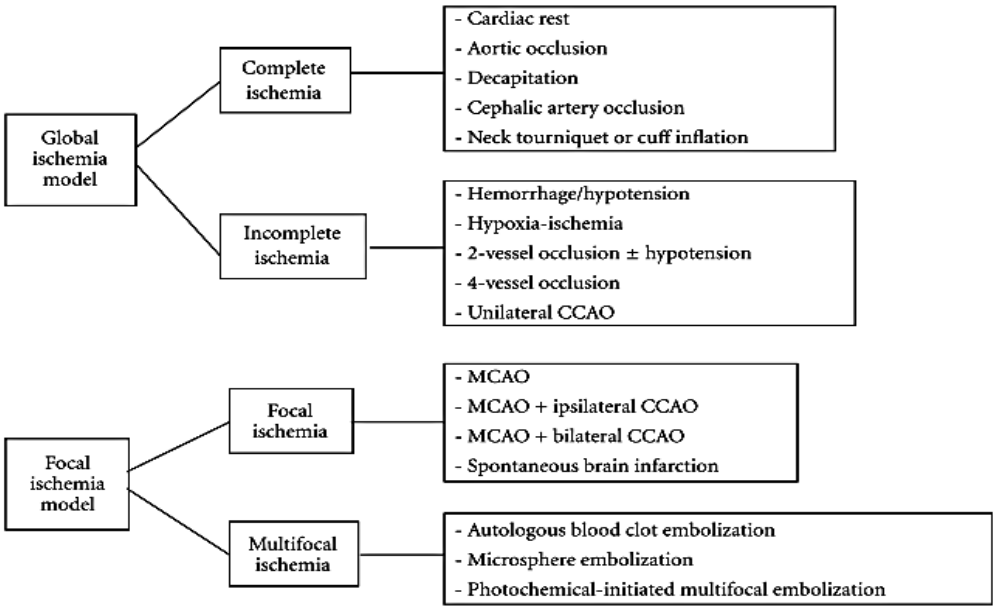

Figure 4 - Major types of animal models for ischemic stroke [116].

1.3.2.1. Intraluminal middle cerebral artery occlusion (MCAo)

Among the transient focal ischemic models that do not require craniectomy, the intraluminal middle cerebral artery occlusion model (MCAo) is the most used, especially with rodents. In addition, it has been considered a gold standard reference in mechanistic studies of ischemic stroke [117]. The method consists of introducing a monofilament into the internal carotid artery (ICA) and further advancing it until blood flow at the middle cerebral artery (MCA) is blocked [118]. Later improvements were introduced by advancing the suture into the MCA *via* the transected external carotid artery (ECA) [119] (Figure), filament guidance by Laser Doppler Flowmetry and increasing the *post*-ischemic temperature after MCAo [120]. The occlusion of the MCA and other surrounding arteries depends on the shape, size and the insertion length of the microfilament [121]. While in rats the most common periods of MCA occlusion are 60, 90 and 120 min [122], in mice occlusion times as short as 15 min result in infarct [123].

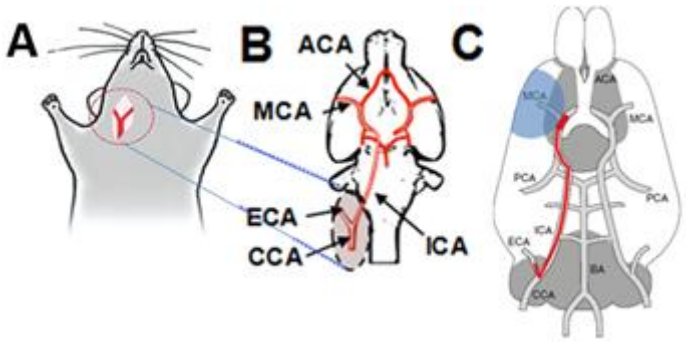

Figure 5 - Scheme of filament introduction in MCAo model of focal brain ischemia.

MCAo presents several benefits as an *in vivo* model of brain ischemia: it is less invasive than other methods, allows an easy control of the ischemic duration and reperfusion, and closely mimics the human cases, exhibiting a penumbra region that is comparable to the one observed in human stroke cases. However, this MCAo model is not suitable for testing therapies combined with tissue plasminogen activator [117]. From the experimental point of view, there is no perfect ischemic stroke model. Therefore, the advantages and disadvantages of each method must be weighted when considering the question(s) to be addressed (Table 5).

In conclusion, establishing new and better animal models, which ultimately consider the various co-morbidities associated with stroke, is a work in progress. In the end, the goal is to develop safer and more efficacious therapies

1.3.2.2. Outcome evaluation

The wide assortment of stroke models enables researchers to explore preventive and neuroprotective strategies for stroke. However, this is only possible if an anatomical, functional and behavioral assessment can be performed. Besides defining the outcome assessment tools, the time at which this evaluation is performed is also a relevant parameter, as well as the analysis of the mortality rate [124].

Table 5 - Advantages and disadvantages of the most used rodent stroke models [119].

Models	Advantages	Disadvantages
Intraluminal suture MCAo	Mimics human ischemic stroke • Exhibits a penumbra • Highly reproducible • Reperfusion highly controllable • No craniectomy	Hyper-/hypothermia • Increased hemorrhage with certain suture types • Not suitable for thrombolysis studies
Craniotomy	High long-term survival rates • Visual confirmation of successful MCAo	High invasiveness and consecutive complications • Requires a high degree of surgical skill
Photothrombosis	Enables well-defined localization of an ischemic lesion • Highly reproducible; Low invasiveness	Causes early vasogenic edema that is uncharacteristic for human stroke • Not suitable for investigating neuroprotective agents
Endothelin-I	Low invasiveness • Induction of ischemic lesion in cortical or subcortical regions • Low mortality	Duration of ischemia not controllable • Induction of astrocytosis and axonal sprounting, which may complicate the interpretation of results
Embolic stroke	Mimics most closely the pathogenesis of human stroke • Appropriate for studies of thrombolytic agents	Low reproducibility of infarcts • Spontaneous recanalization • High variability of lesion size

1.3.2.2.1. Tissue examination

The cerebral infarction area can be evaluated *in vivo* (*e.g.* Magnetic Resonance Imaging (MRI)) or *post-mortem* (*e.g.* triphenyltetrazolium chloride (TTC)). Since infarct volume development changes with time and its measurement is methodology dependent, fresh tissue staining approaches are typically preferred to avoid hemisphere shrinkage due to fixation steps [122]. Nevertheless, tissue processing for histopathological staining is still very useful to detect molecular and cell-specific alterations. TTC staining is still the most common approach to analyze infarct volume. TTC is reduced by enzymes present in functioning mitochondria (in particular, succinate dehydrogenase), staining the intact brain regions dark red (formazan), while the lesion area remains colorless.

Infarct volume correction regarding volume due to brain edema is critical. These volumetric changes are easily corrected using the indirect measurement: subtracting to the contralateral hemisphere volume the health volume of the ipsilateral hemisphere [125]. More recently, brain edema following stroke has gained attention from researchers and its evaluation is also a readout of stroke outcome [126].

1.3.2.2.1.1. Magnetic Resonance Imaging (MRI)

After the first MRI study on a mouse MCAo model in 1997 [127], noninvasive imaging methods were developed to study stroke models in small animals. A growing body of studies can be found where MRI techniques were used in rodent stroke models.

This exponential usage of MRI in preclinical models of stroke is due to the numerous advantages that this technique offers: high spatial and time resolution, longitudinal studies, and multi parameter assessment, among others [128].

1.3.2.2.2. Functional Assessment

Sensorimotor function tests in preclinical stroke models are essential, since neurological function and quality of life are key readouts of stroke recovery in humans. This can be achieved by determination of neurologic scores together with the analysis of behavioral paradigms. Performing more than one behavioral test is recommended to avoid confounding effects (

Figure). Accelerated rotarod, pole test, openfield and adhesive removal test are widely used to evaluate motor coordination and gross motor skills following stroke [129]. Tests to examine the refined sensorimotor function after focal stroke include limb placing, beam walking, grid walking, the sticky label test, and the staircase test [130].

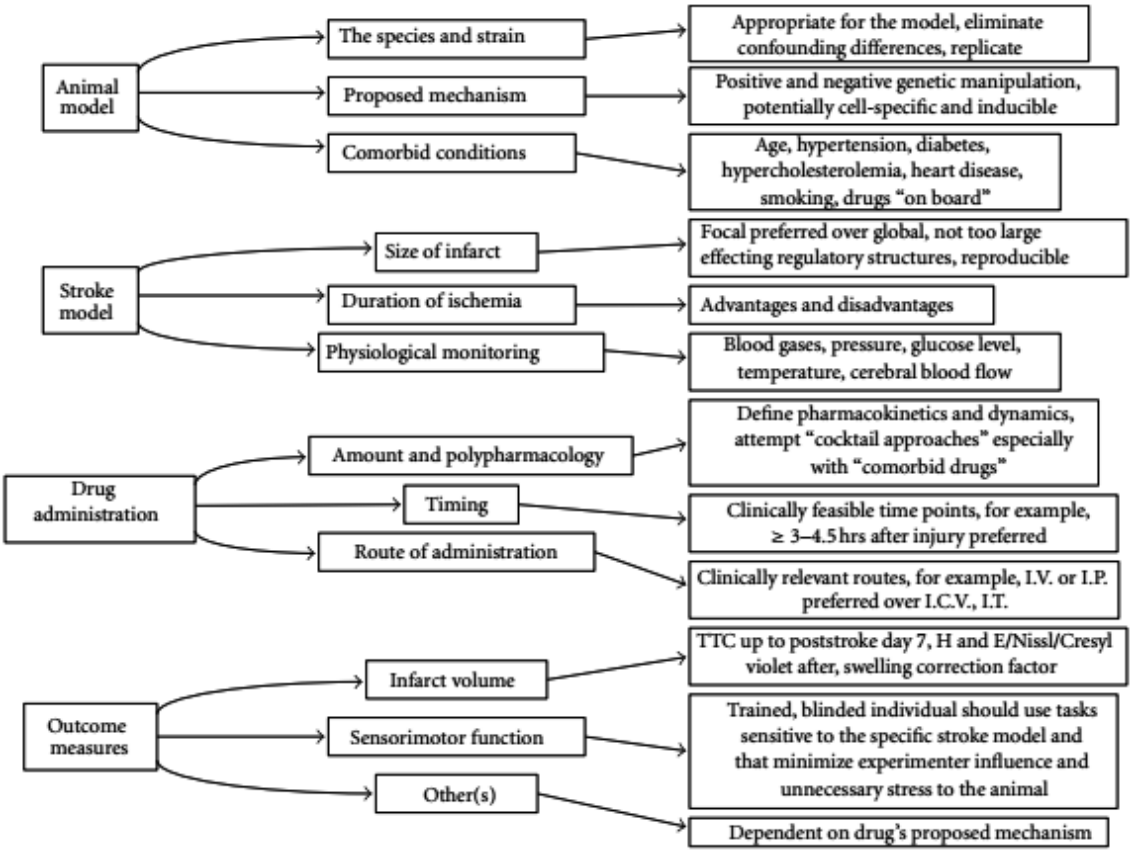

Figure 6 – Summary of the factors to take into consideration to increase the potential of laboratory experimental stroke treatments to be translated to successful clinical trials [131].

2. Carbon monoxide/hemoxygenase axis

Carbon monoxide (CO) is a gasotransmitter, endogenously produced by hemoxygenase (HO) as a product of heme degradation (Figure A). Approximately 86% of endogenous CO is produced *via* HO, while the other 14% originates from lipid peroxidation and xenobiotics (Figure B).

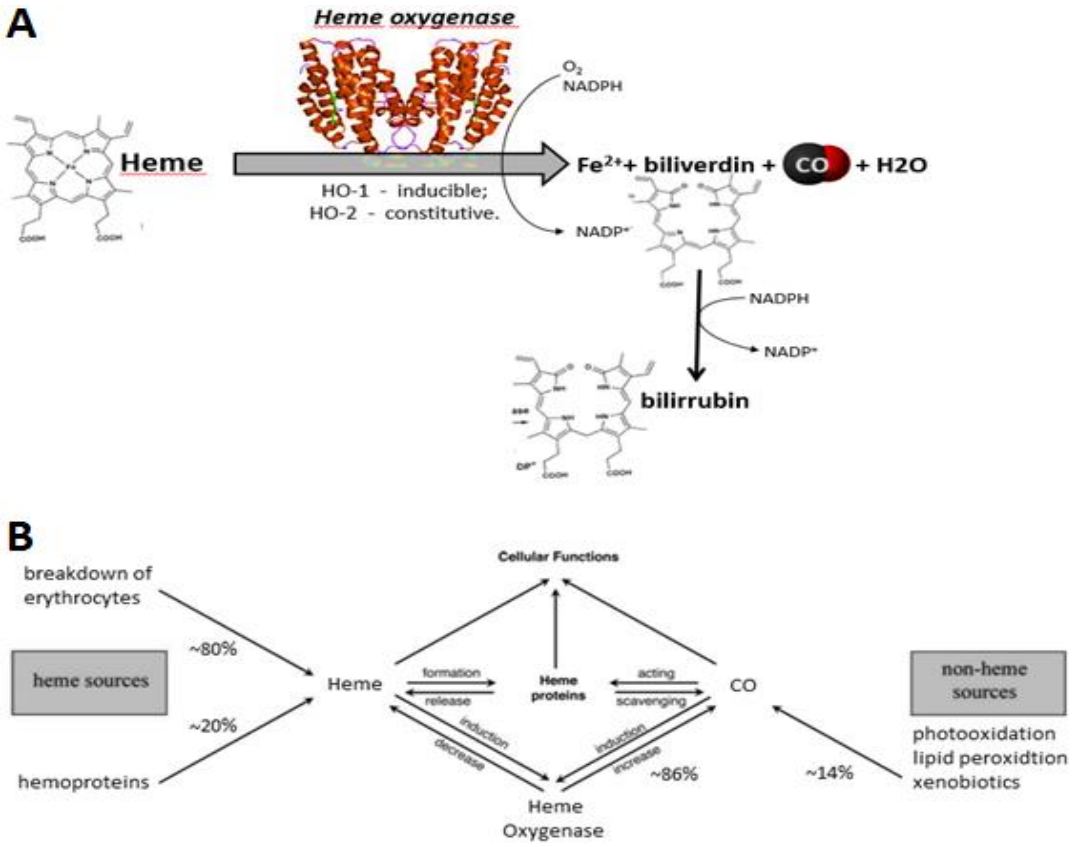

Figure 7 – Carbon monoxide biology. (A) Heme metabolization by the enzyme HO, producing free iron, biliverdin (rapidly converted to bilirubin) and CO; (B) Interplay among heme, HO, and CO [132] and CO sources [133].

To date, two HO isoforms have been well characterized: one is inducible (HO-1) and the other is constitutively expressed (HO-2). HO-1, also known as heat shock protein-32 (HSP32) [134], is an emergency molecule whose expression is induced in response to stress stimuli. Therefore, modulation of HO-1 has therapeutic potential [135]. Moreover, the cytoprotective effects of HO-1 under stress conditions caused by a wide range of stimuli have been described in many tissues and disease scenarios (Table 6). The effects of HO are typically attributed to its endpoint product CO [136].

CO is the most comprehensively studied of all HO-1 products [137]. More than being the endpoint product of the enzymatic activity of HO, CO has its own biological relevance as neurotransmitter, vascular modulator [138], anti-apoptotic agent [139], anti-inflammatory molecule [140], and modulator of the mitochondrial function [141], among other functions. CO is capable of influencing its own production by promoting HO expression (Figure). Average tissue concentrations of CO is at low nanomolar range, but the production rate of CO in the human body is 16.4 µmol/h, reaching more than 12 ml (500 µmol) daily [142].

Table 6 - Protective role of HO-1 expression in diseases [135].

Organs	Disease
Brain	Cerebrovascular accident
Eye	Corneal inflammation • Uveitis • Ocular hypertension
Ear	Noise-induced hearing loss • Drug-induced ototoxicity
Lung	Hyperoxic Injury • Pulmonary hypertension • Pulmonary Fibrosis
Heart	Cardiac transplant rejection • Ischemic heart disease
Gastrointestinal	Inflammatory bowel disease
Liver	Ischemia/reperfusion injury • Drug-induced hepatotoxicity • Transplantation
Vasculature	Transplant arteriosclerosis • Atherosclerosis • Hypertension
Bone marrow	Transplantation
Kidney	Acute kidney injury • Chronic renal allograft rejection • Polycystic kidney disease

CO is inert and more stable than nitric oxide (NO), due to the absence of unpaired electrons. It binds exclusively reversibly to its targets, and this interaction occurs exclusively with metal complexes, either heme iron and nonheme iron complexes, to inhibit their function. Interestingly, CO does not interact with nonmetal cofactors or amino acid residues on the protein surface [143,144].

CO is best known for causing asphyxiation, due to its high affinity to hemoglobin [145]. However, under subtoxic concentrations CO was described to confer several beneficial effects in a wide range of tissues [146]. CO action is very complex, since it is time and dose-dependent, the effects are transient and vary with the delivery method [147].

2.1. Cerebral HO expression

In the brain, HMOX1, the HO-1 coding gene, can be rapidly induced in response to a big variety of stimuli, predominantly in microglia and astrocytes, while HMOX2, the HO-2 coding gene, is preferentially expressed in neurons. Both HO isoforms are induced in the central nervous system (CNS) and in other tissues in response to damaging events, including oxidative stress, heat shock, hypoxia, heavy metals, and toxins [148]. HO-2 is expressed in a subpopulation of cells in the olfactory bulb, as well as in the cortex, hippocampus, hypothalamus, cerebellum, and caudal brain stem [149]. Contrary to the low or undetectable levels of HO-1 protein in the brain, its mRNA is physiologically detectable at high levels in the hippocampus and cerebellum, and to a lower extent in the striatum and cortical type I astrocytes [150,151].

Neuroprotection by the HO system (HO-1/2, CO, Fe and biliverdin) was reported by several authors in a myriad of pathologic and toxic contexts [152–157]. Soares and Bach [158] suggested HO-1 system to be a therapeutic funnel; although each molecule has its own mechanism, the overall protective effect is raised together. Moreover, HO-2-deficient mice present cerebral dysfunction, such as pronounced brain tissue loss and compromised motor function after traumatic brain injury [159]. Similarly, HO-1 knockout mice and primary cultured neurons lacking the enzyme show increased cell death following *N*-methyl-D-aspartate-induced acute toxicity [160]. However, detrimental effects of HO-1 were also described. Glial HO-1 overexpression was implicated in cerebral iron deposition and oxidative mitochondrial injury in neurodegenerative diseases such as Alzheimer's disease [161]. Accordingly, conditional GFAP.HO-1 transgenic mice displayed unregulated glial iron in the hippocampus and subcortical

regions [162]. On the other hand, the upregulation of HO-1 in neurodegenerative diseases might be a cellular response to free heme associated with neurodegeneration, and may allow to convert heme into the antioxidant bilirubin [163].

One can hypothesize that HO-1 is a 'double-edged sword' in brain tissue: it is either neuroprotective or neurotoxic [164]. A deeper understanding of HO-1 function is indispensable to elucidate the exact functions in each context and the mechanisms underlying the effect of HO-1 in the nervous system.

2.2. Exogenous CO administration

The evidence gathered concerning the beneficial effects of endogenous CO pushed the development of new delivery methods aiming at exploring its potential as a therapeutic molecule. For systemic delivery, CO gas can be inhaled or CO-releasing molecules (CORMs) or hemoglobin-based CO carriers (HBCOC) can be administrated intravenously (i.v.) or intraperitoneally (i.p.) [137]. CO/gas mixtures were first used in CO delivery, but unfortunately this strategy presents several disadvantages, since it is difficult to bypass the problems related to the effects of CO on oxygen transport and delivery [142]. To overcome the obvious limitations of this route, efforts have been made to develop molecules to deliver CO in a controlled, directed fashion, called CORMs (Figure).

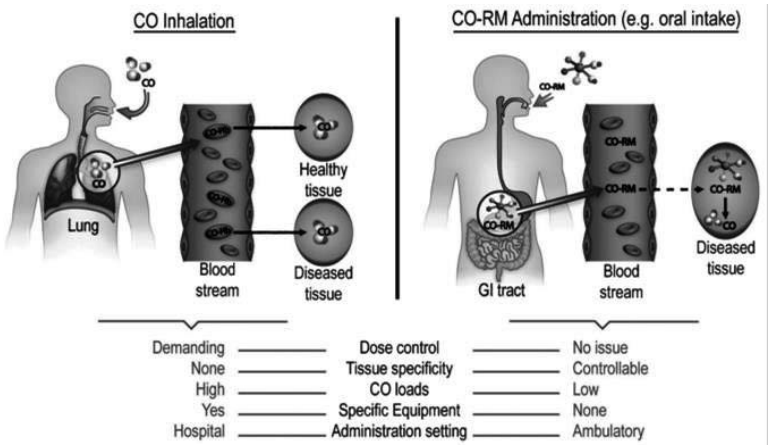

Figure 8 – Comparison between strategies of CO delivery to diseased tissues [165].

The development of CORMs boosted the CO research field and accelerated the potential translation of CO into clinics. An array of CORMs was created to answer the needs of the CO research field. Nowadays, scientists use CORMs to deliver CO in *in vitro*, *ex-vivo* and *in vivo* experimental models of disease [166]. CORMs are chemical structures constituted by metal carbonyls to which one or more CO molecules are covalently bound. The release of CO can be elicited by several triggers: pH [167], temperature [165], ligand substitutions [168], click-and-release [169], UV light [170,171] and visible light [172]. In addition, faster or slower CO release can also be achieved (Table 7).

Table 7 - Chemical properties and pharmacological activities of the most commonly studied CORMs [173].

Compound	Chemical structure	CO release kinetic and properties	Pharmacological action
CORM-1		Fast ($t_{1/2}$ < 1 min) CO release is light-dependent Soluble in ethanol and DMSO	Vasodilator; Reno-protective
CORM-2	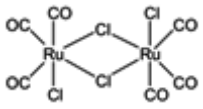	Fast ($t_{1/2}$ ≈ 1 min) CO release induced by ligand substitution Soluble in ethanol and DMSO	Vasodilator; Reno-protective; Anti-inflammatory; Anti-carcinogenic; Pro-angiogenesis; Anti-apoptotic; Inhibitor of cell proliferation
CORM-3	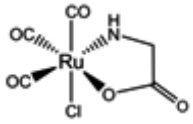	Fast ($t_{1/2}$ ≈ 1 min at pH = 7.4, 37ºC) CO release induced by ligand substitution Water-soluble	Vasodilator; Reno-protective; Cardioprotective; Anti-inflammatory; Anti-ischemic; Inhibitor of platelet aggregation
CORM-A1	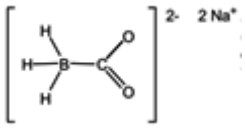	Slow ($t_{1/2}$ ≈ 21 min at pH = 7.4, 37ºC) CO release is strictly pH-dependent Water-soluble	Vasodilator; Reno-protective; Anti-ischemia; Anti-apoptotic

The CORMs' half-life ($t_{1/2}$) is defined as the time taken to release 0.5 equivalents of CO [165]. In an attempt to improve some CORMs, "encapsulation" strategies were explored, as described in Table 8.

Table 8 - Encapsulated CORMs and their properties [174].

Macromolecular Carriers	CORMs	Trigger Release	Release Rate
Micelles	CORM-3	Thiol-containing compounds	Thiol concentration dependent. About 10% CO release after 60 min at 10 mM of cysteine
SiO_2 nanoparticles	Photo-CORM	Light	Similar to the parent CORMs
Nano porous fibrous nonwovens	CORM-1	Light	Wavelength dependent
Proteins (BSA)	CORM-3	Proteins	In 1 mg/ml BSA with 50 eq. CO-RM-3, CO release finished in 4h

HBCOC [175] usage did not become yet as popular as CORMs, possibly due to the unclear pharmacology of polyethylene glycol (PEG, its outer constituent) aggravated by the fact that it can only be administered intravenously.

2.2.1. CORM-A1

Motterlini and colleagues first described CORM-A1 ($Na_2[H_3BCO_2]$) in 2005 [166]. This CORM, being sodium boranocarbonate, does not contain a transition metal carbonyl

but a carboxylic group instead. As the threshold for CO toxicity is at 10% of carboxyhemoglobin in blood stream, CORM dosages have been established to induce less than the 10% limit. With this in mind, Csongradi found that 5 mg/kg CORM-A1 would guarantee the nontoxic carboxyhemoglobin concentration in bl6/c57 mice [176].

CORM-A1 releases CO under physiologic conditions (37°C and pH = 7.4) in a slow fashion ($t_{1/2}$≈21 min). CO release from CORM-A1 is pH- (as it becomes faster in acidic conditions) and temperature- (as it becomes slower in colder conditions) dependent. One of the major advantages of this CORM is its solubility in water, which makes its suitable for biological applications [166].

Numerous studies have assessed the effect of CORM-A1 in many different biological contexts: neurogenesis [177], obesity [178], intestinal oxidative stress [179], diabetes [180], experimental autoimmune uveoretinitis [181], seizures [182], BBB dysfunction [183], antibacterial activity [184], renal vasculature [185] and immune response [186].

Additional studies are required to characterize CORM-A1 pharmacokinetics. Before this CORM can be used therapeutically, it is imperative to know where the inactive CORM-A1 accumulates, and how it is absorbed, metabolized and excreted.

2.3. Binding targets and pathways regulated by CO

CO has a high affinity towards transition metals, such as iron, manganese, vanadium, cobalt, tungsten, copper, nickel and molybdenum. These metal centers can be found in structural and functional proteins. Contrary to NO, which accepts electrons from Fe^{3+} and Fe^{2+}, CO only binds to the latter oxidation state, narrowing the possibilities to target hemeproteins with CO [187]. The molecules targeted by CO in mammals are not restricted to heme-containing proteins, as several reports present evidence of CO targeting non-hemeproteins (Table).

Table 9 - Carbon monoxide targets and function [137].

Hemoprotein	Primary location	Function
sGC	Vascular smooth muscle	Vasodilation
Hemoglobin	Erythrocytes	CO delivery
NOS2	Leukocytes	NO generation
NOS3	Endothelial cells	NO generation
NPAS2	Neurons	Transcriptional regulation
Cytochrome oxidases	All cells	Bioenergetics
Non-hemoproteins	Primary location	Function
MAPKs	All cells	Signal transduction
PPARɣ	All cells	Signal transduction
HIF1α	All cells	Transcriptional regulation
STAT3	All cells	Signal transduction
NADPH oxidase	Leukocytes	Free radical generation

The effects of CO are exerted through multiple pathways [188]. It acts via activation of soluble guanylyl cyclase (sGC) and nitric oxide synthase (NOS), as well as through modulation of mitogen-activated protein kinase (MAPK) family members, potassium,

sodium, calcium and ATP-gated channels and ROS production [143,189]. Moreover, the mitochondria also plays a central role in CO signaling, since its last electron transport chain complex, cytochrome c oxidase, is also one of CO targets (

Figure). The first line of CO effectors then activate the transcription of a myriad of genes, several of them IEGs [190,191].

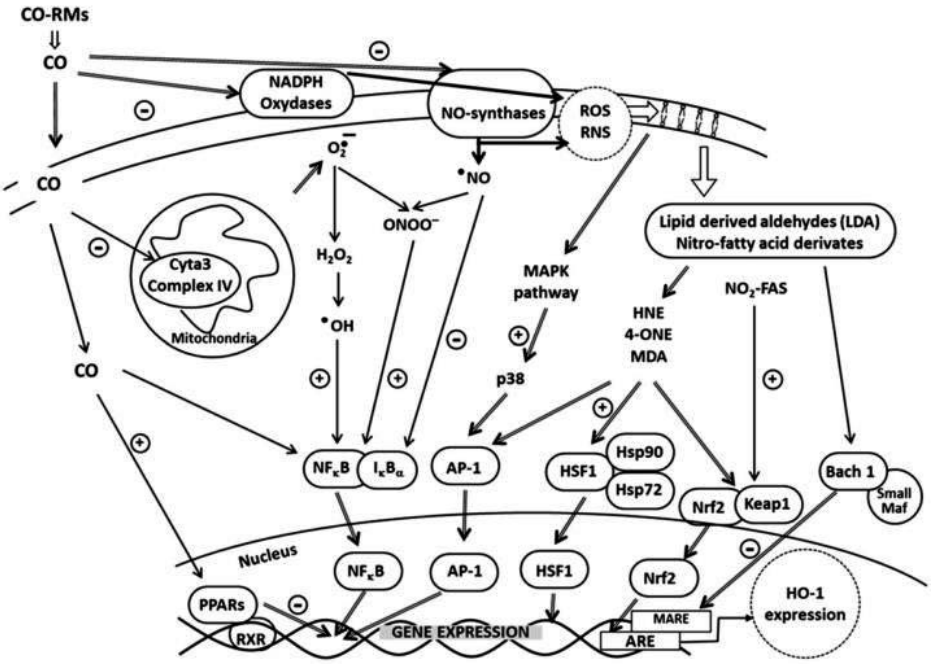

Figure 9 - CO modulation of cellular pathways and downstream regulation of gene expression. Induction of these genes, which include antioxidant and HO-1 genes, contributes to adaptive responses that enhance the resistance of cells to environmental stresses. Reactive Oxygen Species: ROS, Reactive Nitrogen Species: RNS, Lipid Derived Aldehydes: LDA, nitro-fatty acid derivatives: NO2-FAs), antioxidant response element: ARE, *Musca domestica* antifungal: Maf, Maf-recognition element: MARE [143].

In addition to the CO cellular targets, CO sensing is also fundamental. In mammals, neuronal PAS domain protein 2 (NPAS2) is a specific CO sensor [192], as well as cystathionine β-synthase (CBS) [193]. CO sensor proteins are crucial regulators of CO cellular response, since different CO concentrations trigger distinct signals. For example, CBS affinity towards CO is in the physiologically relevant micromolar range, thus endogenous CO may act as an inhibitor of human CBS [194].

2.4. Effect of CO on mitochondria

The most accepted CO cellular target is the mitochondria. This is not surprising for three reasons: (i) the leading potential candidates for CO to coordinate with are mitochondrial hemeproteins, (ii) the biological actions of CO depend on mitochondrial ROS signaling and (iii) the last step of HO's substrate heme is located within the mitochondria [141]. Indeed, one of the best described CO binding candidates is cytochrome c oxidase (mitochondrial complex IV, COX), at the cytochrome a and a3 (

Figure).

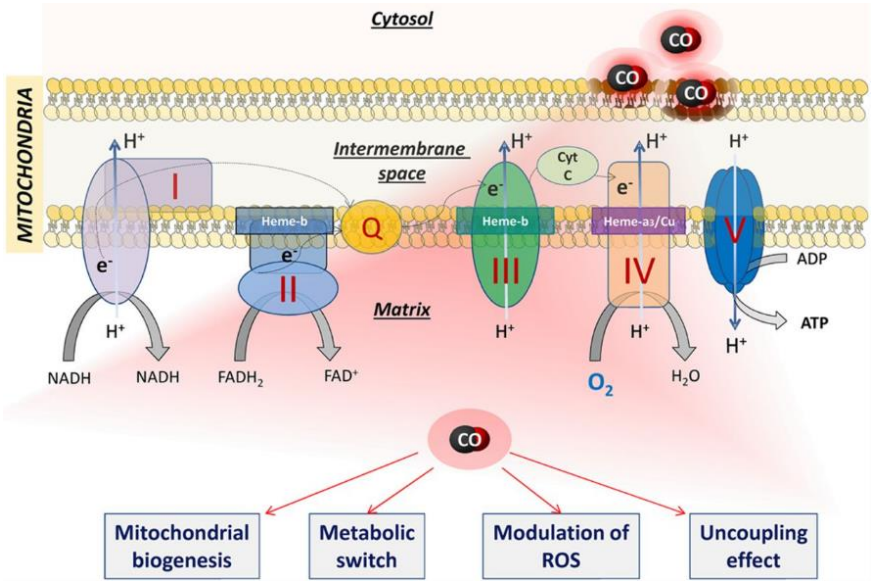

Figure 10 – Interaction of carbon monoxide (CO) with mitochondria [195].

CO cytotoxicity is linked to COX inhibition, being dependent on the oxygen levels [196]. However, low concentrations of CO partially inhibit mitochondrial respiration, producing innocuous ROS amounts which act as signaling molecules [197]. Reinforcing the key role of mitochondria in the activity of CO is the fact that it has no cytoprotective effects in mitochondrial DNA-deficient cells [198]. One may hypothesize that the reduction in CO-induced mitochondrial respiration can induce a compensatory response, resulting in mitochondrial biogenesis, which was observed in several studies [199]. One consequence of CO-triggered ROS signaling is the increased ratio oxidized/reduced (GSSG/GSH) glutathione [200]. Moreover, mild mitochondrial uncoupling is a cellular strategy to control oxidative stress, and CORM-3 was reported to protect mitochondria against oxidative stress by contributing to mild uncoupling [201]. Additionally, in intact cell-free mitochondria preparations from the brain cortex [200] and liver [202], CO gas administered in low doses inhibited several processes related with the regulation of mitochondrial membrane permeabilization (MMP) and cell death, namely (i) mitochondrial swelling, (ii) loss of mitochondrial membrane potential, (iii) permeabilization of the inner membrane to molecules lower than 800 Da and (iv) the release of cytochrome c. Furthermore, CO not only modulates the mechanism whereby Ca^{2+} regulates mitochondrial function and MMP, but also appears to augment the mitochondrial capacity to uptake Ca^{2+}, thus inhibiting cell death [203]. Moreover, CO is also able to promote metabolic improvement and increased mitochondrial population [204].

In conclusion, CO arises as a key gasotransmitter which controls several cellular functions of mitochondria: metabolism, cell death, Ca^{2+} signaling, among others (

Figure ***4***). Particularly, the capacity of CO to modulate metabolism might play a key role in the cellular response to diseases, namely cancer and ischemia.

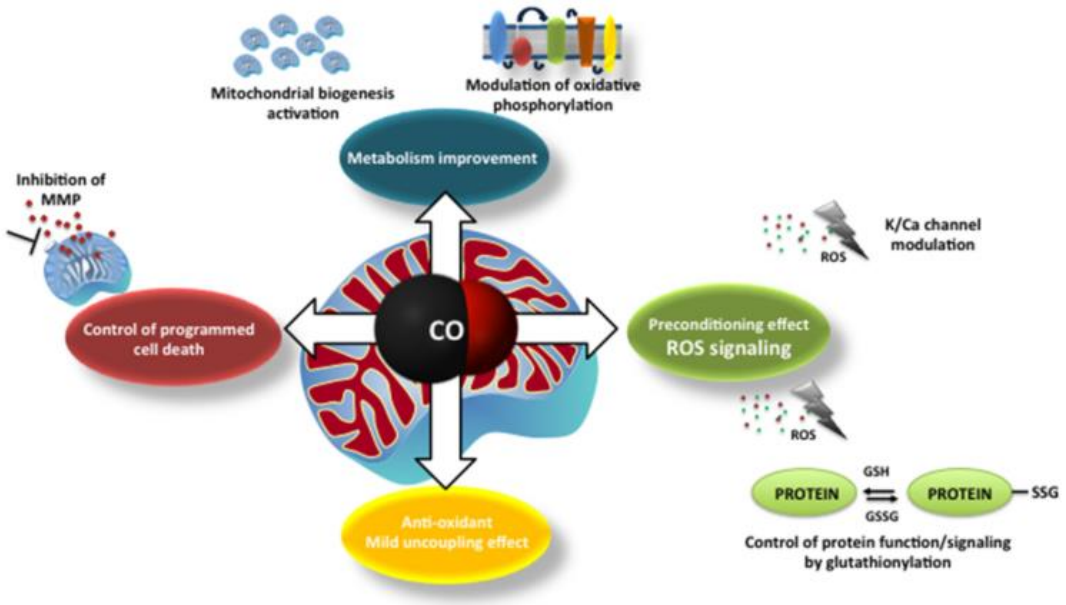

Figure 4 - The main described mechanisms of CO on mitochondria [141].

2.5. Carbon monoxide as a therapeutic agent

Introducing CO as a therapeutic agent, alone or in combination with other strategies, is relatively simple, since it would not involve specialized equipment or invasive procedures. Furthermore, other gasotransmitters are already applied therapeutically, such as NO which is chemically similar to CO. Moreover, as CO is endogenously produced, the organism is fully adapted to it, which is an enormous pharmacologic advantage.

The cytoprotective effects of CO were previously described in innumerous biological systems. The gasotransmitter has been studied for its anti-inflammatory and anti-apoptotic effects, the capacity to maintain tissue homeostasis, the anti-proliferative and vasodilator properties and its activity in metabolic improvement [147,204–207]. The cytoprotective effects resulting from CO administration were evaluated in the brain [206], lung [208], intestine [209], liver [210], pancreas [211], heart [195], kidney [176], lungs [212], immune system [186], and in the retina [213] among other tissues (Figure 5).

One may hypothesize that these general cytoprotective actions of CO can be an advantage to achieve effective therapies in the case of patients presenting comorbidities. For example, in a simplistic scenario, a patient that suffered a stroke and is diabetic would benefit from a CO-based treatment, since CO is known to be helpful against both pathologies.

Currently there are nine clinical trials accessing CO gas therapeutic potential, mainly addressing the respiratory system: severe pulmonary arterial hypertension (NCT01523548), acute respiratory distress syndrome (NCT02425579), intestinal paralysis after colon surgery. (NCT01050712), idiopathic pulmonary fibrosis (NCT01214187), adult respiratory distress syndrome (NCT00094406), stable chronic obstructive pulmonary disease (COPD) (NCT00122694), mitochondrial biogenesis in human cardiac muscle (NCT01727167), and *ex-vivo* lung perfusion reconditionning (NCT02032082)

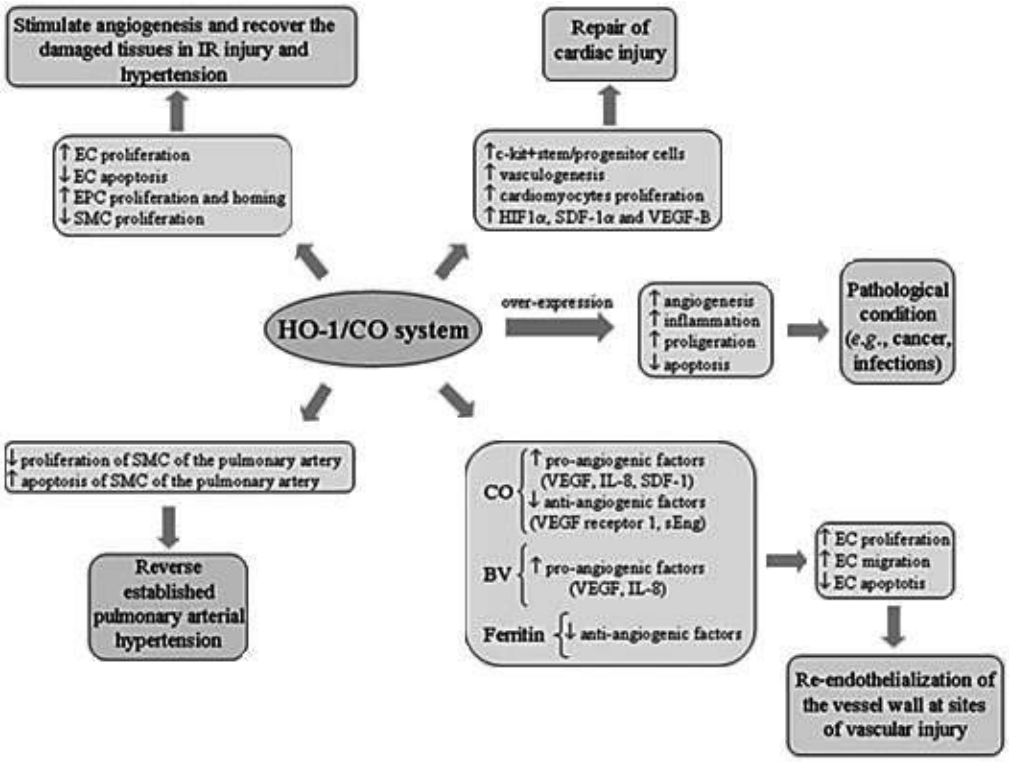

Figure 5 - ‘‘Pro’’ and ‘‘anti’’ physiologic effects of the HO-1/CO system. Overexpression of the HO-1/CO system may be responsible of several pathological conditions, such as cancer (↓, decreased expression; ↑, increased expression) [194].

In the future, the CO dose and administration timing needs to be defined for human treatment. In parallel, the mechanisms of CO action still urge for deeper understanding. All parameters influencing the CO mode of action should be disease tailored in order to guarantee an optimal outcome and here is where the complexity and challenge of CO research resides.

2.5.1. CO therapy to the CNS

Low doses of CO improve the outcome in several *in vivo* models of acute and chronic neurodegenerative diseases [206]. CO gas administrated immediately after permanent MCAo reduced injury in 30% [214]. Similarly, inhalation of 125 to 250 ppm of CO given up to 3h after onset of reperfusion also decreased infarct size after 48 h in transient MCAO models [215]. A rat model of hemorrhagic stroke confirmed the time-dependence of CO effects. Administration of CORM-3 5 min before or 3 days after damage decreased the inflammatory responses, in contrast with the results obtained when CORM-3 was injected 3 h after the hemorrhagic insult [216]. Accordingly, CO gas also minimized hippocampal apoptosis by 64% in a perinatal rat model of cerebral HIR [217]. In a piglet model mimicking open-heart surgery procedures, CO gas pretreatment reduced cell death in the neocortex and hippocampus [218]. Moreover, administration of CORM-A1 (2 mg/kg, i.p.) prior to chemical seizure-induction protected from neonatal vascular injury in newborn piglets [219,220]. CO was also shown to be effective in the alleviation of the symptoms in multiple sclerosis [221]. Furthermore, a single i.p. injection

of CORM-2 ameliorated the outcome and enhanced opioid effect in a rat model of neuropathic pain [222].

The observed effects of CO in the *in vivo* studies described above were also confirmed *in vitro*, using neuronal cultures. A recent CORM (ALF 186) protects the SH-SY5Y neuronal cell line and retinal ganglion cells against rotenone and retinal ischemia-reperfusion, respectively, *via* sGC activity and cGMP production [223]. Both endogenous CO and CORM-2 protected SH-SY5Y cells against Aβ(1-42) toxicity in a concentration-dependent manner [224]. CO effects are also extend to glia cells, since CO gas limited astrocytic apoptosis induced by diamide or *t*-BHP by preventing mitochondrial membrane permeabilization and mitochondrial release of pro-apoptotic factors [200], as well as by improving astrocytic metabolism *via* oxidative phosphorylation and increasing the mitochondrial population [204]. Furthermore, BV-2 microglial cells challenged with CORM-3 decreased their NO production and TNF-α release in response to LPS, thrombin and IFN-γ stimuli [225,226].

Brain tissue is extremely intricate, as it is not only constituted by neural cells, but also by its own vasculature. Cerebral vessels can also benefit from the effects of CO [138]. For example, endogenous and exogenous CO modulate Nox4 NADPH activity, thereby promoting endothelial cell survival [227,228]. Likewise, CORM-A1 prevents BBB dysfunction by minimizing glutamate-induced apoptosis and oxidative stress in cerebral microvascular endothelial cells [183].

Taken together, the multiple responses induced by CO in brain cells are effective against different CNS pathologies; these include the ability of CO to mediate cytoprotection and modulate cell death, inflammation, cell metabolism, cellular redox responses and vasomodulation, as well as targeting different neural cells. These positive effects of CO have an enormous potential as a therapeutic strategy for many cerebral diseases, as depicted in Figure 6 for stroke.

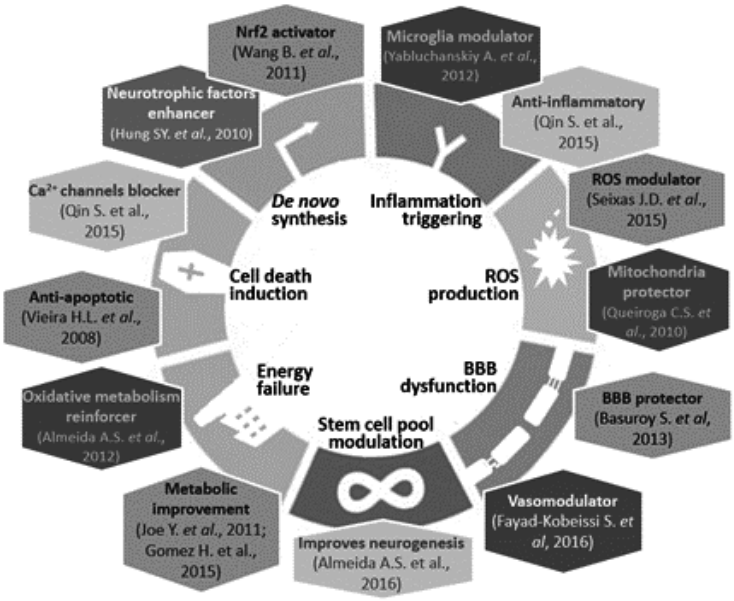

Figure 6 - Hallmarks of stroke and cytoprotective effects of CO.

3. Aims and scope of the thesis

The present work aims at contributing to a deeper understanding of the cellular pathways and effectors involved in cytoprotection by carbon monoxide (CO), focusing on astrocytes and on ischemic stroke scenarios. More specifically we investigated:

(i) **CO-induced transcriptome alterations in primary cultures of astrocytes.** This was analyzed using RNASeq (Chapter II.I). Furthermore, internal reference genes (Chapter II.II) and genes differentially expressed were validated and one candidate, FosB, was selected for protein and functional studies (Chapter II.III).

(ii) **The impact of a low CO dose at the cerebral vasculature in healthy animals.** The vascular responses to CO were studied in different brain regions, in male and female mice (Chapter II.IV).

(iii) **The anatomical, vascular, metabolic and functional role of CO in a rodent model of focal cerebral ischemia, when administered in a clinical relevant timing.** Several outcome readouts were assessed and integrated for further understanding the complex CO biology and its potential in stroke therapy (Chapter II.V).

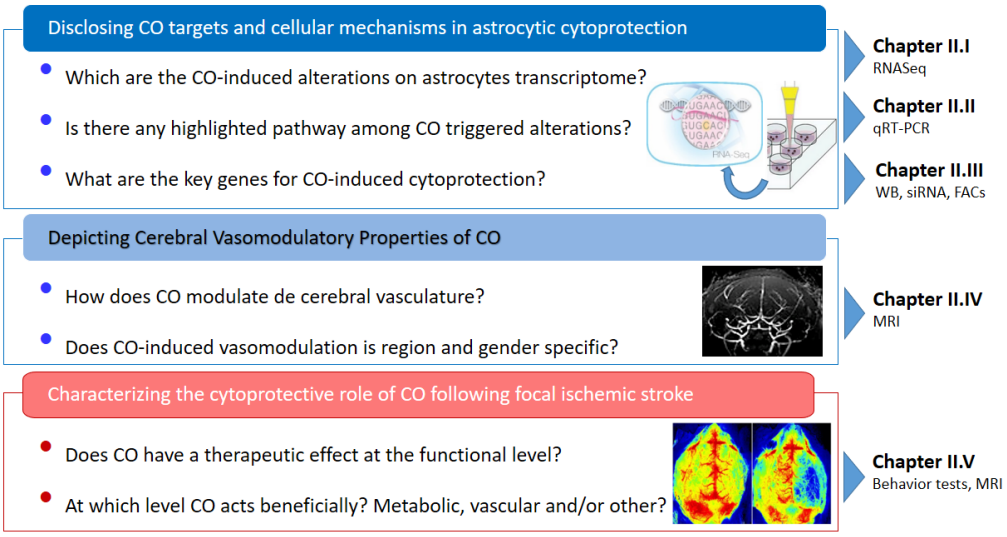

Figure 7 - Main questions addressed in this thesis and the techniques used. The column on the right shows the chapters where each question is discussed and the main method applied.

References

[1] V. Thijs, U. Grittner, M. Dichgans, C. Enzinger, F. Fazekas, A.K. Giese, C. Kessler, E. Kolodny, P. Kropp, P. Martus, B. Norrving, E.B. Ringelstein, P.M. Rothwell, R. Schmidt, C. Tanislav, T. Tatlisumak, B. Von Sarnowski, A. Rolfs, Family History in Young Patients with Stroke, Stroke. 46 (2015) 1975–1978. doi:10.1161/STROKEAHA.115.009341.

[2] A. Oliveira, A.J.R. Cabral, J.M. Mendes, M.R.O. Martins, P. Cabral, Spatiotemporal analysis of the relationship between socioeconomic factors and stroke in the Portuguese mainland population under 65 years old., Geospat. Health. 10 (2015) 365. doi:10.4081/gh.2015.365.

[3] L. De Wit, P. Theuns, E. Dejaeger, S. Devos, A.R. Gantenbein, E. Kerckhofs, B. Schuback, W. Schupp, K. Putman, Long-term impact of stroke on patients' health-related quality of life, Disabil. Rehabil. 8288 (2016) 1–6. doi:10.1080/09638288.2016.1200676.

[4] N.S. Association, No Title, Http://www.stroke.org/understand-Stroke/what-Stroke/ischemic-Stroke. (n.d.).

[5] U. Dirnagl, M. Endres, Found in translation: Preclinical stroke research predicts human pathophysiology, clinical phenotypes, and therapeutic outcomes, Stroke. 45 (2014) 1510–1518. doi:10.1161/STROKEAHA.113.004075.

[6] U. Dirnagl, Pathobiology of injury after stroke: The neurovascular unit and beyond, Ann. N. Y. Acad. Sci. 1268 (2012) 21–25. doi:10.1111/j.1749-6632.2012.06691.x.

[7] U. Dirnagl, C. Iadecola, M. a Moskowitz, Pathobiology of ischaemic stroke: an integrated view, Trends Neurosci. 22 (1999) 391–397. doi:10.1016/S0166-2236(99)01401-0.

[8] A. Moretti, F. Ferrari, R.F. Villa, Neuroprotection for ischaemic stroke: Current status and challenges, Pharmacol. Ther. 146 (2015) 23–34. doi:10.1016/j.pharmthera.2014.09.003.

[9] H. Chen, H. Yoshioka, G.S. Kim, J.E. Jung, N. Okami, H. Sakata, C.M. Maier, P. Narasimhan, C.E. Goeders, P.H. Chan, Oxidative stress in ischemic brain damage: mechanisms of cell death and potential molecular targets for neuroprotection., Antioxid. Redox Signal. 14 (2011) 1505–17. doi:10.1089/ars.2010.3576.

[10] B.R.S. Broughton, D.C. Reutens, C.G. Sobey, Apoptotic Mechanisms After Cerebral Ischemia, Stroke. 40 (2009) e331–e339. doi:10.1161/STROKEAHA.108.531632.

[11] D.R. Green, F. Llambi, Cell Death Signaling, Cold Spring Harb. Perspect. Biol. 7 (2015) a006080. doi:10.1101/cshperspect.a006080.

[12] Y. Kiraz, A. Adan, M. Kartal Yandim, Y. Baran, Major apoptotic mechanisms and genes involved in apoptosis, Tumor Biol. (2016) 1–16. doi:10.1007/s13277-016-5035-9.

[13] L. Galluzzi, K. Blomgren, G. Kroemer, Mitochondrial membrane permeabilization in neuronal injury, Nat. Rev. Neurosci. 10 (2009) 481–494. doi:10.1038/nrn2665.

[14] A.H. Gittis, D.J. Brasier, Astrocytes tell neurons when to listen up, Science (80-.). 349 (2015) 690–691. doi:10.1126/science.aad0678.

[15] R.C. Koehler, R.J. Roman, D.R. Harder, Astrocytes and the regulation of cerebral blood flow., Trends Neurosci. 32 (2009) 160–9. doi:10.1016/j.tins.2008.11.005.

[16] G. Barreto, R.E. White, Y. Ouyang, L. Xu, R.G. Giffard, Astrocytes: targets for neuroprotection in stroke., Cent. Nerv. Syst. Agents Med. Chem. 11 (2011) 164–73. http://www.pubmedcentral.nih.gov/articlerender.fcgi?artid=3167939&tool=pmcentrez&rendertype=abstract.

[17] S. Sultan, L. Li, J. Moss, F. Petrelli, F. Cassé, E. Gebara, J. Lopatar, F.W. Pfrieger, P. Bezzi, J. Bischofberger, N. Toni, Synaptic Integration of Adult-Born Hippocampal Neurons

Is Locally Controlled by Astrocytes, Neuron. 88 (2015) 957–972. doi:10.1016/j.neuron.2015.10.037.

[18] D.T. Theodosis, D.A. Poulain, S.H.R. Oliet, Activity-Dependent Structural and Functional Plasticity of Astrocyte-Neuron Interactions, Physiol. Rev. 88 (2008) 983–1008. doi:10.1152/physrev.00036.2007.

[19] A. Verkhratsky, R. Zorec, J.J. Rodriguez, V. Parpura, PATHOBIOLOGY OF NEURODEGENERATION: THE ROLE FOR ASTROGLIA., Opera Medica Physiol. 1 (2016) 13–22. doi:10.1016/j.jaac.2013.12.025.

[20] R. Martin, R. Bajo-Graneras, R. Moratalla, G. Perea, A. Araque, Circuit-specific signaling in astrocyte-neuron networks in basal ganglia pathways, Science (80-.). 349 (2015) 730–734. doi:10.1126/science.aaa7945.

[21] N.J. Allen, Astrocyte Regulation of Synaptic Behavior, Annu. Rev. Cell Dev. Biol. 30 (2014) 439–463. doi:10.1146/annurev-cellbio-100913-013053.

[22] N. Vardjan, A. Verkhratsky, R. Zorec, Pathologic Potential of Astrocytic Vesicle Traffic: New Targets to Treat Neurologic Diseases?, Cell Transplant. 24 (2015) 599–612. doi:10.3727/096368915X687750.

[23] I. Allaman, M. Bélanger, P.J. Magistretti, Astrocyte–neuron metabolic relationships: for better and for worse, Trends Neurosci. 34 (2011) 76–87. doi:10.1016/j.tins.2010.12.001.

[24] C. Finsterwald, P. Magistretti, S. Lengacher, Astrocytes: New Targets for the Treatment of Neurodegenerative Diseases, Curr. Pharm. Des. 21 (2015) 3570–3581. doi:10.2174/1381612821666150710144502.

[25] S.M. Rocha, A.C. Cristovão, F.L. Campos, C.P. Fonseca, G. Baltazar, Astrocyte-derived GDNF is a potent inhibitor of microglial activation., Neurobiol. Dis. 47 (2012) 407–15. doi:10.1016/j.nbd.2012.04.014.

[26] R.C. Turner, S.C. Dodson, C.L. Rosen, J.D. Huber, The science of cerebral ischemia and the quest for neuroprotection: navigating past failure to future success., J. Neurosurg. 118 (2013) 1072–85. doi:10.3171/2012.11.JNS12408.

[27] H.K. Eltzschig, T. Eckle, review Ischemia and reperfusion — from mechanism to translation, Nat. Med. 17 (2011) 1391–1401. doi:10.1038/nm.2507.

[28] B.M. Famakin, Y. Mou, K. Johnson, M. Spatz, J. Hallenbeck, A new role for downstream Toll-like receptor signaling in mediating immediate early gene expression during focal cerebral ischemia, J. Cereb. Blood Flow Metab. 34 (2014) 258–267. doi:10.1038/jcbfm.2013.182.

[29] H.-M. Huang, J.-Y. Yu, H.-C. Ou, K.C. Jeng, Effect of naloxone on the induction of immediately early genes following oxygen- and glucose-deprivation in PC12 cells, Neurosci. Lett. 438 (2008) 252–256. doi:10.1016/j.neulet.2008.04.036.

[30] M. Rickhag, M. Teilum, T. Wieloch, Rapid and long-term induction of effector immediate early genes (BDNF, Neuritin and Arc) in peri-infarct cortex and dentate gyrus after ischemic injury in rat brain, Brain Res. 1151 (2007) 203–210. doi:10.1016/j.brainres.2007.03.005.

[31] J. Fernandes, M. Vieira, L. Carreto, M. a S. Santos, C.B. Duarte, A.L. Carvalho, A.E. Santos, In vitro ischemia triggers a transcriptional response to down-regulate synaptic proteins in hippocampal neurons, PLoS One. 9 (2014) 6–9. doi:10.1371/journal.pone.0099958.

[32] M.G. Adamski, Y. Li, E. Wagner, H. Yu, C. Seales-Bailey, S.A. Soper, M. Murphy, A.E. Baird, Expression profile based gene clusters for ischemic stroke detection, Genomics.

104 (2014) 163–169. doi:10.1016/j.ygeno.2014.08.004.

[33] J. Hess, P. Angel, M. Schorpp-Kistner, AP-1 subunits: quarrel and harmony among siblings., J. Cell Sci. 117 (2004) 5965–5973. doi:10.1242/jcs.01589.

[34] Y. Kambe, A. Miyata, Mitochondrial c-Fos May Increase the Vulnerability of Neuro2a Cells to Cellular Stressors, J. Mol. Neurosci. 59 (2016) 106–112. doi:10.1007/s12031-015-0710-7.

[35] K. Ogita, M. Kubo, N. Nishiyama, M. Watanabe, R. Nagashima, Y. Yoneda, Enhanced binding activity of nuclear antioxidant-response element through possible formation of Nrf2/Fos-B complex after in vivo treatment with kainate in murine hippocampus., Neuropharmacology. 46 (2004) 580–9. doi:10.1016/j.neuropharm.2003.11.002.

[36] S.W. Rau, D.B. Dubal, M. Böttner, P.M. Wise, Estradiol differentially regulates c-Fos after focal cerebral ischemia., J. Neurosci. 23 (2003) 10487–10494. doi:23/33/10487 [pii].

[37] T. Yamashita, K. Abe, Recent Progress in Therapeutic Strategies for Ischemic Stroke, Cell Transplant. 25 (2016) 893–898. doi:10.3727/096368916X690548.

[38] T. Herdegen, J.D. Leah, Inducible and constitutive transcription factors in the mammalian nervous system: control of gene expression by Jun, Fos and Krox, and CREB/ATF proteins., Brain Res. Brain Res. Rev. 28 (1998) 370–490. http://www.ncbi.nlm.nih.gov/pubmed/9858769.

[39] K. Milde-Langosch, The Fos family of transcription factors and their role in tumourigenesis, Eur. J. Cancer. 41 (2005) 2449–2461. doi:10.1016/j.ejca.2005.08.008.

[40] E.J. Nestler, Transcriptional mechanisms of drug addiction., Clin. Psychopharmacol. Neurosci. 10 (2012) 136–43. doi:10.9758/cpn.2012.10.3.136.

[41] N. Hiroi, G.J. Marek, J.R. Brown, H. Ye, F. Saudou, V. a Vaidya, R.S. Duman, M.E. Greenberg, E.J. Nestler, Essential role of the fosB gene in molecular, cellular, and behavioral actions of chronic electroconvulsive seizures., J. Neurosci. 18 (1998) 6952–6962.

[42] M. Zerial, L. Toschi, R.P. Ryseck, M. Schuermann, R. Müller, R. Bravo, The product of a novel growth factor activated gene, fos B, interacts with JUN proteins enhancing their DNA binding activity., EMBO J. 8 (1989) 805–13. http://www.ncbi.nlm.nih.gov/pubmed/2498083.

[43] T.L. Carle, Y.N. Ohnishi, Y.H. Ohnishi, I.N. Alibhai, M.B. Wilkinson, A. Kumar, E.J. Nestler, Proteasome-dependent and -independent mechanisms for FosB destabilization: identification of FosB degron domains and implications for ΔFosB stability, Eur. J. Neurosci. 25 (2007) 3009–3019. doi:10.1111/j.1460-9568.2007.05575.x.

[44] I.N. Alibhai, T. a. Green, J. a. Potashkin, E.J. Nestler, Regulation of fosB and ΔfosB mRNA expression: In vivo and in vitro studies, Brain Res. 1143 (2007) 22–33. doi:10.1016/j.brainres.2007.01.069.

[45] T.L. Carle, M.E.G. Phillips, G.D.E. Martino, L. Monteggia, E.J. Nestler, Biochemical Characterization of Delta Fosb, Texas Southwestern Medical Canter at Dallas, 2006.

[46] N. Yutsudo, T. Kamada, K. Kajitani, H. Nomaru, A. Katogi, Y.H. Ohnishi, Y.N. Ohnishi, K. Takase, K. Sakumi, H. Shigeto, Y. Nakabeppu, fosB-Null Mice Display Impaired Adult Hippocampal Neurogenesis and Spontaneous Epilepsy with Depressive Behavior, Neuropsychopharmacology. 38 (2013) 895–906. doi:10.1038/npp.2012.260.

[47] Y. Nakabeppu, D. Nathans, A naturally occurring truncated form of FosB that inhibits Fos/Jun transcriptional activity., Cell. 64 (1991) 751–759. doi:10.1016/0092-8674(91)90504-R.

[48] E. Jindal, S.K. Goswami, In cardiac myoblasts, cellular redox regulates FosB and Fra-1 through multiple cis-regulatory modules, Free Radic. Biol. Med. 51 (2011) 1512–1521. doi:10.1016/j.freeradbiomed.2011.07.008.

[49] T.L. Butler, K.R. Pennypacker, Temporal and regional expression of Fos-related proteins in response to ischemic injury., Brain Res. Bull. 63 (2004) 65–73. doi:10.1016/j.brainresbull.2003.12.005.

[50] S. Al-Noori, N.M. Sanders, G.J. Taborsky, C.W. Wilkinson, A. Zavosh, C. West, C.M. Sanders, D.P. Figlewicz, Recurrent hypoglycemia alters hypothalamic expression of the regulatory proteins FosB and synaptophysin., Am. J. Physiol. Regul. Integr. Comp. Physiol. 295 (2008) R1446–R1454. doi:10.1152/ajpregu.90511.2008.

[51] P.S. Lazo, K. Dorfman, T. Noguchi, M.G. Mattéi, R. Bravo, Structure and mapping of the fosB gene. FosB downregulates the activity of the fosB promoter., Nucleic Acids Res. 20 (1992) 343–50. http://www.ncbi.nlm.nih.gov/pubmed/1741260.

[52] K.O. Kuroda, V.G. Ornthanalai, T. Kato, N.P. Murphy, FosB null mutant mice show enhanced methamphetamine neurotoxicity: potential involvement of FosB in intracellular feedback signaling and astroglial function., Neuropsychopharmacology. 35 (2010) 641–55. doi:10.1038/npp.2009.169.

[53] V. Vialou, A. Robison, FosB in brain reward circuits mediates resilience to stress and antidepressant responses, Nat. …. 13 (2010) 745–752. doi:10.1038/nn.2551.

[54] K.O. Kuroda, M.J. Meaney, N. Uetani, T. Kato, Neurobehavioral basis of the impaired nurturing in mice lacking the immediate early gene FosB, Brain Res. 1211 (2008) 57–71. doi:10.1016/j.brainres.2008.02.100.

[55] S.P.M. Reddy, B.T. Mossman, Role and regulation of activator protein-1 in toxicant-induced responses of the lung, Am J Physiol Lung Cell Mol Physiol. 283 (2002) 1161–1178. doi:10.1152/ ajplung.00140.2002.

[56] M.A. Alfonso-Jaume, M.R. Bergman, R. Mahimkar, S. Cheng, Z.Q. Jin, J.S. Karliner, D.H. Lovett, Cardiac ischemia-reperfusion injury induces matrix metalloproteinase-2 expression through the AP-1 components FosB and JunB., Am. J. Physiol. Heart Circ. Physiol. 291 (2006) H1838-46. doi:10.1152/ajpheart.00026.2006.

[57] M.L. Gavala, L.M. Hill, L.Y. Lenertz, M.R. Karta, P.J. Bertics, Activation of the transcription factor FosB/activating protein-1 (AP-1) is a prominent downstream signal of the extracellular nucleotide receptor P2RX7 in monocytic and osteoblastic cells, J. Biol. Chem. 285 (2010) 34288–34298. doi:10.1074/jbc.M110.142091.

[58] Y. Zhang, K. Chen, S.A. Sloan, M.L. Bennett, A.R. Scholze, S. O'Keeffe, H.P. Phatnani, P. Guarnieri, C. Caneda, N. Ruderisch, S. Deng, S.A. Liddelow, C. Zhang, R. Daneman, T. Maniatis, B.A. Barres, J.Q. Wu, An RNA-sequencing transcriptome and splicing database of glia, neurons, and vascular cells of the cerebral cortex, J. Neurosci. 34 (2014) 11929–11947. doi:10.1523/JNEUROSCI.1860-14.2014.

[59] E.J. Nestler, M.B. Kelz, J. Chen, ΔFosB: a molecular mediator of long-term neural and behavioral plasticity, Brain Res. 835 (1999) 10–17. doi:10.1016/S0006-8993(98)01191-3.

[60] V. Vialou, M. Thibault, S. Kaska, S. Cooper, P. Gajewski, A. Eagle, M. Mazei-Robison, E.J. Nestler, A.J. Robison, Differential induction of FosB isoforms throughout the brain by fluoxetine and chronic stress, Neuropharmacology. 99 (2015) 28–37. doi:10.1016/j.neuropharm.2015.07.005.

[61] K. Lidwell, R. Griffiths, Possible role for the FosB/JunD AP-1 transcription factor complex in glutamate-mediated excitotoxicity in cultured cerebellar granule cells, J. Neurosci. Res. 62 (2000) 427–439. doi:10.1002/1097-4547(20001101)62:3<427::AID-JNR13>3.0.CO;2-

O.

[62] K. Kumar, X. Wu, a. T. Evans, Expression of c-fos and fos-B proteins following transient forebrain ischemia: Effect of hypothermia, Mol. Brain Res. 42 (1996) 337–343. doi:10.1016/S0169-328X(96)00181-7.

[63] V. Kormos, L. Gáspár, L.Á. Kovács, J. Farkas, T. Gaszner, V. Csernus, A. Balogh, H. Hashimoto, D. Reglődi, Z. Helyes, B. Gaszner, Reduced response to chronic mild stress in PACAP mutant mice is associated with blunted FosB expression in limbic forebrain and brainstem centers, Neuroscience. 330 (2016) 335–358. doi:10.1016/j.neuroscience.2016.06.004.

[64] D. Phillips, E. Choleris, K.S.J. Ervin, C. Fureix, L. Harper, K. Reynolds, L. Niel, G.J. Mason, Cage-induced stereotypic behaviour in laboratory mice covaries with nucleus accumbens FosB/??FosB expression, Behav. Brain Res. 301 (2016) 238–242. doi:10.1016/j.bbr.2015.12.035.

[65] Q. Zhang, Q. Liu, T. Li, Y. Liu, L. Wang, Z. Zhang, H. Liu, M. Hu, Y. Qiao, H. Niu, Expression and colocalization of NMDA receptor and FosB/ΔFosB in sensitive brain regions in rats after chronic morphine exposure, Neurosci. Lett. 614 (2016) 70–76. doi:10.1016/j.neulet.2015.11.052.

[66] E.F. Wagner, AP-1 – Introductory remarks, Oncogene. 20 (2001) 2334–2335. doi:10.1038/sj.onc.1204416.

[67] M. Skinner, S. Qu, C. Moore, R. Wisdom, Transcriptional activation and transformation by FosB protein require phosphorylation of the carboxyl-terminal activation domain, Mol Cell Biol. 17 (1997) 2372–2380. http://www.ncbi.nlm.nih.gov/entrez/query.fcgi?cmd=Retrieve&db=PubMed&dopt=Citation&list_uids=9111306.

[68] B. Kaminska, G. Mosieniak, M. Gierdalski, M. Kossut, L. Kaczmarck, Elevated AP-1 transcription factor DNA binding activity at the onset of functional plasticity during development of rat sensory cortical areas., Brain Res. Mol. Brain Res. 33 (1995) 295–304. http://www.ncbi.nlm.nih.gov/pubmed/8750889.

[69] J.W. Edmunds, MAP kinases as structural adaptors and enzymatic activators in transcription complexes, J. Cell Sci. 117 (2004) 3715–3723. doi:10.1242/jcs.01346.

[70] J.-G. Lehoux, A. Fleury, L. Ducharme, The Acute and Chronic Effects of Adrenocorticotropin on the Levels of Messenger Ribonucleic Acid and Protein of Steroidogenic Enzymes in Rat Adrenal in Vivo 1, Endocrinology. 139 (1998) 3913–3922. doi:10.1210/endo.139.9.6196.

[71] M. Benkoussa, C. Brand, M.-H. Delmotte, P. Formstecher, P. Lefebvre, Retinoic Acid Receptors Inhibit AP1 Activation by Regulating Extracellular Signal-Regulated Kinase and CBP Recruitment to an AP1-Responsive Promoter, Mol. Cell. Biol. 22 (2002) 4522–4534. doi:10.1128/MCB.22.13.4522-4534.2002.

[72] D. Inoue, S. Kido, T. Matsumoto, Transcriptional Induction of FosB /Δ FosB Gene by Mechanical Stress in Osteoblasts, J. Biol. Chem. 279 (2004) 49795–49803. doi:10.1074/jbc.M404096200.

[73] H.-J. Byun, I.-K. Hong, E. Kim, Y.-J. Jin, D.-I. Jeoung, J.-H. Hahn, Y.-M. Kim, S.H. Park, H. Lee, A Splice Variant of CD99 Increases Motility and MMP-9 Expression of Human Breast Cancer Cells through the AKT-, ERK-, and JNK-dependent AP-1 Activation Signaling Pathways, J. Biol. Chem. 281 (2006) 34833–34847. doi:10.1074/jbc.M605483200.

[74] D.G. Romero, S. Rilli, M.W. Plonczynski, L.L. Yanes, M.Y. Zhou, E.P. Gomez-Sanchez,

C.E. Gomez-Sanchez, Adrenal transcription regulatory genes modulated by angiotensin II and their role in steroidogenesis, Physiol. Genomics. 30 (2007) 26–34. doi:10.1152/physiolgenomics.00187.2006.

[75] B. Li, T. Du, H. Li, L. Gu, H. Zhang, J. Huang, L. Hertz, L. Peng, Signalling pathways for transactivation by dexmedetomidine of epidermal growth factor receptors in astrocytes and its paracrine effect on neurons., Br. J. Pharmacol. 154 (2008) 191–203. doi:10.1038/bjp.2008.58.

[76] E. Chaum, J. Yin, H. Yang, F. Thomas, J.C. Lang, Quantitative AP-1 gene regulation by oxidative stress in the human retinal pigment epithelium, J. Cell. Biochem. 108 (2009) 1280–1291. doi:10.1002/jcb.22358.

[77] L.Y. Lenertz, M.L. Gavala, L.M. Hill, P.J. Bertics, Cell signaling via the P2X7 nucleotide receptor: linkage to ROS production, gene transcription, and receptor trafficking, Purinergic Signal. 5 (2009) 175–187. doi:10.1007/s11302-009-9133-7.

[78] L.Y. Lenertz, M.L. Gavala, Y. Zhu, P.J. Bertics, Transcriptional Control Mechanisms Associated with the Nucleotide Receptor P2X7, a Critical Regulator of Immunologic, Osteogenic and Neurologic Functions, Immunol. Res. 50 (2011) 22–38. doi:10.1007/s12026-011-8203-4.Transcriptional.

[79] A. Ramachandran, E.M. Gong, K. Pelton, S.A. Ranpura, M. Mulone, A. Seth, P. Gomez, R.M. Adam, FosB Regulates Stretch-Induced Expression of Extracellular Matrix Proteins in Smooth Muscle, Am. J. Pathol. 179 (2011) 2977–2989. doi:10.1016/j.ajpath.2011.08.034.

[80] J.B. Tee, Y. Choi, A. Dnyanmote, M. Decambre, C. Ito, K.T. Bush, S.K. Nigam, GDNF-independent ureteric budding: role of PI3K-independent activation of AKT and FOSB/JUN/AP-1 signaling, Biol. Open. 2 (2013) 952–959. doi:10.1242/bio.20135595.

[81] L.E. Wickert, J.B. Blanchette, N. V. Waldschmidt, P.J. Bertics, J.M. Denu, L.C. Denlinger, L.Y. Lenertz, The C-Terminus of Human Nucleotide Receptor P2X7 Is Critical for Receptor Oligomerization and N-Linked Glycosylation, PLoS One. 8 (2013). doi:10.1371/journal.pone.0063789.

[82] E. Del-Bel, F.E. Padovan-Neto, M. Bortolanza, V. Tumas, A.S. Aguiar, R. Raisman-Vozari, R.D. Prediger, Nitric oxide, a new player in L-DOPA-induced dyskinesia?, Front. Biosci. (Elite Ed). 7 (2015) 168–92. http://www.ncbi.nlm.nih.gov/pubmed/25553372.

[83] I. Ruiz-DeDiego, B. Mellstrom, M. Vallejo, J.R. Naranjo, R. Moratalla, Activation of DREAM (Downstream Regulatory Element Antagonistic Modulator), a Calcium-Binding Protein, Reduces L-DOPA-Induced Dyskinesias in Mice, Biol. Psychiatry. 77 (2015) 95–105. doi:10.1016/j.biopsych.2014.03.023.

[84] R. Weijer, M. Broekgaarden, R.F. van Golen, E. Bulle, E. Nieuwenhuis, A. Jongejan, P.D. Moerland, A.H.C. van Kampen, T.M. van Gulik, M. Heger, Low-power photodynamic therapy induces survival signaling in perihilar cholangiocarcinoma cells, BMC Cancer. 15 (2015) 1014. doi:10.1186/s12885-015-1994-2.

[85] X. Cao, D. Hou, L. Wang, S. Li, S. Sun, Q. Ping, Y. Xu, Effects and molecular mechanism of chitosan-coated levodopa nanoliposomes on behavior of dyskinesia rats, Biol. Res. 49 (2016) 32. doi:10.1186/s40659-016-0093-4.

[86] C. a Godman, K.P. Chheda, L.E. Hightower, G. Perdrizet, D.-G. Shin, C. Giardina, Hyperbaric oxygen induces a cytoprotective and angiogenic response in human microvascular endothelial cells, Cell Stress Chaperones. 15 (2010) 431–442. doi:10.1007/s12192-009-0159-0.

[87] T.H. Saito, S. Uda, T. Tsuchiya, Y. Ozaki, S. Kuroda, Temporal Decoding of MAP Kinase

and CREB Phosphorylation by Selective Immediate Early Gene Expression, PLoS One. 8 (2013) e57037. doi:10.1371/journal.pone.0057037.

[88] N. Yukimasa, K. Isobe, H. Nagai, Y. Takuwa, T. Nakai, Successive occupancy by immediate early transcriptional factors of the tyrosine hydroxylase gene TRE and CRE sites in PACAP-stimulated PC12 pheochromocytoma cells, Neuropeptides. 33 (1999) 475–482. doi:10.1054/npep.1999.0765.

[89] Y. Chen, B. Samal, C.R. Hamelink, C.C. Xiang, Y. Chen, M. Chen, D. Vaudry, M.J. Brownstein, J.M. Hallenbeck, L.E. Eiden, Neuroprotection by endogenous and exogenous PACAP following stroke, Regul. Pept. 137 (2006) 4–19. doi:10.1016/j.regpep.2006.06.016.

[90] I.Y. Elgendy, A.N. Mahmoud, H. Mansoor, M.K. Mojadidi, A.A. Bavry, Evolution of acute ischemic stroke therapy from lysis to thrombectomy: Similar or different to acute myocardial infarction?, Int. J. Cardiol. 222 (2016) 441–447. doi:10.1016/j.ijcard.2016.07.251.

[91] B.S.P. Sean I. Savitz, B.S.P. Marc Fisher, Prophylactic Neuroprotection, Curr. Drug Targets. 8 (2007) 846–849. doi:10.2174/138945007781077382.

[92] S. V. Narayanan, K.R. Dave, M.A. Perez-Pinzon, Ischemic preconditioning and clinical scenarios, Curr. Opin. Neurol. 26 (2013) 1–7. doi:10.1097/WCO.0b013e32835bf200.

[93] J.T. Neumann, J.W. Thompson, A.P. Raval, C.H. Cohan, K.B. Koronowski, M.A. Perez-Pinzon, Increased BDNF protein expression after ischemic or PKC epsilon preconditioning promotes electrophysiologic changes that lead to neuroprotection, J. Cereb. Blood Flow Metab. 35 (2015) 121–130. doi:10.1038/jcbfm.2014.185.

[94] Y. Wang, C. Reis, R. Applegate, G. Stier, R. Martin, J.H. Zhang, Ischemic conditioning-induced endogenous brain protection: Applications pre-, per- or post-stroke, Exp. Neurol. 272 (2015) 26–40. doi:10.1016/j.expneurol.2015.04.009.

[95] J.A. Desai, E.E. Smith, Prenotification and Other Factors Involved in Rapid tPA Administration, Curr. Atheroscler. Rep. 15 (2013) 337. doi:10.1007/s11883-013-0337-5.

[96] A. Szijártó, Z. Czigány, Z. Turóczi, L. Harsányi, Remote ischemic perconditioning—a simple, low-risk method to decrease ischemic reperfusion injury: Models, protocols and mechanistic background. A review, J. Surg. Res. 178 (2012) 797–806. doi:10.1016/j.jss.2012.06.067.

[97] P.M. Holloway, F.N.E. Gavins, Modeling Ischemic Stroke In Vitro: Status Quo and Future Perspectives, Stroke. (2016) STROKEAHA.115.011932. doi:10.1161/STROKEAHA.115.011932.

[98] M. Mehra, N. Henninger, J.A. Hirsch, J. Chueh, A.K. Wakhloo, M.J. Gounis, Preclinical acute ischemic stroke modeling, J. Neurointerv. Surg. 4 (2012) 307–313. doi:10.1136/neurintsurg-2011-010101.

[99] J.L. Werth, T.S. Park, D.L. Silbergeld, S.M. Rothman, Excitotoxic swelling occurs in oxygen and glucose deprived human cortical slices., Brain Res. 782 (1998) 248–54. http://www.ncbi.nlm.nih.gov/pubmed/9519270.

[100] M. Gumbleton, K.L. Audus, Progress and limitations in the use of in vitro cell cultures to serve as a permeability screen for the blood-brain barrier., J. Pharm. Sci. 90 (2001) 1681–98. http://www.ncbi.nlm.nih.gov/pubmed/11745727.

[101] A. Asthana, W.S. Kisaalita, Biophysical microenvironment and 3D culture physiological relevance, Drug Discov. Today. 18 (2013) 533–540. doi:10.1016/j.drudis.2012.12.005.

[102] Q. Li, X. Han, J. Wang, Organotypic Hippocampal Slices as Models for Stroke and

Traumatic Brain Injury., Mol. Neurobiol. 53 (2016) 4226–37. doi:10.1007/s12035-015-9362-4.

[103] V.A. Sardão, P.J. Oliveira, J. Holy, C.R. Oliveira, K.B. Wallace, Vital imaging of H9c2 myoblasts exposed to tert-butylhydroperoxide – characterization of morphological features of cell death, BMC Cell Biol. 8 (2007) 11. doi:10.1186/1471-2121-8-11.

[104] R.H. Hughes, V.A. Silva, I. Ahmed, D.I. Shreiber, B. Morrison, Neuroprotection by genipin against reactive oxygen and reactive nitrogen species-mediated injury in organotypic hippocampal slice cultures, Brain Res. 1543 (2014) 308–314. doi:10.1016/j.brainres.2013.11.020.

[105] G.A. Kurian, B. Pemaih, Standardization of in vitro Cell-based Model for Renal Ischemia and Reperfusion Injury., Indian J. Pharm. Sci. 76 (2014) 348–53. http://www.ncbi.nlm.nih.gov/pubmed/25284933.

[106] J. von Engelhardt, I. Coserea, V. Pawlak, E.C. Fuchs, G. Köhr, P.H. Seeburg, H. Monyer, Excitotoxicity in vitro by NR2A- and NR2B-containing NMDA receptors, Neuropharmacology. 53 (2007) 10–17. doi:10.1016/j.neuropharm.2007.04.015.

[107] M.P. Goldberg, D.W. Choi, Combined oxygen and glucose deprivation in cortical cell culture: calcium-dependent and calcium-independent mechanisms of neuronal injury., J. Neurosci. 13 (1993) 3510–24. http://www.ncbi.nlm.nih.gov/pubmed/8101871.

[108] J. Kofler, K. Hattori, M. Sawada, A.C. DeVries, L.J. Martin, P.D. Hurn, R.J. Traystman, Histopathological and behavioral characterization of a novel model of cardiac arrest and cardiopulmonary resuscitation in mice, J. Neurosci. Methods. 136 (2004) 33–44. doi:10.1016/j.jneumeth.2003.12.024.

[109] A. Durukan, T. Tatlisumak, Acute ischemic stroke: Overview of major experimental rodent models, pathophysiology, and therapy of focal cerebral ischemia, Pharmacol. Biochem. Behav. 87 (2007) 179–197. doi:10.1016/j.pbb.2007.04.015.

[110] R.J. Traystman, Animal models of focal and global cerebral ischemia., ILAR J. 44 (2003) 85–95. http://www.ncbi.nlm.nih.gov/pubmed/12652003.

[111] K.-A. Hossmann, The two pathophysiologies of focal brain ischemia: implications for translational stroke research, J. Cereb. Blood Flow Metab. 32 (2012) 1310–1316. doi:10.1038/jcbfm.2011.186.

[112] A. Durukan, T. Tatlisumak, Ischemic Stroke in Mice and Rats, in: K. DiPetrillo (Ed.), Humana Press, Totowa, NJ, 2009: pp. 95–114. doi:10.1007/978-1-60761-247-6_6.

[113] A. Kumar, Aakriti, V. Gupta, A review on animal models of stroke: An update, Brain Res. Bull. 122 (2016) 35–44. doi:10.1016/j.brainresbull.2016.02.016.

[114] J. Bogousslavsky, G. Van Melle, F. Regli, The Lausanne Stroke Registry: analysis of 1,000 consecutive patients with first stroke., Stroke. 19 (1988) 1083–92. http://www.ncbi.nlm.nih.gov/pubmed/3413804.

[115] A. Tamura, D.I. Graham, J. McCulloch, G.M. Teasdale, Focal Cerebral Ischaemia in the Rat: 1. Description of Technique and Early Neuropathological Consequences Following Middle Cerebral Artery Occlusion, J. Cereb. Blood Flow Metab. 1 (1981) 53–60. doi:10.1038/jcbfm.1981.6.

[116] F. Liu, L.D. McCullough, Middle cerebral artery occlusion model in rodents: methods and potential pitfalls., J. Biomed. Biotechnol. 2011 (2011) 464701. doi:10.1155/2011/464701.

[117] P.S. Herson, R.J. Traystman, Animal models of stroke: translational potential at present and in 2050, Future Neurol. 9 (2014) 541–551. doi:10.2217/fnl.14.44.

[118] E.Z. Longa, P.R. Weinstein, S. Carlson, R. Cummins, Reversible middle cerebral artery occlusion without craniectomy in rats., Stroke. 20 (1989) 84–91. http://www.ncbi.nlm.nih.gov/pubmed/2643202.

[119] F. Fluri, M. Schuhmann, C. Kleinschnitz, Animal models of ischemic stroke and their application in clinical research, Drug Des. Devel. Ther. 9 (2015) 3445. doi:10.2147/DDDT.S56071.

[120] L. Wu, L. Xu, X. Xu, X. Fan, Y. Xie, L. Yang, W. Lan, J. Zhu, G. Xu, J. Dai, Y. Jiang, X. Liu, Keep warm and get success: the role of postischemic temperature in the mouse middle cerebral artery occlusion model., Brain Res. Bull. 101 (2014) 12–7. doi:10.1016/j.brainresbull.2013.12.003.

[121] H. Abrahám, A. Somogyvári-Vigh, J.L. Maderdrut, S. Vigh, A. Arimura, Filament size influences temperature changes and brain damage following middle cerebral artery occlusion in rats., Exp. Brain Res. 142 (2002) 131–8. doi:10.1007/s00221-001-0909-4.

[122] S. Liu, G. Zhen, B.P. Meloni, K. Campbell, H.R. Winn, RODENT STROKE MODEL GUIDELINES FOR PRECLINICAL STROKE TRIALS (1ST EDITION)., J. Exp. Stroke Transl. Med. 2 (2009) 2–27. http://www.ncbi.nlm.nih.gov/pubmed/20369026.

[123] E. Pedrono, A. Durukan, D. Strbian, I. Marinkovic, S. Shekhar, M. Pitkonen, U. Abo-Ramadan, T. Tatlisumak, An optimized mouse model for transient ischemic attack., J. Neuropathol. Exp. Neurol. 69 (2010) 188–95. doi:10.1097/NEN.0b013e3181cd331c.

[124] G.C. Jickling, F.R. Sharp, Improving the translation of animal ischemic stroke studies to humans, Metab. Brain Dis. 30 (2015) 461–467. doi:10.1007/s11011-014-9499-2.

[125] T.N. Lin, Y.Y. He, G. Wu, M. Khan, C.Y. Hsu, Effect of brain edema on infarct volume in a focal cerebral ischemia model in rats., Stroke. 24 (1993) 117–21. http://www.ncbi.nlm.nih.gov/pubmed/8418534.

[126] J.A. Stokum, V. Gerzanich, J.M. Simard, Molecular pathophysiology of cerebral edema., J. Cereb. Blood Flow Metab. 36 (2016) 513–38. doi:10.1177/0271678X15617172.

[127] G. Zaharchuk, H. Hara, P.L. Huang, M.C. Fishman, M.A. Moskowitz, B.G. Jenkins, B.R. Rosen, Neuronal nitric oxide synthase mutant mice show smaller infarcts and attenuated apparent diffusion coefficient changes in the peri-infarct zone during focal cerebral ischemia., Magn. Reson. Med. 37 (1997) 170–5. http://www.ncbi.nlm.nih.gov/pubmed/9001139.

[128] X. Milidonis, I. Marshall, M.R. Macleod, E.S. Sena, Magnetic Resonance Imaging in Experimental Stroke and Comparison With Histology, Stroke. 46 (2015) 843–851. doi:10.1161/STROKEAHA.114.007560.

[129] M. Balkaya, J.M. Kröber, A. Rex, M. Endres, Assessing post-stroke behavior in mouse models of focal ischemia., J. Cereb. Blood Flow Metab. 33 (2013) 330–8. doi:10.1038/jcbfm.2012.185.

[130] A.J. Hunter, J. Hatcher, D. Virley, P. Nelson, E. Irving, S.J. Hadingham, A.A. Parsons, Functional assessments in mice and rats after focal stroke., Neuropharmacology. 39 (2000) 806–16. http://www.ncbi.nlm.nih.gov/pubmed/10699446.

[131] M.P. Kahle, G.J. Bix, Successfully Climbing the “STAIRs”: Surmounting Failed Translation of Experimental Ischemic Stroke Treatments, Stroke Res. Treat. 2012 (2012) 1–8. doi:10.1155/2012/374098.

[132] L. Wu, R. Wang, Carbon Monoxide : Endogenous Production , Physiological Functions , and Pharmacological Applications, Pharmacol. Rev. 57 (2005) 585–630. doi:10.1124/pr.57.4.3.585.

[133] H. Vreman, R. Wong, D. Stevenson, Sources, Sinks, and Measurement of Carbon Monoxide, in: Carbon Monoxide Cardiovasc. Funct., CRC Press, 2001: pp. 273–307. doi:10.1201/9781420041019.ch15.

[134] J.F. Ewing, V.S. Raju, M.D. Maines, Induction of heart heme oxygenase-1 (HSP32) by hyperthermia: possible role in stress-mediated elevation of cyclic 3':5'-guanosine monophosphate., J. Pharmacol. Exp. Ther. 271 (1994) 408–14. http://www.ncbi.nlm.nih.gov/pubmed/7525927.

[135] A. Agarwal, S. Bolisetty, Adaptive responses to tissue injury: role of heme oxygenase-1., Trans. Am. Clin. Climatol. Assoc. 124 (2013) 111–22. http://www.pubmedcentral.nih.gov/articlerender.fcgi?artid=3715920&tool=pmcentrez&rendertype=abstract.

[136] N.G. Abraham, A. Kappas, Pharmacological and Clinical Aspects of Heme Oxygenase, Pharmacol. Rev. 60 (2008). doi:10.1124/pr.107.07104.79.

[137] B. Wegiel, D.W. Hanto, L.E. Otterbein, The social network of carbon monoxide in medicine., Trends Mol. Med. 19 (2013) 3–11. doi:10.1016/j.molmed.2012.10.001.

[138] C.W. Leffler, H. Parfenova, J.H. Jaggar, Carbon monoxide as an endogenous vascular modulator, AJP Hear. Circ. Physiol. 301 (2011) H1–H11. doi:10.1152/ajpheart.00230.2011.

[139] H.L.A. Vieira, C.S.F. Queiroga, P.M. Alves, Pre-conditioning induced by carbon monoxide provides neuronal protection against apoptosis, J. Neurochem. 107 (2008) 375–384. doi:10.1111/j.1471-4159.2008.05610.x.

[140] S.W. Ryter, A.M.K. Choi, Targeting heme oxygenase-1 and carbon monoxide for therapeutic modulation of inflammation, Transl. Res. 167 (2016) 7–34. doi:10.1016/j.trsl.2015.06.011.

[141] A.S. Almeida, C. Figueiredo-Pereira, H.L.A. Vieira, Carbon monoxide and mitochondria - modulation of cell metabolism, redox response and cell death, Front. Physiol. 6 (2015) 1–6. doi:10.3389/fphys.2015.00033.

[142] C.A. Piantadosi, Biological chemistry of carbon monoxide., Antioxid. Redox Signal. 4 (2002) 259–70. doi:10.1089/152308602753666316.

[143] L. Rochette, Y. Cottin, M. Zeller, C. Vergely, Carbon monoxide: Mechanisms of action and potential clinical implications, Pharmacol. Ther. 137 (2013) 133–152. doi:10.1016/j.pharmthera.2012.09.007.

[144] T. Shimizu, D. Huang, F. Yan, M. Stranava, M. Bartosova, V. Fojtíková, M. Martínková, Gaseous O 2 , NO, and CO in Signal Transduction: Structure and Function Relationships of Heme-Based Gas Sensors and Heme-Redox Sensors, Chem. Rev. 115 (2015) 6491–6533. doi:10.1021/acs.chemrev.5b00018.

[145] M.L. Bleecker, Carbon monoxide intoxication., Handb. Clin. Neurol. 131 (2015) 191–203. doi:10.1016/B978-0-444-62627-1.00024-X.

[146] B. Olas, Carbon monoxide is not always a poison gas for human organism: Physiological and pharmacological features of CO, Chem. Biol. Interact. 222 (2014) 37–43. doi:10.1016/j.cbi.2014.08.005.

[147] R. Motterlini, L.E. Otterbein, The therapeutic potential of carbon monoxide., Nat. Rev. Drug Discov. 9 (2010) 728–43. doi:10.1038/nrd3228.

[148] K.K. Elbirt, H.L. Bonkovsky, Heme oxygenase: recent advances in understanding its regulation and role., Proc. Assoc. Am. Physicians. 111 (1999) 438–47. http://www.ncbi.nlm.nih.gov/pubmed/10519165.

[149] S.R. Vincent, S. Das, M.D. Maines, Brain heme oxygenase isoenzymes and nitric oxide synthase are co-localized in select neurons., Neuroscience. 63 (1994) 223–31. http://www.ncbi.nlm.nih.gov/pubmed/7534881.

[150] V. Calabrese, G. Scapagnini, A. Ravagna, R.G. Fariello, A.M. Giuffrida Stella, N.G. Abraham, Regional distribution of heme oxygenase, HSP70, and glutathione in brain: Relevance for endogenous oxidant/antioxidant balance and stress tolerance, J. Neurosci. Res. 68 (2002) 65–75. doi:10.1002/jnr.10177.

[151] G. Scapagnini, V. D'Agata, V. Calabrese, A. Pascale, C. Colombrita, D. Alkon, S. Cavallaro, Gene expression profiles of heme oxygenase isoforms in the rat brain, Brain Res. 954 (2002) 51–59. doi:10.1016/S0006-8993(02)03338-3.

[152] G. Wang, D. Han, Y. Zhang, X. Xie, Y. Wu, S. Li, M. Li, PERSPECTIVE A novel hypothesis : up-regulation of HO-1 by activation of PPAR γ inhibits HMGB1-RAGE signaling pathway and ameliorates the development of ALI / ARDS, (n.d.). doi:10.3978/j.issn.2072-1439.2013.08.69.

[153] A.A. Chora, P. Fontoura, A. Cunha, T.F. Pais, S. Cardoso, P.P. Ho, L.Y. Lee, R.A. Sobel, L. Steinman, M.P. Soares, Heme oxygenase-1 and carbon monoxide suppress autoimmune neuroinflammation., J. Clin. Invest. 117 (2007) 438–47. doi:10.1172/JCI28844.

[154] J. Wang, S. Doré, Heme oxygenase 2 deficiency increases brain swelling and inflammation after intracerebral hemorrhage, Neuroscience. 155 (2008) 1133–1141. doi:10.1016/j.neuroscience.2008.07.004.

[155] J. Chen, Heme oxygenase in neuroprotection: from mechanisms to therapeutic implications, Rev. Neurosci. 25 (2014) 269–280. doi:10.1515/revneuro-2013-0046.

[156] Y.N. Huang, C.H. Wu, T.C. Lin, J.Y. Wang, Methamphetamine induces heme oxygenase-1 expression in cortical neurons and glia to prevent its toxicity, Toxicol. Appl. Pharmacol. 240 (2009) 315–326. doi:10.1016/j.taap.2009.06.021.

[157] M. Zhou, H.K. Kimelberg, M.I.N. Zhou, Freshly Isolated Astrocytes From Rat Hippocampus Show Two Distinct Current Patterns and Different [K +] o Uptake Capabilities, J. Neurophysiol. 84 (2013) 2746–2757.

[158] M.P. Soares, F.H. Bach, Heme oxygenase-1: from biology to therapeutic potential., Trends Mol. Med. 15 (2009) 50–8. doi:10.1016/j.molmed.2008.12.004.

[159] E.F. Chang, R.J. Wong, H.J. Vreman, T. Igarashi, E. Galo, F.R. Sharp, D.K. Stevenson, L.J. Noble-Haeusslein, Heme oxygenase-2 protects against lipid peroxidation-mediated cell loss and impaired motor recovery after traumatic brain injury., J. Neurosci. 23 (2003) 3689–96. http://www.ncbi.nlm.nih.gov/pubmed/12736340.

[160] a. S. Ahmad, H. Zhuang, S. Doré, Heme oxygenase-1 protects brain from acute excitotoxicity, Neuroscience. 141 (2006) 1703–1708. doi:10.1016/j.neuroscience.2006.05.035.

[161] H.M. Schipper, Heme oxygenase-1: transducer of pathological brain iron sequestration under oxidative stress., Ann. N. Y. Acad. Sci. 1012 (2004) 84–93. http://www.ncbi.nlm.nih.gov/pubmed/15105257.

[162] W. Song, H. Zukor, S.-H. Lin, A. Liberman, A. Tavitian, J. Mui, H. Vali, C. Fillebeen, K. Pantopoulos, T.-D. Wu, J.-L. Guerquin-Kern, H.M. Schipper, Unregulated brain iron deposition in transgenic mice over-expressing HMOX1 in the astrocytic compartment., J. Neurochem. 123 (2012) 325–36. doi:10.1111/j.1471-4159.2012.07914.x.

[163] V. Calabrese, D.A. Butterfield, G. Scapagnini, A.M.G. Stella, M.D. Maines, Redox

Regulation of Heat Shock Protein Expression by Signaling Involving Nitric Oxide and Carbon Monoxide: Relevance to Brain Aging, Neurodegenerative Disorders, and Longevity, Antioxid. Redox Signal. 8 (2006) 444–477. doi:10.1089/ars.2006.8.444.

[164] E. Barone, F. Di Domenico, C. Mancuso, D.A. Butterfield, The Janus face of the heme oxygenase/biliverdin reductase system in Alzheimer disease: It's time for reconciliation, Neurobiol. Dis. 62 (2014) 144–159. doi:10.1016/j.nbd.2013.09.018.

[165] C.C. Romão, W. a Blättler, J.D. Seixas, G.J.L. Bernardes, Developing drug molecules for therapy with carbon monoxide., Chem. Soc. Rev. 41 (2012) 3571–83. doi:10.1039/c2cs15317c.

[166] R. Motterlini, P. Sawle, J. Hammad, S. Bains, R. Alberto, R. Foresti, C.J. Green, CORM-A1: a new pharmacologically active carbon monoxide-releasing molecule., FASEB J. 19 (2005) 284–6. doi:10.1096/fj.04-2169fje.

[167] D.J. Darensbourg, D.L. Larkins, J.H. Reibenspies, Bis(triphenylphosphine)copper(I) Complexes of Orotate and L-Dihydroorotate., Inorg. Chem. 37 (1998) 6125–6128. http://www.ncbi.nlm.nih.gov/pubmed/11670757.

[168] J.A.S. Howell, P.M. Burkinshaw, Ligand Substitution Reactions at Low-Valent Four-, Five-, and Six-Coordinate Transition-Metal Centers, Chem. Rev. 83 (1983) 557–599.

[169] D. Wang, E. Viennois, K. Ji, K. Damera, A. Draganov, Y. Zheng, C. Dai, D. Merlin, B. Wang, A click-and-release approach to CO prodrugs, Chem. Commun. 50 (2014) 15890–15893. doi:10.1039/C4CC07748B.

[170] R.D. Rimmer, H. Richter, P.C. Ford, A Photochemical Precursor for Carbon Monoxide Release in Aerated Aqueous Media, Inorg. Chem. 49 (2010) 1180–1185. doi:10.1021/ic902147n.

[171] C.S. Jackson, S. Schmitt, Q.P. Dou, J.J. Kodanko, Synthesis, characterization, and reactivity of the stable iron carbonyl complex [Fe(CO)(N4Py)](ClO4)2: photoactivated carbon monoxide release, growth inhibitory activity, and peptide ligation., Inorg. Chem. 50 (2011) 5336–8. doi:10.1021/ic200676s.

[172] M. a Gonzalez, S.J. Carrington, N.L. Fry, J.L. Martinez, P.K. Mascharak, Syntheses, structures, and properties of new manganese carbonyls as photoactive CO-releasing molecules: design strategies that lead to CO photolability in the visible region., Inorg. Chem. 51 (2012) 11930–40. doi:10.1021/ic3018216.

[173] R. Foresti, M.G. Bani-Hani, R. Motterlini, Use of carbon monoxide as a therapeutic agent: promises and challenges., Intensive Care Med. 34 (2008) 649–58. doi:10.1007/s00134-008-1011-1.

[174] X. Ji, K. Damera, Y. Zheng, B. Yu, L.E. Otterbein, B. Wang, Toward Carbon Monoxide-Based Therapeutics: Critical Drug Delivery and Developability Issues, J. Pharm. Sci. 105 (2016) 406–415. doi:10.1016/j.xphs.2015.10.018.

[175] K.D. Vandegriff, M.A. Young, J. Lohman, A. Bellelli, M. Samaja, A. Malavalli, R.M. Winslow, CO-MP4, a polyethylene glycol-conjugated haemoglobin derivative and carbon monoxide carrier that reduces myocardial infarct size in rats, Br. J. Pharmacol. 154 (2009) 1649–1661. doi:10.1038/bjp.2008.219.

[176] E. Csongradi, Role of Carbon Monoxide in Kidney Function: Is a little Carbon Monoxide Good for the Kidney?, Curr. Pharm. Biotechnol. 13 (2012) 819–826. doi:10.2174/138920112800399284.

[177] A.S. Almeida, N.L. Soares, M. Vieira, J.B. Gramsbergen, H.L.A. Vieira, Carbon monoxide releasing molecule-A1 (CORM-A1) improves neurogenesis: increase of neuronal

differentiation yield by preventing cell death, PLoS One. in press (2016) 1–24. doi:10.1371/journal.pone.0154781.

[178] P.A. Hosick, A.A. AlAmodi, M.W. Hankins, D.E. Stec, Chronic treatment with a carbon monoxide releasing molecule reverses dietary induced obesity in mice, Adipocyte. 5 (2016) 1–10. doi:10.1080/21623945.2015.1038443.

[179] D. Babu, G. Leclercq, V. Goossens, Q. Remijsen, P. Vandenabeele, R. Motterlini, R.A. Lefebvre, Antioxidant potential of CORM-A1 and resveratrol during TNF-α/cycloheximide-induced oxidative stress and apoptosis in murine intestinal epithelial MODE-K cells., Toxicol. Appl. Pharmacol. 288 (2015) 161–78. doi:10.1016/j.taap.2015.07.007.

[180] I. Nikolic, T. Saksida, M. Vujicic, I. Stojanovic, S. Stosic-Grujicic, Anti-diabetic actions of carbon monoxide-releasing molecule (CORM)-A1: Immunomodulation and regeneration of islet beta cells., Immunol. Lett. 165 (2015) 39–46. doi:10.1016/j.imlet.2015.03.009.

[181] P. Fagone, K. Mangano, S. Mammana, E. Cavalli, R. Di Marco, M.L. Barcellona, L. Salvatorelli, G. Magro, F. Nicoletti, Carbon monoxide-releasing molecule-A1 (CORM-A1) improves clinical signs of experimental autoimmune uveoretinitis (EAU) in rats., Clin. Immunol. 157 (2015) 198–204. doi:10.1016/j.clim.2015.02.002.

[182] J. Liu, A.L. Fedinec, C.W. Leffler, H. Parfenova, Enteral supplements of a carbon monoxide donor CORM-A1 protect against cerebrovascular dysfunction caused by neonatal seizures., J. Cereb. Blood Flow Metab. 35 (2015) 193–9. doi:10.1038/jcbfm.2014.196.

[183] S. Basuroy, C.W. Leffler, H. Parfenova, CORM-A1 prevents blood-brain barrier dysfunction caused by ionotropic glutamate receptor-mediated endothelial oxidative stress and apoptosis, AJP Cell Physiol. 304 (2013) C1105–C1115. doi:10.1152/ajpcell.00023.2013.

[184] M. Desmard, R. Foresti, D. Morin, M. Dagouassat, A. Berdeaux, E. Denamur, S.H. Crook, B.E. Mann, D. Scapens, P. Montravers, J. Boczkowski, R. Motterlini, Differential Antibacterial Activity Against Pseudomonas aeruginosa by Carbon Monoxide-Releasing Molecules, Antioxid. Redox Signal. 16 (2012) 153–163. doi:10.1089/ars.2011.3959.

[185] M.J. Ryan, N.L. Jernigan, H.A. Drummond, G.R. McLemore, J.M. Rimoldi, S.R. Poreddy, R.S. V Gadepalli, D.E. Stec, Renal vascular responses to CORM-A1 in the mouse., Pharmacol. Res. 54 (2006) 24–9. doi:10.1016/j.phrs.2006.01.012.

[186] I. Nikolic, M. Vujicic, I. Stojanovic, S. Stosic-Grujicic, T. Saksida, Carbon Monoxide-Releasing Molecule-A1 Inhibits Th1/Th17 and Stimulates Th2 Differentiation In vitro, Scand. J. Immunol. 80 (2014) 95–100. doi:10.1111/sji.12189.

[187] J. Boczkowski, J.J. Poderoso, R. Motterlini, CO-metal interaction: Vital signaling from a lethal gas., Trends Biochem. Sci. 31 (2006) 614–21. doi:10.1016/j.tibs.2006.09.001.

[188] C. Peers, D.S. Steele, Carbon monoxide: a vital signalling molecule and potent toxin in the myocardium., J. Mol. Cell. Cardiol. 52 (2012) 359–65. doi:10.1016/j.yjmcc.2011.05.013.

[189] M. Knauert, S. Vangala, M. Haslip, P. Lee, Therapeutic Applications of Carbon Monoxide, Oxid. Med. Cell. Longev. 2013 (2013) 1–11. doi:10.1155/2013/360815.

[190] J. Dulak, A. Józkowicz, Carbon monoxide — a " new " gaseous modulator of gene, Acta Bioch. Pol. 50 (2003).

[191] A.A. Untereiner, L. Wu, R. Wang, Gasotransmitters: Physiology and Pathophysiology, Springer Berlin Heidelberg, Berlin, Heidelberg, 2012. doi:10.1007/978-3-642-30338-8.

[192] E.M. Dioum, J. Rutter, J.R. Tuckerman, G. Gonzalez, M.-A. Gilles-Gonzalez, S.L.

McKnight, NPAS2: a gas-responsive transcription factor., Science. 298 (2002) 2385–7. doi:10.1126/science.1078456.

[193] M. Kajimura, R. Fukuda, R.M. Bateman, T. Yamamoto, M. Suematsu, Interactions of multiple gas-transducing systems: hallmarks and uncertainties of CO, NO, and H2S gas biology., Antioxid. Redox Signal. 13 (2010) 157–92. doi:10.1089/ars.2009.2657.

[194] F. Gullotta, A. di Masi, M. Coletta, P. Ascenzi, CO metabolism, sensing, and signaling, BioFactors. 38 (2012) 1–13. doi:10.1002/biof.192.

[195] L.E. Otterbein, R. Foresti, R. Motterlini, Heme Oxygenase-1 and Carbon Monoxide in the Heart, Circ. Res. 118 (2016) 1940–1959. doi:10.1161/CIRCRESAHA.116.306588.

[196] S.D. Brown, C.A. Piantadosi, In vivo binding of carbon monoxide to cytochrome c oxidase in rat brain., J. Appl. Physiol. 68 (1990) 604–10. http://www.ncbi.nlm.nih.gov/pubmed/2156793.

[197] C.S.F. Queiroga, A.S. Almeida, H.L.A. Vieira, Carbon Monoxide Targeting Mitochondria, Biochem. Res. Int. 2012 (2012) 1–9. doi:10.1155/2012/749845.

[198] B.Y. Chin, G. Jiang, B. Wegiel, H.J. Wang, T. MacDonald, X.C. Zhang, D. Gallo, E. Cszimadia, F.H. Bach, P.J. Lee, L.E. Otterbein, Hypoxia-inducible factor 1 stabilization by carbon monoxide results in cytoprotective preconditioning, Proc. Natl. Acad. Sci. 104 (2007) 5109–5114. doi:10.1073/pnas.0609611104.

[199] C.A. Piantadosi, H.B. Suliman, Redox regulation of mitochondrial biogenesis, Free Radic. Biol. Med. 53 (2012) 2043–2053. doi:10.1016/j.freeradbiomed.2012.09.014.

[200] C.S.F. Queiroga, A.S. Almeida, C. Martel, C. Brenner, P.M. Alves, H.L.A. Vieira, Glutathionylation of adenine nucleotide translocase induced by carbon monoxide prevents mitochondrial membrane permeabilization and apoptosis., J. Biol. Chem. 285 (2010) 17077–88. doi:10.1074/jbc.M109.065052.

[201] L. Lo Iacono, J. Boczkowski, R. Zini, I. Salouage, A. Berdeaux, R. Motterlini, D. Morin, A carbon monoxide-releasing molecule (CORM-3) uncouples mitochondrial respiration and modulates the production of reactive oxygen species., Free Radic. Biol. Med. 50 (2011) 1556–64. doi:10.1016/j.freeradbiomed.2011.02.033.

[202] C.S.F. Queiroga, A.S. Almeida, P.M. Alves, C. Brenner, H.L.A. Vieira, Carbon monoxide prevents hepatic mitochondrial membrane permeabilization., BMC Cell Biol. 12 (2011) 10. doi:10.1186/1471-2121-12-10.

[203] S.R. Oliveira, C.S.F. Queiroga, H.L.A. Vieira, Mitochondria and carbon monoxide: cytoprotection and control of cell metabolism - a role for Ca 2+ ?, J. Physiol. 594 (2016) 4131–4138. doi:10.1113/JP270955.

[204] A.S. Almeida, C.S.F. Queiroga, M.F.Q. Sousa, P.M. Alves, H.L.A. Vieira, Carbon monoxide modulates apoptosis by reinforcing oxidative metabolism in astrocytes: role of Bcl-2., J. Biol. Chem. 287 (2012) 10761–70. doi:10.1074/jbc.M111.306738.

[205] M. Bilban, A. Haschemi, B. Wegiel, B.Y. Chin, O. Wagner, L.E. Otterbein, Heme oxygenase and carbon monoxide initiate homeostatic signaling, J Mol Med. 86 (2008) 267–279. doi:10.1007/s00109-007-0276-0.

[206] C.S.F. Queiroga, A. Vercelli, H.L.A. Vieira, Carbon monoxide and the CNS: Challenges and achievements, Br. J. Pharmacol. (2014) 1–13. doi:10.1111/bph.12729.

[207] A. Almeida, U. Sonnewald, P.M. Alves, H.L.A. Vieira, Carbon monoxide improves neuronal differentiation and yield by increasing the functioning and number of mitochondria, J Neurochem. (2016). doi:10.1111/jnc.13653.

[208] T. Ohtsuka, K. Kaseda, T. Shigenobu, T. Hato, I. Kamiyama, T. Goto, M. Kohno, M. Shimoda, Carbon monoxide-releasing molecule attenuates allograft airway rejection, Transpl. Int. 27 (2014) 741–747. doi:10.1111/tri.12314.

[209] K. Katada, T. Takagi, K. Uchiyama, Y. Naito, Therapeutic roles of carbon monoxide in intestinal ischemia-reperfusion injury., J. Gastroenterol. Hepatol. 30 Suppl 1 (2015) 46–52. doi:10.1111/jgh.12742.

[210] M. Suematsu, K. Tsukada, T. Tajima, T. Yamamoto, D. Ochiai, H. Watanabe, Y. Yoshimura, N. Goda, Carbon monoxide as a guardian against hepatobiliary dysfunction., Alcohol. Clin. Exp. Res. 29 (2005) 134S–139S. doi:00000374-200511001-00010 [pii].

[211] L. Vítek, H. Gbelcová, L. Muchová, K. Váňová, J. Zelenka, R. Koníčková, J. Suk, M. Zadinova, Z. Knejzlík, S. Ahmad, T. Fujisawa, A. Ahmed, T. Ruml, Antiproliferative effects of carbon monoxide on pancreatic cancer., Dig. Liver Dis. 46 (2014) 369–75. doi:10.1016/j.dld.2013.12.007.

[212] J. Ruiz, B.T. Ameredes, The cellular effects of carbon monoxide in the airway., Curr. Mol. Med. 13 (2013) 94–108. http://www.ncbi.nlm.nih.gov/pubmed/22834843.

[213] J. Biermann, W. a Lagrèze, C. Dimitriu, C. Stoykow, U. Goebel, Preconditioning with inhalative carbon monoxide protects rat retinal ganglion cells from ischemia/reperfusion injury., Invest. Ophthalmol. Vis. Sci. 51 (2010) 3784–3791. doi:10.1167/iovs.09-4894.

[214] B. Wang, W. Cao, S. Biswal, S. Doré, Carbon monoxide-activated Nrf2 pathway leads to protection against permanent focal cerebral ischemia., Stroke. 42 (2011) 2605–10. doi:10.1161/STROKEAHA.110.607101.

[215] E. Zeynalov, S. Doré, Low Doses of Carbon Monoxide Protect Against Experimental Focal Brain Ischemia, Neurotox. Res. 15 (2009) 133–137. doi:10.1007/s12640-009-9014-4.

[216] A. Yabluchanskiy, P. Sawle, S. Homer-Vanniasinkam, C.J. Green, R. Foresti, R. Motterlini, CORM-3, a carbon monoxide-releasing molecule, alters the inflammatory response and reduces brain damage in a rat model of hemorrhagic stroke., Crit. Care Med. 40 (2012) 544–52. doi:10.1097/CCM.0b013e31822f0d64.

[217] C.S.F. Queiroga, S. Tomasi, M. Widerøe, P.M. Alves, A. Vercelli, H.L.A. Vieira, Preconditioning Triggered by Carbon Monoxide (CO) Provides Neuronal Protection Following Perinatal Hypoxia-Ischemia, PLoS One. 7 (2012) e42632. doi:10.1371/journal.pone.0042632.

[218] V.L. Mahan, D. Zurakowski, L.E. Otterbein, F. a Pigula, Inhaled carbon monoxide provides cerebral cytoprotection in pigs., PLoS One. 7 (2012) e41982. doi:10.1371/journal.pone.0041982.

[219] A. Zimmermann, C.W. Leffler, D. Tcheranova, A.L. Fedinec, H. Parfenova, A. Zimmermann, L. Cw, D. Tcheranova, F. Al, Cerebroprotective effects of the CO-releasing molecule CORM-A1 against seizure-induced neonatal vascular injury, Am J Physiol Hear. Circ Physiol. 38163 (2007) 2501–2507. doi:10.1152/ajpheart.00354.2007.

[220] H. Parfenova, D. Tcheranova, S. Basuroy, A.L. Fedinec, J. Liu, C.W. Leffler, Functional role of astrocyte glutamate receptors and carbon monoxide in cerebral vasodilation response to glutamate., Am. J. Physiol. Heart Circ. Physiol. 302 (2012) H2257–H2266. doi:10.1152/ajpheart.01011.2011.

[221] P. Fagone, K. Mangano, M. Coco, V. Perciavalle, G. Garotta, C.C. Romao, F. Nicoletti, Therapeutic potential of carbon monoxide in multiple sclerosis., Clin. Exp. Immunol. 167 (2012) 179–87. doi:10.1111/j.1365-2249.2011.04491.x.

[222] A.M. Jurga, A. Piotrowska, J. Starnowska, E. Rojewska, W. Makuch, J. Mika, Treatment

with a carbon monoxide-releasing molecule (CORM-2) inhibits neuropathic pain and enhances opioid effectiveness in rats., Pharmacol. Rep. 68 (2016) 206–13. doi:10.1016/j.pharep.2015.08.016.

[223] N. Schallner, C.C. Romão, J. Biermann, W.A. Lagrèze, L.E. Otterbein, H. Buerkle, T. Loop, U. Goebel, Carbon Monoxide Abrogates Ischemic Insult to Neuronal Cells via the Soluble Guanylate Cyclase-cGMP Pathway, PLoS One. 8 (2013). doi:10.1039/c2dt32174b.

[224] N. Hettiarachchi, M. Dallas, M. Al-Owais, H. Griffiths, N. Hooper, J. Scragg, J. Boyle, C. Peers, Heme oxygenase-1 protects against Alzheimer's amyloid-β1-42-induced toxicity via carbon monoxide production, Cell Death Dis. 5 (2014) e1569. doi:10.1038/cddis.2014.529.

[225] M.G. Bani-Hani, D. Greenstein, B.E. Mann, C.J. Green, R. Motterlini, Modulation of thrombin-induced neuroinflammation in BV-2 microglia by carbon monoxide-releasing molecule 3., J. Pharmacol. Exp. Ther. 318 (2006) 1315–22. doi:10.1124/jpet.106.104729.

[226] M.G. Bani-Hani, D. Greenstein, B.E. Mann, C.J. Green, R. Motterlini, A carbon monoxide-releasing molecule (CORM-3) attenuates lipopolysaccharide- and interferon-gamma-induced inflammation in microglia., Pharmacol. Rep. 58 Suppl (2006) 132–44. http://www.ncbi.nlm.nih.gov/pubmed/17332683.

[227] S. Basuroy, S. Bhattacharya, C.W. Leffler, H. Parfenova, Nox4 NADPH oxidase mediates oxidative stress and apoptosis caused by TNF- in cerebral vascular endothelial cells, AJP Cell Physiol. 296 (2008) C422–C432. doi:10.1152/ajpcell.00381.2008.

[228] S. Basuroy, D. Tcheranova, S. Bhattacharya, C.W. Leffler, H. Parfenova, Nox4 NADPH oxidase-derived reactive oxygen species, via endogenous carbon monoxide, promote survival of brain endothelial cells during TNF-α-induced apoptosis., Am. J. Physiol. Cell Physiol. 300 (2011) C256-65. doi:10.1152/ajpcell.00272.2010.

[229] A. Lau, M. Tymianski, Glutamate receptors, neurotoxicity and neurodegeneration, Pflügers Arch. - Eur. J. Physiol. 460 (2010) 525–542. doi:10.1007/s00424-010-0809-1.

[230] U. Dirnagl, R.P. Simon, J.M. Hallenbeck, Ischemic tolerance and endogenous neuroprotection, Trends Neurosci. 26 (2003) 248–254. doi:10.1016/S0166-2236(03)00071-7.

Chapter II

RESULTS

Chapter II.I

RNASeq Analysis

This chapter is based on the following manuscript:

RNASeq analysis reveals pathways and candidate genes associated with carbon monoxide treatment in astrocytes
Sara R. Oliveira, Carlos B Duarte, Helena L. A. Vieira
(in preparation)

INDEX

ABSTRACT

Carbon monoxide (CO) has been studied as a possible therapeutic agent in several systems, namely CNS. Low doses of CO are involved in cell death reduction and metabolic improvement, both in neurons and astrocytes. A wide variety of other beneficial outcomes have been associated with CO administration, however the detailed function of this gasotransmitter in neuronal cells remains unknown. Previous work from our group showed that astrocytes pre-treated with CO could induce cytoprotection in neurons when in co-culture. To interpret the astrocytic alterations caused by CO, we performed transcriptome comparison of astrocyte primary cultures after CO exposure. Cultured astrocytes were treated with the CO-releasing molecule CORM-A1 (12.5 μM) for 40 min, and transcriptional changes were analyzed through RNASeq. A total of 162 genes were found differentially expressed due to CO exposure, from which 100 were upregulated and 62 were downregulated. Differentially-expressed genes (DEGs) were then selected and underwent Gene Ontology annotation and pathway analysis using the Kyoto Encyclopedia of Genes and Genomes. The most represented transcription factors were identified and gene-act networks were also constructed. The functional annotation revealed that the main pathways involved were related to: Hedgehog and basal cell carcinoma pathways and phosphatidylinositol signaling system. Moreover, the pathway and network analysis showed that the AP-1 transcription factor and cytoskeleton organization were intimately involved in the CO effect on astrocytes.

Our work provides valuable information on the transcriptional changes in astrocytes promoted by CO. This study reveals the diverse regulatory mechanisms of astrocytes upon a non-toxic CO exposure.

KEYWORDS

Carbon monoxide, astrocytes, RNASeq, transcriptome, differential gene expression.

ABBREVIATIONS

Actg1 - actin gamma 1
AP-1 - activator protein 1
ATF - activating transcription factor
BDNF - brain-derived neurotrophic factor
CBP - CREB binding protein
CO - carbon monoxide
CORM-A1 - carbon monoxide-releasing molecule A1
CREB - cAMP-response element-binding protein
DEGs - differentially expressed genes
ERK - extracellular signal-regulated kinase
FDR - false discovery rate
GFAP – glial fibrillary acidic protein
GLAST - glutamate aspartate transporter
HO-1 – heme oxygenase 1
JAK - Janus kinase
JNK - c Jun N-terminal kinase
MAPK - mitogen-activated protein kinase
MMP - mitochondria membrane potential
PPARɣ - peroxisome proliferator-activated receptor gamma
PI - propidium iodide
qRT-PCR - quantitative real-time reverse transcription-polymerase chain reaction
t-BHP - *tert*-butyl hydroperoxide
ROS - reactive oxygen species.

1. INTRODUCTION

Carbon monoxide (CO) is an endogenously produced gasotransmitter, which is generated by the activity of heme oxygenase (HO). This gasotransmitter has been shown to confer cytoprotection by boosting cellular resistance against a wide variety of harmful events [1]. Thus, low concentrations of exogenous CO and/or expression of heme oxygenase 1 (HO-1) promotes neuroprotection in central nervous system by limiting neuroinflammation and neural cell death, as well as by inducing vasodilation (for review see [2]). In cellular models of brain tissue, CO has anti-apoptotic properties in neurons [3,4] and in astrocytes [5,6], promotes neurogenesis [7], and reduces neuroinflammation by acting on microglia [8–10]. Likewise, administration of low doses of CO revealed beneficial properties and improved the outcome in several rodent models of brain disease, namely ischemic stroke [11,12], hemorrhagic stroke [13] and multiple sclerosis [14,15]. Although several cytoprotective properties have been described for CO, the molecular mechanisms underlying the effect of CO are far from being completely understood. Up to date, the transcriptomic alterations contributing to the cytoprotective effects induced by exogenous CO have not been investigated.

Because CO holds great potential for therapeutic purposes, several strategies based on small molecules able to deliver CO gas under controlled conditions have been developed. These CO-releasing molecules (CORM) [16] present yet several issues to be addressed before their use in biological systems, namely: water insolubility, toxic chemical structures, promotion of high levels of carboxyhemoglobin and chemical instability, among others [17]. The CORM-A1 was developed by Motterlini and colleagues and presents as main advantages the fact that it is water soluble and a slow CO releaser under physiological conditions in a pH- and temperature-dependent manner [18].

Astrocytes are the most abundant cell type in the brain and provide structural, metabolic and trophic support to other neural cells, in particular to neurons [19]. Recently, neuroscientists have been giving increasing attention to astrocytes. Due to the tightly regulated cross talk between neurons and astrocytes, one can suggest that improving astrocytic function can promote neuroprotection. Astrocytes are enriched in signaling pathways such as p38/MAPK, ERK, and PPAR [20–22], which are reported to be modulated by low concentrations of CO [23,24]. Also, astrocytes are metabolically very active cells, being key players in brain metabolism, in particular in astrocyte-neuron lactate shuttle [25]. Likewise, some of the biological effects of CO have been attributed to the regulation of cell metabolism [6,26,27]. Finally, CO-induced modulation of astrocytic metabolism increased neuronal survival upon challenging neurons to death by oxidative stress in a co-culture system [28]. Therefore, in the present work, we investigated the putative alterations on gene expression due to exogenous CO treatment are studied in primary cultures of astrocytes.

The aim of this work was: (i) to identify the molecular effectors of CO-induced transcriptomic alteration in astrocytes by mRNA sequencing; (ii) to categorize the most relevant set of pathways; (iii) to disclose the interaction network and cluster of genes; and (iv) to find the key transcription factors associated with CO treatment. Finally, the characterization of CO-induced alterations in gene expression will contribute for better understanding CO's beneficial and detrimental effects and to the potential development of novel therapeutic strategies against cerebral diseases.

2. MATERIALS AND METHODS

2.1. Cortical astrocyte cultures

Primary cultures of mouse cortical astrocytes were prepared from the cortices of P1–P2 Bl6/c57 mice pups after mechanical dissociation, as previously described [29]. Briefly, cerebral hemispheres were carefully freed of the meninges and the dissected cortices were washed in ice-cold PBS, dissociated mechanically and passed through a 70 µm nylon cell strainer (BD Falcon™) into Dulbecco's minimum essential medium containing 1 g/L glucose (Sigma) and supplemented with 20% (v/v) fetal bovine serum (FBS; Gibco® Life Technologies) and 1% (v/v) penicillin/streptomycin (Gibco® Life Technologies). Single-cell suspensions were plated in cell culture flasks (8 to 10 cortices/75 cm^2; Orange Scientific) and maintained in a humidified atmosphere of 5% CO_2 / 95% air at 37°C. After 8 days in culture, the phase dark cells growing on the astrocytic cell layer were detached by vigorous shaking and removed. Culture medium was replaced twice a week for 3 weeks with gradual reduction in FBS content (2^{nd} week 15%; 3^{rd} week 10%). The confluent astrocytic cultures were mildly trypsinized (0.05% (w/v) trypsin/EDTA; Gibco® Life Technologies) and subcultured in 6-well plates until full confluence.

2.2. Administration of CO to astrocytic culture

CORM-A1, a CO releasing molecule [18], was used to deliver CO to astrocytes. CORM-A1 (Sigma) stock solutions were prepared in MilliQ water to a final concentration of 10 mM and stored at -20°C to avoid loss of released CO, and diluted in PBS just before use. Cells were exposed to a final concentration of 12.5 µM of CORM-A1 for 40 min prior to RNA extraction. Controls without CORM-A1 were performed in parallel.

The time of CORM-A1 treatment was selected based on the cytoprotective effects of CO in astrocytes subjected to oxidative stress (data not shown).

2.3. Total RNA isolation and assessment of quality and concentration of RNA

Astrocyte RNA was purified using RNeasy Qiagen kit accordingly to manufacturer's procedure followed by lyophilisation. Samples of 15 µg of dried RNA *per* condition were sent for RNA sequencing using Illumina 2000 HiSeq instrument at BGI Genomics (Cambridge, MA).

RNA quality and integrity was assessed using the Experion RNA StdSens automated gel electrophoresis system (Bio-Rad). A virtual gel was created for each sample, allowing the detection of degradation of the reference markers RNA18S and 28S. The system labels each sample with a RNA Quality Indicator (RQI), ranging from 1 to 10. Samples were discarded when showing RQI ≤7, indicating that they presented RNA degradation, poor integrity or contamination with DNA.

2.4. RNAseq and bioinformatics analysis

RNA extracted from 4 primary astrocyte cultures from mice cortices was used to prepare mRNA libraries using the Illumina's HiSeq technology. At least 10 million clean reads were generated *per* sample. Raw sequencing data were first evaluated by FastQC [30], and then mapped to the Mus_musculus.GRCm38.73.dna.toplevel genome using Tophat 2.0 [31] based on Bowtie2 [32]. The read count for each gene was obtained from the mapping results using Cufflinks [33] and normalized to reads per kilobase of exon model *per* million mapped reads (RPKM). The alignment of read counts was analyzed with Qualimap [34], AligmentQC (samstats) and CummeRbund [35] (Supplementary Data, Figure S1). Differentially expressed genes (DEGs) between the CO-treated samples and controls were identified with FDR (false discovery rate) ≤ 0.05 and fold change ≥ 1. GO analyses were performed with GoMiner and pathway enrichment analyses were performed with Enrichr [36]. Gene-act network analyses were performed with STRING [37].

3. RESULTS

3.1. CO induces transcriptional regulation in cortical astrocytes

To investigate the transcriptional events in astrocytes exposed to CO, we performed a transcriptional profiling *via* RNASeq. Primary cultures of mice cortical astrocytes were stimulated with CORM-A1 at 12.5 μM ($t_{1/2}$ = 21 min at 37ºC and pH = 7.4). Alterations in gene expression due to CO exposure were previously described to occur at incubation periods ranging from 30 min up to 60 min [38]. Thus, any CO-induced transcriptional alteration responsible for the acquired tolerance must occur within this early period after CO exposure. Furthermore, a previous study performed in our laboratory showed that pre-incubation of primary cultures of astrocytes with CORM-A1 for 1h prior to exposure to the pro-oxidant *t*-BHP reduced cell death by 50%, when determined by propidium iodide staining (data not shown). Therefore, a period of 40 min of CORM-A1 exposure was chosen for gene expression profiling studies. A total of 162 transcripts were found to be differentially expressed, being 100 of these genes upregulated and 62 downregulated by more than 1-fold in the CORM-A1 treated cultures, with a false discovery rate (FDR) < 0.05 (Supplementary Data, Table S1).

Gene ontology analysis using GoMiner showed the 'primary metabolic processes' as one of the most represented categories regulated upon exposure of astrocytes to CO (Figure 1), corresponding to 10% of all altered genes (data not shown). This category includes, for example, the metabolic processes of carbohydrates, cellular amino acids, lipids, proteins and the tricarboxylic acid cycle. These reactions guarantee the cellular basic needs, especially the energy status. This result is in accordance with the evidence showing a role for CO in the modulation of mitochondrial function [6,26,27]. Functional annotation also showed that genes acting on the control of gene expression and on the response to stimuli were the biological processes presenting higher amounts of upregulated genes upon CO treatment (Figure 1). This is not surprising since HO-1 is a stress response gene, the expression of which contributes to cell response against deleterious events, boosting cytoprotection and tissue tolerance [39,40]. Likewise, CO may trigger other cellular pathways to respond to stressful stimuli, thus resulting in an overall upregulation of genes belonging to the categories of this ontology. Interestingly, the only biological process presenting higher levels of downregulated than upregulated DEGs was 'cell differentiation' (Figure 1).

Concerning the evaluation of DEG molecular functions, protein and ion binding are the major actions of the upregulated genes, representing 39% of all DEGs. On the other hand, down-regulated DEGs have mainly catalytic activity functions, which represent a total of 26% (Figure 2). In addition to the functional annotation of the DEGs, we also analyzed whether there was any gene family represented by more than 1 gene. A total of 11 gene families were found, namely: Rho GTPase activating protein (Arhgap#, downregulated), coiled-coil domain-containing protein (Ccdc#, mostly upregulated), family with sequence similarity (Fam#, downregulated), FBJ murine osteosarcoma viral oncogene homolog (Fos, upregulated), interleukin receptors (Il#r, upregulated), Protocadherins (Pcdh), Protein tyrosine phosphatase (Ptp, downregulated), ribosomal RNA (Rn#s, downregulated), solute carrier family (Slc#a#, mostly downregulated), wingless-type MMTV integration site family (Wnt#), and zinc finger proteins (Zfp#, upregulated). Altogether, these families represent 16.7% of the 162 DEGs.

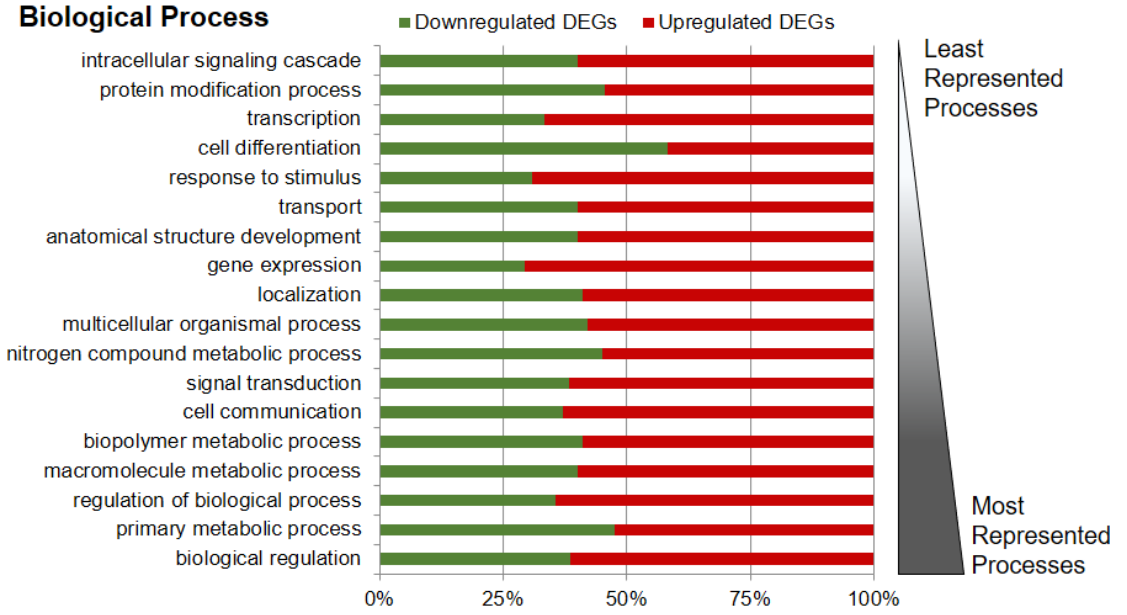

Figure 1 – Biological processes represented among the differentially expressed genes (DEGs) detected following treatment of cortical astrocytes with CORM-A1. Percentage of upregulated and downregulated DEGs in each biological process identified by GoMiner.

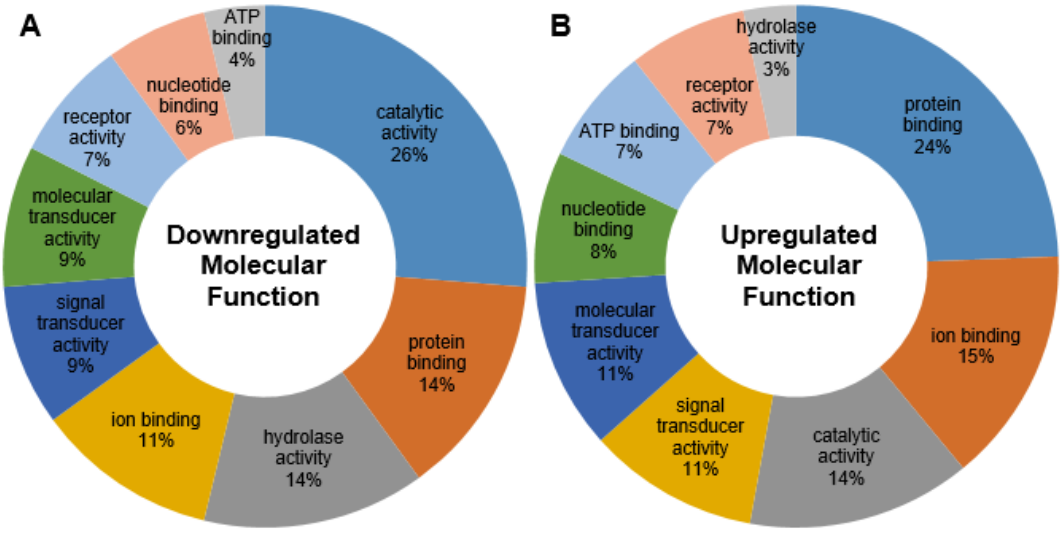

Figure 2 – Most represented molecular functions among CORM-A1-induced DEGs in cortical astrocytes. Molecular functions of upregulated(A) and downregulated (B) DEGs, as analyzed by GoMiner.

3.2. CO mainly modulates the expression of genes regulated by AP-1, Jun, HNF and STAT transcription factors in cortical astrocytes

In addition to the functional annotation of the DEGs, we used SABiosciences' proprietary database DECipherment of DNA Elements (DECODE, http://www.sabiosciences.com/chipqpcrsearch.php?app=TFBS) to identify transcription

factors acting upstream the identified DEGs, which are therefore likely to be candidate gene regulators in CO triggered cytoprotection in astrocytes (Table 1). This analysis identified several targets of the transcriptional mediators of AP-1, Jun, HNF and STAT as the most significantly enriched among the genes with altered expression. In Figure 3 are depicted which DEGs bind to which TF.

Table 1 – Most represented transcription factors that regulate CORM-A1-induced DEGs in cortical astrocytes. Enriched transcription factors were identified by the SABiosciences database (http://www.sabiosciences.com/chipqpcrsearch.php?app=TFBS).

AP	JUN	HNF	STAT	MYC	NFkB	PAX	GATA	PPAR	POU#F	ATF
Cish	Cyth1	Aass	Cish	Aspscr1	Dpp4	Ccdc85c	Aass	Dpp4	Aass	Dpp4
Cyth1	Dab1	Ccdc85c	Hmgb1	Camta1	Hmgb1	Ndufb2	Hmgb1	Fap	Lars2	FosB
Dab1	FosB	Dpp4	Il2ra	Dpp4	Il2ra	Pcsk1n	Map3k14	Gadd45a	Ndufb2	Lrrtm2
Gadd45a	Gadd45a	Nkain4	Il2ra	Gadd45a	Lrrc23	Pde10a	Npr1	Srd5a1	Pik3cd	Ndufb2
Il2ra	Il2ra	Rps6ka1	Lrrtm2	Gli2	Pik3cd	Pex12	Plxnd1	Wnt7a	Slc4a10	Pcsk1n
Lrrc23	Lrrc23	Scand1	Ndufb2	Kdm4b	Rps6ka1	Zbtb20	Rarres2			
Nkain4	Ndufb2	Srd5a1	Scand1	Wnt7a	Ugcg					
Pex12	Nkain4	Stk36	Tnfsf13b							
Tnfsf13b	Tnfsf13b	Wnt7a								

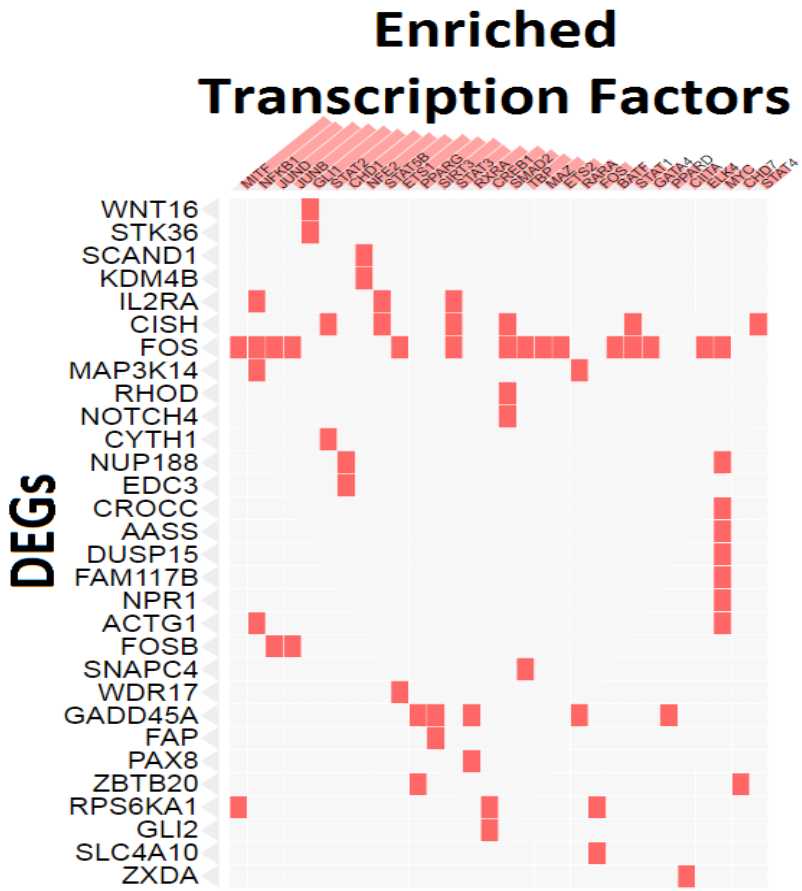

Figure 3 - Enriched transcription factors with protein-protein interaction with DEGs. Clustergram obtained by Enrichr [36].

3.3. CO alters different pathways in cortical astrocytes

To investigate the regulatory mechanisms induced by CO in astrocytes, the Gene Ontology (GO) and Kyoto Encyclopedia of Genes and Genomes (KEGG) pathway enrichment analyses were performed. Genes regulated in astrocytes were associated with important biological processes (Figure 4A). Transcription and gene expression are among the biological processes with higher percentage of upregulated genes, which is in accordance with the majority of the upregulation responses taking place in the nucleus (Figure 4C). The only biological process with more downregulated DEGs then upregulated ones is cell differentiation.

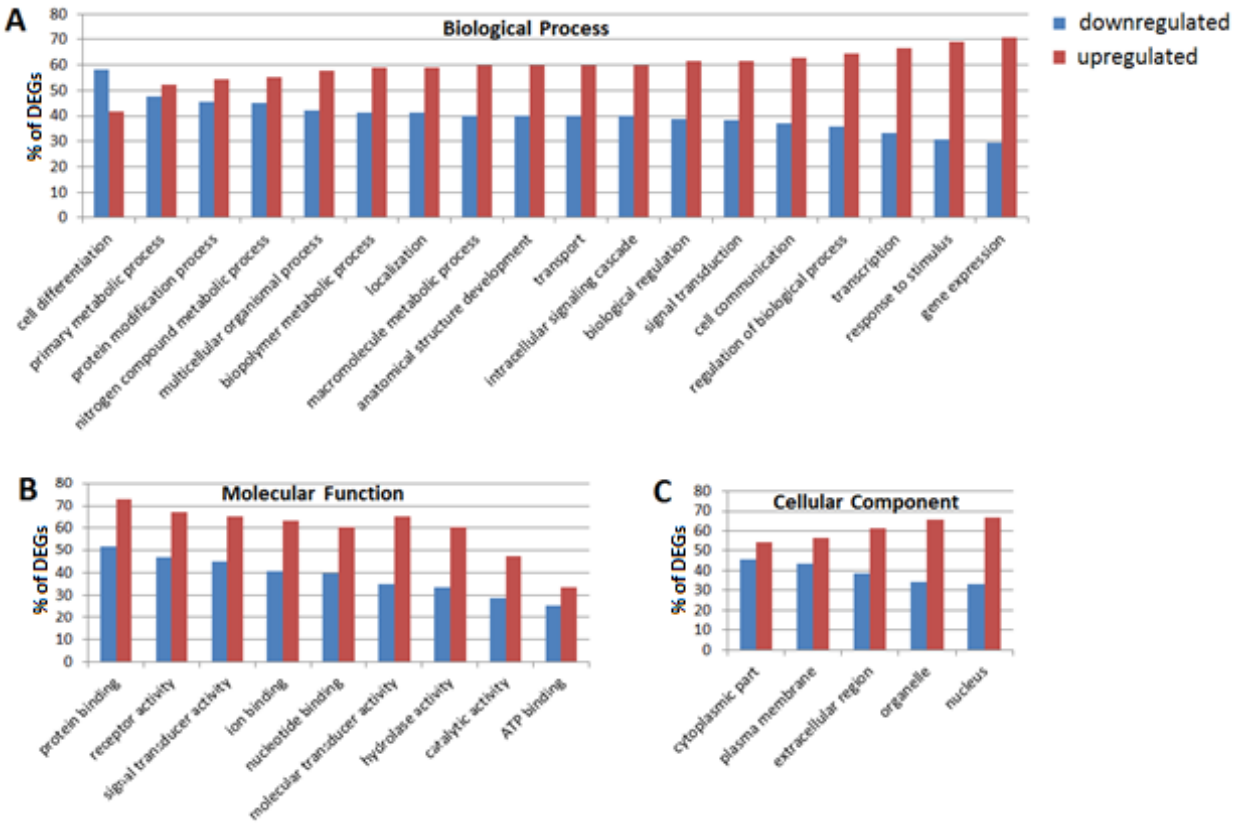

Figure 4 - Gene Ontology (GO) for genes regulated following CO administration. The GO terms identified by GoMiner and the percentage of down and upregulated genes in each category for (A) biological process, (B) molecular function and (C) cellular component.

On the other hand, the most enriched pathways in the KEGG pathway analysis were the basal cell carcinoma and hedgehog signaling pathways, which are related to cell proliferation and stem cell maintenance (Table 2). Another pathway with low *p*-value was the phosphatidylinositol signaling system, which can be related to calcium signaling and PI3K-Akt signaling pathway. Pathways in cancer is the most represented with 7 DEGs, which is not surprising since this term covers several other pathways.

Table 2 - Enrichment analysis of DEGs as determined by the KEGG pathway. Pathway terms with high enrichment scores of DEGs between control and CO-treated cultures of astrocytes. The pathways shown present *p*-values ≤ 0.751.

PATHWAY TERM	Nº OF GENES	*P*-VALUE
Pathways in cancer	7	0.323
MAPK signaling pathway	5	0.751
Hedgehog signaling pathway	4	0.0756
Basal cell carcinoma	4	0.0756
T cell receptor signaling pathway	4	0.334
Phosphatidylinositol signaling system	4	0.186
Inositol phosphate metabolism	3	0.323
Intestinal immune network for IgA production	3	0.323
Drug metabolism – Cytochrome P450	3	0.508
Fc epsilon RI signaling pathway	3	0.508
Melanogenesis	3	0.748
Aminoacyl-tRNA biosynthesis	2	0.748

3.4. Protein-protein interaction network analysis

Protein-protein interaction networks were built with the genes regulated upon CO exposure in order to investigate the regulatory relationships between them in astrocytes (Figure 5). The networks were composed of upregulated and downregulated genes. We found a central cluster which connected to three other clusters. This central cluster was composed of genes related to the AP-1 transcription factor (one of the most represented TF; see Table 1), which includes Fos, FosB, Cish, Il2ra and Gadd45a. The most enriched genes in the basal cell carcinoma and hedgehog signaling pathways (Gli2, Stk36, Wnt7a, Wnt16) and DEGs related to cytoskeleton reorganization (Actg1, Rhod, Arhgap27/32 and Cdk14) formed two branches of the network, suggesting that these pathways might constitute an independent regulatory mechanism in astrocytes upon CO exposure. On the other hand, the genes regulated in astrocytes belonging to the phosphatidylinositol signaling system and the inositol phosphate metabolism (Dgkq, Inpp5a, Itpkc, Pik3cd and Plcb1) formed a third branch with less apparent interactions. This third cluster is described to be involved in cellular reorganization and locomotion, signal transduction and modulation of energetic status. This supported the model indicating that astrocytes modulate their metabolic performance and are more prone to alter their morphology in response to CO.

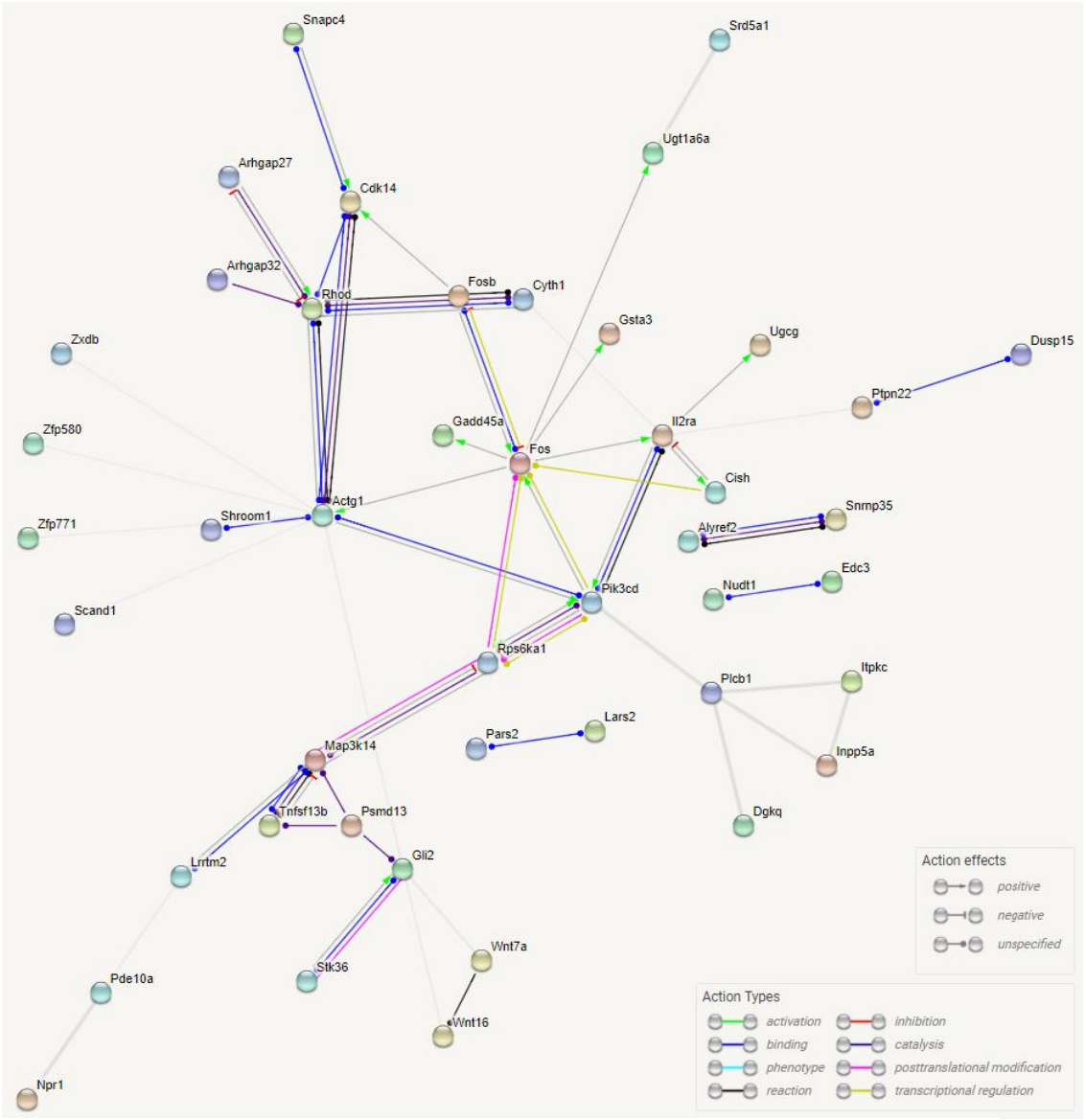

Figure 5 - Network of interaction between the genes regulated by CO in astrocytes. STRING identified 134 DEGs from the 162. Molecular actions are represented with a minimum required interaction score of medium confidence (0.04). The DEGs displaying no interactions are not presented. Action effects and types are described on the right lower corner.

4. DISCUSSION

Astrocytes are essential elements participating in the maintenance of numerous functions of the CNS. A better understanding of the cellular and molecular regulation of the astrocytic components after CO exposure, to promote neuroprotection, is one of the critical steps for the development of new therapeutic strategies in several CNS disorders. In this work, we investigated the transcriptional profiles of astrocyte cultures after CO administration, and found that these underwent different transcriptional changes.

Transcriptome sequencing showed that CO induces multiple transcriptional responses in cultured astrocytes. Previous reports have shown alteration in gene expression in astrocytes upon CO exposure, including changes in the expression of the Bdnf, Bcl-2 [38] and Nrf-2 [41] genes. In the case of neurons, these effects on gene expression are crucial for conferring protection against cytotoxicity factors, since blocking *de novo* protein synthesis abolished the CO-induced protection [4]. As previous studies were focused on specific genes, the whole transcriptome analysis was still required in order to fully understand the diversity of effects of CO.

Functional annotation with GoMiner revealed preferential effects of CO on the abundance of transcripts coding for proteins with relevance in biological regulation and in primary metabolic processes in astrocytes. Furthermore, KEGG pathway analysis showed an enrichment in the hedgehog signaling pathway, basal cell carcinoma, and phosphatidylinositol signaling system in astrocytes exposed to CO. It is worth noting that the central clustered genes, observed in the STRING obtained interactome, were found to be all upregulated and combined into a regulatory sub-network in the protein-protein interaction network. These DEGs share AP-1 as a common transcription factor, which is important in the response to a wide range of stimuli, playing different roles in the CNS. Under normal physiological conditions, AP-1 is involved in many CNS signaling pathways, including immune response, redox-sensitive first line responses, memory formation, maturation and differentiation of neuronal cells, circadian rhythm and plasticity. AP-1 proteins are also triggered in fundamental physiological responses to injury in non-neuronal cells, such as astrocytes *in vivo* [42]. The effects of AP-1 activation are intimately dependent on the dimer constituents forming it. For example, Jun and its upstream activators JNKs were described to be involved in processes underlying neuroregeneration or neuroprotection. In the case of protection of ischemic retinal ganglion cells by intravitreal BDNF, the presence of c-Jun is required [43]. Moreover, JunD can confer protection by antagonization of the p53 expression; thus, c-Jun might be involved in neuroprotection as a docking molecule for JNKs, allowing these kinases to activate JunD [44]. Our results showed that Fos family members were more represented among DEGs in astrocytes upon CO exposure when compared with the Jun counterparts, so the former family of genes may have a different expression timing or be less relevant in astrocytes.

Several genes related to cytoskeleton were also differentially expressed in astrocytes incubated with CO, and their roles are involved in protrusions formation, cell motility and morphology. Astrocytes present an increased number of processes when in a reactive state, and therefore, it is not surprising that the components of the cytoskeleton machinery show altered expression upon exposure to external stimuli. On the other

hand, considering that the cancer-related pathways are composed of large gene networks, perhaps some of these pathways would be beneficial in astrocytes when activated. The latter group includes genes that allow apoptosis escape, proliferation, energy maintenance and sensitivity to growth factors and cytokines. In the last few years, evidence became available for effects of CO on differentiation of neuronal cells [7,27], T-cells [45] and cardiomyocytes [46]. Nevertheless, one reason for CO to promote differentiation might reside on its ability to modulate cell metabolism, cell death and redox responses, rather than triggering specific differentiation pathways.

Although the primary cultures used in this work are enriched in cortical astrocytes, other cell types may also be present in residual number. Therefore, it cannot be excluded that the response of the latter population of cells to CO treatment might be greater and surpass the change in gene expression in astrocytes in some cases. To overcome these limitations, single-cell RNAseq or qRT-PCR would be performed for further validation. Moreover, transcriptional alterations may occur due to RNA stability rather than altered gene expression. To clarify this, validating the RNA sequencing results with nuclear run-on assay would be an option to collect data independent of RNA stability [47].

To investigate the role of the identified pathways in CO-induced astrocytic responses, additional studies are required, several key players in each pathway should be selected for further studies.

Recent studies showed that astrocytes are functionally and morphologically diverse [48]. Building evidence points to the fact that this heterogeneity is expressed at different levels, including development, genomes, astrogliosis, and cell-cell interactions [49]. Each subtype of astrocytes express different markers and play important roles in several CNS trauma and diseases. For example, the astrocytes located in the subventricular zone present high expression of GFAP, GLAST, and nestin being able to migrate towards a lesion site and give rise to new neurons following injury [49]. Therefore, it is possible that different subtypes of astrocytes may respond in a distinct manner to CO treatment. Characterization of vital genes of different subtypes of astrocytes may clarify the detailed roles of astrocytes in neuroprotection and in regeneration and how CO can help in this process.

It is also well-established that the mRNA expression does not always convert into similar changes in the abundance of the respective protein. As this work was performed with transcriptome sequencing, it is possible that the protein expression of fundamental genes might not precisely mirror the gene expression data reported. Thus, future work should be focused in the validation of the alterations in protein expression and the role of these changes in the responses to CO.

In conclusion, astrocytes may be an indirect target for neuroprotection upon CO treatment. This work provides information for a cell-type-specific approach to CO treatment, while further exploration of the detailed functions and regulatory mechanisms is required.

ACKNOWLEDGEMENTS

We thank Pedro Fernandes for his support and expertise on RNAseq data analysis. SRO was supported by a fellowship from Fundação para a Ciência e a Tecnologia (FCT) with reference SFRH/BD/51969/2012. This work was supported by FEDER (QREN) through Programa Mais Centro, under projects CENTRO-07-ST24-FEDER-002002, CENTRO-07-ST24-FEDER-002006 and CENTRO-07-ST24-FEDER-002008, through Programa Operacional Factores de Competitividade - COMPETE and national funds via FCT under projects Pest-C/SAU/LA0001/2013-2014, PTDC/SAU-NMC/120144/2010, PTDC/NEU-NMC/0198/2012 and FCT-ANR/NEU-NMC/0022/2012.

REFERENCES

[1] B. Wegiel, D.W. Hanto, L.E. Otterbein, The social network of carbon monoxide in medicine., Trends Mol. Med. 19 (2013) 3–11. doi:10.1016/j.molmed.2012.10.001.

[2] C.S.F. Queiroga, A. Vercelli, H.L.A. Vieira, Carbon monoxide and the CNS: Challenges and achievements, Br. J. Pharmacol. (2014) 1–13. doi:10.1111/bph.12729.

[3] N. Schallner, C.C. Romão, J. Biermann, W.A. Lagrèze, L.E. Otterbein, H. Buerkle, T. Loop, U. Goebel, Carbon Monoxide Abrogates Ischemic Insult to Neuronal Cells via the Soluble Guanylate Cyclase-cGMP Pathway, PLoS One. 8 (2013). doi:10.1371/journal.pone.0060672.

[4] H.L.A. Vieira, C.S.F. Queiroga, P.M. Alves, Pre-conditioning induced by carbon monoxide provides neuronal protection against apoptosis, J. Neurochem. 107 (2008) 375–384. doi:10.1111/j.1471-4159.2008.05610.x.

[5] C.S.F. Queiroga, A.S. Almeida, C. Martel, C. Brenner, P.M. Alves, H.L.A. Vieira, Glutathionylation of adenine nucleotide translocase induced by carbon monoxide prevents mitochondrial membrane permeabilization and apoptosis., J. Biol. Chem. 285 (2010) 17077–88. doi:10.1074/jbc.M109.065052.

[6] A.S. Almeida, C.S.F. Queiroga, M.F.Q. Sousa, P.M. Alves, H.L.A. Vieira, Carbon monoxide modulates apoptosis by reinforcing oxidative metabolism in astrocytes: role of Bcl-2., J. Biol. Chem. 287 (2012) 10761–70. doi:10.1074/jbc.M111.306738.

[7] A.S. Almeida, N.L. Soares, M. Vieira, J.B. Gramsbergen, H.L.A. Vieira, Carbon monoxide releasing molecule-A1 improves neurogenesis:increase of neuronal differentiation yield by preventing cell death,PLoSOne.(2016)1–24. doi:10.1371/journal.pone.0154781.

[8] F. Ulbrich, U. Goebel, D. Böhringer, P. Charalambous, W.A. Lagrèze, J. Biermann, Carbon monoxide treatment reduces microglial activation in the ischemic rat retina., Graefes Arch. Clin. Exp. Ophthalmol. 254 (2016) 1967–1976. doi:10.1007/s00417-016-3435-6.

[9] M.G. Bani-Hani, D. Greenstein, B.E. Mann, C.J. Green, R. Motterlini, Modulation of thrombin-induced neuroinflammation in BV-2 microglia by carbon monoxide-releasing molecule 3, J Pharmacol Exp Ther. 318 (2006) 1315–1322. doi:10.1124/jpet.106.104729.

[10] R. Foresti, S.K. Bains, T.S. Pitchumony, L.E. De Castro Brás, F. Drago, J.L. Dubois-Randé, C. Bucolo, R. Motterlini, Small molecule activators of the Nrf2-HO-1 antioxidant axis modulate heme metabolism and inflammation in BV2 microglia cells, Pharmacol. Res. 76 (2013) 132–148. doi:10.1016/j.phrs.2013.07.010.

[11] B. Wang, W. Cao, S. Biswal, S. Doré, Carbon monoxide-activated Nrf2 pathway leads to protection against permanent focal cerebral ischemia., Stroke. 42 (2011) 2605–10. doi:10.1161/STROKEAHA.110.607101.

[12] C.S.F. Queiroga, S. Tomasi, M. Widerøe, P.M. Alves, A. Vercelli, H.L.A. Vieira, Preconditioning Triggered by CO Provides Neuronal Protection Following Perinatal Hypoxia-Ischemia,PLoSOne7(2012)e42632. doi:10.1371/journal.pone.0042632.

[13] A. Yabluchanskiy, P. Sawle, S. Homer-Vanniasinkam, C.J. Green, R. Foresti, R. Motterlini, CORM-3, a carbon monoxide-releasing molecule, alters the inflammatory response and reduces brain damage in a rat model of hemorrhagic stroke., Crit. Care Med. 40 (2012) 544–52. doi:10.1097/CCM.0b013e31822f0d64.

[14] Â.A. Chora, P. Fontoura, A. Cunha, T.F. Pais, S. Cardoso, P.P. Ho, L.Y. Lee, R.A. Sobel, L. Steinman, M.P. Soares, Heme oxygenase–1 and carbon monoxide suppress autoimmune neuroinflammation, J.Clin.Invest.117(2007)438–447. doi:10.1172/JCI28844.

[15] P. Fagone, K. Mangano, C. Quattrocchi, R. Motterlini, R. Di Marco, G. Magro, N. Penacho, C.C. Romao, F. Nicoletti, Prevention of clinical and histological signs of proteolipid protein (PLP)-induced experimental allergic encephalomyelitis (EAE) in mice by the water-soluble carbon monoxide-releasing molecule (CORM)-A1, Clin.Exp.Immunol.163(2011)368–374. doi:10.1111/j.1365-2249.2010.04303.x.

[16] R. Motterlini, J.E. Clark, R. Foresti, P. Sarathchandra, B.E. Mann, C.J. Green, Carbon Monoxide-Releasing Molecules: Characterization of Biochemical and Vascular Activities, Circ. Res. 90 (2002) e17–e24. doi:10.1161/hh0202.104530.

[17] C.C. Romão, W. a Blättler, J.D. Seixas, G.J.L. Bernardes, Developing drug molecules for therapy with CO.,Chem.Soc.Rev.41(2012)3571–83. doi:10.1039/c2cs15317c.

[18] R. Motterlini, P. Sawle, J. Hammad, S. Bains, R. Alberto, R. Foresti, C.J. Green, CORM-A1: a new pharmacologically active carbon monoxide-releasing molecule., FASEB J. 19 (2005) 284–6. doi:10.1096/fj.04-2169fje.

[19] I. Allaman, M. Be, P.J. Magistretti, Astrocyte – neuron metabolic relationships : for better and for worse, Trends Neurosci. 34 (2011). doi:10.1016/j.tins.2010.12.001.

[20] J.D. Cahoy, B. Emery, A. Kaushal, L.C. Foo, J.L. Zamanian, K.S. Christopherson, Y. Xing, J.L. Lubischer, P.A. Krieg, S.A. Krupenko, W.J. Thompson, B.A. Barres, A Transcriptome Database for Astrocytes , Neurons , and Oligodendrocytes : A New Resource for Understanding Brain Development and Function, 28 (2008) 264–278. doi:10.1523/JNEUROSCI.4178-07.2008.

[21] J. Dulak, A. Józkowicz, Carbon monoxide — a " new " gaseous modulator of gene, Acta Bioch. Pol. 50 (2003).

[22] S.W. Ryter, A.M.K. Choi, Targeting heme oxygenase-1 and CO for therapeutic modulation of inflammation,Transl.Res.167(2016)7–34. doi:10.1016/j.trsl.2015.06.011.

[23] S.W. Ryter, D. Morse, A.M.K. Choi, Carbon monoxide: to boldly go where NO has gone before, Sci. STKE. 27 (2004) 3145–3165. doi:10.1002/cpe.3463.

[24] N. Schallner, M. Fuchs, C.I. Schwer, T. Loop, H. Buerkle, W.A. Lagrèze, C. van Oterendorp, J. Biermann, U. Goebel, Postconditioning with Inhaled Carbon Monoxide Counteracts Apoptosis and Neuroinflammation in the Ischemic Rat Retina, PLoS One. 7 (2012). doi:10.1371/journal.pone.0046479.

[25] L. Pellerin, P.J. Magistretti, Sweet sixteen for ANLS, J Cereb Blood Flow Metab. 32 (2012) 1152–1166. doi:10.1038/jcbfm.2011.149.

[26] B. Wegiel, D. Gallo, E. Csizmadia, C. Harris, J. Belcher, G.M. Vercellotti, N. Penacho, P. Seth, V. Sukhatme, A. Ahmed, P.P. Pandolfi, L. Helczynski, A. Bjartell, J.L. Persson, L.E. Otterbein, Carbon monoxide expedites metabolic exhaustion to inhibit tumor growth, Cancer Res. 73 (2013) 7009–7021. doi:10.1158/0008-5472.CAN-13-1075.

[27] A. Almeida, U. Sonnewald, P.M. Alves, H.L.A. Vieira, Carbon monoxide improves neuronal differentiation and yield by increasing the functioning and number of mitochondria, J Neurochem. (2016). doi:10.1111/jnc.13653.

[28] C.S.F. Queiroga, R.M.A. Alves, S. V. Conde, P.M. Alves, H.L.A. Vieira, Paracrine effect of carbon monoxide – astrocytes promote neuroprotection through purinergic signaling in mice, J. Cell Sci. 129 (2016) 3178–3188. doi:10.1242/jcs.187260.

[29] L. Hertz, B.H.J. Juurlink, E. Hertz, H. Fosmark, a Schousboe, Preparation of primary cultures of mouse (rat) astrocytes, A Dissection Tissue Cult. Man. Nerv. Syst. (1986).

[30] S. Andrew, FastQC: A quality control tool for high throughput sequence data, Http//www.bioinformatics.babraham.ac.uk/ Proj. (n.d.).

[31] C. Trapnell, L. Pachter, S.L. Salzberg, TopHat: discovering splice junctions with RNA–Seq, Bioinformatics. 25 (2009) 1105–1111.

[32] B. Langmead, S.L. Salzberg, Fast gapped-read alignment with Bowtie 2, Nat Methods. 9 (2012) 357–359.

[33] C. Trapnell, A. Roberts, L. Goff, G. Pertea, D. Kim, D.R. Kelley, H. Pimentel, S.L. Salzberg, J.L. Rinn, L. Pachter, Differential gene and transcript expression analysis of RNA-seq experiments with TopHat and Cufflinks, Nat Protoc. 7 (2012) 562–578. doi:10.1038/nprot.2012.016.

[34] K. García-Alcalde, F. Okonechnikov, J. Carbonell, L.M. Cruz, S. Götz, S. Tarazona, J. Dopazo, T.F. Meyer, A. Conesa, Qualimap: evaluating next-generation sequencing alignment data, Bioinformatics. 28 (2012) 2678–9. doi:10.1093/bioinformatics/bts503.

[35] S. Ghosh, C.K. Chan, Analysis of RNA-Seq Data Using TopHat and Cufflinks, Methods Mol Biol. 1374 (2016) 339–61. doi:10.1007/978-1-4939-3167-5_18.

[36] E.Y. Chen, C.M. Tan, Y. Kou, Q. Duan, Z. Wang, G.V. Meirelles, N.R. Clark, A. Ma'ayan, Enrichr: interactive and collaborative HTML5 gene list enrichment analysis tool, BMC Bioinformatics. 14 (2013). doi:10.1186/1471-2105-14-128.

[37] D. Szklarczyk, A. Franceschini, S. Wyder, K. Forslund, D. Heller, J. Huerta-Cepas, M. Simonovic, A. Roth, A. Santos, K.P. Tsafou, M. Kuhn, P. Bork, L.J. Jensen, C. von Mering, STRING v10: protein-protein interaction networks, integrated over the tree of life., Nucleic Acids Res. 43 (2015) d447-52. doi:10.1093/nar/gku1003.

[38] S.R. Oliveira, H.L.A. Vieira, C.B. Duarte, Effect of carbon monoxide on gene expression in cerebrocortical astrocytes: Validation of reference genes for quantitative real-time PCR, Nitric Oxide. 49 (2015) 80–89. doi:10.1016/j.niox.2015.07.003.

[39] Motterlini, R. and Foresti, R., Heme Oxygenase-1 As a Target for Drug Discovery, Antioxid.RedoxSignal.(2014)1–57. doi/abs/10.1089/ars.2013.5658.

[40] A. Agarwal, S. Bolisetty, Adaptive responses to tissue injury: role of heme oxygenase-1., Trans. Am. Clin. Climatol. Assoc. 124 (2013) 111–22. http://www.pubmedcentral.nih.gov/articlerender.fcgi?artid=3715920&tool=pmcentrez&rendertype=abstract.

[41] P.-L. Chi, C.-C. Lin, Y.-W. Chen, L.-D. Hsiao, C.-M. Yang, CO Induces Nrf2-Dependent Heme Oxygenase-1 Transcription by Cooperating with Sp1 and c-Jun in Rat Brain Astrocytes, Mol. Neurobiol. 52 (2015) 277–292. doi:10.1007/s12035-014-8869-4.

[42] T. Herdegen, V. Waetzig, AP-1 proteins in the adult brain: facts and fiction about effectors of neuroprotection and neurodegeneration, Oncogene. 20 (2001) 2424–2437.

[43] T. Kurokawa, N. Katai, H. Shibuki, S. Kuroiwa, Y. Kurimoto, C. Nakayama, N. Yoshimura, BDNF diminishes caspase-2 but not c-Jun immunoreactivity of neurons in retinal ganglion cell layer after transient ischemia., Invest Ophthalmol Vis Sci. 40 (1999) 3006–11.

[44] T. Kallunki, T. Deng, M. Hibi, M. Karin, c-Jun can recruit JNK to phosphorylate dimerization partners via specific docking interactions., Cell. 87 (1996) 929–39.

[45] I. Nikolic, M. Vujicic, I. Stojanovic, S. Stosic-Grujicic, T. Saksida, Carbon Monoxide-Releasing Molecule-A1 Inhibits Th1/Th17 and Stimulates Th2 Differentiation In vitro, Scand. J. Immunol. 80 (2014) 95–100. doi:10.1111/sji.12189.

[46] H.B. Suliman, F. Zobi, C.A. Piantadosi, Heme Oxygenase-1/Carbon Monoxide System and Embryonic Stem Cell Differentiation and Maturation into Cardiomyocytes., Antioxid. Redox Signal. 24 (2016) 345–60. doi:10.1089/ars.2015.6342.

[47] S.T. Smale, Nuclear run-on assay, Cold Spring Harb Protoc. 2009 (2009). doi:10.1101/pdb.prot5329.

[48] L. Ben Haim, D. Rowitch, Functional diversity of astrocytes in neural circuit regulation, Nat. Publ. Gr. 18 (2016) 31–41. doi:10.1038/nrn.2016.159.

[49] X. Hu, Y. Yuan, D. Wang, Z. Su, Heterogeneous astrocytes : Active players in CNS, Brain Res. Bull. 125 (2016) 1–18. doi:10.1016/j.brainresbull.2016.03.017.

SUPPLEMENTARY DATA

Table S1 – List of genes identified as being differentially expressed. The first two columns list the 100 upregulated DEGs by descending order of log2 (fold change). The last two columns list the 62 downregulated DEGs by descending order of log2 (fold change). All listed DEGs present more than 1-fold in the CORM-A1 treated cultures with a false discovery rate (FDR) < 0.05.

upregulated: 100			
gene	log2(FC)	gene	log2(FC)
Ccl27a	inf	Actg1	1.39
Crybb3	inf	Mirg	1.38
Gm10029	inf	2310061J03Rik	1.37
Gm9783	+ inf	Dph2	1.35
Mroh7	6.51	Sox2ot	1.34
Mak	4.84	Zfp580	1.33
Vwa3a	4.40	Plcb1	1.32
Susd3	4.14	Wfdc2	1.31
Wnt16	3.70	Gm216	1.31
Lrrtm2	3.61	Il18rap	1.29
Npr1	3.58	Dgkq	1.29
Efhb	3.20	Cntnap2	1.29
Cish	3.16	CAAA01147332.1	1.28
Cdnf	3.11	Zfp365	1.28
2010001M06Rik	3.08	Dennd4b	1.27
Scand1	3.05	Pcsk1n	1.27
Fosb	2.98	Cdk14	1.26
Cyp2d22	2.68	Zfp771	1.26
Extl1	2.66	Pcdhga8	1.22
9330101J02Rik	2.58	Cd300lf	1.21
Cbln3	2.55	1810009N02Rik	1.21
Lcp2	2.34	1810043H04Rik	1.21
A630033H20Rik	2.32	E130012A19Rik	1.21
Tnfsf13b	2.29	Ugt1a6a	1.20
Il2ra	2.26	Lyrm1	1.19
Shroom1	2.20	Snrnp35	1.18
4930539J05Rik	2.11	Gli2	1.17
Ccdc114	2.08	Crocc	1.17
Ptchd2	2.05	Slc15a4	1.16
Gm13238	2.02	Rarres2	1.14
1700030K09Rik	2.02	Mllt6	1.13
Angpt2	2.01	Lhfpl2	1.10
Ttc25	1.91	Rgs10	1.09
Car9	1.88	Itpkc	1.09
Gm14303	1.81	Edc3	1.09
Lonrf3	1.76	Rps6ka1	1.07
Cdc42bpg	1.75	Erdr1	1.07
Sts	1.67	Aspscr1	1.06
Trim46	1.65	Zfp593	1.06
Unc13a	1.65	Ndufb2	1.06
Hmgb1-rs17	1.62	Snapc4	1.04
Gm1673	1.59	Mrgpre	1.04
Abcb4	1.55	Camta1	1.04
Dtwd2	1.55	Plxnd1	1.03
Pex12	1.44	Gadd45a	1.03
Pars2	1.43	Fos	1.02
6430548M08Rik	1.42	Mypop	1.01
Tlr13	1.40	2310036O22Rik	1.01
Map3k14	1.39	Ccdc85c	1.00
5430427O19Rik	1.39	Alg12	1.00

downregulated: 62			
gene	log2(FC)	gene	log2(FC)
Gsta3	- inf	Alyref2	-1.23
Adam3	-inf	Zbtb20	-1.22
Notch4	-6.16	Inpp5a	-1.20
Dpp4	-5.70	Srd5a1	-1.18
Dusp15	-4.59	Mettl25	-1.17
Ccdc155	-4.33	A730098P11Rik	-1.15
Nkain4	-4.03	Sapcd2	-1.15
Unc79	-3.91	Slc4a3	-1.10
Impg2	-3.91	Epsti1	-1.05
Has3	-3.77	Ugcg	-1.04
Wdr17	-3.62	Cyth1	-1.03
Pax8	-3.54	Fam117b	-1.00
Pde10a	-3.35		
Arhgap27	-3.26		
Cdh26	-3.16		
Wnt7a	-3.06		
Ptpn22	-2.90		
Slc4a10	-2.77		
Dab1	-2.76		
Pik3cd	-2.42		
Aass	-2.39		
Rn28s1	-2.27		
Kdm4b	-2.13		
Lars2	-1.97		
Lrrc23	-1.93		
Bcam	-1.87		
Rs5-8s1	-1.75		
Rn18s	-1.75		
Pla2g5	-1.74		
Fam126b	-1.68		
Panx1	-1.67		
Stk36	-1.64		
Pcdhb21	-1.64		
Nphp4	-1.63		
Csmd1	-1.58		
Ptprt	-1.57		
Rhod	-1.52		
Vnn1	-1.49		
Nudt1	-1.48		
4933427D14Rik	-1.47		
Fam102a	-1.43		
Psmd13	-1.36		
Mtcp1	-1.34		
Gpr157	-1.33		
Nup188	-1.28		
Fap	-1.28		
Ccser1	-1.28		
Rpusd3	-1.28		
Zxda	-1.24		
Arhgap32	-1.24		

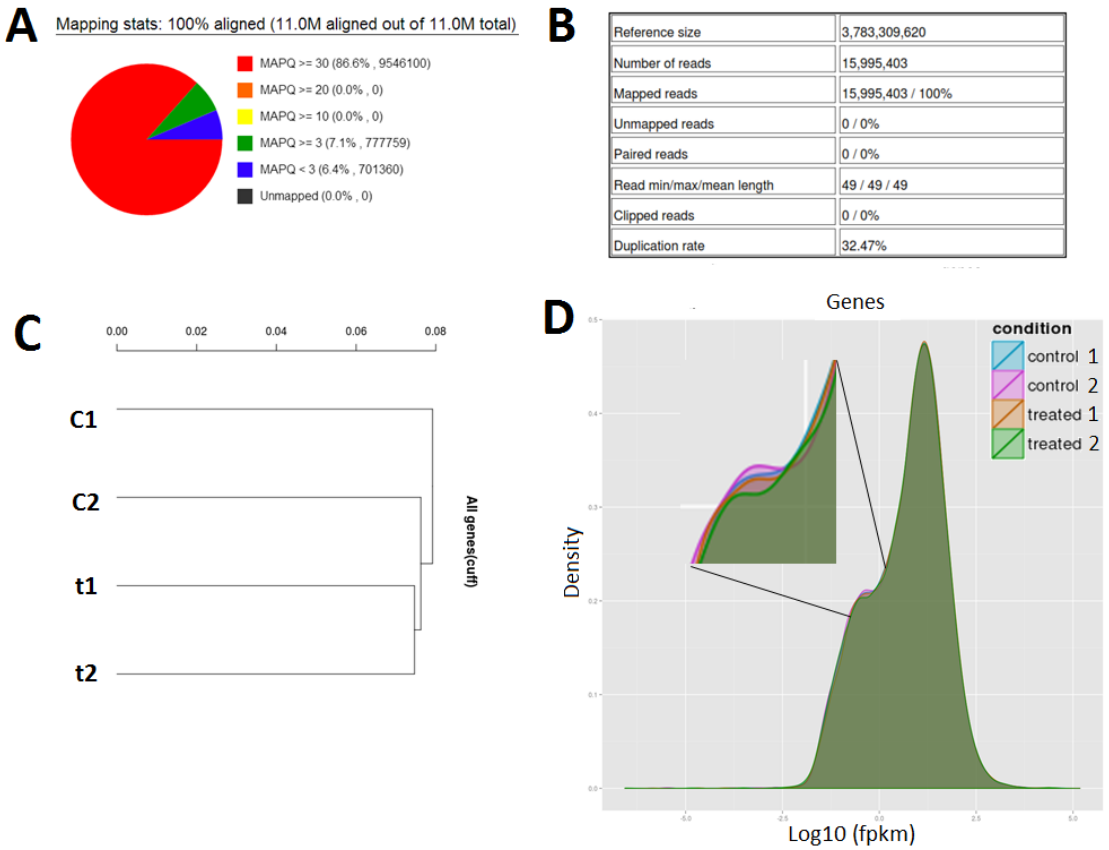

Figure S1 - Assessment of Alignment quality. Alignment was analyzed by 3 different softwares: (A) Qualimap, (B) AlignmentQC (samstats) and (C,D) CummeRbund dendrogram and histogram, respectively. Dendrogram shows the relationship in terms of similarity/closeness among different samples. Density plots show the expression level distribution for all genes in each sample.

Chapter II.II

Validation of Reference Genes

This chapter is based on the following manuscript:

Effect of carbon monoxide on gene expression in cerebrocortical astrocytes: Validation of reference genes for quantitative real-time PCR.
Sara R. Oliveira, Helena L. A. Vieira, Carlos B. Duarte, 2015. *Nitric Oxide*, 49, pp.80–89

INDEX

ABSTRACT

Quantitative real-time reverse transcription-polymerase (qRT-PCR) is a widely-used technique to characterize changes in gene expression in complex cellular and tissue processes, such as cytoprotection or inflammation. The accurate assessment of changes in gene expression depends on the selection of an adequate internal reference gene. Carbon monoxide (CO) affects several metabolic pathways and *de novo* protein synthesis is crucial in the cellular responses to this gasotransmitter.

Herein a selection of commonly used reference genes was analyzed to identify the most suitable internal control genes to evaluate the effect of CO on gene expression in cultured cerebrocortical astrocytes. The cells were exposed to CO by treatment with CORM-A1 (CO releasing molecule A1) and four different algorithms (geNorm, NormFinder, Delta Ct and BestKeeper) were applied to evaluate the stability of eight putative reference genes.

Our results indicate that *Gapdh* (glyceraldehyde-3-phosphate dehydrogenase) together with *Ppia* (peptidylpropyl isomerase A) is the most suitable gene pair for normalization of qRT-PCR results under the experimental conditions used. *Pgk1* (phosphoglycerate kinase 1), *Hprt1* (hypoxanthine guanine phosphoribosyl transferase I), Sdha (Succinate Dehydrogenase Complex, Subunit A), *Tbp* (TATA box binding protein), *Actg1* (actin gamma 1) and *Rn18s* (18S rRNA) genes presented less stable expression profiles in cultured cortical astrocytes exposed to CORM-A1 for up to 60min.

For validation, we analyzed the effect of CO on the expression of *Bdnf* and *Bcl-2*. Different results were obtained, depending on the reference genes used. A significant increase in the expression of both genes was found when the results were normalized with *Gapdh* and *Ppia,* in contrast with the results obtained when the other genes were used as reference.

These findings highlight the need for a proper and accurate selection of the reference genes used in the quantification of qRT-PCR results in studies on the effect of CO in gene expression.

KEYWORDS

Carbon monoxide, astrocytes, reference genes, quantitative real-time reverse transcription PCR

ABBREVIATIONS

Actg1 - actin gamma 1
Bcl-2 - B-cell leukemia/lymphoma 2
Bdnf - Brain-derived neurotrophic factor
CNS – central nervous system
CO – Carbon monoxide
CORM-A1 – Carbon monoxide releasing molecule A1
Gapdh - glyceraldehyde-3-phosphate dehydrogenase
Hprt1 - hypoxanthine guanine phosphoribosyl transferase I
MAPK – mitogen-activated protein kinase
NO – nitric oxide
Pgk1 - phosphoglycerate kinase 1
Ppia - peptidylpropyl isomerase A
PPARɣ - Peroxisome proliferator-activated receptor gamma
qRT-PCR - Quantitative real-time reverse transcription-polymerase
Rn18s - 18S rRNA
Sdha - Succinate Dehydrogenase Complex, Subunit A
sGC – soluble guanylyl cyclase
Tbp - TATA box binding protein

1. INTRODUCTION

Carbon monoxide (CO) is a gasotransmitter with a well-documented role in both inter- and intracellular signaling in the brain as well as in other tissues [1, 2]. Several studies have addressed the molecular mechanisms underlying the effects of CO in the treatment of pathologies as diverse as vascular and cerebral diseases, cancer and inflammation [3–15]. Exogenous administration of CO is beneficial in several pathologies [3–7,16–20] by acting as metabolic modulator [20], anti-apoptotic molecule [21], anti-inflammatory agent [22], stemness regulator [23], vasodilator [24], modulator of proliferation [25] and anti-rejection agent in organ transplantation [26]. The effects of CO, either from exogenous or endogenous sources, are mediated by multiple pathways, including mitogen-activated protein kinases (MAPKs), nitric oxide (NO), soluble guanylyl cyclase (sGC), peroxisome proliferator-activated receptor gamma (PPARɣ) [3–5,27] and mitochondrial function (cell death control and cell metabolism) [28]. In the Central Nervous System (CNS) CO limits neuroinflammation [29,30] and promotes cytoprotection in *in vivo* cerebral ischemia [11,31]. *In vitro* experiments showed that CO prevents apoptosis in neurons [32,33] and in astrocytes [34,35]. Astrocytes play very important roles in the brain, conferring physical and metabolic support to neurons, releasing gliotransmitters and up-taking toxic factors. Astrocytes also modulate the activity of other brain cells (*e.g.* microglia) [9]. Therefore, targeting astrocytes is a promising strategy for promoting neuroprotection and limiting neuroinflammation [36]. In summary, the effects of endogenous or exogenous CO in astrocytes may also have secondary beneficial functions in other brain cell types.

Unveiling the cellular and molecular responses to CO, namely at the transcriptional level, is crucial for further understanding the mechanisms underlying its role in cytoprotection. The evaluation of changes in transcription activity typically relies in quantitative real-time reverse transcription-polymerase chain reaction (qRT-PCR), due to the high sensitivity and accuracy of this powerful tool for measuring specific RNA levels. To minimize gene and sample variations, an internal control is used to normalize the entire set of data for proper comparison between experimental conditions. A multitude of strategies are available for relative quantification of RNA levels, although the most commonly used is the normalization with a reference gene [37]. A reference gene is an endogenous control that is exposed to the same manipulations as the target genes and is measured by the same methodology. An optimal reference gene should present an invariable expression across tissue, manipulation and/or stimuli. Since this may not occur, in particular under conditions that induce multiple changes in gene expression, validation for each specific tissue or cell type and stimulus is needed. For example, the β-actin, β-2 microglobulin and glyceraldehyde-3-phosphate-dehydrogenase genes are classically used as reference genes in qRT-PCR studies, but their expression levels were found to change with cell proliferation and differentiation [38,39]. Therefore, applying unsuitable reference genes can generate false data. The multiple effects of CO on gene expression [40] makes difficult the choice of reference genes for gene expression analysis since some of the genes typically used as internal controls in other systems may also be affected by the gasotransmitter or simply are not the most stable genes.

The aim of this study was to identify accurate endogenous control genes for normalization of gene expression induced by CO in mouse cortical astrocytes. From all the available algorithms to evaluate the stability of gene expression, none can be classified as the optimal, since each of them is based on different assumptions, parameters and statistical approaches [41]. Therefore, and in order to guarantee the choice of the best reference gene(s) with the highest confidence possible, data were processed by four different tools, geNorm [42], NormFinder [43], DeltaCt [44] and BestKeeper [45]. The first two computational tools were used through the GenEx software, while the last two were obtained *via* free online access at the RefFinder integrative platform. Eight potential internal control genes were selected and changes in their expression were analyzed in astrocytic cultures treated with CO. Our results highlight the importance of a cautious assessment of the reference genes in the particular case of CO treatment.

2. MATERIALS AND METHODS

2.1. Selection of reference genes

Candidate reference genes evaluated were carefully chosen from the literature, being the most commonly used and/or suggested to be adequate for studies on the effects of CO on gene expression or its related pathways (Table 1).

2.2. Cortical astrocyte cultures

Primary cultures of mouse cortical astrocytes were prepared from the cortices of P3–P4 Bl6/c57 mice pups after mechanical dissociation, as previously described [46]. Briefly, cerebral hemispheres were carefully freed of the meninges and the dissected cortices were washed in ice-cold PBS, dissociated mechanically and passed through a 70 µm nylon cell strainer (BD Falcon™) into Dulbecco's minimum essential medium containing 1 g/L glucose (Sigma) and supplemented with 20% (v/v) fetal bovine serum (FBS; Gibco® Life Technologies) and 1% (v/v) penicillin/streptomycin solution (Gibco® Life Technologies). Single-cell suspensions were plated in cell culture flasks (8 to 10 cortices/75 cm^2, Orange Scientific) and maintained in a humidified atmosphere of 5% CO_2 / 95% air at 37°C. After 8 days in culture, the phase dark cells growing on the astrocytic cell layer were detached by vigorous shaking and removed. Culture medium was replaced twice a week for 3 weeks with gradual reduction in FBS content (2^{nd} week 15%; 3^{rd} week 10%). The confluent astrocytic cultures were mildly trypsinized (0.05% (w/v) trypsin/EDTA, Gibco®) and subcultured in 6-well plates until full confluence.

2.3. Administration of CO to astrocytic culture

CORM-A1, a CO releasing molecule [47], was used to deliver CO to cultured astrocytes. CORM-A1 (Sigma) stock solution was prepared in PBS to a final concentration of 10 mM and stored at -20°C to avoid loss of released CO. Time points for CORM-A1 treatment were selected from the incubation times that were found to trigger a protective preconditioning effect in astrocytes subjected to oxidative stress (data not shown). RNA extraction was performed at 30 min, 40 min and 60 min after CORM-A1 addition to the culture medium, at a final concentration of 12.5 µM. Non-supplemented PBS was added to controls.

2.4. Total RNA isolation and assessment of quality and concentration of RNA

The full content of a six-well cluster plate, with a density of $4.5x10^5$ cells/well, was collected for each experimental condition and total RNA from cortical astrocytes was extracted with TRIzol (Invitrogen Life Technologies), following the manufacturer's specifications. After addition of chloroform and phase separation, the RNA was precipitated with isopropanol. The precipitated RNA was washed once with 75% ethanol, centrifuged, air dried, and resuspended in 20 µL of RNase free water (Gibco Life

Technologies). The whole procedure was performed at 4°C. RNA concentration and purity were determined by spectrophotometry (NanoDrop 2000; Thermo Scientific). RNA quality and integrity was assessed using the Experion RNA StdSens automated gel electrophoresis system (Bio-Rad). A virtual gel was created for each sample, allowing the detection of degradation of the reference markers RNA18S and 28S. The system labels each sample with a RNA Quality Indicator (RQI), ranging from 1 to 10. Samples were discarded when showing RQI ≤7, indicating that they presented RNA degradation, poor integrity or contamination by DNA. Samples were stored at -80°C until further use.

2.5. Reverse transcription PCR

For cDNA synthesis, 1 µg of total RNA was reverse transcribed using iScript™ cDNA Synthesis Kit (Bio-Rad) according to manufacturer instructions. Briefly, the samples were defrosted on ice, and the PCR reaction mix was added to a 20 µL final volume. The reaction protocol started with a 5-min step at 25ºC, followed by 30 min at 42°C and ended with a 5-min step at 85°C (T100™ Thermal Cycler, Bio-Rad). Samples were stored at -20ºC until further use.

2.6. Primer design

Primers for real-time PCR were designed by Beacon Designer 8.13 software (Premier Biosoft International). In order to guarantee the optimal primer pair, the following considerations were taken: (i) GC content close to 50%; (ii) annealing temperature (T_a) between 52°C and 69°C; (iii) secondary structures and primer–dimers were avoided; (iv) cross homology regions were avoided (database chosen was RefSeqRNA); (v) primer length from 18 to 24 bp; (vi) final product length from 75 to 250 bp. Used primers are detailed described in Table 2.

2.7. Real-time PCR

For the gene expression study, 2 µL of 1:10 diluted cDNA was added to 10 µL 2x SsoFast™ EvaGreen Supermix (Bio-Rad), and the final concentration of each primer was 250 nM in 20 µL final volume. The thermocycling reaction was initiated with activation of Sso7d-fusion DNA polymerase by heating at 95°C during 30 seconds, followed by 40 cycles of a 10-sec denaturation step at 95°C, a 30-second annealing step at 55°C, and a 30-second elongation step at 72°C. The fluorescence was measured after the extension step by the iQ™5 Multicolor Real-Time PCR Detection System (Bio-Rad). After the thermocycling reaction, the melting step was performed, from 55°C up to 95°C, with an increment of 0.5°C each 10 sec. Continuous measurement of fluorescence allowed the detection of possible nonspecific products. The assay included a non-template control and a standard curve (three 1:10 sequential dilution steps) of cDNA for assessing the efficiency of all primer pairs. The reactions were run in duplicate to reduce confounding variance and average results were calculated.

2.8. Gene expression analysis

Since all primer pairs presented efficiency close to 100%, the data was processed using the $2^{-\Delta Ct}$ method, an adapted version of the $2^{-\Delta\Delta Ct}$ method [48], with $\Delta C_t = C_{t\ condition\ x} - C_{t\ control}$. The control corresponds to the reference condition representing 1-fold expression of each gene. The threshold cycle (C_t) refers to the cycle at which the fluorescence signal is detectable above background due to the accumulation of amplified product. This value is proportional to the starting target sequence copy number. C_t was measured in the exponential phase and, therefore, it was not affected by possible limiting components in the reaction. For every run performed, the threshold was set at the same fluorescence value (100 RFU).

2.9. Evaluation of the stability in the expression of reference genes

Data analysis was performed by three different programs and one web-based comprehensive tool to have a stronger confidence about the variability of the genes under study. geNorm and NormFinder algorithms were used through GenEx software for real-time PCR expression profiling (MultiD Analyses; http://www.multid.se/genex/cnt.htm). geNorm calculates the expression stability value (M) for each gene, which is the average pairwise variation of a particular gene compared with the remaining candidate reference genes. The lower the M value, the more stable is the expression of the gene [42]. NormFinder uses a model-based approach to assess the overall variation in the expression of the candidate reference gene. Besides estimating the stability of a particular gene, NormFinder also provides information about the optimal number of reference genes for normalization purposes [43]. The Delta C_t method evaluates the gene expression stability by comparing relative expression of ‘‘gene pairs’’ within each sample [44]. The BestKeeper algorithm uses the geometric mean of the C_t values with a standard deviation (SD) [49]. Furthermore, the RefFinder was used since it combines four different algorithms (geNorm, NormFinder, BestKeeper and comparative ΔC_t method). This comprehensive tool compares and ranks the candidate genes by integrating the results from all the four algorithms (http://www.leonxie.com/referencegene.php).

2.10. Statistical analysis

Data are presented as the mean ± standard error of the mean (SEM). A one-way analysis of variance (ANOVA) test was used to identify significant differences between experimental conditions for each candidate control gene, followed by Dunnett's Multiple Comparison Test. Statistical analysis was performed using GraphPad Prism 5 (GraphPad Software, Inc.).

3. RESULTS

3.1. Evaluation of candidate reference gene expression in astrocytes after administration of CORM-A1

To characterize the effect of exogenous administration of CO at the transcription level in cortical astrocytic cultures, cells were treated with CORM-A1 for different periods of time and eight candidate genes were evaluated as putative internal controls. Since CORM-A1 releases CO in a slow manner, with a half-life of 21 min [47], and aiming to determine early cellular CO effects, the treatment times used in the study were 30, 40 and 60 minutes of CORM-A1 exposure. At the concentration used (12.5 μM) CORM-A1 presents cytoprotective effects on cultured mouse astrocytes exposed to oxidative stress conditions (not shown).

The selection of four of the genes to be studied, *Gapdh*, *Rn18s, Ppia* and *Pgk1*, was based on previously published work (Table 1). These genes have been used as internal controls in studies analyzing the effect in gene expression of both exogenous CO administration and endogenous CO production, across different cell types and tissues. *Hprt1* and *Tbp* were also tested in the present study as they were proposed as internal controls for the analysis of gene expression in mouse tissue (http://www.tataa.com/products-page/gene_expression_assays_panels/single-assays-reference-gene-panel-mouse/). *Sdha* was included in the present analysis due to previous evidence validating it as a suitable reference gene for human brain tissue [50] and for cultured astrocytes after a period of *in vitro* ischemia [51]. Although it is more common to use *Actb* for normalization purposes, *Actg1* was tested as a novel putative reference gene since the beta isoform of actin (*Actb*) was already shown to be altered in several conditions that are also regulated by CO (*e.g.*: proliferation, differentiation) [22,52]. Because β- and ɣ-actin are the only cytoplasm actin isoforms, the selection of *Actg1* as a reference gene aimed at testing a gene that belongs to the cytoskeleton machinery while avoiding problems resulting from low stability in the expression of the *Actb* gene. Actin isoforms are ubiquitous and crucial for cell survival [49]. Together, the eight tested genes are involved in a wide range of pathways, including glycolysis (*Gapdh* and *Pgk1*), cytoskeletal architecture (*Actg1*), regulation of transcription (*Tbp*), protein folding and transport (*Ppia*), purine metabolism (*Hprt1*), oxidative phosphorylation (*Sdha*) and protein synthesis (*Rn18s*).

Table 1 - Reference genes used in the literature to evaluate the expression of CO pathway components or the effect of CO administration.

	Sample Source	Tissue/Cells	Genes Studied	Treatment	Used Controls	Article
Exogenous Carbon Monoxide	-	HepG2	*NQO1, HO-1*	CORM-2 (50μM), CO gas (250 ppm)	*Gapdh*	[53]
	C57BL/6 mouse	HepG2, Liver	*Hepcidin*	CORM-2 (20 μM)	*Gapdh*	[54]
	C57BL/6 and BALB/c mouse	Tracheal tissue	*IFNγ, IL-10, IL-2, IL-17A*	CORM-2 (10 mg/kg)	β-actin (*Actb*)	[55]
	Sprague-Dawley rat	left ventricular apex	*IL-6, IL-10, TNF-α*	CO gas (250 pm)	β-actin (*Actb*)	[56]
	BALB/c mouse and rat	Kidney tissue and UMR106 cells	*Cyp24a1, Cyp27b1, Klotho, FGF23*	CORM-2 (20 mg/kg or 20 μM)	*Gapdh*	[57]
	Human	vastus lateralis muscle tissue	*NRF-1, NRF-2, PGC-1α, Tfam*	CO gas (100 pm)	18S rRNA (*Rn18s*)	[58]
	Wistar rat	Heart tissue	*HCN2, HCN4*	CO gas (150 pm)	*Gapdh*	[59]
	Sprague-Dawley rat	Cerebellar tissue	*Ngb, Cygb*	CO gas (25 ppm)	β-actin (*Actb*)	[60]
	Wistar rat	cerebellar neurons	*Bcl-2*	CO gas (30 μM)	Cyclophilin A (*Ppia*)	[11]
	-	HUVECs	*TF, PAI-1*	CORM-2 (50 μM)	*Gapdh*	[61]
	Wistar rat	cortical astrocytes	*Bcl-2*	CO gas (50 μM)	Cyclophilin A (*Ppia*)	[35]
	Wistar rat	cortical astrocytes	*GDNF*	CORM-2 (30μM)	*Gapdh*	[62]
Endogenous Carbon Monoxide	Wistar rat	cortical astrocytes	*GDNF*	bilirubin (10 μM)	*Gapdh*	[62]
	human	CCF-STTG1	*HO-1, HO-2*	PGD_2 (10 μM)	*Gapdh*	[63]
	Sprague Dawley rat	Cortical neuron/glia cocultures	*HO-1*	METH (5 mM)	β-actin (*Actb*)	[64]
	Sprague Dawley rat	Cortical microglia	*HO-1*	astrocytic conditioned medium	*Gapdh*	[65]
	Sprague Dawley rat	Cortical tissue	*HO-1, AQP-4*	ZnPP and CoPP (0.2 M)	β-actin (*Actb*)	[66]
	Wistar rat	brain tissue, cortical neurons and astrocytes	*HO-1, HO-2, HO-3*	-	*Pgk1*	[67]
	mouse	C26	*HO-1*	hemin (1 μM), THP (0.01 μM)	β-actin (*Actb*)	[68]

Table 2 – Detailed description of the primers used.

Gene	Acession number	Description	Primer sequence (foward & reverse)	Ta (ºC)	Tm (ºC)	Product length (bp)	Primer efficiency (average)	Cell function
Gapdh	NM_008084.2	Mouse glyceraldehyde-3-phosphate dehydrogenase	ACAATGAATACGGCTACAG	57,6	58,8	78	109	Glycolytic enzyme
			GGTCCAGGGTTTCTTACT		59,8			
Ppia	BC059141	Rat peptidylprolyl isomerase A	TTTGGGAAGGTGAAAGAAGGC	54,3	74.9	157	95	Protein folding and transport
			ACAGAAGGAATGGTTTGATGGG					
Pgk1	NM_053291	Rat phosphoglycerate kinase 1	ACAACCAGATAACGAATAAC	53,5	77.2	200	94	Glycolytic enzyme
			CTTCAAGAACAGAACATCC					
Hprt1	NM_012583	Rat hypoxanthine guanine phosphoribosyl transferase 1	CCTTGACTATAATGAGCACTTC	51,1	72.1	126	94	Metabolic salvage of purines in mammals
			GCCACATCAACAGGACTC					
Sdha	NM_023281.1	Mouse succinate dehydrogenase complex, subunit A	CTCATCAACAGTCAAGGT	56,6	57,9	91	96	Glycolytic enzyme, oxidative phosphorylation
			TCATGGATCGAGACACAA		59,4			
Tbp	NM_001004198	Rat TATA box binding protein	CTAACCACAGCACCATTG	53,3	76.5	152	97	Regulation of transcription
			TTACAGCCAAGATTCACG					
Actg1	NM_009609.2	Mouse actin, gamma, cytoplasmic 1	CTGGAATAAGCCTTTGAAA	55,0	56,9	137	105	Cytoskeletal structural protein
			GCACAGGGTATTAAACATAT		56,8			
Rn18s	NR_003278.3	Mouse 18S ribosomal RNA	ACAGGATTGACAGATTGA	56,3	56,8	97	102	Ribosomal protein
			TATCGGAATTAACCAGACA		57			
Bdnf	NM_007540.4	Rat brain-derived neurotrophic factor	TAACCTCGCTCATTCATTA	57,3	49	146	110	Cell Survival
			TCAACTCTCATCCACCTT		50			
Bcl-2	NR_009741.4	Rat B-cell leukemia/lymphoma 2	GGTGGAGGAACTCTTCAGGG	64,2	67,2	251	110	Programmed cell death
			GAGACAGCCAGGAGAAATCA		64,7			

NOTE: The database source is the NCBI Reference Sequence (http://www.ncbi.nlm.nih.gov). Annealing temperature (Ta), melting temperature (Tm) and product length were determined by Beacon Designer software. Primer efficiency was determined by a standard curve of cDNA samples (see Materials and Methods).

As expected, the eight putative reference genes tested were differentially expressed in cultured cortical astrocytes, as determined by the threshold cycle (C_t) for the same fluorescence intensity in qPCR experiments (Fig. 1). Rn18s presented the highest expression level, which is not surprising since it represents the bulk of total RNA.

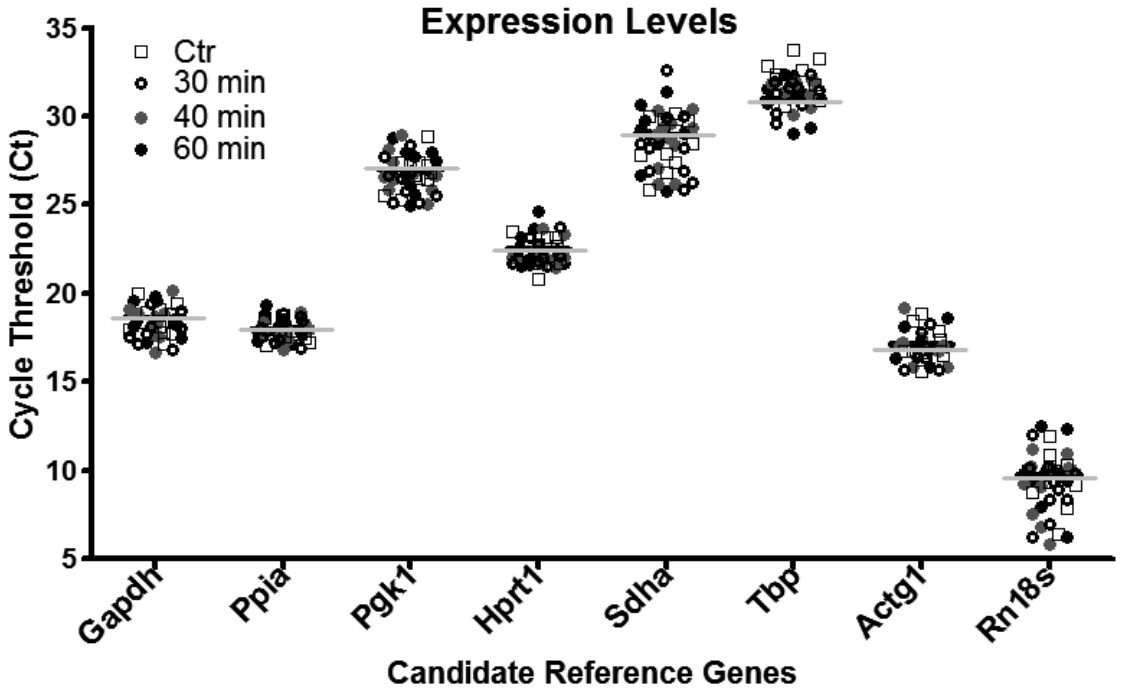

Figure 1 – Expression levels (C_t) of eight putative reference genes tested in primary cultures of cerebrocortical astrocytes. The relative expression values of Gapdh, Ppia, Pgk1, Hprt1, Sdha, Tbp, Actg1 and Rn18s were determined in cultured cortical astrocytes, under control conditions (empty squares) and following incubation with 12.5 µM CORM-A1 for 30 (empty circles), 40 (grey circles) or 60 min (black circles). The data points are the results of at least 9 independent experiments, performed in different cell preparations. The horizontal bars indicate the mean C_t values.

The results of gene expression for *Gapdh*, *Ppia*, *Pgk1*, *Hprt1*, *Sdha*, *Tbp*, *Actg1* and *Rn18s* in cortical astrocytes exposed or not to 12.5 µM of CORM-A1 for 30 min, 40 min and 60 min are presented in Fig. 2. The expression level of *Tbp* was the only one to show significant differences among the conditions evaluated, namely after 30 min (p value < 0.05) and 60 min (p value < 0.01) of exposure to CORM-A1, when compared to the respective untreated control. As shown in Fig. 2F, CORM-A1 induced a near 2-fold increase in *Tbp* expression.

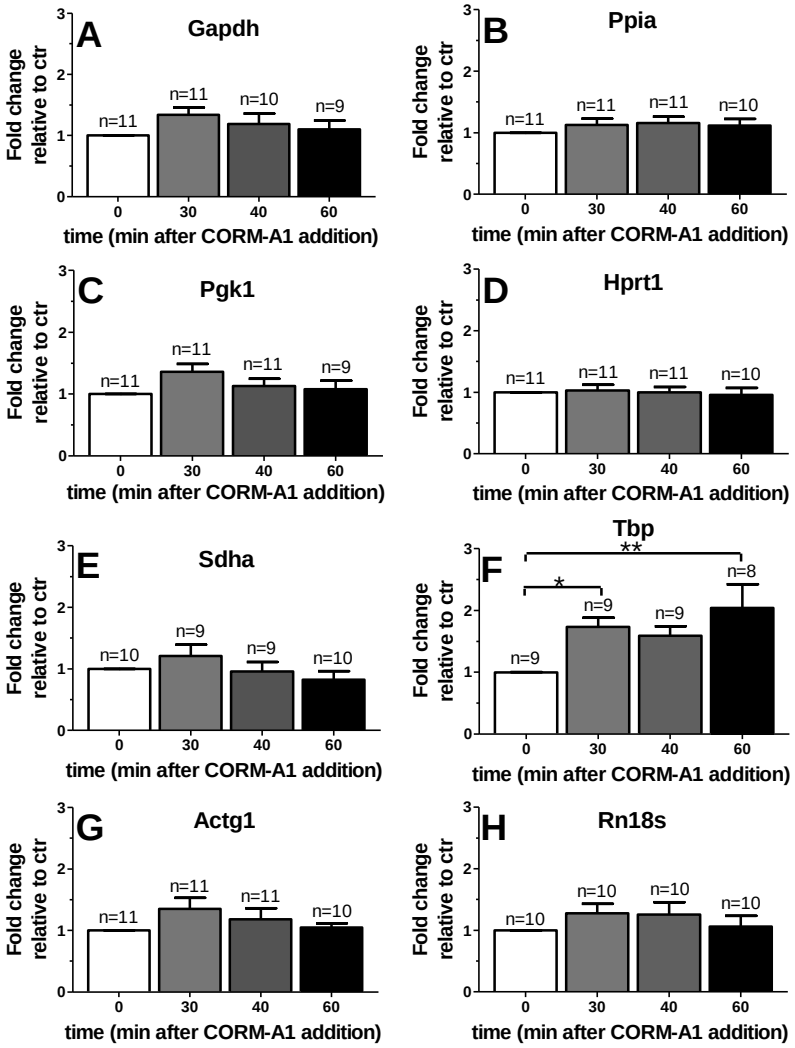

Figure 2 - Effects of CORM-A1 in the expression of putative reference genes in cultured cortical astrocytes. Fold change in the expression of Gapdh (A), Ppia (B), Pgk1 (C), Hprt1 (D), Sdha (E), Tbp (F), Actg1 (G) and Rn18s (H) was analysed by the $2^{-\Delta Ct}$ (see methods for further details). The results are the mean ± SEM of at least 9 independent experiments, performed in different cell preparations. *p<0.05, **p<0.01 when compared with the control.

3.2. Determination of candidate reference genes expression stability in astrocytes following administration of CORM-A1

As shown in the scatterplot of Fig. 1, none of the genes under study presented a constant expression in cortical astrocytes subjected to CO stimulation. The effect of CO on the expression of *Gapdh* (A), *Ppia* (B), *Pgk1* (C), *Hprt1* (D), *Sdha* (E), *Tbp* (F), *Actg1* (G) and *Rn18s* (H) is shown in Fig. 2. The difference between the minimum and maximum C_t values spanned from 2.5 (*Ppia*) to 6.8 (*Sdha*). Therefore, further criteria are needed to choose any gene for normalization purposes. For an accurate selection of the internal control genes, we analyzed the expression stability of the selected genes using four different algorithms: geNorm [42], NormFinder [43], Delta C_t [44] and BestKeeper [45], and merged all the resulting scores in RefFinder.

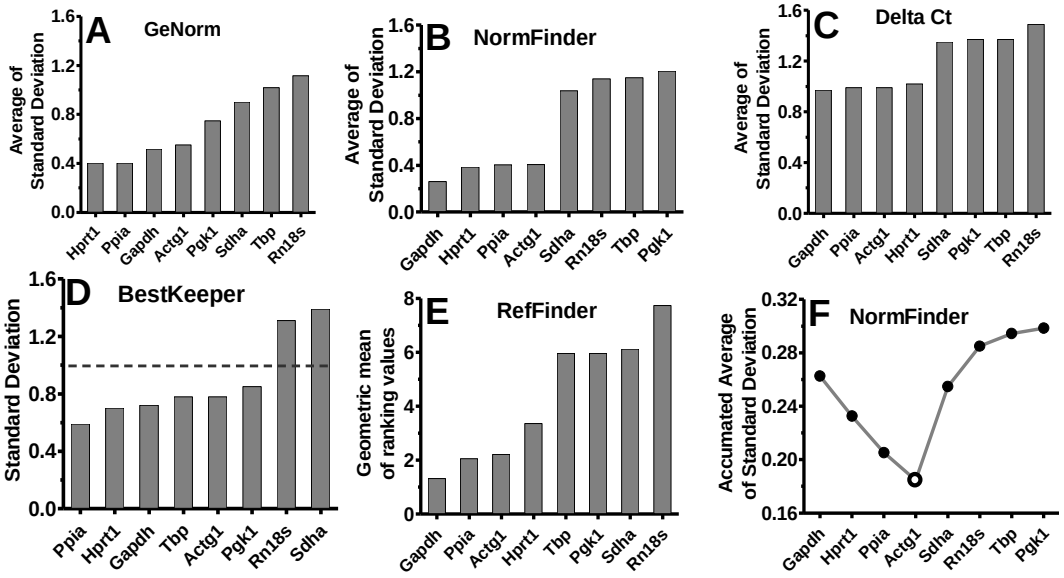

Figure 3 - Stability in the expression of putative reference genes in cultured cortical astrocytes incubated with CORM-1. The stability of gene expression was calculated using GeNorm (A), NormFinder (B, F), Delta Ct (C), BestKeeper (D) and RefFinder (E). The lowest values correspond to the most stable genes. The dashed line in the BestKeeper plot represents the SD threshold for the gene to be considered stable. The empty circle at the NormFinder Acc SD plot indicates the optimal number of reference genes. The raw data analysed is presented in Fig.1.

From the input list of eight candidate reference genes, geNorm identified Hprt1 and Ppia as the most stable genes, with a shared M value of 0.4. On the other hand, Tbp and Rn18s were recognized as the least stable genes with M values higher than 1 (Fig. 3A).

NormFinder, on the other hand, indicated Gapdh and Hprt1 as the most stable genes, with an average standard deviation of 0.2625 and 0.3841, respectively. In partial agreement with the results obtained with geNorm, the least stable genes identified by NormFinder were Tbp and Pgk1 (Fig. 3B). Since NormFinder allows considering different treatment groups, we have also computed gene expression variability under this restriction. The intragroup variation estimated is the standard deviation for the genes belonging to each treatment group (0, 30, 40 and 60 min after CORM-A1 addition), while the intergroup variation is the differential expression and sums to zero for every gene considering all the groups. Suitable reference genes shall present low intragroup variation in all groups and negligible intergroup variation. When considering each one of the groups per experimental condition, NormFinder indicated Gapdh as the most stable gene (standard deviation of 0.1395) and the best pair was Gapdh and Ppia (combined standard deviation of 0.1108) (data not shown).

Analysis of the same sets of data using the Delta C_t method identified Gapdh, Actg1 and Ppia as the most stable genes, with an average standard deviation of 0.97 for the first gene and 0.99 for the last two genes. Tbp and Rn18s presented the highest average standard deviation with this method (Fig. 3C).

The BestKeeper algorithm identified Ppia and Hprt1 as the most stable genes, with standard deviation values of 0.594 and 0.700, respectively. On the other hand, Rn18s

and Sdha genes were found to be the least stable, presenting a standard deviation above 1, which is the recommend threshold [45].

Combining the different outcomes of the four methods with RefFinder, Gapdh and Ppia were found to be the most stable genes with a geometric mean of ranking values of 1.32 and 2.00, respectively. The least stable genes are Sdha and Rn18s, presenting geometric mean of ranking values of 6.12 and 7.74, respectively. When comparing the result of both GeNorm and NormFinder calculated via GenEx (Fig. 3A and 3B) and via RefFinder (Fig. 3E), the ranking order is slightly distinct. The differential results obtained may be due to the fact that RefFinder does not take into account the treatment groups, while this is considered when GenEx is used to run NormFinder.

Although the different methods used to identify gene expression stability are based on different assumptions, it is noticeable that the ranking orders of the four algorithms do not differ much, giving a strong confidence in the obtained results concerning the reference genes to be used for normalization purposes.

3.3. Validation of reference genes with known CO-induced alterations on gene expression

To validate the chosen reference genes, we analyzed the changes in expression of two genes known to be regulated by CO. Administration of CO at low doses or manipulation of its producing enzyme HO-1 was shown to upregulate *Bdnf* (Brain-derived neurotrophic factor) gene expression in several cell types, including diverse populations of neurons, microglia and astrocytes [9,10,62,69]. Similarly, the effect of CO in the upregulation of *Bcl-2* (B-cell leukemia/lymphoma 2) gene expression has been described in different cellular systems, namely brain, retina and kidney [11,35,70–72]. *Bdnf* and *Bcl-2* mRNA levels were evaluated in cultured cerebrocortical astrocytes treated with CORM-A1, and their expression levels was normalized with different groups of the studied reference genes. Prior validation, it is relevant to choose the optimal number of reference genes to use for normalization, in order to minimize costs without compromising accuracy. This can be achieved by using no more than the strictly necessary reference genes, besides being advisable to combine two or more genes to compensate for fluctuations on gene expression in response to CO exposure. For that, since the NormFinder algorithm also calculates the recommended number of reference genes, this information was used to support the decision regarding the number of reference genes used. NormFinder computes this number by accumulated standard deviations. The minimal value corresponds to the result obtained, which was 0.1846 (Fig. 3F), consisting on the combination of the four most stable genes (*Gapdh*, *Hprt1*, *Ppia* and *Actg1*).

Since Gapdh and Ppia were among the three most stable genes identified by every algorithm tested, we compared results for CO-induced expression of Bdnf and Bcl-2 after normalization with Gapdh and Ppia versus Gapdh, Hprt1, Ppia and Actg1 (Fig. 4). When Gapdh and Ppia were used as reference gene pair for assessing the expression of Bdnf and Bcl-2, a significant increase in the expression of both genes was observed in cerebrocortical astrocytes stimulated with CORM-A1 ($p<0.01$ and $p<0.05$, respectively) (Fig. 4A). The same results were obtained when performing the normalization with

Gapdh, Ppia, Hprt1, and Actg1, the genes recommended by the analysis with NormFinder (Fig. 4B). This supports the decision of using only two reference genes instead of four, saving time and reducing expenses without losing statistical power. To further investigate the impact of the number of reference genes used in the normalization procedure, we performed a normalization using only Gapdh. The results obtained for Bdnf expression were similar to those obtained when the normalization was performed with Gapdh and Ppia together. In contrast, the effect on Bcl-2 expression was not statistically significant (Fig. 4C).

To further investigate the importance of selecting appropriate control genes, the effect of CO on the expression of Bdnf and Bcl-2 was analyzed using as reference the two least stable genes identified in this study, Pgk1 and Rn18s (Fig. 5). In contrast with the results obtained when Gapdh and Ppia were used as reference genes, normalization with the two least stable genes showed no significant increase in the expression of Bdnf and Bcl-2 when cerebrocortical astrocytes were treated with CORM-A1 (Fig. 5A). Finally, when Rn18s was used alone in the normalization, no significant effect of CORM-A1 on Bcl-2 expression was observed. Furthermore, the levels of BDNF mRNA at 30 and 40 min after CORM-A1 addition were almost 1-fold lower when compared with those obtained with the best reference genes (Fig. 5B).

In summary, our results identified Gapdh and Ppia as the most suitable endogenous reference genes to evaluate the effects of CORM-A1 treatment on gene expression in cultured murine cerebrocortical astrocytes. Actg1, Hprt1, Tbp, Pgk1, Sdha and Rn18s were identified as the least stable genes and therefore should not be used as a reference.

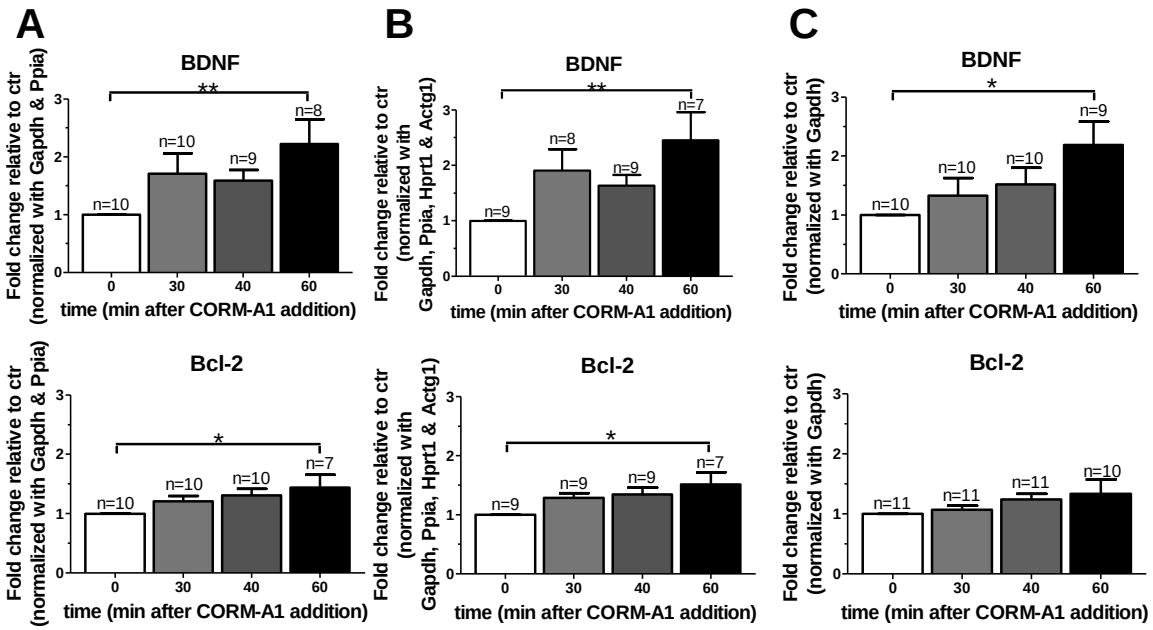

Figure 4 - CORM-A1-induced expression of Bdnf and Bcl-2 as evaluated using different sets of reference genes. Cortical astrocytes were treated or not with 12.5 µM CORM-A1 from 30, 40 or 60 min. Normalizations were performed with (A) the most stable gene pair, (B) the best four genes with the lowest accumulated Standard Deviation (acc SD) as determined with NormFinder and (C) the best gene. The results are the mean ± SEM of the indicated number of independent experiments, performed in different cell preparations. *p<0.05, **p<0.01 when compared with control.

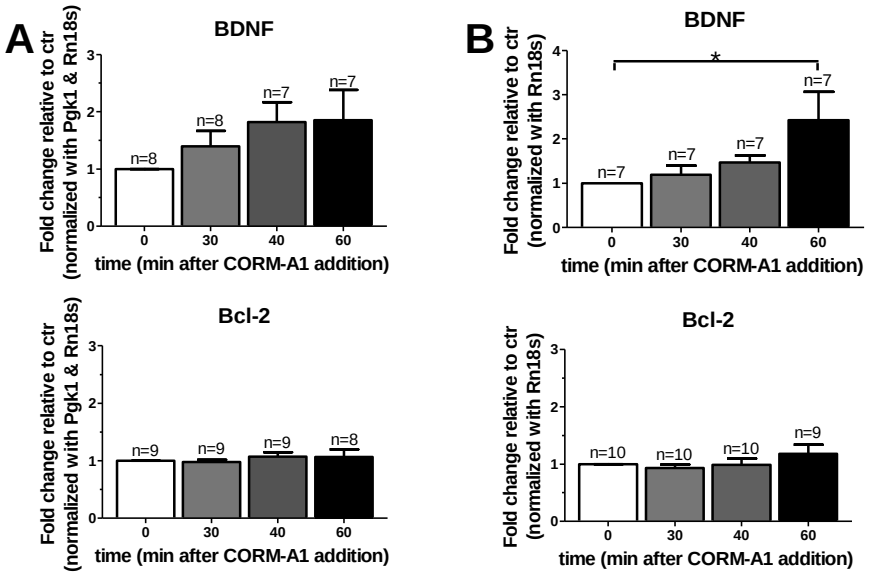

Figure 5 - Effect of different sets of normalization genes in in the evaluation of CORM-A1-induced expression of Bdnf and Bcl-2. Cerebrocortical astrocytes were treated or not with 12.5 µM CORM-A1 from 30, 40 or 60 min. Normalizations were performed with (A) the least stable pair and (B) the gene showing the lowest stability. The results are the mean ± SEM of the indicated number of independent experiments, performed in different cell preparations. *p<0.05 when compared with the control.

4. DISCUSSION

Endogenous reference genes are commonly used to normalize qRT-PCR data, nevertheless they need to be carefully selected since classically used reference genes have already been reported to vary depending on a multitude of variables [37]. In the present work, the variability in the expression of a set of eight putative reference genes was studied in mouse cerebrocortical astrocytes following CORM-A1 treatment. CORM-A1 is a well-established and accepted CO releasing molecule. The optimal conditions at which the CO is released from the chemical backbone structure of CORM-A1 are fully characterized [47], and are similar to those used in the present work to incubate cultured astrocytes (pH = 7.4 and 37ºC). Four distinct algorithms were used for data analysis, giving rise to distinct results. However, *Gapdh* and *Ppia* were among the top three most stable genes in all tested methods. It is interesting to notice that the three most stable genes selected by the applied algorithms (*Gapdh*, *Ppia* and *Actg1*) present a similar expression level, with an average Cycle Threshold of 17.85 $\pm$ 0.65.

The NormFinder algorithm recommended the usage of four of the putative reference genes tested to normalize the results on the effect of CORM-A1 on gene expression. However, analyzing such a large number of genes is cost ineffective and time consuming. Therefore, the degree of improvement and the overall noise contributed by the reference genes should be considered when making a decision about the total number of reference genes to be used. In general, it is a good policy to perform the normalization with at least two genes, since they may compensate each other variation, in particular when the mRNA level of one gene presents more copies at one condition and the other gene presents less copies at the same condition. In fact, in the present study the largest improvement was observed when including the second reference gene (Acc. SD variation of 0.03).

Analysis of the effect of CORM-A1 treatment on the expression of *Bdnf* and *Bcl-2* in astrocytes gave statistically significant differences when the most stable genes were used as a reference, while no effect was observed when the same analysis was performed using the least stable genes. These results show the importance of a careful choice of the reference genes used in gene expression studies testing the effect of CO. In particular, using genes that are upregulated under the same experimental conditions as reference, leads to an underestimation of the effects of CO and vice-versa. The CO-induced upregulation of *Bdnf* expression, with a consequent increase in the signaling activity by TrkB receptors expressed in astrocytes [73], it is likely to affect transcription activity [74,75]. This includes the expression of genes that are often used as reference, being *Rn18s* among the genes which expression is affected by BDNF in cultured hippocampal neurons [76]. Therefore, the activation of neurotrophin receptors may have contributed to the changes in the expression of *Rn18s* observed in this study, particularly for longer incubation periods with CORM-A1.

The use of suitable and unsuitable reference genes was more dramatic in the case of *bcl-2* induction, since the significance was completely lost under the latter conditions (Fig. 5), which would lead to an erroneous conclusion that CO could not induce *bcl-2* gene expression in the present conditions. This problem may occur with other target genes presenting small fold change of their expression. This is particularly critical in cases of fine-tuning complex events or when the concentration and mode of treatment

delivery confers different responses, which is the case of CO. For example, the level of induction of *bcl-2* obtained in the present study is consistent with the previous reported results [35], although an earlier time point was studied here. This difference may be caused by the slower and controlled CO deliver, prompted by the CORM-A1 used in this work, which is distinct from the effects resulting from the use of CO-saturated solutions [35]. The latter method delivers a bolus of CO, to which cells are exposed for a shorter period of time, because CO rapidly diffuses to the atmosphere.

The CORM-2 was shown to upregulate HO-1 gene expression and protein levels in RBA-1 cells, which are derived from primary cultures of neonatal rat astrocytes [77]. The effects of CORM-2 on gene expression were observed upon 2 h of incubation, and were sensitive to inhibitors of reactive oxygen species and protein kinases. Since CORM-A1 releases CO at a slower rate, the rapid effects of this CO donor on gene expression reported here cannot be attributed to the upregulation of HO-1 protein levels. Whether DNA methylation contributes to the effect of CORM-A1 on gene expression in cultured astrocytes remains to be investigated.

To our knowledge, this is the first time that a careful analysis is performed for assessing the impact of a gasotransmitter at the gene expression level. Since CO shares several signaling pathways with other gasotransmitters, namely Nitric Oxide (NO) and hydrogen sulfide (H_2S) [78], it would also be of interest to validate appropriate reference genes in the case of NO or H_2S cell treatment. In fact, since CORM-A1 was previously shown to induce the expression of the inducible and endothelial isoforms of nitric oxide synthase (NOS) [79], thereby increasing NO production, this pathway may also contribute to the delayed responses in gene expression. Whether CORM-A1 regulates H_2S production remains to be determined.

In conclusion, the results from our work emphasize the importance of proper selection of reference genes and the need for validation of their stability in studies where changes in the levels of CO are observed. Furthermore, the results point to the importance of using different algorithms in this type of analysis to guarantee strong confidence in the correct choice of the reference genes.

ACKNOWLEDGEMENTS

We thank Miranda Mele for all the expertise in RNA processing and analysis. We are also thankful to Marta Vieira and Ana Sofia Almeida for the primers provided. We thank Pedro Afonso and Ana Rita Santos as well for the fruitful discussions. SRO was supported by a fellowship from Fundação para a Ciência e a Tecnologia (FCT) with reference SFRH/BD/51969/2012. This work was supported by FEDER (QREN) through Programa Mais Centro, under projects CENTRO-07-ST24-FEDER-002002, CENTRO-07-ST24-FEDER-002006 and CENTRO-07-ST24-FEDER-002008, through Programa Operacional Factores de Competitividade - COMPETE and national funds via FCT under projects Pest-C/SAU/LA0001/2013-2014, PTDC/SAU-NMC/120144/2010, PTDC/NEU-NMC/0198/2012 and FCT-ANR/NEU-NMC/0022/2012.

REFERENCES

[1] L. Wu, R. Wang, Carbon Monoxide : Endogenous Production , Physiological Functions , and Pharmacological Applications, Pharmacol.Rev.57(2005)585–630. doi:10.1124/pr.57.4.3.585.

[2] B. Olas, Carbon monoxide is not always a poison gas for human organism: Physiological and pharmacological features of CO, Chem.Biol.Interact.222(2014)37–43. doi:10.1016/j.cbi.2014.08.005.

[3] F. Gullotta, A. di Masi, M. Coletta, P. Ascenzi, CO metabolism, sensing, and signaling, BioFactors. 38 (2012) 1–13. doi:10.1002/biof.192.

[4] S. Ghosh, J. Gal, N. Marczin, Carbon monoxide: endogenous mediator, potential diagnostic and therapeutic target, Ann.Med.42(2010)1–12. doi:10.3109/07853890903482877.

[5] A.-M. Aberg, Carbon Monoxide in biological systems: An experimental and clinical study, Acta Anaesthesiol. Scand. 52 (2008) 716–7. doi:10.1111/j.1399-6576.2008.01619.x.

[6] E.O. Owens, Endogenous carbon monoxide production in disease, Clin. Biochem. 43 (2010) 1183–1188. doi:10.1016/j.clinbiochem.2010.07.011.

[7] M. Knauert, S. Vangala, M. Haslip, P. Lee, Therapeutic Applications of Carbon Monoxide, Oxid. Med. Cell. Longev. 2013 (2013) 1–11. doi:10.1155/2013/360815.

[8] F. Gullotta, A. di Masi, P. Ascenzi, Carbon monoxide: an unusual drug., IUBMB Life. 64 (2012) 378–86. doi:10.1002/iub.1015.

[9] S. Hung, H. Liou, K. Kang, R.-M. Wu, C. Wen, W.-M. Fu, Overexpression of heme oxygenase-1 protects dopaminergic neurons against 1-methyl-4-phenylpyridinium-induced neurotoxicity., Mol. Pharmacol. 74 (2008) 1564–1575. doi:mol.108.048611.

[10] D. Qi, C. Ouyang, Y. Wang, S. Zhang, X. Ma, Y. Song, H. Yu, J. Tang, W. Fu, L. Sheng, L. Yang, M. Wang, W. Zhang, L. Miao, T. Li, X. Huang, H. Dong, HO-1 attenuates hippocampal neurons injury via the activation of BDNF–TrkB–PI3K/Akt signaling pathway in stroke, Brain Res. 1577 (2014) 69–76. doi:10.1016/j.brainres.2014.06.031.

[11] C.S.F. Queiroga, S. Tomasi, M. Widerøe, P.M. Alves, A. Vercelli, H.L.A. Vieira, Preconditioning Triggered by Carbon Monoxide (CO) Provides Neuronal Protection Following Perinatal Hypoxia-Ischemia, PLoS One. 7 (2012) e42632. doi:10.1371/journal.pone.0042632.

[12] M.L. Dallas, J.P. Boyle, C.J. Milligan, R. Sayer, T.L. Kerrigan, C. McKinstry, P. Lu, J. Mankouri, M. Harris, J.L. Scragg, H. a Pearson, C. Peers, Carbon monoxide protects against oxidant-induced apoptosis via inhibition of Kv2.1., FASEB J. 25 (2011) 1519–30. doi:10.1096/fj.10-173450.

[13] A. Hervera, S. Leánez, R. Negrete, R. Motterlini, O. Pol, Carbon monoxide reduces neuropathic pain and spinal microglial activation by inhibiting nitric oxide synthesis in mice, PLoS One. 7 (2012) 1–10. doi:10.1371/journal.pone.0043693.

[14] K.A. Hanafy, J. Oh, L.E. Otterbein, Carbon Monoxide and the Brain: Time to Rethink the Dogma, Curr Pharm Des. 19 (2013) 2771–2775.

[15] M.D. Maines, The heme oxygenase system: a regulator of second messenger gases., Annu.Rev.Pharmaco.Toxic.37(1997)517–554. doi:10.1146/annurev.pharmtox.37.1.517.

[16] S.W. Ryter, A.M.K. Choi, Carbon monoxide: present and future indications for a medical gas., Korean J. Intern. Med. 28 (2013) 123–40. doi:10.3904/kjim.2013.28.2.123.

[17] R. Foresti, M.G. Bani-Hani, R. Motterlini, Use of carbon monoxide as a therapeutic agent: promises and challenges.,IntCareMed.34(2008)649–58.doi:10.1007/s00134-008-1011-1.

[18] S.W. Ryter, J. Alam, A.M.K. Choi, Heme oxygenase-1/carbon monoxide: from basic science to therapeutic applications., Physiol. Rev. 86 (2006) 583–650. doi:10.1152/physrev.00011.2005.

[19] R. Motterlini, L.E. Otterbein, The therapeutic potential of carbon monoxide., Nat. Rev. Drug Discov. 9 (2010) 728–43. doi:10.1038/nrd3228.

[20] B. Wegiel, D. Gallo, E. Csizmadia, C. Harris, J. Belcher, G.M. Vercellotti, N. Penacho, P. Seth, V. Sukhatme, A. Ahmed, P.P. Pandolfi, L. Helczynski, A. Bjartell, J.L. Persson, L.E. Otterbein, Carbon monoxide expedites metabolic exhaustion to inhibit tumor growth, Cancer Res. 73 (2013) 7009–7021. doi:10.1158/0008-5472.CAN-13-1075.

[21] S. Zhao, Q. Lin, H. Li, Y. He, X. Fang, F. Chen, C. Chen, H. Z, Carbon monoxide releasing molecule-2 attenuated ischemia/reperfusion-induced apoptosis in cardiomyocytes via a mitochondrial pathway, Mol. Med. Rep. 9 (2014) 754–762. doi:10.3892/mmr.2013.1861.

[22] I. Nikolic, M. Vujicic, I. Stojanovic, S. Stosic-Grujicic, T. Saksida, Carbon Monoxide-Releasing Molecule-A1 Inhibits Th1/Th17 and Stimulates Th2 Differentiation In vitro, Scand. J. Immunol. 80 (2014) 95–100. doi:10.1111/sji.12189.

[23] L. Vanella, C. Sanford, D.H. Kim, N.G. Abraham, N. Ebraheim, Oxidative stress and heme oxygenase-1 regulated human mesenchymal stem cells differentiation, Int. J. Hypertens. 2012 (2012). doi:10.1155/2012/890671.

[24] C. Leffler, H. Parfenova, J. Jaggar, Carbon monoxide as an endogenous vascular modulator,AmJPhysiolHear.CircPhysi.301(2011)1–11.doi:10.1152/ajpheart.00230.2011.

[25] S.-J. Kim, K.-S. Min, H.-W. Ryu, H.-J. Lee, E.-C. Kim, The role of heme oxygenase-1 in the proliferation and odontoblastic differentiation of human dental pulp cells., J. Endod. 36 (2010) 1326–1331. doi:10.1016/j.joen.2010.04.011.

[26] P.M. Snijder, E. Van Den Berg, M. Whiteman, S.J.L. Bakker, H.G.D. Leuvenink, H. Van Goor, Emerging role of gasotransmitters in renal transplantation, Am. J. Transplant. 13 (2013) 3067–3075. doi:10.1111/ajt.12483.

[27] H.P. Kim, S.W. Ryter, A.M.K. Choi, CO as a cellular signaling molecule., Annu. Rev. Pharmacol. Toxicol. 46(2006)411–49. doi:10.1146/annurev.pharmtox.46.120604.141053.

[28] A.S. Almeida, C. Figueiredo-Pereira, H.L.A. Vieira, Carbon monoxide and mitochondria - modulation of cell metabolism, redox response and cell death, Front. Physiol. 6 (2015) 1–6. doi:10.3389/fphys.2015.00033.

[29] A. Yabluchanskiy, P. Sawle, S. Homer-Vanniasinkam, C.J. Green, R. Foresti, R. Motterlini, CORM-3, a carbon monoxide-releasing molecule, alters the inflammatory response and reduces brain damage in a rat model of hemorrhagic stroke., Crit. Care Med. 40 (2012) 544–52. doi:10.1097/CCM.0b013e31822f0d64.

[30] R. Foresti, S.K. Bains, T.S. Pitchumony, L.E. De Castro Brás, F. Drago, J.L. Dubois-Randé, C. Bucolo, R. Motterlini, Small molecule activators of the Nrf2-HO-1 antioxidant axis modulate heme metabolism and inflammation in BV2 microglia cells, Pharmacol. Res. 76 (2013) 132–148. doi:10.1016/j.phrs.2013.07.010.

[31] B. Wang, W. Cao, S. Biswal, S. Doré, Carbon monoxide-activated Nrf2 pathway leads to protection against permanent focal cerebral ischemia., Stroke. 42 (2011) 2605–10. doi:10.1161/STROKEAHA.110.607101.

[32] H.L.A. Vieira, C.S.F. Queiroga, P.M. Alves, Pre-conditioning induced by carbon monoxide provides neuronal protection against apoptosis, J. Neurochem. 107 (2008) 375–384. doi:10.1111/j.1471-4159.2008.05610.x.

[33] N. Schallner, C.C. Romão, J. Biermann, W.A. Lagrèze, L.E. Otterbein, H. Buerkle, T. Loop, U. Goebel, Carbon Monoxide Abrogates Ischemic Insult to Neuronal Cells via the Soluble

Guanylate Cyclase-cGMP Pathway, PLoS One. 8 (2013). doi:10.1039/c2dt32174b.

[34] C.S.F. Queiroga, A.S. Almeida, C. Martel, C. Brenner, P.M. Alves, H.L.A. Vieira, Glutathionylation of adenine nucleotide translocase induced by carbon monoxide prevents mitochondrial membrane permeabilization and apoptosis., J. Biol. Chem. 285 (2010) 17077–88. doi:10.1074/jbc.M109.065052.

[35] A.S. Almeida, C.S.F. Queiroga, M.F.Q. Sousa, P.M. Alves, H.L.A. Vieira, Carbon monoxide modulates apoptosis by reinforcing oxidative metabolism in astrocytes: role of Bcl-2., J. Biol. Chem. 287 (2012) 10761–70. doi:10.1074/jbc.M111.306738.

[36] I. Allaman, M. Bélanger, P.J. Magistretti, Astrocyte–neuron metabolic relationships: for better and for worse, Trends Neurosci. 34 (2011) 76–87. doi:10.1016/j.tins.2010.12.001.

[37] J. Huggett, K. Dheda, S. Bustin, A. Zumla, Real-time RT-PCR normalisation; strategies and considerations., Genes Immun. 6 (2005) 279–284. doi:10.1038/sj.gene.6364190.

[38] S. Dupasquier, A.-S. Delmarcelle, E. Marbaix, J.-P. Cosyns, P.J. Courtoy, C.E. Pierreux, Validation of housekeeping gene and impact on normalized gene expression in clear cell renal cell carcinoma: critical reassessment of YBX3/ZONAB/CSDA expression., BMC Mol. Biol. 15 (2014) 9. doi:10.1186/1471-2199-15-9.

[39] P.R. Amable, M.V.T. Teixeira, R.B.V. Carias, J.M. Granjeiro, R. Borojevic, Identification of appropriate reference genes for human mesenchymal cells during expansion and differentiation., PLoS One. 8 (2013) e73792. doi:10.1371/journal.pone.0073792.

[40] L. Rochette, Y. Cottin, M. Zeller, C. Vergely, Carbon monoxide: Mechanisms of action and potential clinical implications, Pharmacol. Ther. 137 (2013) 133–152. doi:10.1016/j.pharmthera.2012.09.007.

[41] D. Chen, X. Pan, P. Xiao, M. a. Farwell, B. Zhang, Evaluation and identification of reliable reference genes for pharmacogenomics, toxicogenomics, and small RNA expression analysis, J. Cell. Physiol. 226 (2011) 2469–2477. doi:10.1002/jcp.22725.

[42] J. Vandesompele, K. De Preter, F. Pattyn, B. Poppe, N. Van Roy, A. De Paepe, F. Speleman, Accurate normalization of real-time quantitative RT-PCR data by geometric averaging of multiple internal control genes., Genome Biol. 3 (2002) RESEARCH0034. doi:10.1186/gb-2002-3-7-research0034.

[43] C.L. Andersen, J.L. Jensen, T.F. Ørntoft, Normalization of Real-Time Quantitative Reverse Transcription-PCR Data : A Model-Based Variance Estimation Approach to Identify Genes Suited for Normalization , Applied to Bladder and Colon Cancer Data Sets Normalization of Real-Time Quantitative Reverse, Cancer Res. 64 (2004) 5245–5250. doi:10.1158/0008-5472.CAN-04-0496.

[44] N. Silver, S. Best, J. Jiang, S.L. Thein, Selection of housekeeping genes for gene expression studies in human reticulocytes using real-time PCR., BMC Mol. Biol. 7 (2006) 33. doi:10.1186/1471-2199-7-33.

[45] M.W. Pfaffl, A. Tichopad, C. Prgomet, T.P. Neuvians, Determination of stable housekeeping genes, differentially regulated target genes and sample integrity: BestKeeper - Excel-based tool using pair-wise correlations, Biotechnol. Lett. 26 (2004) 509–515. doi:10.1023/B:BILE.0000019559.84305.47.

[46] L. Hertz, B.H.J. Juurlink, E. Hertz, H. Fosmark, a Schousboe, Preparation of primary cultures of mouse (rat) astrocytes, A Dissection Tissue Cult. Man. Nerv. Syst. (1986)

[47] R. Motterlini, P. Sawle, J. Hammad, S. Bains, R. Alberto, R. Foresti, C.J. Green, CORM-A1: a new pharmacologically active carbon monoxide-releasing molecule., FASEB J. 19 (2005) 284–6. doi:10.1096/fj.04-2169fje.

[48] K.J. Livak, T.D. Schmittgen, Analysis of Relative Gene Expression Data Using Real- Time

Quantitative PCR and the 2^(-2ΔΔCt) Method, Methods. 25 (2001) 402–408. doi:10.1006/meth.2001.1262.

[49] J. Harborth, S.M. Elbashir, K. Bechert, T. Tuschl, K. Weber, Identification of essential genes in cultured mammalian cells using siRNAs.,JCSci114(2001)4557–65.

[50] D.T.R. Coulson, S. Brockbank, J.G. Quinn, S. Murphy, R. Ravid, G.B. Irvine, J. a Johnston, Identification of valid reference genes for the normalization of RT qPCR gene expression data in human brain tissue., BMC Mol. Biol. 9 (2008) 46. doi:10.1186/1471-2199-9-46.

[51] C. Gubern, O. Hurtado, R. Rodríguez, J.R. Morales, V.G. Romera, M.A. Moro, I. Lizasoain, J. Serena, J. Mallolas, Validation of housekeeping genes for quantitative real-time PCR in in-vivo and in-vitro models of cerebral ischaemia., BMC Mol. Biol. 10 (2009) 57. doi:10.1186/1471-2199-10-57.

[52] H. Duckles, H.E. Boycott, M.M. Al-Owais, J. Elies, E. Johnson, M.L. Dallas, K.E. Porter, F. Giuntini, J.P. Boyle, J.L. Scragg, C. Peers, Heme oxygenase-1 regulates cell proliferation via carbon monoxide-mediated inhibition of T-type Ca2+ channels, Pflügers Arch. - Eur. J. Physiol. (2014) 415–427. doi:10.1007/s00424-014-1503-5.

[53] H.J. Kim, M. Zheng, S.-K. Kim, J.J. Cho, C.H. Shin, Y. Joe, H.T. Chung, CO/HO-1 Induces NQO-1 Expression via Nrf2 Activation, Immune Netw. 11 (2011) 376. doi:10.4110/in.2011.11.6.376.

[54] D.Y. Shin, J. Chung, Y. Joe, H.O. Pae, K.C. Chang, G.J. Cho, S.W. Ryter, H.T. Chung, Pretreatment with CO-releasing molecules suppresses hepcidin expression during inflammation and endoplasmic reticulum stress through inhibition of the STAT3 and CREBH pathways, Blood. 119 (2012) 2523–2532. doi:10.1182/blood-2011-07-366690.

[55] T. Ohtsuka, K. Kaseda, T. Shigenobu, T. Hato, I. Kamiyama, T. Goto, M. Kohno, M. Shimoda, Carbon monoxide-releasing molecule attenuates allograft airway rejection, Transpl. Int. 27 (2014) 741–747. doi:10.1111/tri.12314.

[56] J.N. Pulido, J.R. Neal, C.B. Mantilla, S. Agarwal, W.-Y. Lee, P.D. Scott, R.D. Hubmayr, W.-Z. Zhan, G.C. Sieck, G. Farrugia, M.H. Ereth, Inhaled Carbon Monoxide Attenuates Myocardial Inflammatory Cytokine Expression in a Rat Model of Cardiopulmonary Bypass, J. Extra Corpor Technol. 43 (2011) 137–143.

[57] M. Feger, A. Fajol, A. Lebedeva, A. Meissner, D. Michael, J. Voelkl, I. Alesutan, E. Schleicher, C. Reichetzeder, B. Hocher, S.M. Qadri, F. Lang, Effect of carbon monoxide donor CORM-2 on vitamin D3 metabolism, Kidney Blood Press. Res. 37 (2013) 496–505. doi:10.1159/000355730.

[58] M.A. Rhodes, M.S. Carraway, C.A. Piantadosi, C.M. Reynolds, A.D. Cherry, T.E. Wester, M.J. Natoli, E.W. Massey, R.E. Moon, H.B. Suliman, Carbon monoxide, skeletal muscle oxidative stress, and mitochondrial biogenesis in humans, Am J Physiol Hear. Circ Physiol. 297 (2009) 392–399. doi:10.1152/ajpheart.00164.2009.

[59] L. Sartiani, F. Stillitano, C. Luceri, S. Suffredini, S. Toti, C. De Filippo, V. Cuomo, M. Tattoli, P. Dolara, A. Mugelli, E. Cerbai, Prenatal exposure to carbon monoxide delays postnatal cardiac maturation., Lab. Invest. 90 (2010) 1582–1593. doi:10.1038/labinvest.2010.122.

[60] L. Beltran-Parrazal, D. Acuna, A.M. Ngan, E. Kim, A. Ngan, K. Kawakami, J. Edmond, I. a. Lopez, Neuroglobin, cytoglobin, and transcriptional profiling of hypoxia-related genes in the rat cerebellum after prenatal chronic very mild carbon monoxide exposure (25 ppm), Brain Res. 1330 (2010) 61–71. doi:10.1016/j.brainres.2010.03.005.

[61] K. Maruyama, E. Morishita, T. Yuno, A. Sekiya, H. Asakura, S. Ohtake, A. Yachie, Carbon monoxide (CO)-releasing molecule-derived CO regulates tissue factor and plasminogen activator inhibitor type 1 in human endothelial cells, Thromb. Res. 130 (2012) e188–e193. doi:10.1016/j.thromres.2012.07.002.

[62] S.-Y.S. Hung, H.-C.H. Liou, W.-M.W. Fu, The mechanism of heme oxygenase-1 action involved in the enhancement of neurotrophic factor expression., Neuropharmacology. 58 (2010) 321–329. doi:10.1016/j.neuropharm.2009.11.003. Epub 2009 Nov 20.

[63] J. Kuesap, K. Na-Bangchang, Possible role of heme oxygenase-1 and prostaglandins in the pathogenesis of cerebral malaria: Heme oxygenase-1 induction by prostaglandin D2 and metabolite by a human astrocyte cell line, Korean J. Parasitol. 48 (2010) 15–21. doi:10.3347/kjp.2010.48.1.15.

[64] Y.N. Huang, C.H. Wu, T.C. Lin, J.Y. Wang, Methamphetamine induces heme oxygenase-1 expression in cortical neurons and glia to prevent its toxicity, Toxicol. Appl. Pharmacol. 240 (2009) 315–326. doi:10.1016/j.taap.2009.06.021.

[65] K.-J. Min, M. Yang, S.-U. Kim, I. Jou, E. Joe, Astrocytes induce hemeoxygenase-1 expression in microglia: a feasible mechanism for preventing excessive brain inflammation., J. Neurosci. 26 (2006) 1880–7. doi:10.1523/JNEUROSCI.3696-05.2006.

[66] Q.-M. Wang, X.-Y. Yin, Z.-J. Duan, S.-B. Guo, X.-Y. Sun, Role of the heme oxygenase/carbon monoxide pathway in the pathogenesis and prevention of hepatic encephalopathy, Mol. Med. Rep. 8 (2013) 67–74. doi:10.3892/mmr.2013.1472.

[67] G. Scapagnini, V. D'Agata, V. Calabrese, A. Pascale, C. Colombrita, D. Alkon, S. Cavallaro, Gene expression profiles of heme oxygenase isoforms in the rat brain, Brain Res. 954 (2002) 51–59. doi:10.1016/S0006-8993(02)03338-3.

[68] H. Yin, J. Fang, L. Liao, H. Maeda, Q. Su, Upregulation of heme oxygenase-1 in colorectal cancer patients with increased circulation carbon monoxide levels, potentially affects chemotherapeutic sensitivity., BMCCancer.14(2014)436. doi:10.1186/1471-2407-14-436.

[69] K. Morita, M.-S. Lee, S. Her, Possible Relation of Hemin-Induced HO-1 Expression to the Upregulation of VEGF and BDNF mRNA Levels in Rat C6 Glioma Cells, J. Mol. Neurosci. 38 (2009) 31–40. doi:10.1007/s12031-008-9156-5.

[70] N. Panahian, M. Yoshiura, M.D. Maines, Overexpression of heme oxygenase-1 is neuroprotective in a model of permanent middle cerebral artery occlusion in transgenic mice., J. Neurochem. 72 (1999) 1187–1203. doi:10.1111/j.1471-4159.1999.721187.x.

[71] N. Schallner, M. Fuchs, C.I. Schwer, T. Loop, H. Buerkle, W.A. Lagrèze, C. van Oterendorp, J. Biermann, U. Goebel, Postconditioning with Inhaled Carbon Monoxide Counteracts Apoptosis and Neuroinflammation in the Ischemic Rat Retina, PLoS One. 7 (2012). doi:10.1371/journal.pone.0046479.

[72] A. Sener, K.C. Tran, J.P. Deng, B. Garcia, Z. Lan, W. Liu, T. Sun, J. Arp, M. Salna, P. Acott, G. Cepinskas, A.M. Jevnikar, P.P.W. Luke, Carbon monoxide releasing molecules inhibit cell death resulting from renal transplantation related stress, J. Urol. 190 (2013) 772–778. doi:10.1016/j.juro.2012.12.020.

[73] E. Climent, M. Sancho-Tello, R. Miñana, D. Barettino, C. Guerri, Astrocytes in culture express the full-length Trk-B receptor and respond to brain derived neurotrophic factor by changing intracellular calcium levels: effect of ethanol exposure in rats., Neurosci Lett. 288 (2000) 53–56. doi:10.1016/S0304-3940(00)01207-6.

[74] S. Finkbeiner, S.F. Tavazoie, A. Maloratsky, K.M. Jacobs, K.M. Harris, M.E. Greenberg, CREB: a major mediator of neuronal neurotrophin responses., Neuron. 19 (1997) 1031–1047. doi:10.1016/S0896-6273(00)80395-5.

[75] L.F. Reichardt, Neurotrophin-regulated signalling pathways., Philos. Trans. R. Soc. Lond. B. Biol. Sci. 361 (2006) 1545–1564. doi:10.1098/rstb.2006.1894.

[76] A.R. Santos, C.B. Duarte, Validation of internal control genes for expression studies: Effects of the neurotrophin BDNF on hippocampal neurons, J. Neurosci. Res. 86 (2008)

3684–3692. doi:10.1002/jnr.21796.

[77] P.-L. Chi, C.-C. Lin, Y.-W. Chen, L.-D. Hsiao, C.-M. Yang, CO Induces Nrf2-Dependent Heme Oxygenase-1 Transcription by Cooperating with Sp1 and c-Jun in Rat Brain Astrocytes, Mol. Neurobiol. 52 (2015) 277–292. doi:10.1007/s12035-014-8869-4.

[78] R. Wang, Shared signaling pathways among gasotransmitters., Proc. Natl. Acad. Sci. U. S. A. 109 (2012) 8801–2. doi:10.1073/pnas.1206646109.

[79] A. Moustafa, Y. Habara, A novel role for carbon monoxide as a potent regulator of intracellular Ca2+ and nitric oxide in rat pancreatic acinar cells., Am. J. Physiol. Cell Physiol. 307 (2014) C1039-49. doi:10.1152/ajpcell.00252.2014.

Chapter II.III

Altered Genes Validation – FosB Role

This chapter is based on the following manuscript:

Gene expression alterations in astrocytes due to carbon monoxide treatment – is there a role for FosB in cytoprotection?

Sara R. Oliveira, Carlos B Duarte, Helena L. A. Vieira

(in preparation)

INDEX

ABSTRACT

Carbon monoxide (CO) is an endogenous gasotransmitter produced by heme oxygenase-mediated cleavage of the heme group, which has been shown to limit inflammation and to prevent apoptosis in several tissues, including brain. Likewise, small amounts of exogenous CO are cytoprotective in astrocytes, neurons and microglia. Nevertheless, the molecular mechanisms underlying CO's beneficial role remain poorly understood.

This work aims at identifying the molecular effectors that may account for CO-induced cytoprotection by assessing the gene expression alterations conferred by CO in primary cultures of cortex astrocytes. Cultured astrocytes were treated with the CO-releasing molecule CORM-A1 (12.5 μM) for 40 min, and transcriptional changes were analysed using RNASeq. A total of 162 genes were differentially expressed due to CO treatment, which were systematically selected up to 7 genes: FosB, Scand1, Rgs10, Actg1, Panx1, Pcbdh21, Rn18s. This selected group of differentially expressed genes were further validated using qRT-PCR at 30, 40 and 60 min following CO treatment. According to RNAseq, FosB mRNA increase was validated by qRT-PCR and showed the highest expression following CO treatment at 30 - 60 min. Likewise, western blot analysis also showed a transient increase in FosB protein levels in cortical astrocytes after 40 min of incubation with the CO donor. The increase on FosB mRNA expression revealed to be dependent on activation of the ATP receptor P2X7 and independent on reactive oxygen species (ROS) generation.

The functional importance of FosB in CO-induced survival in astrocytes was investigated by knocking down its expression with FosB siRNA. Astrocytes were challenged to death with oxidative stress (pro-oxidant *tert*-butylhydroperoxide) and cell viability was assessed by flow cytometry 24h later. Down-regulation of FosB did not affect the CO-induced cytoprotection of cortical astrocytes exposed to CORM-A1, suggesting that FosB is not essential for CO to prevent cell death. Nevertheless, generated transcriptomic data related to CO treatment open new opportunities for further studies about CO-induced cytoprotective pathways.

KEYWORDS

Carbon monoxide, astrocytes, FosB, cytoprotection, ROS, transcriptome

ABBREVIATIONS

Actg1 - actin gamma 1
AP-1 - activator protein 1
ATF - activating transcription factor
Bcl-2 - B-cell leukemia/lymphoma 2
BDNF - brain-derived neurotrophic factor
CBP - CREB binding protein
CO - carbon monoxide
CORM-A1 - Carbon monoxide-releasing molecule A1
CREB - cAMP-response element-binding protein
DEGs - differentially expressed genes
DiOC – 3,3'-Dihexylocarbocyanine iodide
ERK - extracellular signal-regulated kinase
FRK - Fos regulating kinase
Gapdh - glyceraldehyde-3-phosphate dehydrogenase
HO-1 – heme oxygenase 1
Hprt1 - hypoxanthine guanine phosphoribosyl transferase I
JAK - Janus kinase
JNK - c Jun N-terminal kinase
MAPK - mitogen-activated protein kinase
MMP - mitochondria membrane potential
NAC - *N*-acetylcysteine
Ppia - peptidylpropyl isomerase A
PPARɣ - Peroxisome proliferator-activated receptor gamma
PI - propidium iodide
P2X7R - P2X7 receptor
qRT-PCR - Quantitative real-time reverse transcription-polymerase chain reaction
Rn18s - 18S rRNA
ROS - Reactive oxygen species
Sdha - Succinate dehydrogenase complex, Subunit A
sGC - soluble guanylyl cyclase
siRNA - small interfering RNA
SRE - serum response element
t-BHP - *tert*-butyl hydroperoxide
TCF - ternary complex factor
TRE - 12-*O*-tetradecanoylphorbol-13-acetate (TPA) response element (consensus sequence 5'-TGAG/CTCA-3')

1. INTRODUCTION

Carbon monoxide (CO) is a gas produced endogenously due to the breakdown of heme by heme oxygenase (HO) and is able to cytoprotect different cell types by boosting cellular resistance against a wide variety of harmful events [1]. In central nervous system, low concentrations of exogenous CO and/or expression of heme oxygenase-1 (HO-1) promotes neuroprotection by limiting neuroinflammation and neural cell death, as well as by modulating vasodilation (for review see [2]). In cell models of brain tissue, CO has anti-apoptotic properties in neurons [3,4] and in astrocytes [5,6]; promotes neurogenesis [7], and reduces neuroinflammation by acting on microglia [8–10]. Likewise, administration of low doses of CO revealed beneficial properties and improved the outcome in several rodent models of brain diseases, namely ischemic stroke [11,12], haemorrhagic stroke [13] and multiple sclerosis [14,15].

Historically, the effect of CO in cerebral ischemia was tested in preconditioning studies (therapy administration prior to injury) and some of the molecular changes underlying the protective effects of CO were characterized. The neuroprotective effects of CO were associated with the modulation of HO-1, ROS and BDNF [17]. Later, the therapeutic potential of CO was tested during the hypoxic phase and after starting reperfusion. Its neuroprotective effects were demonstrated in different animal models of stroke and other diseases [2], [18]. The growing body of evidence pointing to a possible therapeutic application of CO led to the development of CO releasing molecules, which allow the control of CO release. From the clinical point of view these molecules allow minimization of adverse effects and local release, among other advantages ([6], [19], [20]).

Astrocytes are the most abundant cell type in the brain and provide structural, metabolic and trophic support to other neural cells, in particular to neurons [16]. Recently, neuroscientists have been given increasing attention to astrocytes. Because the tightly regulated cross talk between neurons and astrocytes, one can suggest that by improving astrocytic function neuroprotection could be promoted.

From the data presented in Chapter II.I, several validations were needed to gather further evidence for the CO effect on astrocytes. Moreover, with the validated reference genes presented in Chapter II.II, a qRT-PCR approach was possible. Thus, the aim of this work is: (i) to validate a set of these differentially expressed genes (DEGs) at mRNA and protein levels and finally (ii) to functionally validate the most promising found gene: FosB and (iii) to verify the importance of FosB mediating CO-induced cytoprotection in astrocytes subjected to oxidative stress. Finally, the characterization of CO-induced gene expression alterations will contribute to better understanding CO’s cytoprotective pathways and to the potential development of novel therapeutic strategies against cerebral diseases.

2. MATERIALS AND METHODS

2.1. Cortical astrocyte cultures

Primary cultures of mouse cortical astrocytes were prepared from the cortices of P1–P2 Bl6/c57 mice pups after mechanical dissociation, as previously described [17]. Briefly, cerebral hemispheres were carefully freed of the meninges and the dissected cortices were washed in ice-cold PBS, dissociated mechanically and passed through a 70 µm nylon cell strainer (BD Falcon™) into Dulbecco's minimum essential medium containing 1 g/L glucose (Sigma) and supplemented with 20% (v/v) fetal bovine serum (FBS; Gibco® Life Technologies) and 1% (v/v) penicillin/streptomycin (Gibco® Life Technologies). Single-cell suspensions were plated in cell culture flasks (8 to 10 cortices/75 cm^2, Orange Scientific) and maintained in a humidified atmosphere of 5% CO_2 / 95% air at 37°C. After 8 days in culture, the phase dark cells growing on the astrocytic cell layer were detached by vigorous shaking and removed. Culture medium was replaced twice a week for 3 weeks with gradual reduction in FBS content (2^{nd} week 15%; 3^{rd} week 10%). The confluent astrocytic cultures were mildly trypsinized (0.05% (w/v) trypsin/EDTA, Gibco® Life Technologies) and subcultured in 6-well plates until full confluence.

2.2. Administration of CO to astrocytic cultures

CORM-A1, a CO releasing molecule [18], was used to deliver CO to astrocytes. CORM-A1 (Sigma) stock solutions were prepared in MilliQ water to a final concentration of 10 mM and stored at -20°C to avoid loss of released CO, and diluted in PBS before use. Time points for CORM-A1 treatment were selected based on the cytoprotective effects of CO in astrocytes subjected to oxidative stress (data not shown). RNA extraction for RNASeq experiments was performed after 40 min of incubation with CORM-A1 (12.5 µM); for qRT-PCR experiments, the cells were incubated with CORM-A1 for 30 min, 40 min and 60 min at a final concentration of 12.5 µM. Protein extracts were prepared at 40 min, 1h, 2h, 3h, 4h, 5h, 6h, 8h, 24h following CORM-A1 administration. Non-supplemented PBS was added to control points without CORM-A1 treatment.

2.3. Total RNA isolation and assessment of quality and concentration of RNA

For RNA sequencing, astrocytes were cultured at 75cm^2 cell culture flasks for each condition. RNA was purified using RNeasy Qiagen kit accordingly to manufacturers procedure, followed by lyophilisation, and 15 µg of dried RNA per sample was sent to BGI for RNA sequencing using Illumina 2000 HiSeq instrument.

For qRT-PCR experiments, the full content of a six-well cluster plate, with a density of $4.5x10^5$ cells/well, was collected for each experimental condition and total RNA from cortical astrocytes was extracted with TRIzol (Invitrogen® Life Technologies), following the manufacturer's specifications. After addition of chloroform and phase separation, the RNA was precipitated with isopropanol. The precipitated RNA was washed once with

75% ethanol, centrifuged, air dried, and resuspended in 20 µL of RNase free water (Gibco Life Technologies). The whole procedure was performed at 4°C. RNA concentration and purity were determined by spectrophotometry (NanoDrop 2000; Thermo Scientific). RNA quality and integrity was assessed using the Experion RNA StdSens automated gel electrophoresis system (Bio-Rad). A virtual gel was created for each sample, allowing the detection of degradation of the reference markers RNA18S and 28S. The system labels each sample with a RNA Quality Indicator (RQI), ranging from 1 to 10. Samples were discarded when showing RQI ≤7, indicating that they presented RNA degradation, poor integrity or contamination by DNA. Samples were stored at -80°C until further use in qRT-PCR.

2.4. Reverse transcription PCR

For cDNA synthesis, 1 µg of total RNA was reverse transcribed using iScript™ cDNA Synthesis Kit (Bio-Rad) according to manufacturer's instructions. Briefly, the samples were defrosted on ice, and the PCR reaction mix was added to a 20 µL final volume. The reaction protocol started with a 5-min step at 25ºC, followed by 30 min at 42°C and ended with a 5-min step at 85°C (T100™ Thermal Cycler, Bio-Rad). Samples were stored at -20ºC until further use.

2.5. Primer design

Primers for real-time PCR were designed with Beacon Designer 8.13 software (Premier Biosoft International) as described in previous work [19]. The primers used are described in detail in (Supplementary Data, Table S1).

2.6. Real-time PCR

For the gene expression studies, 2 µL of 1:10 diluted cDNA were added to 10 µL 2x SsoFast™ EvaGreen Supermix (Bio-Rad), with a final concentration of each primer of 250 nM in 20 µL final volume. The thermocycling reaction was initiated with activation of Sso7d-fusion DNA polymerase by heating at 95°C during 30 seconds, followed by 40 cycles of a 10-sec denaturation step at 95°C, a 30-sec annealing step at 55°C, and a 30-sec elongation step at 72°C. The fluorescence was measured after the extension step by the iQ™5 Multicolor Real-Time PCR Detection System (Bio-Rad). After the thermocycling reaction, the melting step was performed, from 55°C up to 95°C, with an increment of 0.5°C each 10 sec. Continuous measurement of fluorescence allowed the detection of possible nonspecific products. The assay included a non-template control and a standard curve (three 1:10 sequential dilution steps) of cDNA for assessing the efficiency of all primer pairs. The reactions were run in duplicate to reduce confounding variance and average results were calculated.

2.7. Gene expression analysis

Since all primer pairs presented an efficiency close to 100%, the data were processed using the $2^{-\Delta Ct}$ method, an adapted version of the $2^{-\Delta\Delta Ct}$ method [20], with $\Delta C_t = C_{t\ condition\ x} - C_{t\ control}$. The control corresponds to the reference condition representing 1-fold expression of each gene. The threshold cycle (C_t) refers to the cycle at which the fluorescence signal is detectable above background due to the accumulation of amplified product. This value is proportional to the starting copy number of the target sequence. C_t was measured in the exponential phase and, therefore, it was not affected by possible limiting components in the reaction. All C_t values were normalized to two internal control genes, Gapdh and Ppia, which were already validated to be the most suitable ones for the conditions used in this study [19]. For every run performed, the threshold was set at the same fluorescence value (100 RFU).

2.8. Total protein isolation and concentration calculation

After washing the astrocytes twice with ice-cold PBS (137 mM NaCl, 2.7 mM KCl, 1.8 mM K_2HPO_4, 10 mM $NaH_2PO_4 \cdot 2H_2O$), total protein was extracted using RIPA lysis buffer (150 mM NaCl, 50 mM Tris-HCl, 5 mM EGTA, 1% Triton X-100, 0.5% deoxycholic acid, 0.1% sodium dodecyl sulfate) freshly supplemented with 1X cocktail protease inhibitor (Roche, pH 7.5). Cells were then scraped and samples were stored at -20°C until further use. Protein concentration was quantified using a bicinchoninic acid (BCA) protein assay kit (Pierce®) using the manufacturer's specifications. Absorvance was measured using a TECAN infinite F200PRO microplate reader.

2.9. Immunoblotting

Samples from cell extracts were separated under reducing electrophoresis on a 1 mm thick 12% sodium dodecyl sulfate-polyacrylamide (SDS-PAGE) gel. Samples were transferred to a nitrocellulose membrane (HybondTMC extra, GE Healthcare). FosB protein was stained with an anti-FosB antibody (Santa Cruz Biotechnology) at 1:333 dilution, overnight at 4ºC. Blots were developed using the ECL (enhanced chemiluminescence) detection system after incubation with HRP-labelled anti-rabbit IgG antibody (1:5000 dilution) (GE Healthcare), for 1h at room temperature.

2.10. siRNA Transfection

FosB expression was silenced by FosB coding siRNA transfection according to the manufacturer's instructions (Invitrogen). Astrocytes at 40% of confluence were transfected using Lipofectamine TM RNAiMAX and OptiMEM® medium (Invitrogen); for 2 cm^2 of astrocytic culture area, 6 pmol of siRNA were used. siRNA and culture medium were mixed gently with Lipofectamine at room temperature, to form liposomes, and the astrocytes were then transfected in the absence of antibiotics.

2.11. Viability analysis by Flow Cytometry

To detect apoptosis induced by *tert*-butyl hydroperoxide (*t*-BHP), cell samples were collected by trypsinization, and the cells were gated by the forward and side scatter. Two dyes were used: 3,3-dihexyloxacarbocyanine iodide ($DiOC_6(3)$; 20 nM) (Invitrogen) to quantify the mitochondrial transmembrane potential, and propidium iodide (1 µM) (Invitrogen) to determine cell viability, based on plasma membrane integrity. A flow cytometer (Canto II, Becton Dickinson) was used to analyze apoptosis-associated parameters. This cytometer contains a blue solid-state laser (488 nm) with FL1 green fluorescence channel for $DiOC_6(3)$ at 530 nm, and a FL3 red fluorescence channel for propidium iodide detection at 650 nm. The acquisition was performed with Diva software and data analysis was performed with Flowing software (http://www.uskonaskel.fi/flowingsoftware/).

2.12. Administration of chemical compounds to astrocytic cultures

The stock solution of A-438079 (Sigma), a specific P2X7 receptor inhibitor [21,22], was prepared in PBS to a final concentration of 2.5 mM and stored at -20°C. Astrocytic cultures were incubated with 10 µM of A-438079. Non-supplemented PBS was added to controls. Two antioxidants, *N*-acetylcysteine (NAC; a precursor of Glutathione) and β-carotene (prepared in DMSO), were applied to astrocytes to a final concentration of 1 µM.

2.13. Measurement of ROS generation

Hydrogen peroxide (H_2O_2) production was assessed by the conversion of 2',7'-dichlorofluorescein diacetate (H_2DCFDA, Invitrogen) to fluorescent 2',7'-dichlorofluorescein (DCF). Superoxide anion generation was monitored using MitoSOX Red mitochondrial superoxide indicator (Life Technologies). Astrocytes cultured in 96-well plates (8000 cells/well) were incubated with 5 µM of H_2DCFDA or MitoSOX for 20 min. After being washed twice, astrocytes were treated with 12.5 or 25 µM of CORM-A1 or 230 µM *t*-BHP in PBS, as a positive control. Fluorescence (λ_{ex} 485 nm/λ_{em} 530nm and λ_{ex} 510 nm/λ_{em} 580nm, respectively) was measured using a TECAN infinite F200PRO Spectrofluorometer for 30 min at 37°C. ROS generation was calculated as an increase in fluorescence intensity over baseline levels (determined for untreated cells) and considering 100% the ROS generation in the presence of *t*-BHP. Where indicated, β-carotene or NAC (1 µM) were added to astrocytes 1h prior to CORM-A1 treatment.

2.14. Statistical analysis

Data are presented as the mean ± standard error of the mean (SEM). Student's *t*-test, one-way or two-way analysis of variance (ANOVA) test was used to identify significant differences between experimental conditions. ANOVAs were followed by the Dunnett's Multiple Comparison Test. Statistical analysis was performed using GraphPad Prism 6 (GraphPad Software, Inc.).

3. RESULTS

3.1. CO-induced differential gene expression in cortical astrocytes

In order to filter down the 162 DEGs to a workable number, we applied sequential filters to reduce down to 7 the number of DEGs used in additional validation steps (Figure 1). The first 59 DEGs (33 up-regulated and 26 down-regulated) were shown to have relevant roles in the brain, both under physiological or pathological conditions, namely ischemia, inflammation, neurogenesis, energy balance and redox response. From this smaller group of DEGs, we further selected the ones common to at least two of the three algorithms applied in DEGs screening. This filtering step ensures a higher confidence on the candidate genes under analysis. The latter filter resulted in a group of 14 potential candidate DEGs (9 up-regulated and 3 down-regulated). Finally, a pool of 7 DEGs out the previous 14 was selected based on their function, which might be important in previously described effects of CO such as neuroprotection and calcium signaling [23]. In summary, we identified 162 DEGs in astrocytes treated with CO; metabolic and signaling pathways were found to be the most affected by CO treatment.

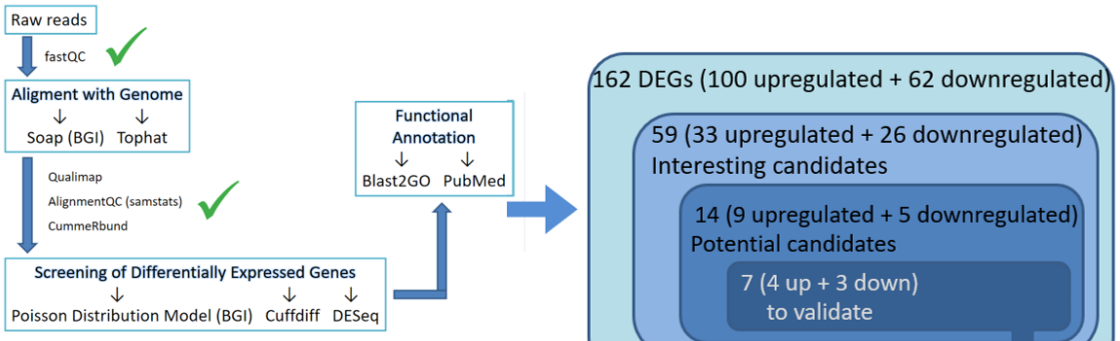

gene	average Δfold	Function relevant in HIR
Scand1	7.01	protective, iron homeostasis, zinc finger protein
FosB	6.54	IEGPs protective, AP-1 activation, neurogenesis
Actg1	2.62	dysregulation implicated in neuro disorders, fibrosis, linked to HIF1α
Rgs10	2.13	neuroprotective in Parkinson, via ↑CREB and ↓NFkB
Rn18s	-3.71	expression levels increase with BDNF treatment
Panx1	-3.18	activation of inflammassome which activates caspases, channel of ATP release
Pcdhb21	-2.72	Ca^{2+}- dependent; adhesion, astro-neuro contact, synapse formation

Figure 1 – Analysis and filtering steps applied to the RNASeq data for the effects of CO on gene expression in astrocytes. The upper left corner depicts the processing and quality control steps applied to obtain the 162 DEGs. The upper right corner represents the different filters used to obtain the final 7 DEGs to validate: from the 162 DEGs, 59 candidates were interesting for being relevant in brain; these 59 candidates were further filtered to 14 candidates due to their high potential in CO action involvement. The table presents the 7 DEGs selected for RT-PCR validation, their fold change and some relevant functions

3.2. CO induces FosB, Rgs10 and Scand1 transcription in cortical astrocytes

From the 162 DEGs, 7 genes were selected to be validated by qRT-PCR. As mentioned above, this subset of DEGs were chosen based on two main criteria: (i) their expression was identified to be significantly altered by two of the 3 algorithms used and (ii) the candidate DEGs were relevant in the context of this study (Figure 1). Thus, *FosB* (FBJ osteosarcoma oncogene B), *Rgs10* (regulator of G-protein signaling 10), *Scand1* (SCAN domain-containing 1), *Rn18s* (18S ribosomal RNA), Actg1 (actin, gamma, cytoplasmic 1), *Pcdhb21* (protocadherin beta 21) and *Panx1* (pannexin 1) mRNA levels were quantified in cultured cortical astrocytes incubated with CORM-A1 (12.5 µM) for 30 to 60 min. We validated the results obtained for 3 DEGs from the 7 selected: *FosB, Rgs10* and *Scand1* (Figure 2 A, B and C). The *Rn18s* qRT-PCR data (Figure 2 D) showed a 2-fold increase in gene expression following incubation with CORM-A1, which contrast with the results obtained in the RNASeq experiments (3.71-fold decrease). This discrepancy may be due to the fact that these two techniques identify alterations in gene expression based on different assumptions and algorithms. The other 3 DEGs did not present a significant variation in expression when analyzed by qRT-PCR: *Actg1, Pcdhb21* and *Panx1* (Figure 2 E, F and G). Since *FosB* showed the strongest alteration in mRNA expression among the 3 genes validated, this gene was chosen for protein and functional validation. Interestingly, FosB is one of the constituents of AP-1, one of the most represented transcription factors identified based on the analysis of the changes in gene expression resulting from the incubation of astrocytes with CO (Figure 3, Chapter I).

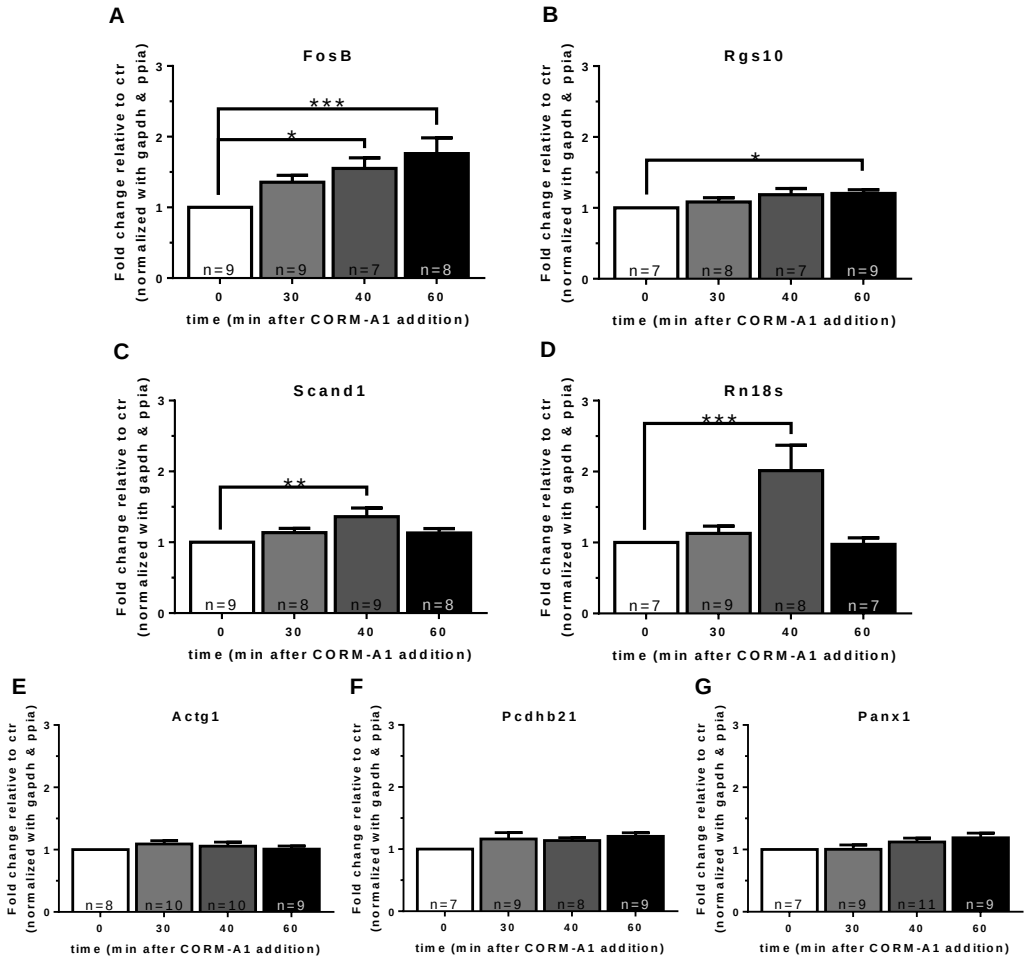

Figure 2 - Effects of CORM-A1 on gene expression in cultured cortical astrocytes. Fold change in the expression of *FosB* (A), *Rgs10* (B), *Scand1* (C), *Rn18s* (D), *Actg1* (E), *Pcdhb21* (F) and *Panx1* (G) was analyzed by qPCR (see methods for further details). Cortical astrocytes were incubated with CORM-A (12.5 µM) for 30 to 60 min. The results are the mean ± SEM of at least 9 independent experiments, performed in different cell preparations. **p*<0.05, ***p*<0.01, ****p*<0.001 as compared to the control with one-way ANOVA.

3.3. CO induces cytoprotective AP-1 products expression

The activator protein-1 transcription factor (AP-1) is formed by FosB paired with Jun family members [24]. To better understand the consequences of FosB induction, and ultimately AP-1 activation, the regulation of several downstream targets was analysed (Figure 3). AP-1 induction is an important cellular response to several stimuli, particularly redox response, cell cycle, cell death control and inflammation. Besides controlling a wide variety of biological processes, AP-1 expression may induce bidirectional responses [25]: its negative or positive regulation of a specific pathway depends on the type of dimers formed within the cellular context [26,27].

Alterations in the expression of several AP-1 target genes following stimulation of cortical astrocytes with CORM-A1 (12.5 µM for 30 to 60 min) were confirmed by qRT–PCR. These AP-1 target genes are: BDNF [28], Bcl-2 [29] and Gria2 (gene coding for glutamate ionotropic receptor AMPA type subunit 2) [30], (Figure 3 B, C and D, respectively). Importantly, the expression of two classical genes of cell survival signaling

was up-regulated: Bdnf and Bcl-2 (Figure 3 C and D) [31,32]. An increased membrane availability of GluA2-containing AMPAR was also proposed to provide protection against excitotoxic damage [33–35]. Since it was observed that Gria2 is up-regulated after 40 min of incubation with CORM-A1, ultimately this event may also contribute to an increased tolerance.

Because mitochondria play a critical role in cell fate [36,37] and are involved in CO-induced pathways [38,39], a gene involved in mitochondrial function was studied. Sdha is a gene coding for a major catalytic subunit of the complex II of the electron chain and its levels were quantified following CO treatment (Figure 3 A). As Sdha inhibition was described to be protective in an ischemia context [40–42], the observed down-regulation in Sdha expression after 60 min of CO treatment may also contribute to the overall tendency for cell survival.

In conclusion, incubation of cortical astrocytes with CORM-A1 may induce multiple pathways, including the AP-1 transcription factor, which protects cells against stress conditions.

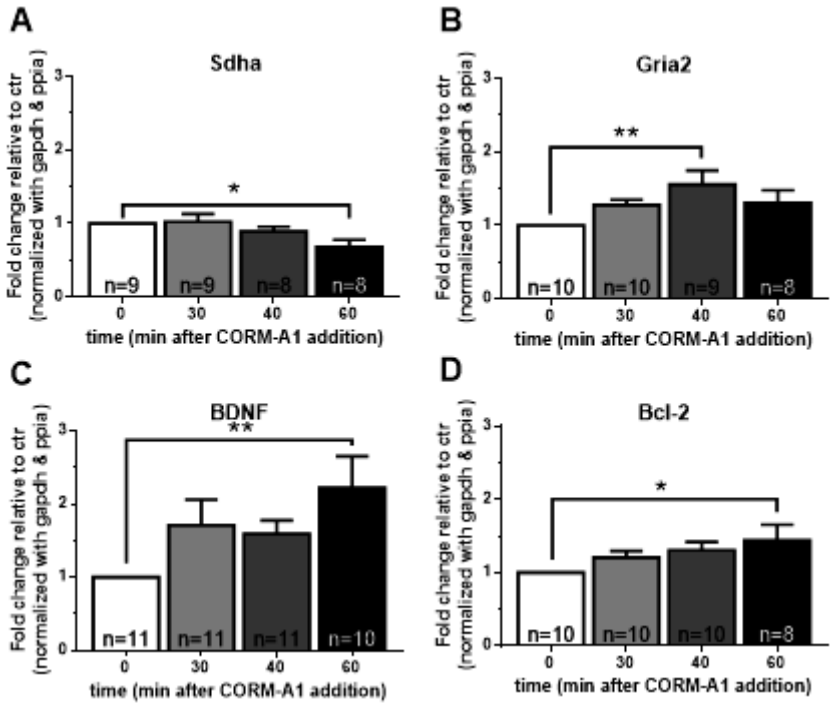

Figure 3 - Effects of CORM-A1 on the expression of AP-1 target genes in cultured cortical astrocytes. The cells were incubated with 12.5 µM CORM-A1 for the indicated periods of time. Fold change in the expression of AP-1 target genes (*Sdha, Bdnf, Bcl-2* and *Gria2*) was analyzed by the $2^{-\Delta Ct}$ (see methods for further details). The results are the mean ± SEM of at least 8 independent experiments, performed in different cell preparations. **p*<0.05, ***p*<0.01 as compared to the control with one-way ANOVA.

3.4. CO-induced FosB protein production

Validation of CO-induced FosB expression was performed by quantification of protein expression following CORM-A1 (12.5 µM) treatment of astrocytes. The immunoblotting results showed a transient increase of FosB protein expression following 40 min of CO treatment. While, FosB protein levels returned to the baseline 20 min later and maintained at basal levels up to 5h (Figure 4). Thus, CO does promote FosB expression in a transitory manner.

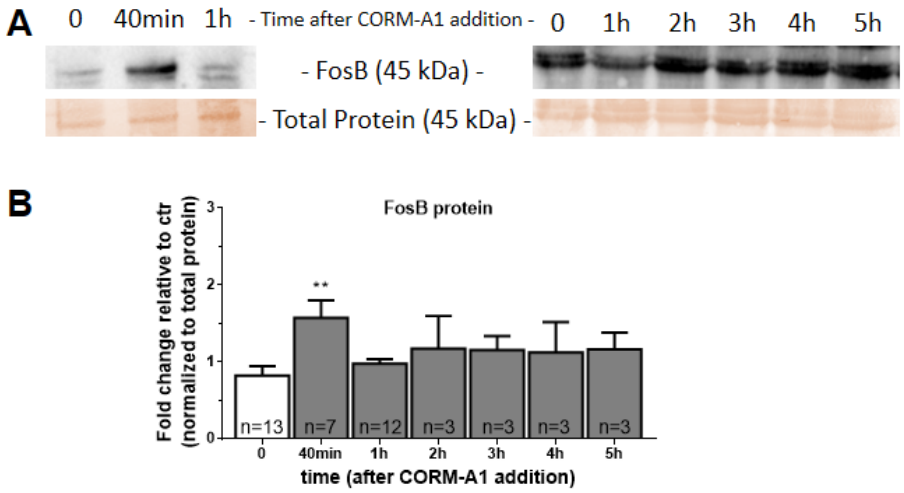

Figure 4 - Effect of CORM-A1 on the expression of the FosB protein in cultured cortical astrocytes. (A) Representative blots of immune detection of FosB and respective loading control with Rouge Ponceau. The first image corresponds to astrocytes treated with CORM-A1 after 0min, 40 min and 1h (early effects) and the second image corresponds to astrocytes treated with CORM-A1 after 0 min, 1h, 2h, 3h, 4h and 5h (later effects). (B) Fold change in the expression of FosB was analyzed by western blot. The results are the mean ± SEM of at least 3 independent experiments, performed in different cell preparations and normalized to total protein. Total protein was evaluated by Rouge Ponceau staining. ***p*<0.01 as compared to the control with one-way ANOVA.

3.5. CO-induced FosB expression is dependent on P2X7 receptor activation

Recent studies showed that activation of the P2X7 receptor (P2X7R) results in a robust induction of FosB [43,44]. Considering that (i) activation of P2X receptors is implicated in the role of CO in astrocyte-neuron paracrine neuroprotection [45] and (ii) P2X7R astrocytic expression was reported to be essential in ischemic preconditioning and cytoprotection [46], we investigated whether CO-induced FosB expression is mediated by P2X7R activation. Primary cultures of cortical astrocytes were treated with A-438079, a specific P2X7R inhibitor, for 10 min prior to CORM-A1 addition, and FosB protein levels were quantified after 40 min of incubation with CORM-A1 (Figure 5). The P2X7R inhibitor abrogated the effect of CORM-A1 on increasing FosB protein expression. One can suggest that CO promotes an autocrine effect, which could be mediated by the release of ATP from cortical astrocytes. Indeed, CO increases ATP production in astrocytes [6], which can be released to the extracellular environment [45].

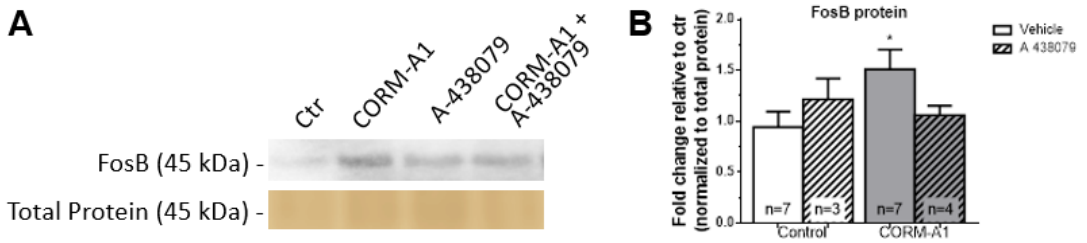

Figure 5 - Role of P2X7R in CORM-A1-induced expression of FosB in cultured cortical astrocytes. (A) Representative blot of immune detection of FosB and respective loading control with Rouge Ponceau. The lanes correspond respectively to astrocytes without treatment, treated with CORM-A1 for 40 min, treated with P2X7R inhibitor (A-438079) and treated both with P2X7R inhibitor and CORM-A1 (B) Fold change in the expression of FosB 40 min after CORM-A1 (12.5 µM) addition was analyzed by western blot. The results are the mean ± SEM of at least 3 independent experiments, performed in different cell preparations and normalized to total protein. Total protein was evaluated by Rouge Ponceau staining. **p*<0.05 as compared to the control with one-way ANOVA.

3.6. CORM-A1 induces mitochondrial ROS production

A strong link between P2X7, ROS and FosB was reported on a study using macrophages, where P2X7 stimulates ROS production, which then activates FosB [47]. Furthermore, ROS signaling plays an important role in CO mediated cytoprotection [7,23,38]. Therefore, we assessed whether ROS signaling is activated downstream of the P2X7R following CO treatment of cortical astrocytes. The H_2O_2 sensitive H_2DCFDA fluorescent probe was used to determine whether CORM-A1 induces ROS generation under physiological conditions, which may be relevant to FosB induction. No increase on H_2O_2 production was found upon 12.5 and 25 µM of CORM-A1 treatment after 45 min. In contrast, it was observed a significant increase in H_2O_2 generation in cortical astrocytes incubated with *t*-BHP concentrations for 25 or 45 min, which were used as positive control (Figure 6A).

In contrast with the results obtained for H_2O_2 generation, CORM-A1 significantly increased mitochondrial anion superoxide, which was quantified by the specific mitochondrial probe (MitoSOX). CORM-A1 increased mitochondrial generation of anion superoxide in a dose dependent manner after 25 min (Figure 6B). For a longer period of CORM-A1 treatment (45 min), an increase in mitochondrial superoxide anion production was only observed for the higher concentration of the CO donor tested (Figure 6B). These results are in accordance to the fact that CO targets mitochondrial and ROS are important signaling molecules. Moreover, since CO-triggered ROS signaling was observed following 25 min of CORM-A1 treatment, this may account for the up-regulation of FosB expression, which was detected after 40 - 60 min of incubation with the CO donor (Figures 2A and 4). In conclusion, these results suggest that the formation of ROS may contribute to the up-regulation in FosB expression observed in cortical astrocytes incubated with the CO donor CORM-A1. Likewise, FosB expression induced by ROS has been reported in several contexts [48,49].

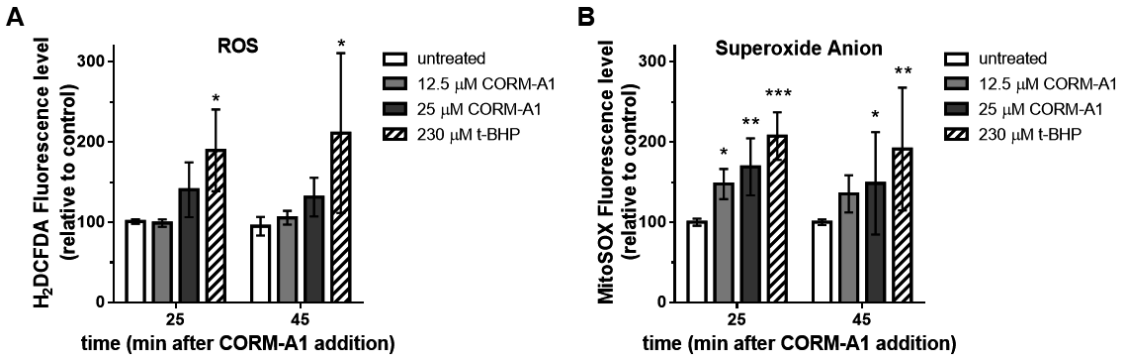

Figure 6 - CORM-A1-induced superoxide anion production in cultured cortical astrocytes. Fold change in the production of ROS was analyzed by (A) H_2DCFDA and (B) MitoSOX. Data was normalized to dye-free samples and quantified relative to control samples. The results are the mean ± SD of at least 3 independent experiments, performed in different cell preparations. **p*<0.05, ***p*<0.01, ****p*<0.001 as compared to the control with two-way ANOVA with Bonferroni post-test.

3.7 – CO-induced FosB expression is independent of ROS production

Because CO-induced early accumulation of ROS in cortical astrocytes, which is before up-regulation of FosB, it was assessed whether CO-induced FosB expression is mediated by ROS production. To address this question cultured astrocytes were incubated with two antioxidants (*N*-acetylcysteine, NAC and β-carotene) 1 h prior to CORM-A1 treatment, and FosB expression was evaluated by Western blot technique. FosB expression is not dependent on ROS production (Figure 7). At 60 min after CORM-A1 addition, no alteration on FosB protein level was observed in all conditions. Interestingly, astrocytes incubated with NAC alone for 40 min showed a strong and transient up-regulation in FosB expression. The same was observed for β-carotene, although to a minor extent. Nevertheless, it was not observed a cumulative effect between the antioxidants and CORM-A1. Further studies are necessary to disclose the anti-oxidant effect on FosB expression. Taken all together, the results show that although the CORM-A1-induced FosB expression might be initiated by P2X7R activation, the effect is independent on ROS production.

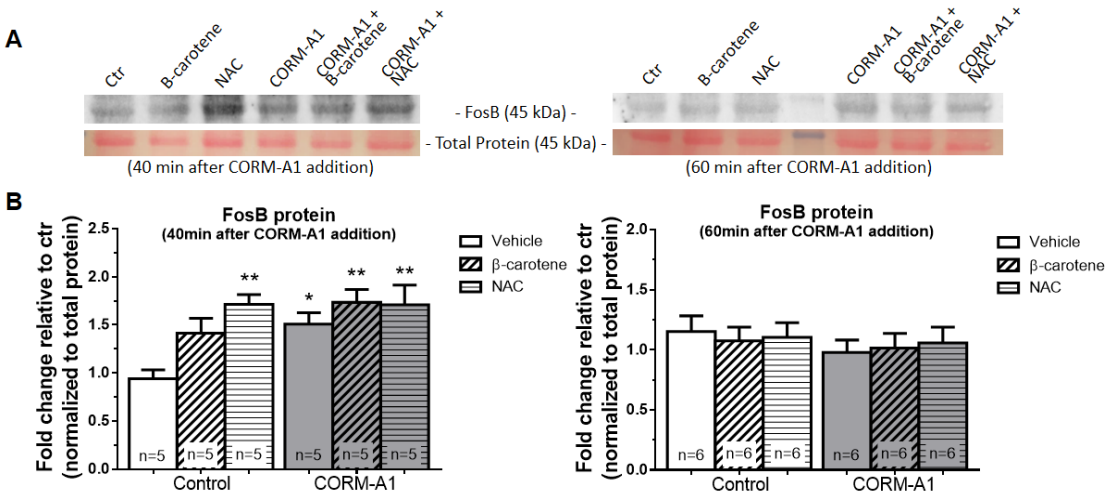

Figure 7 - Role of ROS in CORM-A1-induced expression of the FosB protein in cultured cortical astrocytes. (A) Representative blots of immune detection of FosB and respective loading control with Rouge Ponceau. The lanes correspond respectively to astrocytes without treatment, treated with β-carotene, treated with NAC, treated with CORM-A1 alone, treated with CORM-A1 together with β-carotene and treated with CORM-A together with NAC. The left images correspond to FosB levels after 40 min of CORM-A1 addition, and the right images correspond to FosB levels after 60 min of CORM-A1 addition (B). The cells were incubated with CORM-A1 (12.5 µM) and fold change in the expression of FosB was analyzed by western blot. The results are the mean ± SEM of at least 5 independent experiments, performed in different cell preparations. **p*<0.05, ***p*<0.01, ****p*<0.001 as compared with the vehicle with the Student's *t*-test.

3.8 – CO-induced cytoprotection is independent on FosB expression in astrocytes

Astrocytes, followed by microglia, are neural cells presenting the highest levels of FosB expression [50]. This high expression in glia cells may indicate that FosB is particularly important for their function, both under physiologic and pathologic conditions [51–54]. To determine whether FosB is essential in CO-induced cytoprotection, its expression was down-regulated using a specific siRNA. To verify gene silencing, FosB expression was analyzed by Western blot at 12, 24 and 48 h after siRNA transfection (Supplementary Data, Figure S1). Since FosB downregulation was more efficient at 48 h, FosB silenced astrocytes were used within this time frame.

Astrocytic cell death induced by the pro-oxidant *t*-BHP (156 µM) was assessed by PI internalization and by measuring mitochondrial membrane potential (DiOC dye). Astrocytic cultures that were pre-treated with CORM-A1 showed a significant decrease in cell death when exposed to 160 µM, as expected (Figure 8). Nevertheless, knocking down FosB did not affect the cytoprotective effect of CO, which suggest that despite being up-regulated by CO, FosB is not essential for CO to promote cytoprotection. Surprisingly, a significant cytoprotective effect was observed upon knocking down FosB expression (Figure 8).

Thus, these data open new possibilities for the CO cytoprotective mode of action: (i) CO-induced FosB expression is not relevant in the protection of astrocytes by CO; (ii) astrocytes may up-regulate other components of AP-1 to compensate for the lack of FosB; (iii) a prolonged blockage of AP-1 activation is beneficial and further protection is

achieved when CORM-A1 is added by activating antiapoptotic pathways (*e.g.* Bdnf, Bcl-2); (iv) upon downregulation of FosB, its truncated isoform may be expressed in a compensatory form to contribute to cytoprotection. Taken together, the results presented in this section suggest that the cytoprotective properties of CO are independent of FosB expression.

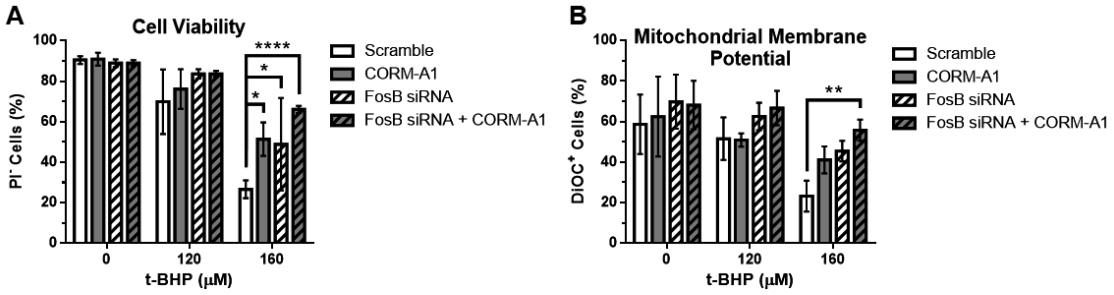

Figure 8 - Role of FosB in CORM-A1-induced protection of cortical astrocytes exposed to t-BHP. Astrocyte viability was assessed by PI internalization and assessment of mitochondrial membrane potential with DiOC. Cortical astrocytes were stimulated with *t*-BHP 20 h, and cell viability was evaluated then. (A) The viability of cortical astrocytes incubated with *t*-BHP (120 µM or 160 µM) was assessed by evaluating the uptake of PI and (B) mitochondrial membrane potential was assessed by staining with DiOC. Where indicated, cells were pre-treated with an siRNA against FosB. The effect of CORM-A1 was tested by pre-incubating the cells with the CO-donor for 60 min before stimulation with *t*-BHP. The results are the mean ± SD of at least 3 independent experiments, performed in different cell preparations. **p*<0.05, ***p*<0.01, *****p*<0.0001 as compared to the respective scramble with two-way ANOVA.

4. DISCUSSION

In order to characterize the CO-induced alterations in gene expression, the whole transcriptome from cultured cortical astrocytes was sequenced using the RNASeq technique and DEGs were identified with Poisson Distribution Model, Cuffdiff and DESeq programs. Applying RNASeq in CO research brings novelty to the field since it allows the discovery of unmapped effectors of the gasotransmitter, for example transcripts resulting from alternative splicing or novel isoforms. Additionally, another advantage of RNASeq regarding microarrays is the fact that this technique is quantitative and allows the identification of transcripts with lower abundance. Furthermore, since we addressed this question at a fairly early time point following CO exposure the approach used is expected to identify initial players contributing to CO-induced cytoprotection. Pathway analysis and functional annotation were performed *via* GoMiner and DAVID. Several genes were identified (Chapter II.I, Table S1), opening future and novel potential lines of research in CO's Biology field. Following a careful DEG data analysis, an important candidate gene was pointed out: the FBJ murine osteosarcoma viral oncogene homolog B (FosB). Indeed, CO treatment did increase the expression of FosB gene at mRNA and protein levels in astrocytes, which were assessed by qRT-PCR and Western blot techniques, respectively (Figures 2A and 4).

The CO-induced upregulation of FosB protein expression in cultured astrocytes was found to be transient, reaching its maximal at 40 min and going back to basal levels after 1h of treatment. As FosB is an immediate early gene, its expression occurs within a short time window, and presents a short half-life, upon a wide range of stimuli [26,55,56]. The FosB C-terminus contains two degron domains (amino acid sequences that regulate its own degradation rates), which are recognized as a signal for ubiquitination and proteasome-mediated degradation [57]. Herein we report a very transient effect of CORM-A1 on the expression of the FosB protein. Upon CO treatment the abundance of FosB protein decreased back to control levels at a faster rate than FosB transient induction by drugs of abuse [58]. This difference can be explained by several factors: (i) the majority of FosB studies in brain tissue were performed in neurons, and the machinery involved in the regulation of the protein half-life in astrocytes may be distinct; (ii) differences in the nature of the stimulus; (iii) CO may modulate the major pathways involved in FosB degradation. Indeed, CO decreases iNOS protein levels in hepatocytes by inducing autophagy and the ubiquitin-proteasome system [59].

In the present study, CORM-A1 was found to induce the expression of FosB by a mechanism dependent on the activation of P2X7 receptors (Figure 5). P2X7R activation has been shown to trigger FosB expression in different models [44,60]. Furthermore, P2X7Rs are implicated in cell death signaling, both in astrocytes [61,62] and other cells [63,64]. P2X7R-induced cell death can be triggered by different stimuli, in particular ischemia [65,66]. The presence and function of P2X7R in cortical astrocytes has been largely documented [60,67–69], and these receptors have a protective role in brain ischemia [46,70].

CO has been shown to induce the production of small amounts of ROS, which may function as signaling molecules to promote cytoprotection (for review see [71,72]). Indeed, herein CORM-A1 did promote mitochondrial generation of ROS (Figure 6).

Nevertheless, CO-induced increased on FosB expression was shown to be independent on ROS generation (Figure 7).

Finally, despite CORM-A1 cytoprotective role, the decreased FosB expression did not prevent the cytoprotective effects of the CO-donor in cultured cortical astrocytes subjected to oxidative stress conditions (Figure 8). These data open new possibilities for the CO cytoprotective mode of action: (i) CO-induced protection of astrocytes may depend on the combined activity of different pathways and, therefore, inhibition of one of the mechanisms involved does not change the effect of the gasotransmitter on cell survival; (ii) astrocytes may up-regulate other components of AP-1 to compensate for the lack of FosB; (iii) a prolonged blockage of AP-1 activation is beneficial and further protection is achieved when CORM-A1 is added by activating antiapoptotic pathways (*e.g.* Bdnf, Bcl-2); (iv) upon downregulation of FosB, its truncated isoform may be expressed in a compensatory form to contribute to cytoprotection; (v) CO-induced FosB expression may not be relevant in the protection of astrocytes by CO. Taken together, the results presented in this section suggest that the cytoprotective properties of CO are independent of FosB expression. The role of FosB and its isoforms has been studied most comprehensively in the context of drug addiction, but a building body of evidence also points to an important beneficial role for FosB in several pathologies, namely seizures [73], ischemia [74–76], hypoglycemia [77], nurturing defect [78,79] and Parkinson's disease [80]. However, further studies are required to understand the role FosB role and its mechanisms of action in these pathologies.

The AP-1 transcription factor is mainly composed of heterodimers of c-Jun/c-Fos or homodimers of c-Jun. It has been reported that ERK signaling pathway leads to activation of c-Fos, while JNK leads to c-Jun activation. The ERK pathway induces cell proliferation and differentiation, whereas the JNK pathway mediates inhibition of proliferation or cell death [26,30,43,81]. The results obtained in the RNASeq experiments suggest that Jun family members are not regulated by CO treatment, since no members of this family were identified in the DEGs list (Chapter II.I, Table S1), at least after 40 min of incubation with CORM-A1. Nevertheless, the cytoprotective effects of CO/HO-1 have been partially linked to AP-1 modulation via c-Fos-Jun [81–84]. Thus, it remains to be determined whether CO modulates FosB containing AP-1 and its potential role in CO-induced cytoprotection. Likewise, in the TGF-β1-dependent apoptosis, only the JunD and FosB components of AP-1 are significantly induced [85]. The same might occur in CO-dependent AP-1 induction. In the present study we found that CORM-A1 enhances the expression of FosB in cortical astrocytes. Other AP-1 components, such as the c-Jun, are known to be expressed after CO treatment, as in the case of astrocytes exposed to CORM-2 [86]. Additional studies are required to identify FosB binding partners in this context. Besides c-Jun, JunB is a probable candidate as it presents a similar induction profile to FosB in astrocytes after glutamate treatment [87].

The observed CO-induced increase in the expression of Bdnf (Figure 3) is in accordance with previous results reported by others [19,88]. Similarly, the Bcl-2 induction following CO administration was also previously described [6,7,12,89,90]. These pieces of evidence support the data showing CO as a molecule with beneficial effects, since both Bdnf and Bcl-2 are anti-apoptotic players and can contribute to the cytoprotective actions of CO. Moreover, inhibition of TrkB receptors was shown to abrogate

neuroprotection prompted by CO in astrocytes [45], further corroborating the key role of Bdnf in the protective effects of the gasotransmitter.

In conclusion, the current study indicates that CORM-A1 reduces the apoptotic death of cortical astrocytes subjected to oxidative stress conditions through a FosB-independent pathway. Whether P2X7R play a role in CO-induced protection of cortical astrocytes should be further investigated. Furthermore, the new DEG identified in astrocytes treated with CO open new opportunities for studying pathways mediating the cytoprotection role of the gasotransmitter.

ACKNOWLEDGEMENTS

We thank Pedro Fernandes for his support and expertise on RNAseq data analysis and Miranda Mele for helping in RNA processing and analysis. We thank Claudia Figueiredo-Pereira as well for the fruitful discussions regarding siRNA and flow cytometry. SRO was supported by a fellowship from Fundação para a Ciência e a Tecnologia (FCT) with reference SFRH/BD/51969/2012. This work was supported by FEDER (QREN) through Programa Mais Centro, under projects CENTRO-07-ST24-FEDER-002002, CENTRO-07-ST24-FEDER-002006 and CENTRO-07-ST24-FEDER-002008, through Programa Operacional Factores de Competitividade - COMPETE and national funds via FCT under projects Pest-C/SAU/LA0001/2013-2014, PTDC/SAU-NMC/120144/2010, PTDC/NEU-NMC/0198/2012 and FCT-ANR/NEU-NMC/0022/2012.

REFERENCES

[1] B. Wegiel, D.W. Hanto, L.E. Otterbein, The social network of carbon monoxide in medicine., Trends Mol. Med. 19 (2013) 3–11. doi:10.1016/j.molmed.2012.10.001.

[2] C.S.F. Queiroga, A. Vercelli, H.L.A. Vieira, Carbon monoxide and the CNS: challenges and achievements., Br. J. Pharmacol. (2014) 1–13. doi:10.1111/bph.12729.

[3] N. Schallner, C.C. Romão, J. Biermann, W.A. Lagrèze, L.E. Otterbein, H. Buerkle, T. Loop, U. Goebel, Carbon Monoxide Abrogates Ischemic Insult to Neuronal Cells via the Soluble Guanylate Cyclase-cGMP Pathway, PLoS One. 8 (2013). doi:10.1371/journal.pone.0060672.

[4] H.L.A. Vieira, C.S.F. Queiroga, P.M. Alves, Pre-conditioning induced by carbon monoxide provides neuronal protection against apoptosis, J. Neurochem. 107 (2008) 375–384. doi:10.1111/j.1471-4159.2008.05610.x.

[5] C.S. Queiroga, A.S. Almeida, C. Martel, C. Brenner, P.M. Alves, H.L. Vieira, Glutathionylation of adenine nucleotide translocase induced by carbon monoxide prevents mitochondrial membrane permeabilisation and apoptosis, J Biol Chem. 285 (2010) 17077–17088. doi:10.1074/jbc.M109.065052.

[6] A.S. Almeida, C.S.F. Queiroga, M.F.Q. Sousa, P.M. Alves, H.L.A. Vieira, Carbon monoxide modulates apoptosis by reinforcing oxidative metabolism in astrocytes: role of Bcl-2., J. Biol. Chem. 287 (2012) 10761–70. doi:10.1074/jbc.M111.306738.

[7] A.S. Almeida, N.L. Soares, M. Vieira, J.B. Gramsbergen, H.L.A. Vieira, Carbon Monoxide Releasing Molecule-A1 (CORM-A1) Improves Neurogenesis: Increase of Neuronal Differentiation Yield by Preventing Cell Death, PLoS One. 11 (2016) e0154781. doi:10.1371/journal.pone.0154781.

[8] F. Ulbrich, U. Goebel, D. Böhringer, P. Charalambous, W.A. Lagrèze, J. Biermann, Carbon monoxide treatment reduces microglial activation in the ischemic rat retina., Graefes Arch. Clin. Exp. Ophthalmol. 254 (2016) 1967–1976. doi:10.1007/s00417-016-3435-6.

[9] M.G. Bani-Hani, D. Greenstein, B.E. Mann, C.J. Green, R. Motterlini, Modulation of thrombin-induced neuroinflammation in BV-2 microglia by carbon monoxide-releasing molecule 3, J Pharmacol Exp Ther. 318 (2006) 1315–1322. doi:10.1124/jpet.106.104729.

[10] R. Foresti, S.K. Bains, T.S. Pitchumony, L.E. De Castro Brás, F. Drago, J.L. Dubois-Randé, C. Bucolo, R. Motterlini, Small molecule activators of the Nrf2-HO-1 antioxidant axis modulate heme metabolism and inflammation in BV2 microglia cells, Pharmacol. Res. 76 (2013) 132–148. doi:10.1016/j.phrs.2013.07.010.

[11] B. Wang, W. Cao, S. Biswal, S. Doré, Carbon monoxide-activated Nrf2 pathway leads to protection against permanent focal cerebral ischemia, Stroke. 42 (2011) 2605–2610. doi:10.1161/STROKEAHA.110.607101.

[12] C.S.F. Queiroga, S. Tomasi, M. Widerøe, P.M. Alves, A. Vercelli, H.L.A. Vieira, Preconditioning Triggered by Carbon Monoxide (CO) Provides Neuronal Protection Following Perinatal Hypoxia-Ischemia, PLoS One. 7 (2012). doi:10.1371/journal.pone.0042632.

[13] A. Yabluchanskiy, P. Sawle, S. Homer-Vanniasinkam, C.J. Green, R. Foresti, R. Motterlini, CORM-3, a carbon monoxide-releasing molecule, alters the inflammatory response and reduces brain damage in a rat model of hemorrhagic stroke., Crit. Care Med. 40 (2012) 544–52. doi:10.1097/CCM.0b013e31822f0d64.

[14] Â.A. Chora, P. Fontoura, A. Cunha, T.F. Pais, S. Cardoso, P.P. Ho, L.Y. Lee, R.A. Sobel, L. Steinman, M.P. Soares, Heme oxygenase–1 and carbon monoxide suppress autoimmune neuroinflammation, J. Clin. Invest. 117 (2007) 438–447. doi:10.1172/JCI28844.

[15] P. Fagone, K. Mangano, C. Quattrocchi, R. Motterlini, R. Di Marco, G. Magro, N. Penacho, C.C. Romao, F. Nicoletti, Prevention of clinical and histological signs of proteolipid protein (PLP)-induced experimental allergic encephalomyelitis (EAE) in mice by the water-soluble carbon monoxide-releasing molecule (CORM)-A1, Clin. Exp. Immunol. 163 (2011) 368–374. doi:10.1111/j.1365-2249.2010.04303.x.

[16] I. Allaman, M. Be, P.J. Magistretti, Astrocyte – neuron metabolic relationships : for better and for worse, Trends Neurosci. 34 (2011). doi:10.1016/j.tins.2010.12.001.

[17] L. Hertz, B.H.J. Juurlink, E. Hertz, H. Fosmark, a Schousboe, Preparation of primary cultures of mouse (rat) astrocytes, A Dissection Tissue Cult. Man. Nerv. Syst. (1986) in press.

[18] R. Motterlini, P. Sawle, J. Hammad, S. Bains, R. Alberto, R. Foresti, C.J. Green, CORM-A1: a new pharmacologically active carbon monoxide-releasing molecule., FASEB J. 19 (2005) 284–6. doi:10.1096/fj.04-2169fje.

[19] S.R. Oliveira, H.L.A. Vieira, C.B. Duarte, Effect of carbon monoxide on gene expression in cerebrocortical astrocytes: Validation of reference genes for quantitative real-time PCR, Nitric Oxide. 49 (2015) 80–89. doi:10.1016/j.niox.2015.07.003.

[20] K.J. Livak, T.D. Schmittgen, Analysis of Relative Gene Expression Data Using Real- Time Quantitative PCR and the 2^(-2ΔΔCt) Method, Methods. 25 (2001) 402–408. doi:10.1006/meth.2001.1262.

[21] C. Ficker, K. Rozmer, E. Kat??, R.D. And??, L. Schumann, U. Kr??gel, H. Franke, B. Sperl??gh, T. Riedel, P. Illes, Astrocyte-neuron interaction in the substantia gelatinosa of the spinal cord dorsal horn via P2X7 receptor-mediated release of glutamate and reactive oxygen species, Glia. 62 (2014) 1671–1686. doi:10.1002/glia.22707.

[22] A. Leichsenring, T. Riedel, Y. Qin, P. Rubini, P. Illes, Anoxic depolarization of hippocampal astrocytes: Possible modulation by P2X7 receptors, Neurochem. Int. 62 (2013) 15–22. doi:10.1016/j.neuint.2012.11.002.

[23] S.R. Oliveira, C.S.F. Queiroga, H.L.A. Vieira, Mitochondria and carbon monoxide: cytoprotection and control of cell metabolism - a role for Ca 2+ ?, J. Physiol. 594 (2016) 4131–4138. doi:10.1113/JP270955.

[24] Y. Chinenov, T.K. Kerppola, Close encounters of many kinds: Fos-Jun interactions that mediate transcription regulatory specificity, Oncogene. 20 (2001) 2438–2452. doi:10.1038/sj.onc.1204385.

[25] E. Shaulian, M. Karin, AP-1 as a regulator of cell life and death, Nat Cell Biol. 4 (2002) E131-6. doi:10.1038/ncb0502-e131.

[26] J. Hess, P. Angel, M. Schorpp-Kistner, AP-1 subunits: quarrel and harmony among siblings., J. Cell Sci. 117 (2004) 5965–5973. doi:10.1242/jcs.01589.

[27] P.W. Vesely, P.B. Staber, G. Hoefler, L. Kenner, Translational regulation mechanisms of AP-1 proteins, Mutat. Res. - Rev. Mutat. Res. 682 (2009) 7–12. doi:10.1016/j.mrrev.2009.01.001.

[28] P. Pruunsild, E. Orav, E. Esvald, AP-1 Transcription Factors Mediate BDNF-Positive

Feedback Loop in Cortical Neurons, J. Neurosci. 36 (2013) 1290–1305. doi:10.1523/JNEUROSCI.3360-15.2016.

[29] S. Hu, Y. Zhang, M. Zhang, Y. Guo, P. Yang, S. Zhang, Aloperine Protects Mice against Ischemia-Reperfusion (IR) -Induced Renal Injury by Regulating PI3K / AKT / mTOR Signaling and AP-1 Activity, (2015) 912–923. doi:10.2119/molmed.2015.00056.

[30] Q. Wang, W. Li, X.S. Liu, J.S. Carroll, O.A. Jänne, E. Krasnickas, A.M. Chinnaiyan, K.J. Pienta, M. Brown, ERK-associated changes of AP-1 proteins during fear extinction, Mol Cell Neurosci. 47 (2011) 137–144. doi:10.1016/j.molcel.2007.05.041.A.

[31] C. V Melo, S. Okumoto, J.R. Gomes, M.S. Baptista, B.A. Bahr, W.B. Frommer, C.B. Duarte, Spatiotemporal resolution of BDNF neuroprotection against glutamate excitotoxicity in cultured hippocampal neurons., Neuroscience. 237 (2013) 66–86. doi:10.1016/j.neuroscience.2013.01.054.

[32] E. a Jonas, G. a Porter, K.N. Alavian, Bcl-xL in neuroprotection and plasticity., Front. Physiol. 5 (2014) 355. doi:10.3389/fphys.2014.00355.

[33] P. Van Damme, E. Bogaert, M. Dewil, N. Hersmus, D. Kiraly, W. Scheveneels, I. Bockx, D. Braeken, N. Verpoorten, K. Verhoeven, V. Timmerman, P. Herijgers, G. Callewaert, P. Carmeliet, L. Van Den Bosch, W. Robberecht, Astrocytes regulate GluR2 expression in motor neurons and their vulnerability to excitotoxicity., Proc. Natl. Acad. Sci. U. S. A. 104 (2007) 14825–14830. doi:10.1073/pnas.0705046104.

[34] Y. Xu, H. Xue, P. Zhao, Y. Yang, G. Ji, W. Yu, G. Han, M. Ding, F. Wang, Isoflurane postconditioning induces concentration- and timing-dependent neuroprotection partly mediated by the GluR2 AMPA receptor in neonatal rats after brain hypoxia–ischemia, J. Anesth. (2016) 1–10. doi:10.1007/s00540-015-2132-7.

[35] H. Wang, M. Luo, C. Li, G. Wang, Propofol post-conditioning induced long-term neuroprotection and reduced internalization of AMPAR GluR2 subunit in a rat model of focal cerebral ischemia/reperfusion, J. Neurochem. 119 (2011) 210–219. doi:10.1111/j.1471-4159.2011.07400.x.

[36] P.D. Bhola, A. Letai, Mitochondria—Judges and Executioners of Cell Death Sentences, Mol Cell. 61 (2016) 695–704. doi:http://dx.doi.org/10.1016/j.molcel.2016.02.019.

[37] H.M. Yonutas, H.J. Vekaria, P.G. Sullivan, Mitochondrial specific therapeutic targets following brain injury, Brain Res. 1640 (2016) 77–93. doi:10.1016/j.brainres.2016.02.007.

[38] A.S. Almeida, C. Figueiredo-Pereira, H.L.A. Vieira, Carbon monoxide and mitochondria - modulation of cell metabolism, redox response and cell death, Front. Physiol. 6 (2015) 1–6. doi:10.3389/fphys.2015.00033.

[39] C.S.F. Queiroga, A.S. Almeida, H.L.A. Vieira, Carbon Monoxide Targeting Mitochondria, Biochem. Res. Int. 2012 (2012) 1–9. doi:10.1155/2012/749845.

[40] S. Dröse, Differential effects of complex II on mitochondrial ROS production and their relation to cardioprotective pre- and postconditioning, Biochim. Biophys. Acta - Bioenerg. 1827 (2013) 578–587. doi:10.1016/j.bbabio.2013.01.004.

[41] S. Grimm, Respiratory chain complex II as general sensor for apoptosis., Biochim. Biophys. Acta. 1827 (2013) 565–72. doi:10.1016/j.bbabio.2012.09.009.

[42] A. Hoshi, T. Nakahara, M. Ogata, T. Yamamoto, The critical threshold of 3-nitropropionic acid-induced ischemic tolerance in the rat, Brain Res. 1050 (2005) 33–39. doi:10.1016/j.brainres.2005.05.028.

[43] M.L. Gavala, L.M. Hill, L.Y. Lenertz, M.R. Karta, P.J. Bertics, Activation of the transcription factor FosB/activating protein-1 (AP-1) is a prominent downstream signal of the extracellular nucleotide receptor P2RX7 in monocytic and osteoblastic cells, J. Biol. Chem. 285 (2010) 34288–34298. doi:10.1074/jbc.M110.142091.

[44] L.Y. Lenertz, M.L. Gavala, Y. Zhu, P.J. Bertics, Transcriptional Control Mechanisms Associated with the Nucleotide Receptor P2X7, a Critical Regulator of Immunologic, Osteogenic and Neurologic Functions, Immunol. Res. 50 (2011) 22–38. doi:10.1007/s12026-011-8203-4.Transcriptional.

[45] C.S.F. Queiroga, R.M.A. Alves, S. V. Conde, P.M. Alves, H.L.A. Vieira, Paracrine effect of carbon monoxide – astrocytes promote neuroprotection through purinergic signaling in mice, J. Cell Sci. 129 (2016) 3178–3188. doi:10.1242/jcs.187260.

[46] Y. Hirayama, Y. Ikeda-Matsuo, S. Notomi, H. Enaida, H. Kinouchi, S. Koizumi, Astrocyte-Mediated Ischemic Tolerance, J. Neurosci. 35 (2015) 3794–3805. doi:10.1523/JNEUROSCI.4218-14.2015.

[47] L.Y. Lenertz, M.L. Gavala, L.M. Hill, P.J. Bertics, Cell signaling via the P2X7 nucleotide receptor: linkage to ROS production, gene transcription, and receptor trafficking, Purinergic Signal. 5 (2009) 175–187. doi:10.1007/s11302-009-9133-7.

[48] E. Jindal, S.K. Goswami, In cardiac myoblasts, cellular redox regulates FosB and Fra-1 through multiple cis-regulatory modules, Free Radic. Biol. Med. 51 (2011) 1512–1521. doi:10.1016/j.freeradbiomed.2011.07.008.

[49] T.B.J. Kuo, Z.F. Yuan, Y.S. Lin, Y.N. Lin, W.S. Li, C.C.H. Yang, C.J. Lai, Reactive oxygen species are the cause of the enhanced cardiorespiratory response induced by intermittent hypoxia in conscious rats, Respir. Physiol. Neurobiol. 175 (2011) 70–79. doi:10.1016/j.resp.2010.09.010.

[50] Y. Zhang, K. Chen, S.A. Sloan, M.L. Bennett, A.R. Scholze, S. O'Keeffe, H.P. Phatnani, P. Guarnieri, C. Caneda, N. Ruderisch, S. Deng, S.A. Liddelow, C. Zhang, R. Daneman, T. Maniatis, B.A. Barres, J.Q. Wu, An RNA-sequencing transcriptome and splicing database of glia, neurons, and vascular cells of the cerebral cortex, J. Neurosci. 34 (2014) 11929–11947. doi:10.1523/JNEUROSCI.1860-14.2014.

[51] K.O. Kuroda, V.G. Ornthanalai, T. Kato, N.P. Murphy, FosB null mutant mice show enhanced methamphetamine neurotoxicity: potential involvement of FosB in intracellular feedback signaling and astroglial function., Neuropsychopharmacology. 35 (2010) 641–55. doi:10.1038/npp.2009.169.

[52] L. Peng, B. Li, T. Du, E.K.C. Kong, X. Hu, S. Zhang, X. Shan, M. Zhang, Astrocytic transactivation by alpha2A-adrenergic and 5-HT2B serotonergic signaling, Neurochem. Int. 57 (2010) 421–431. doi:10.1016/j.neuint.2010.04.018.

[53] B. Li, T. Du, H. Li, L. Gu, H. Zhang, J. Huang, L. Hertz, L. Peng, Signalling pathways for transactivation by dexmedetomidine of epidermal growth factor receptors in astrocytes and its paracrine effect on neurons., Br. J. Pharmacol. 154 (2008) 191–203. doi:10.1038/bjp.2008.58.

[54] N. Yutsudo, T. Kamada, K. Kajitani, H. Nomaru, A. Katogi, Y.H. Ohnishi, Y.N. Ohnishi, K. Takase, K. Sakumi, H. Shigeto, Y. Nakabeppu, fosB-Null Mice Display Impaired Adult Hippocampal Neurogenesis and Spontaneous Epilepsy with Depressive Behavior, Neuropsychopharmacology. 38 (2013) 895–906. doi:10.1038/npp.2012.260.

[55] M. Zerial, L. Toschi, R.P. Ryseck, M. Schuermann, R. Müller, R. Bravo, The product of a

novel growth factor activated gene, fos B, interacts with JUN proteins enhancing their DNA binding activity., EMBO J. 8 (1989) 805–13.

[56] I.N. Alibhai, T. a. Green, J. a. Potashkin, E.J. Nestler, Regulation of fosB and ΔfosB mRNA expression: In vivo and in vitro studies, Brain Res. 1143 (2007) 22–33. doi:10.1016/j.brainres.2007.01.069.

[57] T.L. Carle, Y.N. Ohnishi, Y.H. Ohnishi, I.N. Alibhai, M.B. Wilkinson, A. Kumar, E.J. Nestler, Proteasome-dependent and -independent mechanisms for FosB destabilization: identification of FosB degron domains and implications for ΔFosB stability, Eur. J. Neurosci. 25 (2007) 3009–3019. doi:10.1111/j.1460-9568.2007.05575.x.

[58] E.J. Nestler, Transcriptional mechanisms of drug addiction., Clin. Psychopharmacol. Neurosci. 10 (2012) 136–43. doi:10.9758/cpn.2012.10.3.136.

[59] H.S. Kim, P.A. Loughran, T.R. Billiar, Carbon Monoxide Decreases the Level of iNOS protein and Active Dimer in IL-1β–Stimulated Hepatocytes, Nitric Oxide. 18 (2008) 256–265. doi:10.1126/scisignal.2001449.Engineering.

[60] L.E. Wickert, J.B. Blanchette, N. V. Waldschmidt, P.J. Bertics, J.M. Denu, L.C. Denlinger, L.Y. Lenertz, The C-Terminus of Human Nucleotide Receptor P2X7 Is Critical for Receptor Oligomerization and N-Linked Glycosylation, PLoS One. 8 (2013). doi:10.1371/journal.pone.0063789.

[61] E. Salas, L.M.G. Carrasquero, L. a Olivos-Oré, D. Bustillo, A.R. Artalejo, M.T. Miras-Portugal, *E.G.* Delicado, Purinergic P2X7 receptors mediate cell death in mouse cerebellar astrocytes in culture., J. Pharmacol. Exp. Ther. 347 (2013) 802–15. doi:10.1124/jpet.113.209452.

[62] M. Gandelman, H. Peluffo, J.S. Beckman, P. Cassina, L. Barbeito, Extracellular ATP and the P2X7 receptor in astrocyte-mediated motor neuron death: implications for amyotrophic lateral sclerosis., J. Neuroinflammation. 7 (2010) 33. doi:10.1186/1742-2094-7-33.

[63] K. Chu, B. Yin, J. Wang, G. Peng, H. Liang, Z. Xu, Y. Du, M. Fang, Q. Xia, B. Luo, Inhibition of P2X7 receptor ameliorates transient global cerebral ischemia/reperfusion injury via modulating inflammatory responses in the rat hippocampus, J.Neuroinflam.9(2012)69.

[64] J. Arbeloa, A. Pérez-Samartín, M. Gottlieb, C. Matute, P2X7 receptor blockade prevents ATP excitotoxicity in neurons and reduces brain damage after ischemia, Neurobiol. Dis. 45 (2012) 954–961. doi:10.1016/j.nbd.2011.12.014.

[65] H.Y. Bai, A.P. Li, P2X7 receptors in cerebral ischemia, Neurosci. Bull. 29 (2013) 390–398. doi:10.1007/s12264-013-1338-7.

[66] C.S. Bindra, A.S. Jaggi, N. Singh, Role of P2X7 purinoceptors in neuroprotective mechanism of ischemic postconditioning in mice, Mol. Cell. Biochem. 390 (2014) 161–173. doi:10.1007/s11010-014-1967-9.

[67] S. Alloisio, R. Aiello, S. Ferroni, M. Nobile, Potentiation of Native and Recombinant P2X7-Mediated Calcium Signaling by Arachidonic Acid in Cultured Cortical Astrocytes and Human Embryonic Kidney 293 Cells, Mol. Pharmacol. 69 (2006) 1975–1983. doi:10.1124/mol.105.020164.

[68] M. Nobile, I. Monaldi, S. Alloisio, C. Cugnoli, S. Ferroni, ATP-induced, sustained calcium signalling in cultured rat cortical astrocytes: evidence for a non-capacitative, P2X7-like-mediated calcium entry., FEBS Lett. 538 (2003) 71–6. http://www.ncbi.nlm.nih.gov/pubmed/12633855.

[69] K. Nagasawa, C. Escartin, R.A. Swanson, Astrocyte cultures exhibit P2X7 receptor channel opening in the absence of exogenous ligands, Glia. 57 (2009) 622–633. doi:10.1002/glia.20791.

[70] H. Franke, P. Illes, Nucleotide signaling in astrogliosis, Neurosci. Lett. 565 (2014) 14–22. doi:10.1016/j.neulet.2013.09.056.

[71] M. Bilban, A. Haschemi, B. Wegiel, B.Y. Chin, O. Wagner, L.E. Otterbein, Heme oxygenase and carbon monoxide initiate homeostatic signaling, J Mol Med. 86 (2008) 267–279. doi:10.1007/s00109-007-0276-0.

[72] C.S.F. Queiroga, A. Vercelli, H.L.A. Vieira, Carbon monoxide and the CNS: Challenges and achievements, Br. J. Pharmacol. (2014) 1–13. doi:10.1111/bph.12729.

[73] C. Giordano, J. Vinet, G. Curia, G. Biagini, Repeated 6-Hz corneal stimulation progressively increases FosB/δFosB levels in the lateral amygdala and induces seizure generalization to the Hippocampus, PLoS One. 10 (2015) 1–21. doi:10.1371/journal.pone.0141221.

[74] H. Kurushima, M. Ohno, T. Miura, T.Y. Nakamura, H. Horie, T. Kadoya, H. Ooboshi, T. Kitazono, S. Ibayashi, M. Iida, Y. Nakabeppu, Selective induction of DeltaFosB in the brain after transient forebrain ischemia accompanied by an increased expression of galectin-1, and the implication of DeltaFosB and galectin-1 in neuroprotection and neurogenesis., Cell Death Differ. 12 (2005) 1078–96. doi:10.1038/sj.cdd.4401648.

[75] M.A. Alfonso-Jaume, M.R. Bergman, R. Mahimkar, S. Cheng, Z.Q. Jin, J.S. Karliner, D.H. Lovett, Cardiac ischemia-reperfusion injury induces matrix metalloproteinase-2 expression through the AP-1 components FosB and JunB., Am. J. Physiol. Heart Circ. Physiol. 291 (2006) H1838-46. doi:10.1152/ajpheart.00026.2006.

[76] T.L. Butler, K.R. Pennypacker, Temporal and regional expression of Fos-related proteins in response to ischemic injury., Brain Res. Bull. 63 (2004) 65–73. doi:10.1016/j.brainresbull.2003.12.005.

[77] S. Al-Noori, N.M. Sanders, G.J. Taborsky, C.W. Wilkinson, A. Zavosh, C. West, C.M. Sanders, D.P. Figlewicz, Recurrent hypoglycemia alters hypothalamic expression of the regulatory proteins FosB and synaptophysin., Am. J. Physiol. Regul. Integr. Comp. Physiol. 295 (2008) R1446–R1454. doi:10.1152/ajpregu.90511.2008.

[78] J.R. Brown, H. Ye, R.T. Bronson, P. Dikkes, M.E. Greenberg, A defect in nurturing in mice lacking the immediate early gene fosB, Cell. 86 (1996) 297–309. doi:10.1016/S0092-8674(00)80101-4.

[79] K.O. Kuroda, M.J. Meaney, N. Uetani, T. Kato, Neurobehavioral basis of the impaired nurturing in mice lacking the immediate early gene FosB, Brain Res. 1211 (2008) 57–71. doi:10.1016/j.brainres.2008.02.100.

[80] N. Pavón, A.B. Martín, A. Mendialdua, R. Moratalla, ERK Phosphorylation and FosB Expression Are Associated with L-DOPA-Induced Dyskinesia in Hemiparkinsonian Mice, Biol Psychiatry. 59 (2006) 64–74. doi:http://dx.doi.org/10.1016/j.biopsych.2005.05.044.

[81] D. Morse, S.E. Pischke, Z. Zhou, R.J. Davis, R.A. Flavell, T. Loop, S.L. Otterbein, L.E. Otterbein, A.M.K. Choi, Suppression of inflammatory cytokine production by carbon monoxide involves the JNK pathway and AP-1, J. Biol. Chem. 278 (2003) 36993–36998. doi:10.1074/jbc.M302942200.

[82] B.M. Choi, H.O. Pae, Y.M. Kim, H.T. Chung, Nitric oxide-mediated cytoprotection of hepatocytes from glucose deprivation-induced cytotoxicity: Involvement of heme

oxygenase-1, Hepatology. 37 (2003) 810–823. doi:10.1053/jhep.2003.50114.

[83] F. Serizawa, E. Patterson, R.F. Potter, D.D. Fraser, G. Cepinskas, Pretreatment of Human Cerebrovascular Endothelial Cells with CO-releasing Molecule-3 Interferes with JNK/AP-1 Signaling and Suppresses LPS-induced Proadhesive Phenotype, Microcirculation. 22 (2015) 28–36. doi:10.1111/micc.12161.

[84] P.-Y. Cheng, Y.-M. Lee, N.-L. Shih, Y.-C. Chen, M.-H. Yen, Heme oxygenase-1 contributes to the cytoprotection of alpha-lipoic acid via activation of p44/42 mitogen-activated protein kinase in vascular smooth muscle cells., Free Radic. Biol. Med. 40 (2006) 1313–22. doi:10.1016/j.freeradbiomed.2005.11.024.

[85] Y. Yamamura, X. Hua, S. Bergelson, H.F. Lodish, Critical Role of Smads and AP-1 Complex in Transforming Growth Factor- -dependent Apoptosis, J. Biol. Chem. 275 (2000) 36295–36302. doi:10.1074/jbc.M006023200.

[86] P.-L. Chi, C.-C. Lin, Y.-W. Chen, L.-D. Hsiao, C.-M. Yang, CO Induces Nrf2-Dependent Heme Oxygenase-1 Transcription by Cooperating with Sp1 and c-Jun in Rat Brain Astrocytes, Mol. Neurobiol. (2014). doi:10.1007/s12035-014-8869-4.

[87] D.F. Condorelli, P. Dell'Albani, C. Amico, L. Kaczmarek, F. Nicoletti, K. Lukasiuk, A.M.G. Stella, Induction of Primary Response Genes by Excitatory Amino Acid Receptor Agonists in Primary Astroglial Cultures, J. Neurochem. 60 (1993) 877–885. doi:10.1111/j.1471-4159.1993.tb03232.x.

[88] S.-Y.S. Hung, H.-C.H. Liou, W.-M.W. Fu, The mechanism of heme oxygenase-1 action involved in the enhancement of neurotrophic factor expression., Neuropharmacology. 58 (2010) 321–329. doi:10.1016/j.neuropharm.2009.11.003. Epub 2009 Nov 20.

[89] A. Sener, K.C. Tran, J.P. Deng, B. Garcia, Z. Lan, W. Liu, T. Sun, J. Arp, M. Salna, P. Acott, G. Cepinskas, A.M. Jevnikar, P.P.W. Luke, Carbon monoxide releasing molecules inhibit cell death resulting from renal transplantation related stress, J. Urol. 190 (2013) 772–778. doi:10.1016/j.juro.2012.12.020.

[90] N. Schallner, M. Fuchs, C.I. Schwer, T. Loop, H. Buerkle, W.A. Lagrèze, C. van Oterendorp, J. Biermann, U. Goebel, Postconditioning with Inhaled Carbon Monoxide Counteracts Apoptosis and Neuroinflammation in the Ischemic Rat Retina, PLoS One. 7 (2012). doi:10.1371/journal.pone.0046479.

SUPPLEMENTARY DATA

Table S1 – Detailed description of the primers used.

gene	acession number	description	primer sequence (fw & rv)	Cell function
Ppia	BC059141	Rat peptidylprolyl isomerase A	TTTGGGAAGGTGAAAGAAGGC ACAGAAGGAATGGTTTGATGGG	Protein folding and transport
gapdh	NM_008084.2	Mouse glyceraldehyde-3-phosphate dehydrogenase	ACAATGAATACGGCTACAG GGTCCAGGGTTTCTTACT	Glycolytic enzyme
fosB	NM_008036.2	Mouse FBJ osteosarcoma oncogene B	ACACAGTGAAGTTCAAGTC GTGAGGACAAACGAGGAA	Transcription factor
rgs10	NM_026418.2	Mouse regulator of G-protein signalling 10	TGGACTCTTAGGACTGTA AGTATTGGCAGAATCTCA	GTPase deactivating proteir
scand1	NM_020255.3	Mouse SCAN domain-containing 1	CGCCATCCTTAGTGTCAGTA GCCTCCTCTACCAGTCAC	Transcription factor
rn18s	NR_003278.3	Mouse 18S ribossomal RNA	ACAGGATTGACAGATTGA TATCGGAATTAACCAGACA	Ribosomal protein
actg1	NM_009609.2	Mouse actin, gamma, cytoplasmic 1	CTGGAATAAGCCTTTGAAA GCACAGGGTATTAAACATAT	Cytoskeletal structural protein
pcdhb21	NM_053146.2	Mouse protocadherin beta 21	TTAGCAATTTGTTGACTCTC GAAAGTTATCTACTGAATTAGGA	Cell adhesion protein
panx1	NM_019482.2	Mouse pannexin 1	CTGTTGGATCTGTAGTTAGTT TTCTTCTATGACGCTGTTG	Gap junction component, Hemichannel
Sdha	NM_023281.1	Mouse succinate dehydrogenase complex,	CTCATCAACAGTCAAGGT TCATGGATCGAGACACAA	Glycolytic enzyme, oxidative phosphorylation
Gria2		Rat Glutamate receptor, ionotropic, AMPA2	TTTAGCACCGCGGACAGCGCT	
BDNF	NM_007540.4	Rat brain-derived neurotrophic factor	TAACCTCGCTCATTCATTA TCAACTCTCATCCACCTT	Cell Survival
Bcl-2	NR_009741.4	Rat B cell leukemia/lymphoma 2	GGTGGAGGAACTCTTCAGGG GAGACAGCCAGGAGAAATCA	Programmed cell death

NOTE: The database source is the NCBI Reference Sequence (http://www.ncbi.nlm.nih.gov). Annealing temperature (Ta), melting temperature (Tm) and product length were determined by Beacon Designer software. Primer efficiency was determined by a standard curve of cDNA samples (see Materials and Methods).

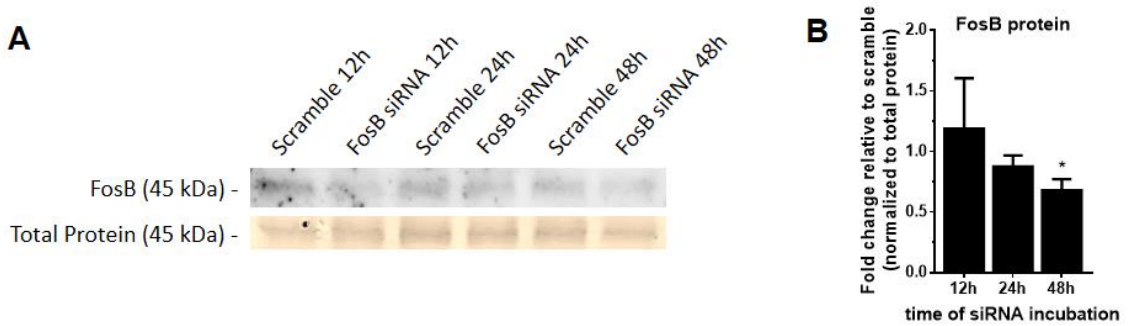

Figure S1 – Efficacy of FosB siRNA in cultured cortical astrocytes. (A) Representative blots of immune detection of FosB and respective loading control with Rouge Ponceau. The lanes correspond respectively to astrocytes with scramble for 12h, with FosB siRNA for 12h, with scramble for 24h, with FosB siRNA for 24h, with scramble for 48h and with FosB siRNA for 48h. (B) fold change in the expression of FosB was analyzed by western blot. The results are the mean ± SEM of at least 3 independent experiments, performed in different cell preparations. *$p<0.05$, as compared with the respective scramble with the student t-test.

Chapter II.IV

Cerebrovascular Effects of CO

This chapter is based on the following manuscript:

Cerebral Vascular Response to systemic Carbon monoxide administration – regional and gender differences

Sara R. Oliveira, João Castelhano, José Sereno, Carlos B Duarte and Miguel Castelo-Branco
(in preparation)

INDEX

ABSTRACT

It is well established that the endogenous gasotransmitter carbon monoxide (CO) modulates the vascular tone. This property presents an enormous therapeutic potential in a wide variety of diseases. In particular, the activity of the brain tissue is highly dependent of the vascular capability to supply its energetic needs. A fine-tuned crosstalk between cerebral vasculature and function of neuronal cells is crucial both in physiological and in pathological conditions. Previous studies where CO effect in the vasculature was addressed, have been performed exclusively in male or sexually-immature animals.

Understanding the gender differences regarding systemic drug processing and pharmacodynamics is an important feature for safety assessment of drug dosing and efficacy. In this work, we used CORM-A1 as source of CO to examine the effects of the gasotransmitter on brain perfusion and the gender-dependent differences. The dynamic contrast-enhanced imaging (DCE) based analysis was used to deeper characterize the properties of CO in the modulation of cerebral vasculature. Perfusion of the temporal muscle, middle cerebral artery and three brain regions (hippocampus, cortex and striatum) were calculated with and without CORM-A1 administration.

Prior to CO exposure, females presented 3-fold less brain perfusion than males. Under CO treatment, they showed an enhanced responsiveness with an overall reduction in perfusion. The results showing a simultaneous vasoconstriction in the hippocampus and striatum following administration of CO can be relevant regarding memory, since these two regions are implicated in memory formation [1].

Future studies should address the molecular players involved in the regional and gender differences observed upon CO administration.

KEYWORDS

Carbon monoxide, vasomodulation, brain, gender, MRI.

ABBREVIATIONS

AUC – Area under the curve
CA – Contrast agent
CBF – Cerebral blood flow
CO – Carbon monoxide
CORM-A1 – Carbon monoxide-releasing molecule A1
CYP - Cytochrome P450
DCE – Dynamic contrast-enhanced
HO - Heme oxygenase
i.p. – Intraperitoneal
MRI – Magnetic resonance imaging
NOS – Nitric oxide synthase
ROI – Region of interest
ROS – Reactive oxygen species
SI – Signal intensity
TTP – Time to peak

1. INTRODUCTION

Several studies have reported anti-inflammatory and anti-apoptotic effects of the gasotransmitter carbon monoxide (CO) ([2,3]), as well as the modulation of cell metabolism ([4]). Furthermore, CO has strong but transient effects at the level of vascular tone in many different disease models and tissues [5–11]. The studies of CO-induced responses on brain vasculature have been focused on the cortical region, by performing cranial windows, and reported CO-induced vasodilation in the pial arteries [12–15]. However, other reports showed that CO inhibits nitric oxide-induced vasodilation [16]. Furthermore, in the hypothalamus, CO had dual indirect effects: vasodilation mediated by prostaglandin E2 and vasoconstriction as a result of nitric oxide synthase (NOS) inhibition [17]. The diversity of vasculature changes induced by CO makes difficult the characterization of the effects of this gasotransmitter. In particular, it is important to understand the regional differences in the physiological response to low doses of CO. Moreover, given the importance of blood perfusion to the brain, it is critical to understand how CO can be modulated and to develop the appropriate tools to modulate brain blood perfusion. A deeper understanding of the effects of CO on the cerebral vasculature can ultimately facilitate drug delivery to the brain, improve oxygenation and nutrient supply, and may contribute as well to CO translation to clinical practice as a therapy.

It is known that cerebrovascular modulation is a complex and multifaceted action, being gender one of the influencing factors. Accordingly, the vascular production of ROS differs among genders and this may be a crucial feature for gender-dependent responses [18]. In addition, it was recently reported that vascular smooth muscle cells from males and females respond differently to stressful stimuli, and mitochondria are the main cell fate orchestrators [19]. These findings are particularly relevant in the study of the vascular role of CO, since this gasotransmitter is able to promote ROS signaling and to modulate oxidative stress [20,21].

Although isolated non-tumor cultured cells or tissue grafts maintained *in vitro* were shown to keep a sort of sexual dimorphism [22], *in vivo* studies continue to be needed and essential. *In vivo* studies regarding vascular sex differences are still scarce, specially using noninvasive methodologies [23,24]. In this work, we used dynamic contrast enhanced (DCE) magnetic resonance imaging (MRI) to evaluate the effects of CORM-A1 on mouse vasculature and its permeability to small molecules in different brain regions. The effects were compared in healthy adult male and female mice, with the aim of characterizing the role of CO on cerebrovascular tone. DCE-MRI is a noninvasive technique that is often used clinically, which provides physiologically meaningful semi-quantitative and quantitative assessment of vascular parameters. DCE-MRI data showed a general decrease in signal intensity (SI) on mice under CORM-A1 effect. This result suggests an overall reduction in the CBF following CORM-A1 treatment. However, sex dimorphism was observed when data was analyzed by gender. Moreover, responses to CORM-A1 were also found to be brain region dependent.

2. MATERIALS AND METHODS

2.1. Animals and experimental design

Healthy adult male (n=4) and female (n=5) Bl6/c57 mice (10-16 weeks-old) were used in the experiments. Animals were maintained with 12 h light/dark cycles and kept on a standard laboratory diet with food and water *ad libitum*. Animal experiments were conducted according to the European Council Directives on Animal Care and were reviewed and approved by DGAV, Portugal.

2.2. Administration of CO to adult mice

CORM-A1, a CO releasing molecule [25], was used to systemically deliver CO in mice. CORM-A1 (Sigma) stock solution was prepared in 0.9% NaCl solution and stored at -20°C to avoid loss of released CO. The period of image acquisition to evaluate the effect of CORM-A1 on brain perfusion was selected based on the work of Zimmermann and colleagues [13]. DCE acquisition was performed for 12 min prior and 108 min after CORM-A1 i.p. administration, at a final concentration of 3 mg/kg and 5 mg/kg.

2.3. MRI protocols

MRI was carried out first without CO treatment and then with CO treatment in the same animal one week later. Anesthetized mice were scanned before and after administration of CORM-A1. Mice were anesthetized with 1.5% (v/v) isoflurane in air, and placed on controlled temperature beds through water baths (Haake SC 100, Thermo Scientific, USA) with tooth bar and head restraint to reduce motion artifact. Body temperature was maintained at 37ºC and assessed cardiorespiratory function (1030, SA Instruments Inc., NY, USA). MRI was performed on a 9.4T MR pre-clinical scanner (Bruker Biospec, Billerica MA, USA) equipped with a standard Bruker crosscoil setup using a volume coil for excitation (86/112 mm of inner/outer diameter) and quadrature mouse surface coil for detection (Bruker Biospin, Ettlingen, Germany). The system was interfaced to a Linux PC running Topspin 3.1PV and Paravision 6.0 (Bruker Biospin). High resolution morphological images were acquired with a 2D T2-weighted turbo RARE (rapid acquisition with relaxation enhancement) sequence with with TR = 3.6 ms, TE = 33.0 ms, matrix 256 × 256 and field of view 20.0 × 20.0 mm reaching an in plane spatial resolution of 78*78 μm^2, rare factor 8, axial slice thickness 0.5 mm and 5 averages resulting in 9 min 36 sec of scan time.

Brain permeability was evaluated after injection of Gadovist® (0.1 mmol/kg) using the dynamic contrast-enhanced magnetic resonance imaging technique. The following parameters were used in 2D DCE-FLASH: TE/TR = 2.5/191.145 ms, flip angle = 70º, FOV = 20 x 20 mm, matrix = 156 x 85, slice thickness 0.5 mm, number of slices = 18, number of repetitions = 80 and time acquisition of 2 h 6 min 40 s. After the first 8 repetitions, a bolus injection of the solutions (saline 0.9% or CORM-A1 and contrast agent) was administered via the catheter.

2.4. Offline processing of imaging data

DCE data were pre-processed (*e.g.* rescaled) and filtering (*e.g.* excluding voxels outside the brain) and movement corrections were applied.

Image analysis was performed within the Regions-of-Interest (ROI). These regions were draw for each animal in a semi-automatic procedure, using MRICron (2015) and custom made Matlab (R2013b) functions. Other in-house Matlab functions were used for further analysis and extraction of perfusion measurements. The perfusion curve (accumulation of contrast agent) was extracted per ROI and animal, and normalized to the baseline (time-window before injection). From these curves, we calculated the Time to peak (TTP; time delay between injection and perfusion peak), the peak amplitude (max perfusion value) and the area under the curve (AUC). Note that the AUC parameter is the overall accumulation of contrast agent in the ROI. These parameters were used for statistical group comparisons as described next.

2.5. Statistical analysis

Data are presented as the mean $\pm$ standard error of the mean (SEM) and were calculated using GraphPad Prism 6 (GraphPad Software, Inc.).

3. RESULTS

3.1. CORM-A1 induces specific perfusion differences detectable by DCE

Two doses of CORM-A1 were tested, 3 and 5 mg/kg, which were reported to be non-toxic in Bl6/c57 mice, giving rise to the production of less than 10% COHb [26]. The latter concentration is the highest CORM-A1 dose that can be administered to mice without exceeding the 10% COHb threshold; a dose of 7.5 mg/kg surpasses that toxic concentration [26]. In a previous study characterizing the effect of 2 mg/kg CORM-A1 on cortical pial dilation over time in newborn piglets, a peak of dilation at 40 min was observed after i.p. injection of the CO donor [13]. Therefore, our experimental design was implemented to estimate the effect of CORM-A1 up to 50 min after i.p. injection (Figure1). Herein the effects observed in the brain were compared with the response in the temporal muscle and in the middle cerebral artery (from now on referred to as vessel). Whole brain analysis showed that after the 20th dynamic, both CORM-A1 doses presented similar signal intensity (SI) values, which were above the control (Figure 1B). In animals injected with 5 mg/kg CORM-A1, the SI of the hippocampus and cortex was lower than that observed upon administration of a lower dose of CORM-A1, but above the SI determined under control conditions. The absence of a dose-response in the hippocampus and cortex suggests that the vasomodulatory effects of CORM-A1 may show a bell-shaped profile. This is not surprising since a bell-shaped profile was already described for CO in cancer modulation [27]. The striatal tissue did not seem to respond significantly to CORM-A1 at the tested doses. In contrast with the brain tissue, the temporal muscle and the middle cerebral artery showed a clear dose-dependent response to the administration of CORM-A1.

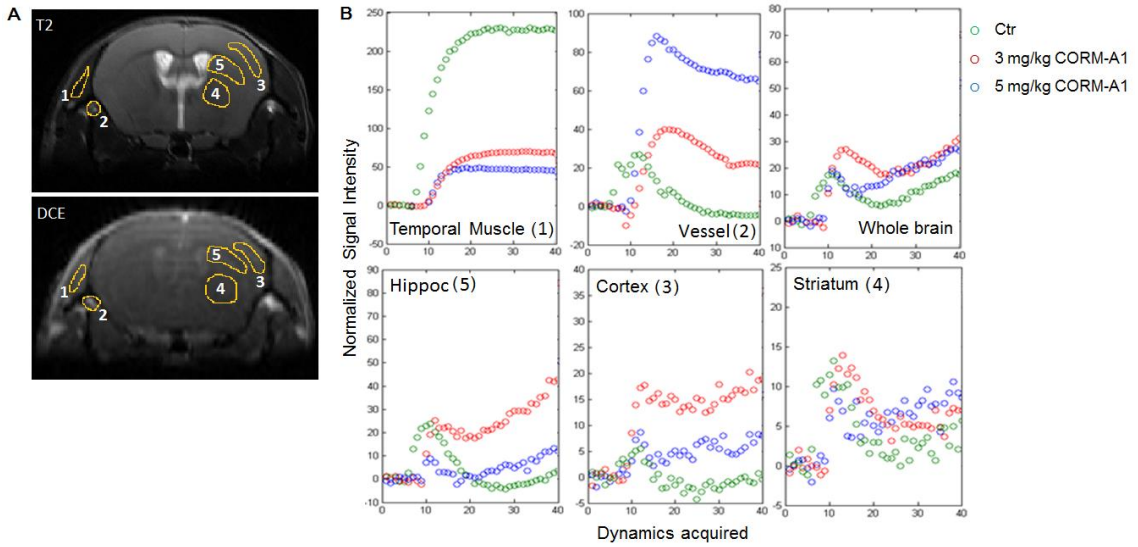

Figure 1 – Effect of CORM-A1 administration on blood perfusion in the brain. Green circles represent the signal intensity under physiological perfusion levels. Red and blue circles represent perfusion after systemic administration of CORM-A1 (3 mg/kg and 5 mg/kg, respectively). (A) Representative images of the drawn ROIs for the tissues under study. ROIs 4 and 5 corresponding to striatum and hippocampus, respectively, where not drawn from the same slice as these two brain structures do not appear in the same representative image. For explanatory reasons and simplicity, these are here represented in the same image. (B) Representative signal profiles for each tissue analyzed. Signal intensity was normalized to the first 8 dynamics obtained without CA injection. Hippoc: hippocampus.

In conclusion, low doses of CO induce alterations in brain vasculature that are detected by DCE in the brain regions studied.

3.2. CORM-A1-induced reduction in brain perfusion

We first evaluated the vascular impact of CORM-A1 administration in a mixed-gender cohort of mice (5 females and 4 males). In control tissues (muscle and vessel), CO did not produce any significant alteration in the perfusion rate (Figure 2A). In contrast, CORM-A1 reduced significantly the blood perfusion in the striatum and hippocampus (Figure 2B). Both areas contributed to an overall reduction in the perfusion rate when the entire brain was analyzed. The cerebral cortex followed the tendency of the other two brain regions evaluated, but the effect was not statistically significant. These results are in contrast with the vasodilation of the cortical area upon CO treatment reported by others [12–16].

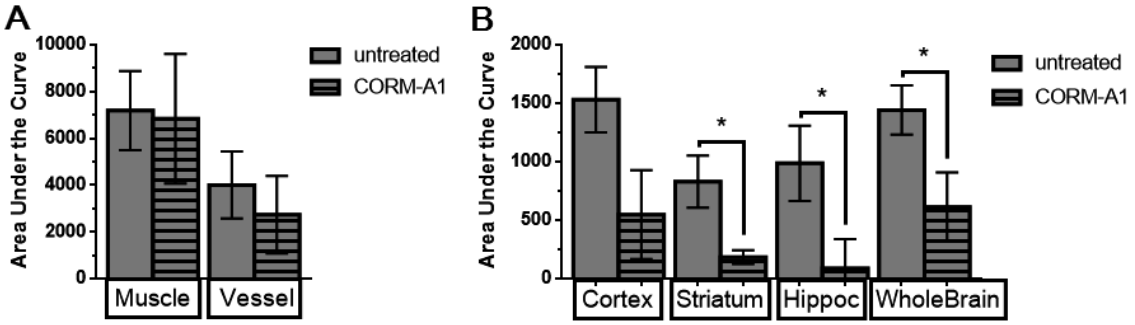

Figure 2 - CORM-A1 decreases general perfusion in the brain of a mixed gender cohort of mice. Grey bars represent physiological perfusion levels. Stripped bars represent perfusion after systemic administration of CORM-A1 (3 mg/Kg). Blood perfusion was analyzed in (A) non-brain tissues (temporal muscle and maxillary vein) and in (B) brain tissue. The area under the curve (AUC) of the signal intensity profile obtained during 2 h of acquisition was calculated. The results are the average ± SEM of 9 animals (5 females and 4 males). Statistical analysis was performed using the unpaired Student's *t*-test. **p*<0.05 as compared to the control (untreated).

Together, these results show that CO induces a reduction in brain perfusion, with a major impact in the striatum and hippocampus.

3.3. Physiological and CO-induced gender differences in perfusion

In additional studies, we analyzed the basal perfusion rate in non-brain tissues (muscle and vessel), distinguishing male and female mice (Figure 3A). A lower regional perfusion rate was observed in female mice upon analysis of the ROI when compared with the male counterparts. The perfusion in the female muscle is less than half of the rate determined in the male muscular tissue. This difference is maintained at the maxillary vein, where the rate of perfusion in males was almost 2 times higher when compared with females. None of regions studied showed higher perfusion in females than in males.

CO strongly reduced perfusion in the temporal muscle and maxillary vein of female mice (Figure 3A). In contrast, in male mice there was an increase in the rate of perfusion in the temporal muscle (but not in the maxillary vein) after administration of CORM-A1, which however was not statistically significant. Brain tissues of both genders showed a decrease in the rate of perfusion upon systemic administration of CORM-A1 addition (not statistically significant), being the only exception the cerebral cortex of male mice. This brain area showed the opposite response to CO when compared to the other brain areas (Figure 3B).

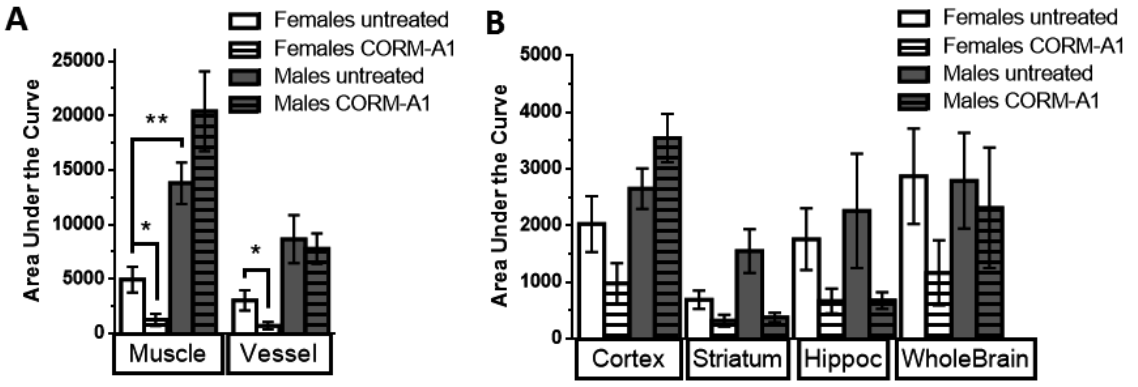

Figure 3 – Gender-dependent effects of CORM-A1 on the rate of perfusion in different tissues. White bars represent perfusion levels under control conditions. Striped bars represent perfusion after systemic administration of CORM-A1 (3 mg/Kg). Blood perfusion was analyzed in (A) non-brain tissues and in (B) the brain tissue. The results show the area under the curve (AUC) of the signal intensity profile of 5 females and 4 males obtained during 2 h of acquisition. *p<0.05 **p<0.01 as compared between genders or to the respective untreated area with unpaired Student's t-test. Hippoc - hippocampus

The overall analysis of the results obtained regarding the rate of perfusion in the different brain regions, and the effect of CO administration in both genders (Figure 3), shows that individual responses follow the same pattern, but there is considerable variability in the absolute values. Therefore, from the results of Figure 3, it was calculated the CORM-A1-induced alteration in the rate of perfusion for each animal, and the average results are plotted in Figure 4. With the AUC fold change representation, it is evident that the cortical region is the only brain ROI with a similar response to the non-cerebral ROIs due to CO administration. In these 3 ROIs (Muscle, Vessel and Cortex), males tend to present an increase of AUC, while females show the opposite CO-induced effect. In both genders, CO contributed for a striatal and hippocampal AUC reduction (Figure 4).

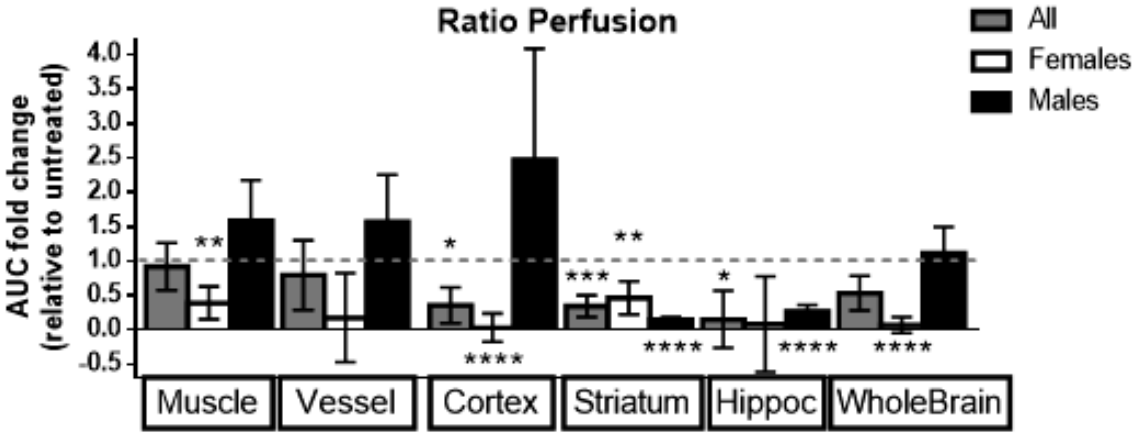

Figure 4 – Effect of CORM-A1 on the rate of perfusion in different tissues. The response to CORM-A1 was expressed as fold change when compared with the control condition. The AUC for the selected ROI was calculated before and after administration of the CO donor. The results correspond to the signal intensity profile (area under the curve [AUC]) obtained during 2 h of acquisition). The results are the average ± SEM (all = 9 animals, females = 5 animals, males = 4 animals). **p*<0.05, ***p*<0.01, ****p*<0.001, *****p*<0.0001 were calculated with unpaired Student's *t*-test.

Altogether, these results show that CO promotes a regional and gender-dependent response in the cerebral vasculature.

3.4. Semi-quantitative analysis of gender differences in cerebral blood flow

Alteration of the vascular density and/or permeability can be quantified by several DCE-MRI metrics. For example, it is widely accepted that an increase in vascular permeability is accompanied by an increase of the wash-in slope (how fast the contrast reagent reaches its maximum), AUC and peak amplitude. A decrease of the time to reach the maximal signal form the contrast agent administered ('time to peak' - TTP) is also observed under the same conditions (for a review, see [28]).

One of the semi-quantitative parameters extracted from a DCE acquisition is the 'time to peak' (TTP), which is inverse to cerebral blood flow (CBF). Administration of CORM-A1 significantly delayed the time to peak in the female hippocampus as well as in non-brain tissues (Figure 5A). This result is in accordance with the AUC data, reinforcing the capacity of CO to reduce CBF in females.

Another semi-quantitative parameter is the amplitude of the change in the signal from the contrast-reagent ('peak amplitude', which can be directly correlated with CBF). Acquisitions performed under the effect of CORM-A1 showed a significant decrease of the peak amplitude in the striatum of female mice (Figure 5A). A decrease was also observed in all the other female ROIs; however, it was not statistically significant. Similarly, analysis of the whole female brain did not show significant effects of CO on the peak amplitude of the response to the administration of the contrast agent. Furthermore, administration of CORM-A1 did not affect significantly the amplitude of the peak after administration of the contrast reagent in the brain of male mice (Figure 5C), and similar results were obtained in the temporal muscle and maxillary vein (Figure 5B).

In conclusion, the results of the DCE-MRI experiments showed that CO impacts the cerebral blood flow of female mice, with no effect on the male counterparts (Figure 5).

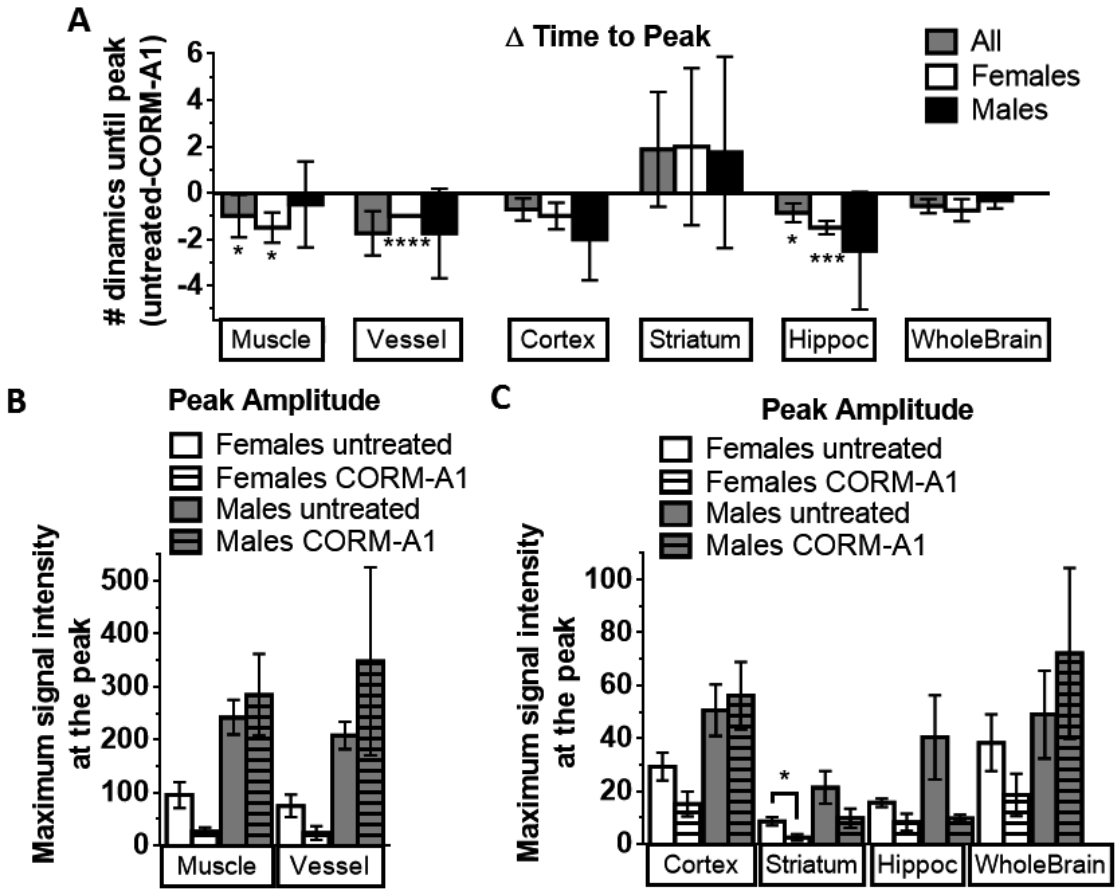

Figure 5 - Effect of CORM-A1 on the cerebral blood flow. (A) Variation of the time to peak after administration of Gadovist® was calculated by subtracting the number of dynamics acquired until the peak was reached in CORM-A1 treated mice from the value obtained under control conditions for each animal. Statistical analysis was performed using the unpaired Student's *t*-test. **p*<0.05, ****p*<0.001, *****p*<0.0001 as compared to the control condition. (B, C) Effect of CORM-A1 on the amplitude of the signal resulting from the administration of the contrast reagent ('Peak amplitude'). Panel (B) shows the signal intensity at the peak in the temporal muscle and in the maxillary vein, while panel (C) shows the effects in different brain regions. The results are the average ± SEM for n≥4. Statistical analysis was performed using the unpaired Student's *t*-test. **p*<0.05, as compared to the respective control.

4. DISCUSSION

In this work, it was found that systemic administration of CORM-A1 induces vasoconstriction in the cerebral cortex of female mice, while the opposite effect was observed in male mice, although the results were not statistically significant in the latter experiments. Similar evidences were obtained when the rate of perfusion was analyzed in the temporal muscle. In contrast with the results obtained in the cerebral cortex, CORM-A1 reduced the rate of perfusion in the striatum and in the hippocampus of male and female mice. Taken together, the changes in brain vascular parameters identified by DCE MRI established that CORM-A1 induces vasomodulation in the brain, in a region and gender-dependent manner. The effects of CO in the vasomodulation are more robust in female than in male mice, since 4 out of the 6 evaluated regions presented significant alterations in the rate of perfusion in females after exposure to the gasotransmitter. In male mice, only 2 out of the 6 regions assessed showed significant changes in the rate of perfusion upon treatment with CO. Furthermore, the results of this study show that systemic CORM-A1 administration robustly reduced cerebral blood flow, especially in females. Only the male cortical tissue did not follow this trend.

The differential effects of CORM-A1 observed in this work may explain, at least in part, some gender differences in the susceptibility to several diseases with a vascular component, such as stroke [29]. Females typically have higher levels of endogenous HO [30], the enzyme that produces CO. Therefore, their sensitivity to this gasotransmitter may vary from that of males and this may account, at least in part, for the gender differences in the response to CO. The vascular response is mediated by many contributors: potassium and calcium channels, astrocyte end feet, hormones and many more [31–33]. As these contributor's function in a gender-dependent manner, it is not surprising the differences observed.

Sexual dimorphism of the brain occurs at different levels, both in rodents and in men. For example, hippocampi of men and women are anatomically and neurochemically distinct, and differences have also been reported in the molecular mechanisms involved in long-term potentiation [34]. Likewise, women have a larger cortical thickness and higher percentage of grey matter, whereas men have a higher percentage of white matter and of CSF [35,36]. Moreover, male rat amygdala has about 80% more excitatory neurons than females. The molecule that has been more associated to gender differences in brain vasculature is perhaps estrogen. Its receptors have been found in the hypothalamus, pituitary gland, hippocampus, and frontal cortex of females, and therefore it may contribute to regional differential reactivity [37]. Human preterm neonate males were also reported to have higher levels of CO [38]. It is also known that cerebral vasoreactivity to several molecules (*e.g.* L-NAME, phenylephrine, NO) differs between genders [39] and it is a predictable marker of acquired dementia [40]. Thus, the differential vasoreactivity to CO in the two genders may also be related with a distinct a susceptibility to neurodegenerative diseases.

We hypothesize that the gender-dependent effects of CO on brain vasculature may be due to a differential expression of CYPs (Cytochrome p450) or through modulation of gender specific CYP pools. A different target of CO may be the soluble epoxide hydrolase (sEH), a key enzyme in the metabolism of vasodilatory epoxyeicosatrienoic acids (EETs). This enzyme is sexually dimorphic, being suppressed by estrogen, and

contributes to the gender differences in cerebral blood flow and injury after cerebral ischemia. CYP-independent pathways responsible for vasomodulation were also described to be gender biased. For example, substance P (a neuropeptide) and shear stress-induced dilation of skeletal muscle arterioles was greater in female than male rats, as a result of the enhanced release of NO in females [41].

DCE-MRI results showed that CO causes an average 2-fold decrease in both control and brain tissues of mice, indicating vasodilation and increase in the blood brain barrier permeability. These vascular changes may contribute to the CO induced cytoprotection reported in several animal models of brain pathologies [12,42,43]. This vasodilatation following administration of CORM-A1 may be exploited in the development of drug delivery strategies.

In conclusion, striking differences were found between the healthy male and female brains after exposure to low doses of CORM-A1. Differences in the vasoreactivity likely play a key role in this dichotomy, as was depicted by the DCE-MRI analysis (Figure 5). These important observations challenge the fundamental assumption that the effects of CO are generally vasodilatory and are not influenced by gender. It is likely that these results also provide a regional clue as to how CO protects the brain during injury.

ACKNOWLEDGEMENTS

We thank Sónia Gonçalves for all the expertise in DCE data processing and analysis. We thank João Peça for the fruitful discussions regarding brain regional differences. SRO was supported by a fellowship from Fundação para a Ciência e a Tecnologia (FCT) with reference SFRH/BD/51969/2012. This work was supported by FEDER (QREN) through Programa Mais Centro, under projects CENTRO-07-ST24-FEDER-002002, CENTRO-07-ST24-FEDER-002006 and CENTRO-07-ST24-FEDER-002008, through Programa Operacional Factores de Competitividade - COMPETE and national funds via FCT under projects Pest-C/SAU/LA0001/2013-2014, PTDC/SAU-NMC/120144/2010, PTDC/NEU-NMC/0198/2012 and FCT-ANR/NEU-NMC/0022/2012.

REFERENCES

[1] L. Schwabe, Memory under stress: from single systems to network changes, Eur. J. Neurosci. (2016). doi:10.1111/ejn.13478.

[2] L. Rochette, Y. Cottin, M. Zeller, C. Vergely, Carbon monoxide: Mechanisms of action and potential clinical implications, Pharmacol. Ther. 137 (2013) 133–152. doi:10.1016/j.pharmthera.2012.09.007.

[3] S.W. Ryter, A.M.K. Choi, Carbon monoxide: present and future indications for a medical gas., Korean J. Intern. Med. 28 (2013) 123–40. doi:10.3904/kjim.2013.28.2.123.

[4] A.S. Almeida, C. Figueiredo-Pereira, H.L.A. Vieira, Carbon monoxide and mitochondria - modulation of cell metabolism, redox response and cell death, Front. Physiol. 6 (2015) 1–6. doi:10.3389/fphys.2015.00033.

[5] C.W. Leffler, H. Parfenova, J.H. Jaggar, Carbon monoxide as an endogenous vascular modulator, AJP Hear. Circ. Physiol. 301 (2011) H1–H11. doi:10.1152/ajpheart.00230.2011.

[6] Y.K. Choi, E.D. Por, Y.-G. Kwon, Y.-M. Kim, Regulation of ROS production and vascular function by carbon monoxide., Oxid. Med. Cell. Longev. 2012 (2012) 794237. doi:10.1155/2012/794237.

[7] R. Motterlini, Carbon monoxide-releasing molecules (CO-RMs): vasodilatory, anti-ischaemic and anti-inflammatory activities., Biochem. Soc. Trans. 35 (2007) 1142–6. doi:10.1042/BST0351142.

[8] H. Lin, J.J. McGrath, Carbon monoxide effects on calcium levels in vascular smooth muscle., Life Sci. 43 (1988) 1813–1816.

[9] S. Salomone, R. Foresti, A. Villari, G. Giurdanella, F. Drago, C. Bucolo, Regulation of vascular tone in rabbit ophthalmic artery: Cross talk of endogenous and exogenous gas mediators, Biochem. Pharmacol. 92 (2014) 661–668. doi:10.1016/j.bcp.2014.10.011.

[10] E. Bor-Seng-Shu, W.S. Kita, *E.G.* Figueiredo, W.S. Paiva, E.T. Fonoff, M.J. Teixeira, R.B. Panerai, Cerebral hemodynamics: concepts of clinical importance., Arq. Neuropsiquiatr. 70 (2012) 352–356. doi:10.1590/S0004-282X2012000500010.

[11] J.C. Van Den Born, H.-P. Hammes, W. Greffrath, H. Van Goor, J.-L. Hillebrands, Gasotransmitters in Vascular Complications of Diabetes, Diabetes. 65 (2016) 331–345. doi:10.2337/db15-1003.

[12] P. Carratu, M. Pourcyrous, A. Fedinec, C.W. Leffler, H. Parfenova, Endogenous heme oxygenase prevents impairment of cerebral vascular functions caused by seizures., Am. J. Physiol. Heart Circ. Physiol. 285 (2003) H1148–H1157. doi:10.1152/ajpheart.00091.2003.

[13] A. Zimmermann, C.W. Leffler, D. Tcheranova, A.L. Fedinec, H. Parfenova, A. Zimmermann, L. Cw, D. Tcheranova, F. Al, Cerebroprotective effects of the CO-releasing molecule CORM-A1 against seizure-induced neonatal vascular injury, Am J Physiol Hear. Circ Physiol. 38163 (2007) 2501–2507. doi:10.1152/ajpheart.00354.2007.

[14] A. Kanu, C.W. Leffler, Arachidonic acid- and prostaglandin E2-induced cerebral vasodilation is mediated by carbon monoxide, independent of reactive oxygen species in piglets, Am. J. Physiol. Heart Circ. Physiol. 301 (2011) H2482-2487. doi:10.1152/ajpheart.00628.2011.

[15] A. Kanu, C.W. Leffler, Roles of Glia limitans astrocytes and carbon monoxide in adenosine diphosphate-induced pial arteriolar dilation in newborn pigs, Stroke. 40 (2009) 930–935. doi:10.1161/STROKEAHA.108.533786.

[16] M. Ishikawa, M. Kajimura, T. Adachi, K. Maruyama, N. Makino, N. Goda, T. Yamaguchi, E. Sekizuka, M. Suematsu, Carbon monoxide from heme oxygenase-2 is a tonic regulator against NO-dependent vasodilatation in the adult rat cerebral microcirculation, Circ. Res. 97 (2005) 104–115. doi:10.1161/01.RES.0000196681.34485.ec.

[17] B. Horváth, L. Hortobágyi, G. Lenzsér, H. Schweer, A. Hrabák, P. Sándor, Z. Benyó, Carbon monoxide-prostaglandin E2 interaction in the hypothalamic circulation., Neuroreport. 19 (2008) 1601–4. doi:10.1097/WNR.0b013e3283129790.

[18] A.A. Miller, T.M. De Silva, K.A. Jackman, C.G. Sobey, EFFECT OF GENDER AND SEX HORMONES ON VASCULAR OXIDATIVE STRESS, Clin. Exp. Pharmacol. Physiol. 34 (2007) 1037–1043. doi:10.1111/j.1440-1681.2007.04732.x.

[19] E. Straface, R. Vona, I. Campesi, F. Franconi, Mitochondria can orchestrate sex differences in cell fate of vascular smooth muscle cells from rats, Biol. Sex Differ. 6 (2015) 34. doi:10.1186/s13293-015-0051-9.

[20] C.S.F. Queiroga, A.S. Almeida, C. Martel, C. Brenner, P.M. Alves, H.L.A. Vieira, Glutathionylation of adenine nucleotide translocase induced by carbon monoxide prevents mitochondrial membrane permeabilization and apoptosis., J. Biol. Chem. 285 (2010) 17077–88. doi:10.1074/jbc.M109.065052.

[21] S.R. Oliveira, C.S.F. Queiroga, H.L.A. Vieira, Mitochondria and carbon monoxide: cytoprotection and control of cell metabolism - a role for Ca 2+ ?, J. Physiol. 594 (2016) 4131–4138. doi:10.1113/JP270955.

[22] C. Penaloza, B. Estevez, S. Orlanski, M. Sikorska, R. Walker, C. Smith, B. Smith, R.A. Lockshin, Z. Zakeri, Sex of the cell dictates its response: differential gene expression and sensitivity to cell death inducing stress in male and female cells, FASEB J. 23 (2009) 1869–1879. doi:10.1096/fj.08-119388.

[23] D.N. Krause, Influence of sex steroid hormones on cerebrovascular function, J. Appl. Physiol. 101 (2006) 1252–1261. doi:10.1152/japplphysiol.01095.2005.

[24] J.F. Laycock, S.A. Whitehead, Vasopressin and vascular regulation: is sex a factor?, J. Endocrinol. 144 (1995) 389–92. http://www.ncbi.nlm.nih.gov/pubmed/7738462.

[25] R. Motterlini, P. Sawle, J. Hammad, S. Bains, R. Alberto, R. Foresti, C.J. Green, CORM-A1: a new pharmacologically active carbon monoxide-releasing molecule., FASEB J. 19 (2005) 284–6. doi:10.1096/fj.04-2169fje.

[26] E. Csongradi, Role of Carbon Monoxide in Kidney Function: Is a little Carbon Monoxide Good for the Kidney?, Curr. Pharm. Biotechnol. 13 (2012) 819–826. doi:10.2174/138920112800399284.

[27] C. Szabo, Gasotransmitters in cancer: from pathophysiology to experimental therapy., Nat. Rev. Drug Discov. 15 (2015) 185–203. doi:10.1038/nrd.2015.1.

[28] S.L. Barnes, J.G. Whisenant, M.E. Loveless, T.E. Yankeelov, Practical dynamic contrast enhanced MRI in small animal models of cancer: data acquisition, data analysis, and interpretation., Pharmaceutics. 4 (2012) 442–78. doi:10.3390/pharmaceutics4030442.

[29] C.M. Davis, S.L. Fairbanks, N.J. Alkayed, Mechanism of the Sex Difference in Endothelial Dysfunction after Stroke, Transl. Stroke Res. 4 (2013) 381–389. doi:10.1007/s12975-012-

0227-0.

[30] A. Pósa, K. Kupai, R. Ménesi, Z. Szalai, R. Szabó, Z. Pintér, G. Pálfi, M. Gyöngyösi, A. Berkó, I. Pávó, C. Varga, Sexual dimorphism of cardiovascular ischemia susceptibility is mediated by heme oxygenase, Oxid. Med. Cell. Longev. (2013). doi:10.1155/2013/521563.

[31] S. Nag, Morphology and Properties of Brain Endothelial Cells, in: 2011: pp. 3–47. doi:10.1007/978-1-60761-938-3_1.

[32] N.J. Abbott, Dynamics of CNS Barriers: Evolution, Differentiation, and Modulation, Cell. Mol. Neurobiol. 25 (2005) 5–23. doi:10.1007/s10571-004-1374-y.

[33] H. Wolburg, S. Noell, A. Mack, K. Wolburg-Buchholz, P. Fallier-Becker, Brain endothelial cells and the glio-vascular complex, Cell Tissue Res. 335 (2009) 75–96. doi:10.1007/s00441-008-0658-9.

[34] L. Frings, K. Wagner, J. Unterrainer, J. Spreer, U. Halsband, A. Schulze-Bonhage, Gender-related differences in lateralization of hippocampal activation and cognitive strategy, Neuroreport. 17 (2006) 417–421. doi:10.1097/01.wnr.0000203623.02082.e3.

[35] E. Luders, C. Gaser, K.L. Narr, A.W. Toga, Why Sex Matters: Brain Size Independent Differences in Gray Matter Distributions between Men and Women, J. Neurosci. 29 (2009) 14265–14270. doi:10.1523/JNEUROSCI.2261-09.2009.

[36] R.C. Gur, B.I. Turetsky, M. Matsui, M. Yan, W. Bilker, P. Hughett, R.E. Gur, Sex differences in brain gray and white matter in healthy young adults: correlations with cognitive performance., J. Neurosci. 19 (1999) 4065–72. http://www.ncbi.nlm.nih.gov/pubmed/10234034.

[37] J. Zhang, W. Cai, D. Zhou, B. Su, Distribution and differences of estrogen receptor beta immunoreactivity in the brain of adult male and female rats, 935 (2002) 73–80.

[38] R.M. Dyson, H.K. Palliser, J.L. Latter, M.A. Kelly, G. Chwatko, R. Glowacki, I.M.R. Wright, Interactions of the gasotransmitters contribute to microvascular tone (Dys)regulation in the preterm neonate, PLoS One. 10 (2015) 1–15. doi:10.1371/journal.pone.0121621.

[39] Gender differences affect blood flow recovery in a mouse model of hindlimb ischemia, Am J Physiol Hear. Circ Physiol. 300 (2011) H2027–H2034. doi:10.1152/ajpheart.00004.2011.

[40] F.J. Wolters, R.F.A.G. De Bruijn, A. Hofman, P.J. Koudstaal, M. Arfan Ikram, Cerebral Vasoreactivity, Apolipoprotein E, and the Risk of Dementia: A Population-Based Study, Arterioscler. Thromb. Vasc. Biol. 36 (2016) 204–210. doi:10.1161/ATVBAHA.115.306768.

[41] a Huang, D. Sun, a Koller, G. Kaley, Gender difference in myogenic tone of rat arterioles is due to estrogen-induced, enhanced release of NO., Am. J. Physiol. 272 (1997) H1804-9. http://www.ncbi.nlm.nih.gov/pubmed/9139966.

[42] C.W. Leffler, H. Parfenova, A.L. Fedinec, S. Basuroy, D. Tcheranova, Contributions of astrocytes and CO to pial arteriolar dilation to glutamate in newborn pigs., Am. J. Physiol. Heart Circ. Physiol. 291 (2006) H2897-904. doi:10.1152/ajpheart.00722.2006.

[43] S. Basuroy, C.W. Leffler, H. Parfenova, CORM-A1 prevents blood-brain barrier dysfunction caused by ionotropic glutamate receptor-mediated endothelial oxidative stress and apoptosis, AJP Cell Physiol. 304 (2013) C1105–C1115. doi:10.1152/ajpcell.00023.2013.

Chapter II.V

Therapeutic Potential of CO Against Stroke

This chapter is based on the following manuscript:

Protective effects of CO against stroke – Behavioral and MRI study

Sara R. Oliveira, João Castelhano, José Sereno, Lorena Petrella, Helena L. A. Vieira, Miguel Castelo-Branco and Carlos B Duarte

(in preparation)

INDEX

ABSTRACT

Although stroke is the main cause of brain damage worldwide, stroke therapies are still scarce. Ischemic stroke (representing 87% of all strokes) causes cerebral damage due to oxygen and tissue energy depletion, which lead to acidosis, inflammation, excitotoxicity and excessive generation of ROS (reactive oxygen species). Carbon monoxide (CO) is an endogenous gasotransmitter produced by heme oxygenase cleavage of the heme group, which promotes cytoprotection. CO limits inflammation in different diseases and prevents apoptosis in several tissues. In the case of brain injury, exogenous CO prevents astrocytic and neuronal cell death by limiting mitochondrial membrane permeabilization and the release of pro-apoptotic factors to the cytosol, in addition to stimulating mitochondrial metabolism and oxidative phosphorylation.

This work aims to explore the putative role of CO in brain cytoprotection following stroke in an *in vivo* model of transient focal ischemia in adult mice, middle cerebral artery occlusion (MCAo). By evaluating the effects of CO with live imaging techniques we aim to elucidate the effect of this gasotransmitter at the metabolic, vascular and anatomic levels. Behavioural tests aimed to further characterize the effects of CO at motor functional level. Additionally, a parallel study was conducted to identify metabolite levels predictive of stroke outcome.

The putative neuroprotective effects of CO were assessed after 45 min of MCAo, by injecting i.p. 3 doses of the CO-releasing molecule CORM-A1 (3 mg/kg), administered after 6 h of reperfusion and daily for the next 2 days. Magnetic Resonance Imaging was performed 1 day and 7 days after reperfusion using T2-weighted, diffusion weighted images, proton spectroscopy (^{1}H-MRS) and perfusion (dynamic contrast enhanced images). ^{1}H-MRS also allowed the comparison between metabolite signatures at day 1 versus 7 day following MCAo. The CO-induced cytoprotection was further evaluated by behavioural analysis every 2 days, starting 1 day after the lesion until the 5th day. Evaluation of motor performance comprised the openfield, accelerated rotarod and pole tests.

A locomotion and motor coordination improvement was observed in CORM-A1 treated cohorts, both MCAo and Sham when compared with the respective untreated controls. Also, CORM-A1 limited the loss of blood-brain barrier (BBB) integrity as it reduced the edema formation. Furthermore, the CO donor minimized the metabolite load loss at an early stage after MCAo, both in striatum and cortex.

By integrating data from behaviour and MRI analysis we concluded that CO has a protective effect in the recovery from stroke injury, mainly by acting on metabolism and on the BBB.

KEYWORDS

Carbon monoxide, brain, ischemia, therapy, behaviour, metabolism, MRI.

ABBREVIATIONS

BBB – Blood-brain barrier
ECA - External carotid artery
FID - Free induction decay
GABA - γ-aminobutyric acid
Glx – Glutamine and glutamate
i.p. - Intraperitoneal
MRI – Magnetic Resonance Imaging
NAA - *N*-acetylaspartate
rCBF – Regional cerebral blood flow
Tau - Taurine
tMCAo - Transient middle cerebral artery occlusion
tPA - Tissue plasminogen activator

1. INTRODUCTION

Carbon monoxide (CO) is a gasotransmitter endogenously produced in many organs. The brain is one of the tissues with the highest activity of heme oxigenase, the enzyme that produces CO [1]. A wide range of physiological roles are played by CO in the brain, including cytoprotective effects such as anti-apoptotic and anti-inflammatory, metabolic improvement, vasomodulation, and promotion of neurogenesis [2,3]. Neuroprotective actions of CO were described in *in vivo* models of Alzheimer's disease [4], epilepsy [5], and in perinatal ischemia [6], among others. However, the mechanisms underlying the neuroprotective effects of CO are still poorly understood. From the molecular point of view, the gasotransmitter binds to heme-containing proteins and induces heme oxygenase, which accounts, at least in part, for neuroprotection in different models [7–9].

Ischemic brain injury is a leading cause of mortality and morbidity in western countries. Tissue plasminogen activator (tPA) and thrombectomy are the only approved therapies for acute non-hemorrhagic stroke [10,11]. However, these therapeutic strategies can only be used in the first 4.5 h and 6 h, respectively, after symptoms onset, making it available for only 4–7 % of these patients [12]. Despite the failure of the previous generation of drugs, new approaches have been pursued for stroke therapy, namely the stimulation of endogenous cytoprotective mechanisms. To overcome the complexity of stroke, one may hypothesize that a molecule that targets as many stroke hallmarks as possible can be a promising therapeutic candidate. Studies have been performed to evaluate the therapeutic potential of CO in stroke models, mainly by administration of CO in a prophylactic manner. A few studies have tested the effect of CO administered after injury at different time points (from several days before injury to 3 days after reperfusion) [6,13–15]. A drawback in most of the studies described above is the choice of the time point of CO administration; treatment with CO before the ischemic insult has a limited clinical relevance. Moreover, since the protective readouts were often collected soon after injury, the long-term effects remain uncharacterized.

In the present study, we investigated the cerebral effects resulting from systemic administration of low doses of CO after brain ischemia, using a mice model of transient middle cerebral artery occlusion (tMCAo). This approach evaluates the therapeutic potential of CO in a clinically relevant scenario: the effect of the gasotransmitter was tested at time periods longer than 4.5 h after the ischemic injury as an effort to overcome the limitation of tPA's short therapeutic window. The route of CO administration, i.p. injection, was also chosen to be easily translated into the clinical practice. As CO presents a complex biology, the effects of this gasotransmitter were evaluated in an integrated manner, characterizing the effects on the vasculature, metabolism, behaviour and histology, in a longitudinal study. We found that 3 intraperitoneal CO injections given within 6h to 48h after the stroke onset promote motor improvement and a robust reduction in BBB permeability. Moreover, CO-treated mice subjected to tMCAo presented a tendency to a reduction in infarct volume measured by MRI at day 1, which was correlated with a limited metabolite loss, in particular in the cortical region.

2. MATERIALS AND METHODS

2.1. Experimental procedure

The mice were randomly divided into four groups (n=5/6 *per* group): i) Sham group, mice were treated with saline; ii) Sham treated with CORM-A1; iii) tMCAo group, mice were treated with saline and iv) tMCAo treated with CORM-A1. The treated groups received CORM-A1 via i.p. injection (3 mg/kg in saline) at 6 h, 1 day and 2 days after MCAo. The behavior tests were conducted for 7 days, once every two days. Mice were sacrificed by anesthetic overdose following the behavioral tests on day 7, and the brains were harvested for histochemical analyses (Supplementary Data, Figure S1).

2.2. Transient middle cerebral artery occlusion (tMCAo)

Surgical procedures were performed according to the protocol published as the latest Standard Operating Procedure (SOP) [16]. The national and local animal welfare authorities approved all animal experiments. Male C57BL/6 mice were obtained from Charles River at the age of 7-8 weeks and were used in the experiments at the age of 8–10 weeks. All animals had access to food and water *ad libitum*, and were kept under a 12 h light/dark cycle. No specific exclusion criteria were set.

The right middle cerebral artery (MCA) was occluded for 45 min. In summary, mice were initially anesthetized by inhalation of 2.5% isoflurane in O_2:N_2O (30:70). Thereafter, mice were placed on a heating pad and anesthesia was subsequently reduced and maintained at 1.5-1.8% (using an open mask). A rectal temperature probe was used to monitor body temperature, which was kept at 37°C (see Figure S2). An optical fiber probe (Probe 318-I, Perimed, Sweden) was firmly attached to the skull and connected to a laser doppler flow meter (Periflux System 5000, Perimed), to monitor changes in regional cerebral blood flow (rCBF). A 6-0 silicon-coated (about 9-10mm is coated silicon) monofilament suture (602334PK10, Doccol Corporation) was introduced into the ECA (external carotid artery), which was monitored by a sudden drop in rCBF (Supplementary Data Figure S2). Bupivacaine (0.150 µL, 0.05%, Marcain™, AstraZeneca, Sweden) was injected around the wound to reduce pain. In order to avoid *post*-surgical hypothermia, animals were placed in an incubator at 35°C for the first 2 h after the procedure and then transferred to an incubator at 33°C (overnight). 30 min we administered 0.5 mL of 5% glucose in saline subcutaneously. As animals were allowed to recover for 7 days, we further administered 0.5 mL of 5% glucose subcutaneously daily, up to day 4 *post*-surgery (which is when weight loss ceases). Body weight was controlled daily up to the experimental endpoint (Supplementary Data, Figure S3). In sham-surgeries, the filament was advanced up to the internal carotid artery, and was withdrawn before reaching the MCA.

2.3. CO administration

CORM-A1, a CO releasing molecule [17], was used to systemically deliver CO in mice. The CORM-A1 (Sigma) stock solution was prepared in 0.9% NaCl solution and

stored at -20°C to avoid loss of released CO. 3 mg/kg of CORM-A1 were administered i.p at 6 h ± 0.2 h, 32 h 39 min ± 5h and 56 h 08 min ± 6 h.

2.4. Histology

At the end of the experiment, all animals were sacrificed and subjected to transcardial perfusion with PBS, followed by brain collection. After fixation with 4 % paraformaldehyde for 48 h, samples were saturated in 30 % sucrose (Sigma) in PBS, then embedded in 7.5 % gelatin (Sigma)/15 % (m/v) sucrose in PBS and subsequently frozen in liquid nitrogen. Transversal sections (starting approximately at 1.70 mm from the Bregma and slicing until -4 mm from Bregma) were cut using a Leica cryostat at 20 µm thickness for Hematoxylin Eosin (H&E) staining, and directly placed on a slide. Sections were cut at 50 µm thickness for immunohistochemistry in a free-floating system and maintained at 4°C afterwards. Three free floating brain slices were placed *per* well in 24-well plates and kept in PBS with 0.02% (m/v) sodium azide until further use. After cutting 9 slices for immunohistochemistry, 1 slice was collected for H&E staining (Supplementary Data, Figure S4).

2.5. Infarct volume quantification by MRI

Stroke volume was quantified by T2-weighted magnetic resonance imaging (T2*-MRI). For stroke volumetry, hyperintense areas of ischemic tissue in T2-weighted images were assigned with a region of interest tool. This enabled a threshold-based segmentation that was performed by connecting all pixels within a specified threshold range around the selected seed pixel and resulted in a 3D object map of the whole stroke region. The total volume of the whole object map was calculated automatically. For quantification of the regional ischemic lesion volumes, axial MR images were divided into three equal slices from medial to lateral with NIH ImageJ. The volume of hyperintense areas in each brain section was calculated with the Analyze 5.0 software. Brain parenchyma was cropped for presentation purposes.

2.6. Quantification of the infarct volume by hematoxylin and eosin staining

Every 10th brain section (20 µm thick; prepared in a cryostate) was stained for hematoxylin and eosin (H&E). Images of H&E-stained brain slices from mice at day 7 after tMCAo were collected using a Zeiss Lumar V12 microscope equipped with a Zeiss MR3 Colour camera. Lower density tissue areas were manually drawn. Direct lesion volumes were calculated from 12 coronal brain sections to allow correlation with the MRI-based quantification.

2.7. Cerebral perfusion quantification by MRI

Mice were anesthetized with 1.5% isoflurane in air, and placed on controlled temperature beds through water baths (Haake SC 100, Thermo Scientific, USA) with tooth bar and head restraint to reduce motion artifact. Body temperature was maintained

at 37ºC with assessment of cardiorespiratory function (1030, SA Instruments Inc., NY, USA). MRI was performed on a 9.4T MR pre-clinical scanner (Bruker Biospec, Billerica MA, USA) equipped with a standard Bruker crosscoil setup using a volume coil for excitation (86/112 mm of inner/outer diameter) and quadrature mouse surface coil for detection (Bruker Biospin, Ettlingen, Germany). The system was interfaced to a Linux PC running Topspin 3.1PV and Paravision 6.0 (Bruker Biospin). High resolution morphological images were acquired with a 2D T2-weighted turbo RARE (rapid acquisition with relaxation enhancement) sequence with TR = 3.6 ms, TE = 33.0 ms, matrix 256 × 256 and field of view 20.0 × 20.0 mm reaching an in plane spatial resolution of 78*78 μm^2, rare factor 8, axial slice thickness 0.5 mm and 5 averages resulting in 9 min 36 s of scan time.

Brain permeability was evaluated after injection of Gadovist® (0.1 mmol/kg) using the dynamic contrast-enhanced magnetic resonance imaging technique. The following parameters were used in 2D DCE-FLASH: TE/TR = 2.5/191.145 ms, flip angel = 70º, FOV= 20 x 20 mm, matrix= 156 x 85, slice thickness 0.5 mm, number of slices= 18, number of repetitions= 40 and time acquisition of 1 h 3 min 20 s.

2.8. ^{1}H-MRS

Data were collected on a volume of interest selected in accordance with coronal, sagittal and axial T2-weighted images, and adjusted to fit the anatomical structure of interest and to minimize partial volume effects. The B0 map was acquired and MAPSHIM was employed to automatically adjust first and second-order shim coils, with iterative correction. Spectral line widths of water around 13–18 Hz were obtained. A PRESS sequence was used in combination with outer volume suppression and VAPOR water suppression. The following parameters were used: TR = 2500 ms, TE = 16.225 ms, number of averages = 720, number of acquired points = 2048, yielding a spectral resolution of 1.22 Hz/point. For each animal, an unsuppressed water signal (TE = 16.225 ms, TR = 2500 ms, 16 averages, scanning time = 40 sec and none water suppression) was acquired immediately before acquiring the water-suppressed spectrum.

Data were saved as Free Induction Decays (FIDs) and corrected for the frequency drift and for residual eddy current effects using the reference water signal. The ^{1}H NMR peak concentrations for major metabolites (*e.g.*, *N*-acetylaspartate (NAA), γ-aminobutyric acid (GABA), taurine, glutamine and glutamate (Glx)) was then analyzed using the LCModel software package (Stephen Provencher Inc., Oakville, Canada; Provencher 1993), and the results were given in relation to the water content in the tissue. Briefly, the LCModel analysis calculates the best fit to the acquired spectrum as a linear combination of a model based on a set of brain metabolites from the LCModel basis set. The Cramer-Rao lower bound provided by LCModel was used as a measure of the reliability, and metabolite concentrations with Cramer-Rao lower bound higher than 24% were not included in the analysis.

2.9. Behavioral Assessment

Mice were subjected to locomotor tests before and 1, 3, 5 and 7 days after tMCAo. Animals were habituated to a quiet room with controlled temperature and ventilation, dimmed lighting (illuminance between 2 and 6 lux) for 1h, and handled prior to behavioral testing.

2.9.1. Openfield

The arena (51 x 30.6 cm) was divided into 15 sub-squares (3 x 5). The mouse was placed in the center of the arena and the behavior of the mouse was observed for 15 min. The number of crossings (a crossing was recorded as each time the mouse crossed the boundary of a sub-square with at least their two forepaws), grooming behaviors (rubbing the body with the paws or mouth and/or rubbing the head with the paws), rearing behaviors (standing on the hind paws), the duration of immobility and the number of fecal pellets excreted were determined.

2.9.2. Pole test

The pole test was performed to analyze sensory motor function. Mice were habituated to the procedure prior to tMCAo. They were placed head upward near the top of a vertical rough-surfaced pole (1 cm diameter, 50 cm height) and then allowed to descend five times during one experimental session, intercalated with 1 min resting time. The total time needed to turn completely head downward (“time-to-turn”) and the time it took the mouse to reach the base with all four paws (“time-to-descend”) were recorded.

2.9.3. Accelerated rotarod

Motor coordination and balance were assessed using rotarod (LE 8200, PanLab, Harvard) as described previously [18]. Sessions consisted of four trials *per* day with a 20-min interval between the second and third run to allow animals to rest. The mean of the three best trials out of four at a given day was used for statistical analysis. The apparatus velocity started at 4 rpm and increased up to 40 rpm over 5 min. The time during which mice remained walking in the rotation drum was recorded.

2.10. Statistical Analysis

Two-way repeated-measures (RM) ANOVA with Bonferroni’s *post hoc* tests for comparison of sample treatment effects within Sham or tMCAo was used. Two-way RM ANOVA, followed by Tukey’s *post hoc* analysis, was performed for statistical analysis of the results obtained in the MRI stroke volume assessment at 1 and 7 days after tMCAo.

2.11. Methods to prevent bias

In summary, out of the 52 animals used, 2 were excluded due to a hemorrhage during surgery and 2 were excluded as they died during MRI acquisition. 48 animals were included in the study from which 21 reached the end point (Supplementary Data, Figure S1).

Animals were randomized before the experiments by a scientist who was not involved in the tMCAo experiments, in the administration of CO or in the behavioral tests. MRI and behavior data analysis were performed blind for the grouping, and the treatment allocation was secret. MRI data acquisition was also performed by scientists who were not involved in the surgery experiments, CO administration or behavioral analysis, and both the grouping and the treatment allocation were concealed.

3. RESULTS

3.1. CO improves motor activity after tMCAo

The putative effects of CO in neuroprotection were evaluated by i.p. injection of the donor CORM-A1 (3 mg/kg) 6 h after tMCAo (45 min occlusion), followed by administration of the same dose 1 and 2 days later. The use of this concentration of CORM-A1 ensures that carboxyhemoglobin was not significantly increased compared to baseline [19], thus avoiding any toxicity.

Neuroprotection by CO administered after tMCAo was first investigated by analyzing the motor behavior of mice 7 days after the lesion. Mice were tested under free and forced-moving paradigms. Free movements were assessed using the open field test, by scoring the number of crossings (the number of times the mice crossed the boundary of a sub-square) and the grooming and rearing behaviors. tMCAo for 45 min did not change the cumulative number of crossings, when tested 7 days after the lesion (Figure 1A), but significantly reduced the exploratory behavior as expected (Figure 1B). However, the latter changes were not significantly affected by administration of CO. Nevertheless, CO treatment restored the grooming behavior to sham levels (Figure 1C). Overall, it was observed that CO partially alleviates motor deficits due to tMCAo in mice.

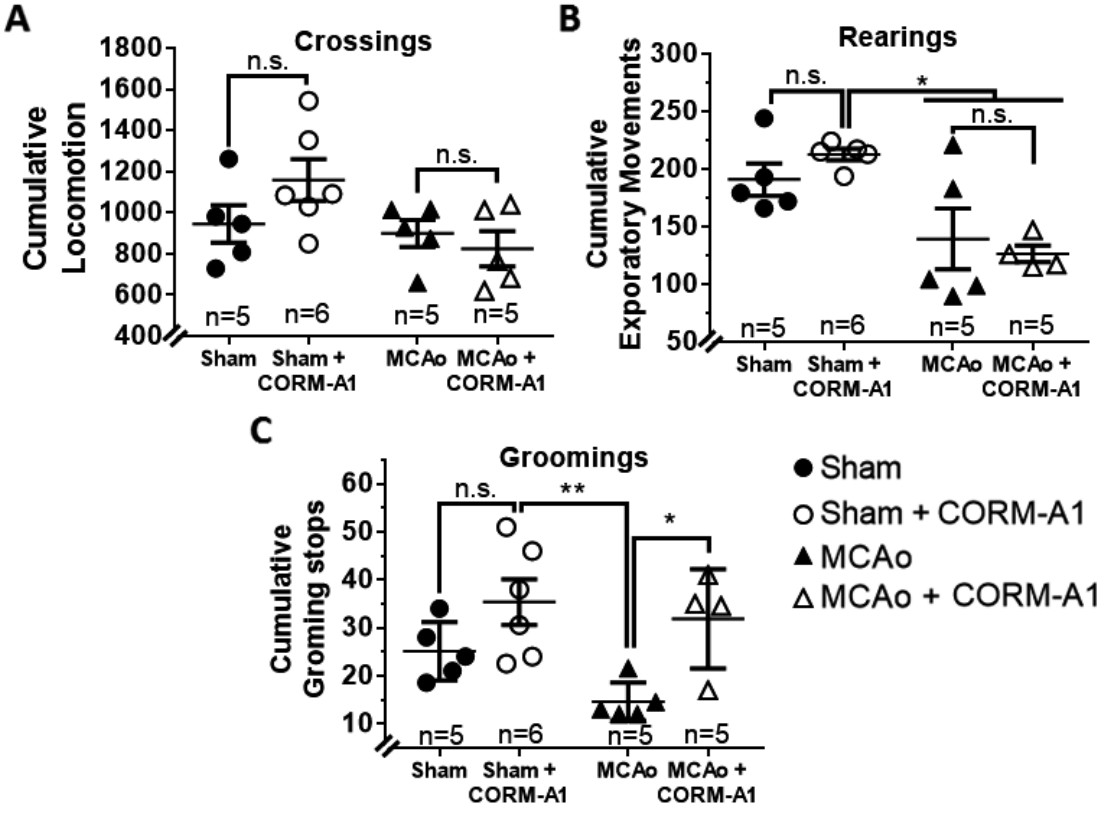

Figure 1 – Open field assessment of motor performance in mice subjected to tMCAo. Where indicated, the animals were treated with CORM-A1 (3 mg/kg) in 3 doses (6 h, 1 day and 2 days *post* injury). Mice were placed at the center of the arena and behavior was recorded for 15 min. The sum of each parameter observed during all open field sessions was calculated: (A) number of crossings; (B) number of rearings and (C) number of groomings. Circles represent sham-operated mice and triangles represent MCAO-operated mice. Filled and empty symbols represent control and CO-treated mice, respectively. *p<0.05 **p<0.01 calculated with unpaired one-way ANOVA with Bonferroni *post*-test. n.s. – not significant.

The vertical pole test and rotarod were used as forced-moving tests to evaluate motor alterations induced by tMCAo, and the putative effects of CORM-A1. In the former test, tMCAo increased the cumulative total descending time, when analyzed 7 days after injury, but this effect was not statistically significant. Furthermore, animals treated with CORM-A1 after tMCAo showed a cumulative total descending time that was similar to the control (Figure 2A). The effects of tMCAo on the performance of mice in this test resulted from a deficit in the ability to turn when placed at the top of the pole (Figure 2B), and a reduced performance when descending the pole was also observed (Figure 2C). Administration of CORM-A1 decreased the rate of turning (Figure 2B) but did not change significantly the performance when descending the pole.

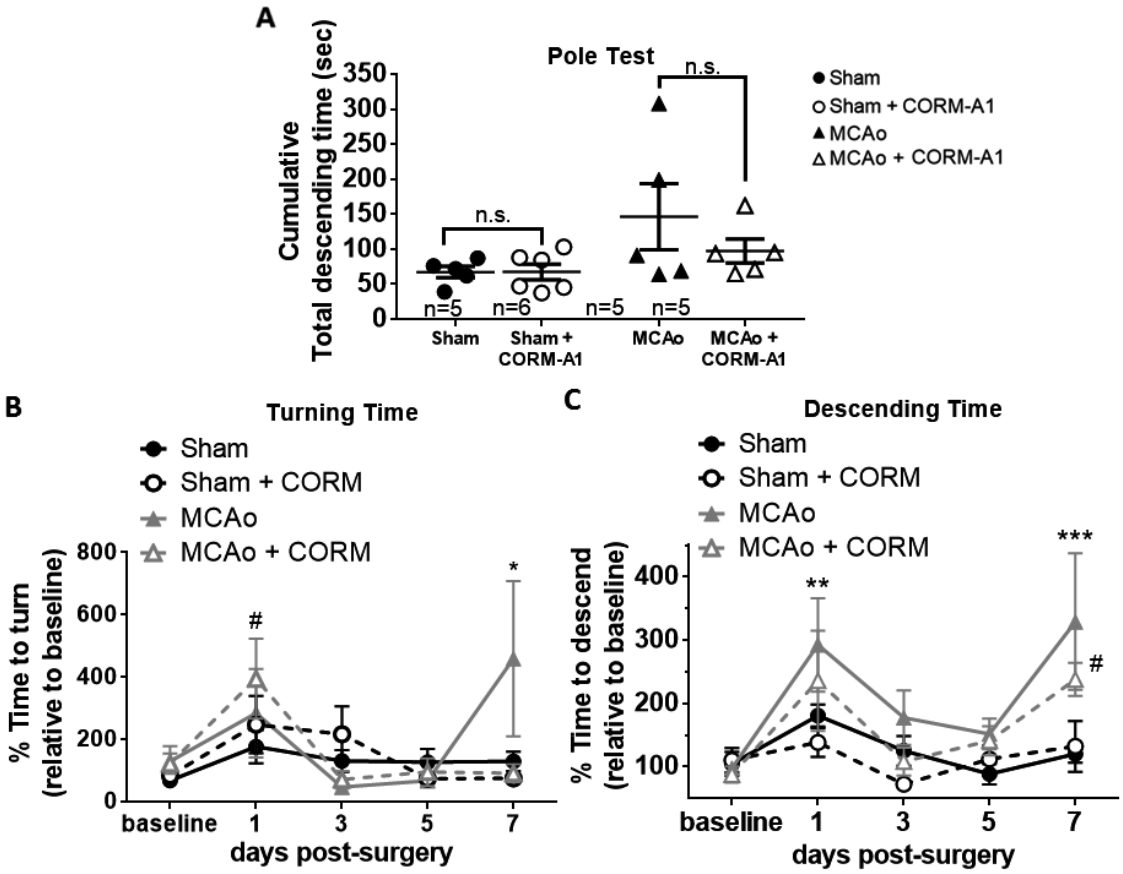

Figure 2 – Vertical pole test assessment of motor performance in mice subjected to tMCAo. Where indicated, the animals were treated with CORM-A1 (3 mg/kg) in 3 doses (6 h, 1 day and 2 days *post* injury). Mice were placed on the top of the pole facing upwards and 5 trials were done per day. (A) The sum of total time to reach the pole base during all sessions was calculated. Panel (B)shows the longitudinal evolution of the Turning time and (C) shows the longitudinal evolution of descending time. Black circles represent sham-operated mice and grey triangles represent MCAO-operated mice. Filled and empty symbols represent control and CO-treated mice, respectively. In (A) unpaired Student's t-test was applied. In (B) and (C) statistical analysis was performed comparing all time points with baseline for each cohort, *p<0.05, **p<0.01, ***p<0.001, n.s. – not significant, for MCAo and #p<0.05 MCAo + CORM. Statistical analysis was performed with two-way ANOVA with Bonferroni *post*-test.

In the accelerated rotarod, which evaluates coordination and balance, no significant differences were observed between control and CO-treated cohorts, under sham conditions or after tMCAo, when analyzed 7 days after tMCAo (Figure 3). This

result follows the same pattern observed when the number of crossings was evaluated in the open field test.

Overall, these results suggest that CO administration improves motor activity to some extent, with the best results obtained in the grooming assessment and in the performance in the pole test.

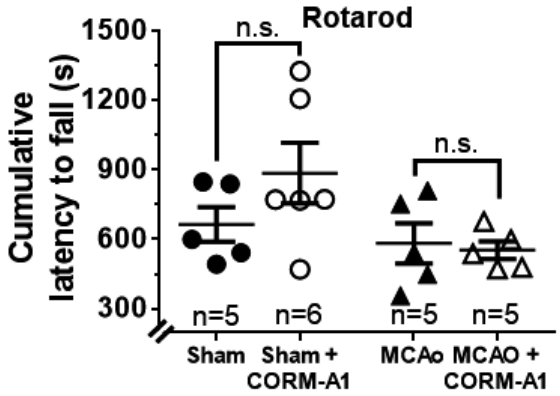

Figure 3 – Effect of tMCAo on motor performance as assessed by the accelerated rotarod method. Where indicated, the animals were treated with CORM-A1 (3 mg/kg) in 3 doses (6 h, 1 day and 2 days *post* injury). Circles represent sham-operated mice and triangles represent MCAO-operated mice. Filled and empty symbols represent control and CO-treated mice, respectively. Statistical analysis was performed using the unpaired Student's *t*-test. n.s. – not significant.

3.2. CO reduces BBB leakiness

Blood-brain barrier (BBB) leakiness plays a major role in neuronal damage after transient brain ischemia, enhancing tissue damage [20,21]. There are multiple evidence for modulatory and protective effects of CO on the vasculature [22,23]. Therefore, we hypothesized that the CORM-A1-induced motor improvement in mice subjected to tMCAo could be mediated by alterations on the BBB. To address this question, a MRI-based technique was used. A gadolinium-based contrast agent was given i.p. and its signal was quantified in brain tissue [24,25]. Since under normal physiological conditions the BBB excludes the contrast agent, any increase in signal intensity is interpreted as BBB breakdown. The results of Figure 4 show a significant increase in the permeability of the BBB when evaluated 1 day or 7 days after tMCAo. Under the latter conditions, CORM-A1 administration significantly reduced BBB damage in mice subjected to tMCAo (Figure 4B), which was very clear when the cumulative signal of the contrast agent was represented with a color code (Figure 4A). The total accumulation of the contrast agent at day 7 in animals exposed to focal ischemic injury followed by administration of CORM-A1 was similar to that observed after tMCAo at day 1, suggesting that CO prevents the delayed increase of BBB permeability, rather than the initial alterations. The untreated MCAo cohort showed a 3-fold increase in the accumulation of contrast agent in the same period of time (Figure 4B).

Taken together, the results show the prolonged effects of CO in the protection of the BBB after ischemic injury, which resulted in preservation of the BBB integrity.

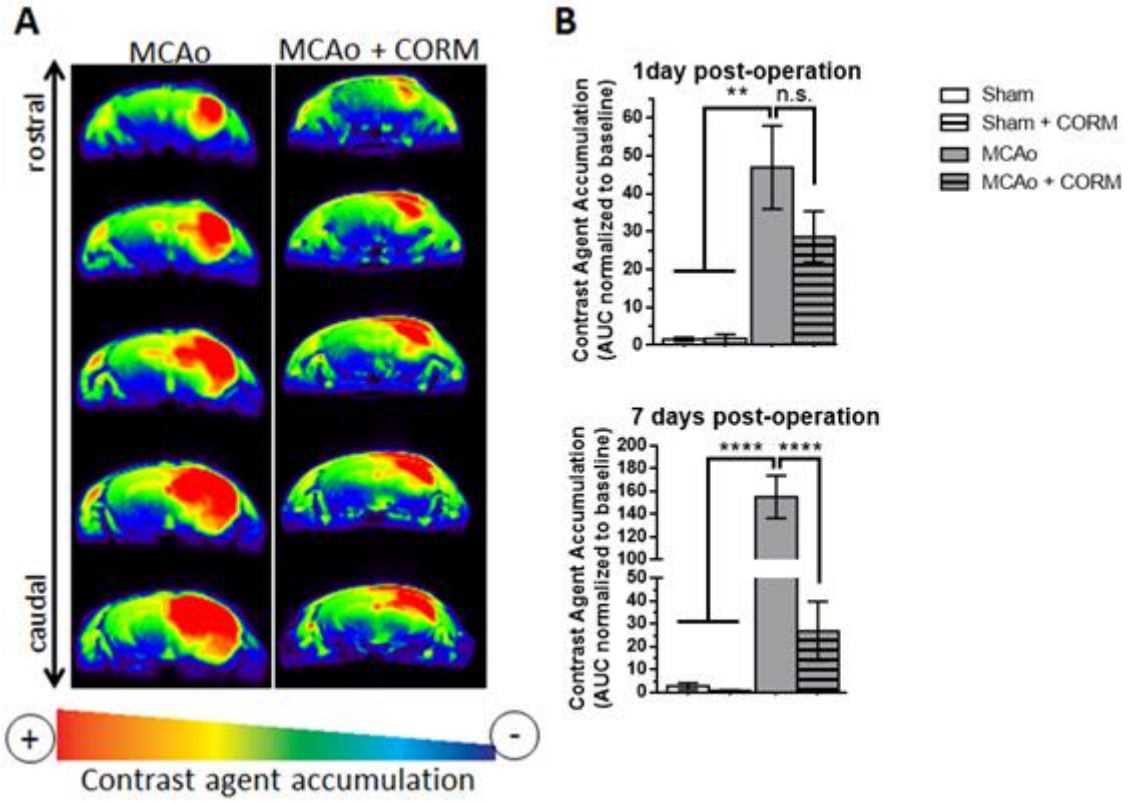

Figure 4 – Alterations in the BBB permeability after tMCAo. Where indicated, the animals were treated with CORM-A1 (3 mg/kg) in 3 doses (6 h, 1 day and 2 days *post* injury). Accumulation of contrast agent in the brain tissue occurs in regions where the BBB in compromised. (A) Representative images showing accumulation of the contrast agent 7 days after tMCAo in mice. (B) Quantification of the signal intensity resulting from the accumulation of the contrast agent. White bars represent sham-operated mice and grey bars represent MCAO-operated mice. Clear and striped bars represent control and CO-treated mice, respectively. ***p*<0.01, *****p*<0.0001, n.s. – not significant, determined with unpaired Student's *t*-test.

3.3. CO limits infarct lesion 24h after MCAo

To determine whether the preservation of the BBB integrity in CO treated mice correlates with a smaller infarcted area, two independent methods were used to quantify the ischemic brain tissue: MRI and H&E staining. When total lesion volume was evaluated by MRI, CO treated animals presented a slightly smaller infarct size at day 1 compared to the untreated group (Figure 5A), but the results were not statistically significant. Since the cerebral cortex and striatum are the most affected brain regions in the MCAo model of transient focal ischemia [26], the ischemic injury was also specifically quantified in these two areas. This categorization showed that the cortical lesion, but not the striatal injury, was slightly reduced when the animals were treated with CORM-A1 after MCAo, but the results were not statistically significant (Figure 5B, C). Analysis of the lesion volume at day 7 after MCAo showed no effect of CORM-A1 administration.

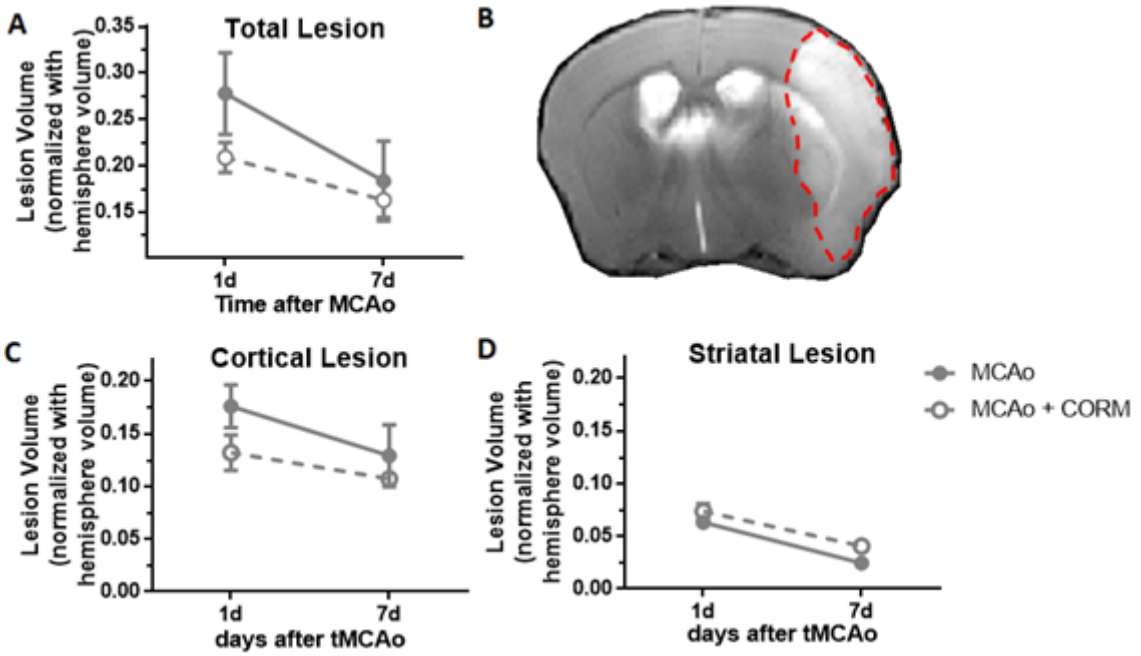

Figure 5 – MRI quantification of infarcted brain volume in mice subjected to tMCAo. Where indicated, the animals were treated with CORM-A1 (3 mg/kg) in 3 doses (6 h, 1 day and 2 days *post* injury). Anatomic volumetries were measured at day 7. The results obtained in untreated mice subjected to MCAo are represented by filled circles, while empty circles showed the results obtained in animals subjected to the ischemic insult followed by CORM-A1 treatment. (A) Total lesion volume; (B) representative image of the infarcted mouse brain with the hyperintense lesioned tissue limited with a dashed red line; (C) lesion volume affecting the cerebral cortex; (D) lesion volume affecting the striatum. The results are the average ± SEM n = 5. Statistical analysis was performed using the two-way ANOVA followed by the Bonferroni *post*-test.

In additional experiments, we quantified the lesion volume in H&E stained brain slices prepared 7 days after MCAo. The results showed no significant effect of CO treatment on the tMCAo-induced brain lesion (Figure 6).

In summary, the CO dosage given was insufficient to decrease the infarct volume in mice subjected to tMCAo, specially at day 7 after the lesion. Although a slight protection was observed in the cerebral cortex at day 1 *post*-MCAo, the effect was not statistically significant and was not observed at a later point.

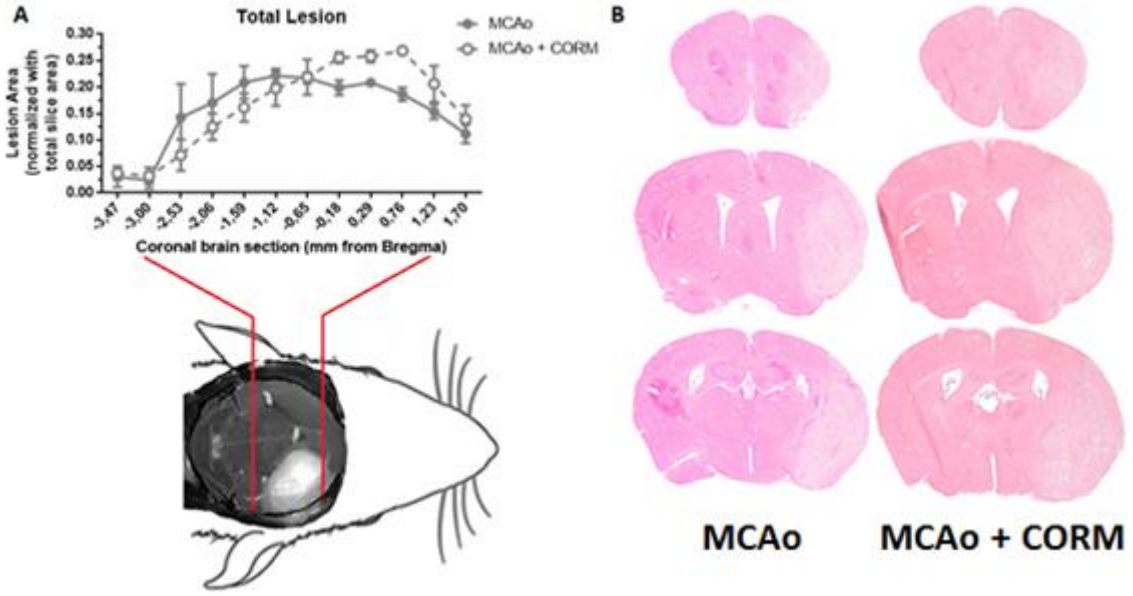

Figure 6 - Quantification of the infarct area by H&E staining in mice subjected to tMCAo. Where indicated, the animals were treated with CORM-A1 (3 mg/kg) in 3 doses (6 h, 1 day and 2 days *post* injury). The total area and lesion area were quantified manually in each of the 12 coronal sections. (A) Quantification of the lesioned area (normalized with the total slice area) at day 7, and representation of the area from which slices were collected. Filled circles represent the results obtained in untreated mice subjected to MCAo and empty circles correspond to the quantification of the injury in mice subjected to MCAo followed by administration of CORM-A1. (B) Representative images from a rostrocaudal series of brain sections from untreated and treated MCAo groups. Values are expressed as a ratio of the total brain structure (means ± SEM; n = 5). Statistical analysis was performed using the two-way ANOVA followed by the Bonferroni *post*-test. No statistical difference was found.

3.4. CO minimizes cortical metabolic loss 24h after tMCAo

To further characterize the differential effects of CO when tested at day 1 and day 7 after tMCAo (*e.g.* in the BBB permeability), metabolic profiles (Figure 7A) were obtained at both time points. ^{1}H-MRS was applied in a voxel placed in the cerebral cortex (Figure 7B) to determine whether CORM-A1 administration prevents the ischemia-induced metabolic changes, as previously describe in other contexts [27–29]. Nine metabolites were analyzed by this method (named here as metabolic load) in order to have a general assessment of the alterations in brain metabolism: alanine, phosphocholine, phosphocreatine, lactate, taurine, *myo*-inositol, glutathione, glutamate, glutamine, GABA, *N*-acetylaspartate. tMCAo reduced the metabolite load in the ipsilateral hemisphere, when assessed 1 day after the ischemic injury, while no effect was observed in the contralateral hemisphere. Administration of CORM-A1 significantly reduced the metabolic changes in the ipsilateral hemisphere at this time point, to levels similar to the sham cohorts (Figure 7C), in contrast with the results obtained at day 7, when CO had no effect on MCAo-evoked metabolite loss (Figure 7D). Under the latter conditions both MCAo subjected groups presented the same metabolite load loss.

CO treatment also reduced the metabolite load in the Sham group at day 1 after ischemia, which however did not have functional consequences since treatment with CORM-A1 did not affect the motor performance (see Figures 1-3).

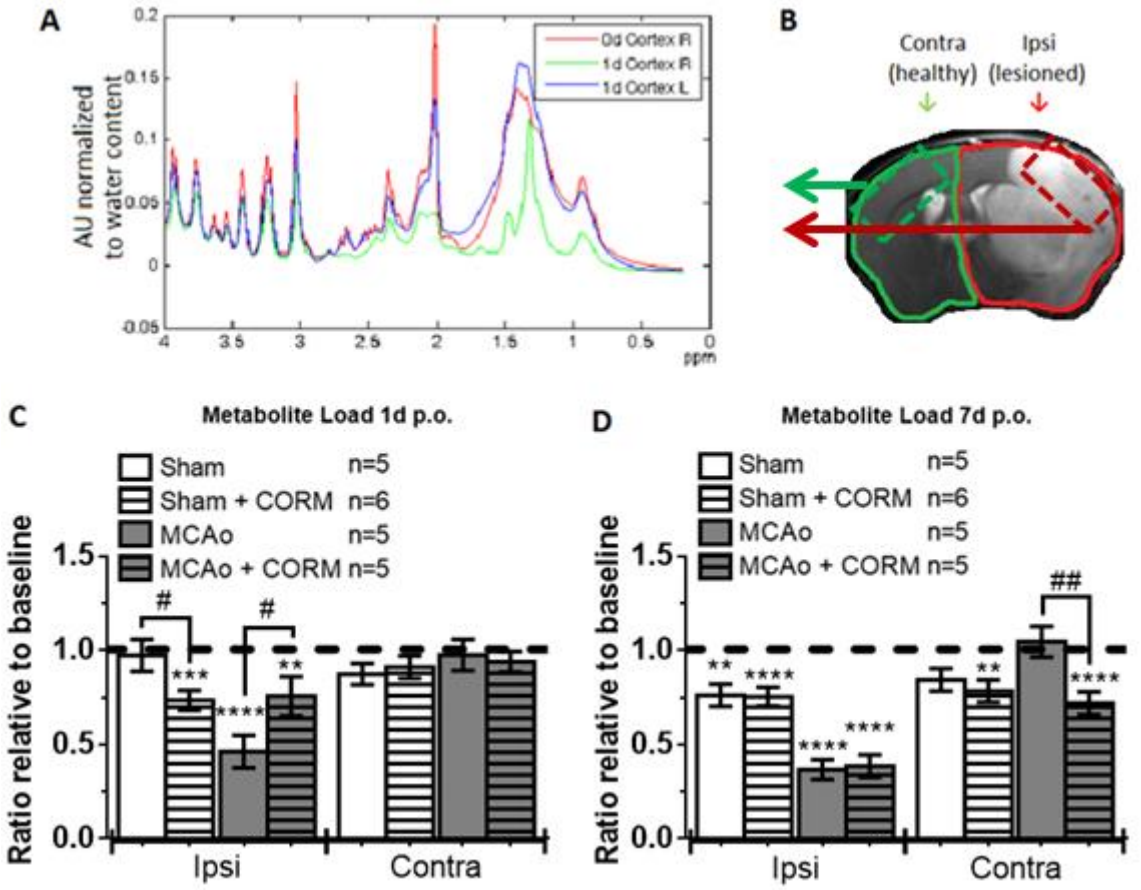

Figure 7 – Modulation of the MCAo-induced alterations in the metabolic profile in the cerebral cortex by CORM-A1. Metabolite load includes the following metabolites: alanine, phosphocholine, phosphocreatine, lactate, taurine, *myo*-inositol, glutathione, glutamate, glutamine, GABA and *N*-acetylaspartate. Where indicated, the animals were treated with CORM-A1 (3 mg/kg) in 3 doses (6 h, 1 day and 2 days *post* injury). (A) Representative plot of distribution of metabolites in control conditions and at days 1 and 7 after MCAo, as determined by ^{1}H-MRS quantification. (B) Voxel placement in the ipsi- and contralateral hemispheres. (C) Ratio of metabolite load at day 1 after MCAo. (D) Ratio of metabolite load at day 7 after MCAo. White bars represent sham-operated mice and grey bars represent MCAO-operated mice. White and striped bars show the results obtained in control conditions and in mice treated with CORM-A1, respectively. **p<0.01, ***p<0.001, ****p<0.0001 calculated with one-way ANOVA with Bonferroni *post*-test calculated as a percentage of the control, determined before the surgery (mean ± SEM). # p<0.05 determined using the unpaired Student's *t*-test.

These data clearly indicate that CO treatment decreases the early (1 day) metabolic changes that occur in the cerebral cortex after tMCAo. However, this was a transient effect since no effect was observed when the metabolic load was evaluated at day 7 after tMCAo.

3.5. CO administration is beneficial for the maintenance of the metabolite load in the neuronal and astrocytic populations in the cerebral cortex

To determine whether CO treatment has a differential effect on the metabolism of neurons and astrocytes, a group of metabolites relevant for neuronal survival (*N*-acetylaspartate (NAA), glutamate (Glu) and taurine (Tau)) [30,31] and a metabolite

enriched in astrocytes (*myo*-inositol) [32] were evaluated in the cerebral cortex at day 1 after tMCAo. As proposed by others [33], the composite score NAA + Glu + Tau predicts better the outcome of an ischemic insult than NAA or lactate alone. In the scatterplot representing glutamine *versus* the composite score, a good separation between Sham and MCAo subjected cohorts was obtained (Figure 8A). In accordance with the metabolic load and infarct volume at day 1, mice subjected to tMCAo followed by administration of CORM-A1 are more similar to the Sham cohorts than to untreated mice subjected to transient focal ischemia. Moreover, as this composite score is constituted by a group of metabolites relevant to the neuronal population, we may hypothesize that this score may account for an increased survival of the neuronal population.

When evaluating the correlation between the levels of *myo*-inositol and glutamine, two metabolites that are enriched in the astrocytic population, mice subjected to tMCAo followed by treatment with CORM-A1 presented a correlation very similar to sham treated groups (Figure 8B). In contrast, untreated mice with an ischemic lesion showed a distinct profile when compared with sham groups. In conclusion, administration of CO after the ischemic injury has a beneficial metabolic effect on both the neuronal and astrocytic populations, decreasing the severity of the lesion.

Taken together, these results reinforce the idea that CO acts in different cell populations, protecting both neurons and astrocytes, at least in part by maintaining the levels of key metabolites.

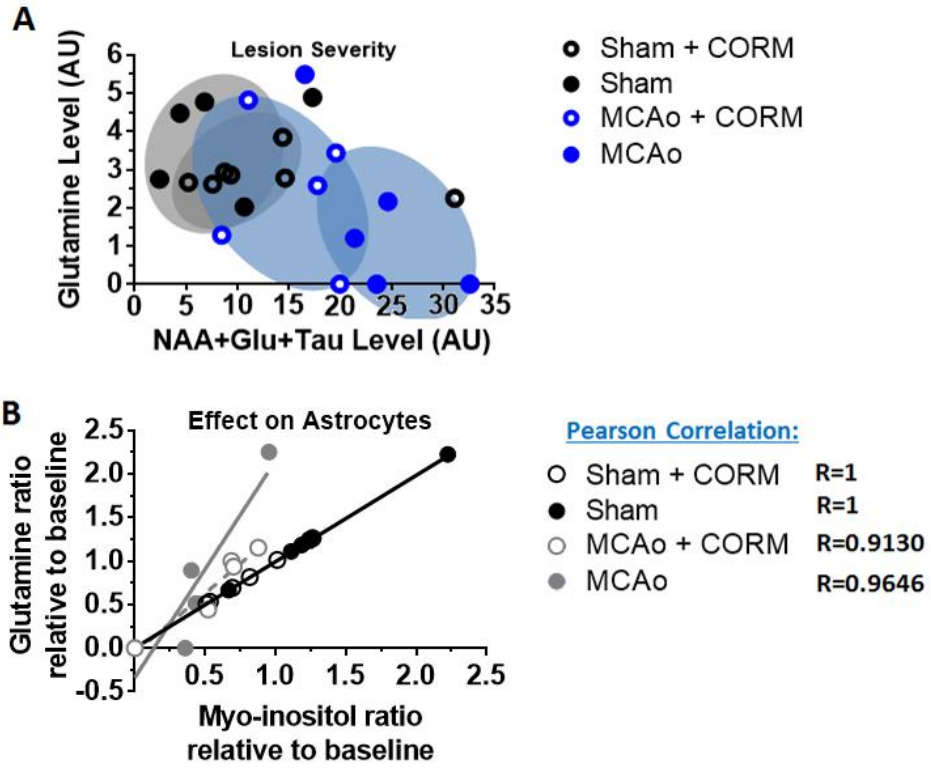

Figure 8 – Severity of the lesion after tMCAo and astrocytic metabolic status in the cerebral cortex. Data were obtained from ^{1}H-MRS at day 1 *post* tMCAo, and where indicated the animals were treated with CORM-A1 (3 mg/kg) in 3 doses (6 h, 1 day and 2 days *post* injury). (A) The distribution of NAA + Glu + Tau is plotted vs glutamine levels. (B) The relation between the levels of two metabolites enriched in astrocytes, glutamine and *myo*-inositol.

3.6. CO ameliorates survival

Mortality reduction is also an important feature when evaluating the effect of putative therapeutic strategies for stroke. Administration of CORM-A1 after tMCAo, at 6 h, 1.3 d and 2.3 d after injury, during the therapeutic window, reduced the rate of mortality (Figure 9). However, the protective effects decreased after the last dose of CO (after day 3), and at day 7 following MCAo mice treated with CORM-A1 showed a survival rate similar to the non-treated controls (Figure 9). Survival data correlates very well with the lesion volume and metabolic load variations, since a certain degree of protection was observed during the therapeutic window (0-2 days after lesion).

In conclusion, the CO dose given has potential to improve outcome after ischemic stroke. However, the CO therapy needs to be optimized, including the timing of administration and the number of CO doses.

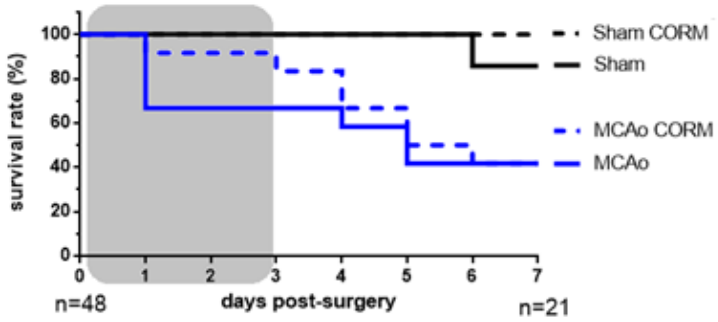

Figure 9 – Effect of CO treatment on the survival rate of mice subjected to MCAo. CORM-A1 (3 mg/kg) was administrated in 3 doses (6 h, 1 day and 2 days *post* injury). The grey rectangle represents the therapeutic window applied. Black lines represent sham-operated mice and blue lines represent MCAO-operated mice. Full and dashed lines represent control and CO-treated mice, respectively.

4. DISCUSSION

In this integrative study, we investigated the putative neuroprotective effects of CO in a mouse stroke model. The results showed protective effects of CO at different levels, when administered from 6 h after injury: i) a significant improvement in motor function and brain connectivity was observed in what concerns self-grooming behavior; ii) improved limb strength and coordination was observed in CO treated mice when evaluated with the vertical pole test; iii) strong reduction of BBB leakage; iv) serial MRI data showed a tendency for smaller brain infarction in the cortical area of CO treated animals at day 1 *post* MCAo; v) at day 7 *post* MCAo, CORM-A1 treatment did not affect the lesion volume as determined by serial histological sections and MRI; vi) minimization of metabolite load loss in the cerebral cortex at day 1 after MCAo; vii) CO reduced the mortality only when administered during the therapeutic window. Together, the evidence gathered in the current study indicates that CO has therapeutic potential as a *post*-stroke treatment.

The evaluation of motor performance showed an effect of CO in preventing the loss in grooming activity in mice subjected to MCAo. Self-grooming is a complex innate rodent behavior and its assessment can be useful in neuronal circuitry studies, as it has been done in translational psychiatry research [34]. Grooming initiation and sequence is mainly linked to striatal functions and connectivity [35]. However, cortical lesions can also induce a mild disruption in grooming activity since corticostriatal connections can modulate self-grooming behavior [36]. Stroke is known to reduce grooming bouts, but grooming in stroke contexts still lacks full characterization. MCAo produces a lesion that affects the cortex and striatum; thus, the effect of CO in preserving self-grooming activity may be reasoned as a protection of the corticostriatal connections responsible for this innate behavior. Moreover, in order for mice to display grooming activity after stroke, they need a proper balance and hind limb strength to sustain itself upright. This fact adds more importance to the effect of CO in the maintenance of grooming behavior.

Motor assessment using the vertical pole test also showed a functional improvement in mice treated with CO after the ischemic lesion when compared with the untreated counterparts. Pole test evaluates simple motor function, such as forelimb strength, ability to grasp and balance in mice [37]. There are some evidence for striatal involvement in the pole test performance [38]. This test showed a motor dysfunction from day 2 after tMCAo up to day 8, with cumulative worsening of the performance up to day 8 after surgery [37]. It is also one of the most reliable tests, remaining sensitive to the severity of ischemic injury up to 4 weeks after ischemia [39]. In the current study, administration of CO prevented the poor performance at day 7 after stroke. At this time point, the treated cohort took the same time to turn as Sham groups, and descending time was not significantly different when compared with sham treated animals, in contrast with untreated injured mice. Overall, the results show that CO treatment ameliorated the balance, limb strength and coordination. This suggests that CO protects striatal function, as it confers functional recovery, in particular to striatum dependent tasks.

BBB experiences several types of damage in a stroke context, with its cellular constituents (astrocyte end feet, pericytes, endothelial cells, smooth muscle cells and a variety of basement membranes) presenting different susceptibilities to the ischemic insult. The contribution of BBB for stroke pathogenesis has recently emerged as a focus for new therapeutic strategies [21]. The results obtained in this work showed that CORM-

A1 administration significantly prevents the early increase in BBB permeability after tMCAo, as evaluated 1 day after the lesion. The protective effects of CO on the integrity of the BBB function resemble the effects previously described for this gasotransmitter in several of its components, namely astrocytes [40,41], pericytes [42] and vasculature [22]. These observations were performed both in ischemic and non-ischemic conditions. Therefore, effects of CO in the stabilization of the BBB may arise from the combined effects on several of its components. However, it remains to be determined whether CO preserves the crosstalk between the different BBB components, acts through its anti-oxidant capacity and/or simply promotes vasodilatation. The latter effect of CO was reported in several other contexts [43–45] and when induced at the right timing after stroke, vasodilation can be crucial in protecting the brain as it allows the supply of energy and nutrients which are in need in the ischemic tissue. The increase of regional blood flow due to cerebral vasodilation was previously found to be protective in stroke [46,47]. The enhancement in the reperfusion of the lesioned tissue can be decisive for the final outcome after focal brain ischemia, and CO may be a good candidate therapeutic strategy acting at this level.

Leakage of the BBB was recently observed as early as 30 min after stroke [48]. However, small and large molecules (≤150 kDa) only cross the BBB 3 h and 6 h after tMCAo. Moreover, permeability to very-large molecules (2000 kDa) was not detected until 24 h after injury [48]. Furthermore, the infarct was found to expand from the striatum to the cerebral cortex within 6 h to 24 h, being the striatum the first brain region to suffer from BBB dysfunction [48]. This body of evidence helps to understand the impact of CORM-A1 administration at 6 h after cerebral ischemia, and may explain the strong effects of CO in protecting the BBB. We might hypothesize that minimizing the BBB leakage to molecules with a size close to 2000 kDa is crucial for a better recovery, and CO may act on this mechanism. Further research is required to characterize whether CO can in fact prevent the stroke-induced increase in the permeability of the BBB to very-large molecules. The fact that CO fully protected the BBB, in contrast with the partial protection of the brain tissue under the conditions of this study, suggests that the vascular system and/or the glio-vascular unit is more responsive to CO treatment.

Functional preservation, rather than histological assessment, is presently considered the best approach to evaluate the outcome of the ischemic injury and the effect of putative protective strategies [49]. In this work, we evaluated the metabolic status of the cortical and striatal regions as an indirect measure of functionality after ischemic injury. At day 1 after MCAo we observed that CO administration promoted the maintenance of the metabolic load in the cerebral cortex, which is in accordance with the MRI results showing a reduced infarct area under the same conditions, although the results were not statistically significant in the latter experiments. At day 7 *post* injury, metabolic and histologic data were also in accordance since no protection was observed when the metabolite load was analyzed, and both cohorts presented a similar infarct volume. The time-dependence of the protective effect of CO is further reinforced by the evidence regarding the effect of CORM-A1 administration on the survival rate. A low rate of mortality was observed in mice subjected to MCAo while the CO-mediated responses were active. From day 3 onwards, when CORM-A1 was no longer administered, the difference between the two mice cohorts decreased, and at day 7 the survival rates were equal.

Quantification of the infarct volume using MRI suggests that the effects of CO are restricted to the cerebral cortex and limited to the early period after tMCAo. Region-specific effects of CO were previously described in the brain, either with low or high doses of CO [50–52]. However, the mechanisms underlying the differences in the regional responses to CO in the brain (*e.g.* cerebral cortex vs striatum) remain to be elucidated. The cortical lesion accounted for more than half of the total lesion under the conditions used in the present work. Therefore, the preferential effects in the cortical region are also reflected in the results obtained when the total lesion volume was analyzed. The fact that there is no significant lesion reduction when the BBB protection was so robust, points out for the need of further studies regarding the effect of CO on stroke.

In conclusion, the present work provides an integrated assessment of the time course of brain tissue and vasculature responses to CO in mice subjected to transient MCAo. Motor activity and metabolic homeostasis were analyzed to characterize the effects of CO from the functional point of view. Damaged tissue responded to CO in a spatiotemporal dependent manner, which highly correlated with the effects in minimizing the loss in metabolic load. Moreover, the results suggest that a strong protection of the BBB and a slight metabolic preservation might contribute to effects of CO in re-establishing the brain and neuronal network and functional recovery after stroke. Causal effects of CO-mediated protection of the BBB on the metabolic stabilization needs to be address in the future. It is also important to determine whether CO prevents the infarct expansion and BBB extravasation from striatum to the cerebral cortex. With the first CO dose administered at 6h *post*-stroke, the present study shows that this strategy has a strong therapeutic potential for later treatments and ultimately may constitute an alternative for those patients that are not qualified for tPA administration. Longer CO treatments might overcome the loss of protection observed at 5 days after the last CO dose. In addition, CO administration may also be a good therapeutic option to minimize the risk of hemorrhagic transformation after tPA treatment, which is a major concern in clinical practice [53].

ACKNOWLEDGEMENTS

We thank Marius Widerøe for all the expertise in ^{1}H-MRI data processing and analysis, as well as the fruitful discussions regarding ischemia. We also thank to Ana Paula Silva and her group for the usage of the rodent behaviour room and equipments. SRO was supported by a fellowship from Fundação para a Ciência e a Tecnologia (FCT) with reference SFRH/BD/51969/2012. This work was supported by FEDER (QREN) through Programa Mais Centro, under projects CENTRO-07-ST24-FEDER-002002, CENTRO-07-ST24-FEDER-002006 and CENTRO-07-ST24-FEDER-002008, through Programa Operacional Factores de Competitividade - COMPETE and national funds via FCT under projects Pest-C/SAU/LA0001/2013-2014, PTDC/SAU-NMC/120144/2010, PTDC/NEU-NMC/0198/2012 and FCT-ANR/NEU-NMC/0022/2012.

REFERENCES

[1] M.D. Maines, The heme oxygenase system and its functions in the brain., Cell. Mol. Biol. (Noisy-Le-Grand). 46 (2000) 573–85. http://www.ncbi.nlm.nih.gov/pubmed/10872744.

[2] C.S.F. Queiroga, A. Vercelli, H.L.A. Vieira, Carbon monoxide and the CNS: Challenges and achievements, Br. J. Pharmacol. (2014) 1–13. doi:10.1111/bph.12729.

[3] A.S. Almeida, N.L. Soares, M. Vieira, J.B. Gramsbergen, H.L.A. Vieira, Carbon monoxide releasing molecule-A1 (CORM-A1) improves neurogenesis: increase of neuronal differentiation yield by preventing cell death, PLoS One. in press (2016) 1–24. doi:10.1371/journal.pone.0154781.

[4] N. Hettiarachchi, M. Dallas, M. Al-Owais, H. Griffiths, N. Hooper, J. Scragg, J. Boyle, C. Peers, Heme oxygenase-1 protects against Alzheimer's amyloid-β1-42-induced toxicity via carbon monoxide production, Cell Death Dis. 5 (2014) e1569. doi:10.1038/cddis.2014.529.

[5] H. Parfenova, C.W. Leffler, S. Basuroy, J. Liu, A.L. Fedinec, Antioxidant roles of heme oxygenase, carbon monoxide, and bilirubin in cerebral circulation during seizures., J. Cereb. Blood Flow Metab. 32 (2012) 1024–34. doi:10.1038/jcbfm.2012.13.

[6] C.S.F. Queiroga, S. Tomasi, M. Widerøe, P.M. Alves, A. Vercelli, H.L.A. Vieira, Preconditioning Triggered by Carbon Monoxide (CO) Provides Neuronal Protection Following Perinatal Hypoxia-Ischemia, PLoS One. 7 (2012) e42632. doi:10.1371/journal.pone.0042632.

[7] K.M. Kim, H.O. Pae, M. Zheng, R. Park, Y.M. Kim, H.T. Chung, Carbon monoxide induces heme oxygenase-1 via activation of protein kinase R-like endoplasmic reticulum kinase and inhibits endothelial cell apoptosis triggered by endoplasmic reticulum stress, Circ. Res. 101 (2007) 919–927. doi:10.1161/CIRCRESAHA.107.154781.

[8] P.-L. Chi, C.-J. Liu, I.-T. Lee, Y.-W. Chen, L.-D. Hsiao, C.-M. Yang, HO-1 Induction by CO-RM2 Attenuates TNF- α -Induced Cytosolic Phospholipase A 2 Expression via Inhibition of PKC α -Dependent NADPH Oxidase/ROS and NF- κ B, Mediators Inflamm. 2014 (2014) 1–18. doi:10.1155/2014/279171.

[9] P.-L. Chi, C.-C. Lin, Y.-W. Chen, L.-D. Hsiao, C.-M. Yang, CO Induces Nrf2-Dependent Heme Oxygenase-1 Transcription by Cooperating with Sp1 and c-Jun in Rat Brain Astrocytes, Mol. Neurobiol. 52 (2015) 277–292. doi:10.1007/s12035-014-8869-4.

[10] J.M. Wardlaw, V. Murray, E. Berge, G.J. del Zoppo, Thrombolysis for acute ischaemic stroke, in: J.M. Wardlaw (Ed.), Cochrane Database Syst. Rev., John Wiley & Sons, Ltd, Chichester, UK, 2014: pp. 1581–1588. doi:10.1002/14651858.CD000213.pub3.

[11] W.J. Meurer, B.E. Barth, G. Gaddis, G.M. Vilke, S.H.F. Lam, Rapid Systematic Review: Intra-Arterial Thrombectomy ("Clot Retrieval") for Selected Patients with Acute Ischemic Stroke, J. Emerg. Med. (2016). doi:10.1016/j.jemermed.2016.10.004.

[12] L.H. Schwamm, S.F. Ali, M.J. Reeves, E.E. Smith, J.L. Saver, S. Messe, D.L. Bhatt, M. V. Grau-Sepulveda, E.D. Peterson, G.C. Fonarow, Temporal Trends in Patient Characteristics and Treatment With Intravenous Thrombolysis Among Acute Ischemic Stroke Patients at Get With the Guidelines-Stroke Hospitals, Circ. Cardiovasc. Qual. Outcomes. 6 (2013) 543–549. doi:10.1161/CIRCOUTCOMES.111.000303.

[13] B. Wang, W. Cao, S. Biswal, S. Doré, Carbon monoxide-activated Nrf2 pathway leads to protection against permanent focal cerebral ischemia., Stroke. 42 (2011) 2605–10.

doi:10.1161/STROKEAHA.110.607101.

[14] E. Zeynalov, S. Doré, Low Doses of Carbon Monoxide Protect Against Experimental Focal Brain Ischemia, Neurotox. Res. 15 (2009) 133–137. doi:10.1007/s12640-009-9014-4.

[15] J.A. Klaus, K.K. Kibler, A. Abuchowski, R.C. Koehler, Early Treatment of Transient Focal Cerebral Ischemia with Bovine PEGylated Carboxy Hemoglobin Transfusion, Artif. Cells, Blood Substitutes, Biotechnol. 38 (2010) 223–229. doi:10.3109/10731199.2010.488635.

[16] V. Prinz, J. Köning, S. Ji, U. Lindauer, A. Rex, U. Dirnagl, Standard operating procedures (SOP) in experimental stroke research: SOP for middle cerebral artery occlusion in the mouse, Nat. Preced. 202213 (2010) 1–5. doi:10.1038/npre.2010.3492.2.

[17] R. Motterlini, P. Sawle, J. Hammad, S. Bains, R. Alberto, R. Foresti, C.J. Green, CORM-A1: a new pharmacologically active carbon monoxide-releasing molecule., FASEB J. 19 (2005) 284–6. doi:10.1096/fj.04-2169fje.

[18] C.J. Hoffmann, U. Harms, A. Rex, F. Szulzewsky, S.A. Wolf, U. Grittner, G. Lattig-Tunnemann, M. Sendtner, H. Kettenmann, U. Dirnagl, M. Endres, C. Harms, Vascular Signal Transducer and Activator of Transcription-3 Promotes Angiogenesis and Neuroplasticity Long-Term After Stroke, Circulation. 131 (2015) 1772–1782. doi:10.1161/CIRCULATIONAHA.114.013003.

[19] E. Csongradi, Role of Carbon Monoxide in Kidney Function: Is a little Carbon Monoxide Good for the Kidney?, Curr. Pharm. Biotechnol. 13 (2012) 819–826. doi:10.2174/138920112800399284.

[20] M. Krueger, I. Bechmann, K. Immig, A. Reichenbach, W. Härtig, D. Michalski, Blood-brain barrier breakdown involves four distinct stages of vascular damage in various models of experimental focal cerebral ischemia., J. Cereb. Blood Flow Metab. 35 (2015) 292–303. doi:10.1038/jcbfm.2014.199.

[21] A. Kassner, Z. Merali, Assessment of Blood–Brain Barrier Disruption in Stroke, Stroke. 46 (2015) 3310–3315. doi:10.1161/STROKEAHA.115.008861.

[22] C.W. Leffler, H. Parfenova, J.H. Jaggar, Carbon monoxide as an endogenous vascular modulator, AJP Hear. Circ. Physiol. 301 (2011) H1–H11. doi:10.1152/ajpheart.00230.2011.

[23] K.R. Knecht, S. Milam, D. a Wilkinson, A.L. Fedinec, C.W. Leffler, Time-dependent action of carbon monoxide on the newborn cerebrovascular circulation., Am. J. Physiol. Heart Circ. Physiol. 299 (2010) H70–H75. doi:10.1152/ajpheart.00258.2010.

[24] Q. Jiang, J.R. Ewing, G.L. Ding, L. Zhang, Z.G. Zhang, L. Li, P. Whitton, M. Lu, J. Hu, Q.J. Li, R. a Knight, M. Chopp, Quantitative evaluation of BBB permeability after embolic stroke in rat using MRI., J. Cereb. Blood Flow Metab. 25 (2005) 583–592. doi:10.1038/sj.jcbfm.9600053.

[25] A. Wunder, K. Schoknecht, D.B. Stanimirovic, O. Prager, Y. Chassidim, Imaging blood-brain barrier dysfunction in animal disease models., Epilepsia. 53 Suppl 6 (2012) 14–21. doi:10.1111/j.1528-1167.2012.03698.x.

[26] B.W. McColl, H. V. Carswell, J. McCulloch, K. Horsburgh, Extension of cerebral hypoperfusion and ischaemic pathology beyond MCA territory after intraluminal filament occlusion in C57Bl/6J mice, Brain Res. 997 (2004) 15–23. doi:10.1016/j.brainres.2003.10.028.

[27] S.W. Ryter, A.M.K. Choi, Heme oxygenase-1/carbon monoxide: from metabolism to

molecular therapy., Am. J. Respir. Cell Mol. Biol. 41 (2009) 251–60. doi:10.1165/rcmb.2009-0170TR.

[28] A.S. Almeida, C.S.F. Queiroga, M.F.Q. Sousa, P.M. Alves, H.L.A. Vieira, Carbon monoxide modulates apoptosis by reinforcing oxidative metabolism in astrocytes: role of Bcl-2., J. Biol. Chem. 287 (2012) 10761–70. doi:10.1074/jbc.M111.306738.

[29] V.L. Mahan, Neuroprotective, neurotherapeutic, and neurometabolic effects of carbon monoxide., Med. Gas Res. 2 (2012) 32. doi:10.1186/2045-9912-2-32.

[30] P. Saransaari, S.S. Oja, Modulation of taurine release in ischemia by glutamate receptors in mouse brain stem slices, Amino Acids. 38 (2010) 739–746. doi:10.1007/s00726-009-0278-z.

[31] H. Lei, C. Berthet, L. Hirt, R. Gruetter, Evolution of the neurochemical profile after transient focal cerebral ischemia in the mouse brain, J. Cereb. Blood Flow Metab. 29 (2009) 811–819. doi:10.1038/jcbfm.2009.8.

[32] J.L. Harris, I.-Y. Choi, W.M. Brooks, Probing astrocyte metabolism in vivo: proton magnetic resonance spectroscopy in the injured and aging brain, Front. Aging Neurosci. 7 (2015). doi:10.3389/fnagi.2015.00202.

[33] C. Berthet, H. Lei, R. Gruetter, L. Hirt, Early Predictive Biomarkers for Lesion After Transient Cerebral Ischemia, Stroke. 42 (2011) 799–805. doi:10.1161/STROKEAHA.110.603647.

[34] A. V Kalueff, A.M. Stewart, C. Song, K.C. Berridge, A.M. Graybiel, J.C. Fentress, Neurobiology of rodent self-grooming and its value for translational neuroscience, Nat. Rev. Neurosci. 17 (2015) 45–59. doi:10.1038/nrn.2015.8.

[35] K. Berridge, I. Whishaw, Cortex, striatum and cerebellum: control of serial order in a grooming sequence, Exp. Brain Res. 90 (1992) 275–290. doi:10.1007/BF00227239.

[36] J.A. Obeso, J.L. Lanciego, Past, Present, and Future of the Pathophysiological Model of the Basal Ganglia, Front. Neuroanat. 5 (2011). doi:10.3389/fnana.2011.00039.

[37] V. Bouët, T. Freret, J. Toutain, D. Divoux, M. Boulouard, P. Schumann-Bard, Sensorimotor and cognitive deficits after transient middle cerebral artery occlusion in the mouse, Exp. Neurol. 203 (2007) 555–567. doi:10.1016/j.expneurol.2006.09.006.

[38] B. Winter, G. Juckel, I. Viktorov, J. Katchanov, A. Gietz, R. Sohr, M. Balkaya, H. Hörtnagl, M. Endres, Anxious and Hyperactive Phenotype Following Brief Ischemic Episodes in Mice, Biol. Psychiatry. 57 (2005) 1166–1175. doi:10.1016/j.biopsych.2005.02.010.

[39] S.-Y. Park, S. Marasini, G.-H. Kim, T. Ku, C. Choi, M.-Y. Park, E.-H. Kim, Y.-D. Lee, H. Suh-Kim, S.-S. Kim, A Method for Generate a Mouse Model of Stroke: Evaluation of Parameters for Blood Flow, Behavior, and Survival, Exp. Neurobiol. 23 (2014) 104. doi:10.5607/en.2014.23.1.104.

[40] Y.K. Choi, J.H. Park, Y.-Y. Baek, M.-H. Won, D. Jeoung, H. Lee, K.-S. Ha, Y.-G. Kwon, Y.-M. Kim, Carbon monoxide stimulates astrocytic mitochondrial biogenesis via L-type Ca(2+) channel-mediated PGC-1α/ERRα activation., Biochem. Biophys. Res. Commun. 479 (2016) 297–304. doi:10.1016/j.bbrc.2016.09.063.

[41] C.S.F. Queiroga, R.M.A. Alves, S. V. Conde, P.M. Alves, H.L.A. Vieira, Paracrine effect of carbon monoxide – astrocytes promote neuroprotection through purinergic signaling in mice, J. Cell Sci. 129 (2016) 3178–3188. doi:10.1242/jcs.187260.

[42] Y.K. Choi, T. Maki, E.T. Mandeville, S.-H. Koh, K. Hayakawa, K. Arai, Y.-M. Kim, M.J.

Whalen, C. Xing, X. Wang, K.-W. Kim, E.H. Lo, Dual effects of carbon monoxide on pericytes and neurogenesis in traumatic brain injury, Nat. Med. (2016). doi:10.1038/nm.4188.

[43] H. Parfenova, D. Tcheranova, S. Basuroy, A.L. Fedinec, J. Liu, C.W. Leffler, Functional role of astrocyte glutamate receptors and carbon monoxide in cerebral vasodilation response to glutamate., Am. J. Physiol. Heart Circ. Physiol. 302 (2012) H2257–H2266. doi:10.1152/ajpheart.01011.2011.

[44] A. Kanu, C.W. Leffler, Arachidonic acid- and prostaglandin E2-induced cerebral vasodilation is mediated by carbon monoxide, independent of reactive oxygen species in piglets, Am. J. Physiol. Heart Circ. Physiol. 301 (2011) H2482-2487. doi:10.1152/ajpheart.00628.2011.

[45] R. Motterlini, Carbon monoxide-releasing molecules (CO-RMs): vasodilatory, anti-ischaemic and anti-inflammatory activities., Biochem. Soc. Trans. 35 (2007) 1142–6. doi:10.1042/BST0351142.

[46] H. Levi, K. Schoknecht, O. Prager, Y. Chassidim, I. Weissberg, Y. Serlin, A. Friedman, Stimulation of the Sphenopalatine Ganglion Induces Reperfusion and Blood-Brain Barrier Protection in the Photothrombotic Stroke Model, PLoS One. 7 (2012) e39636. doi:10.1371/journal.pone.0039636.

[47] M.D. Ginsberg, Expanding the concept of neuroprotection for acute ischemic stroke: The pivotal roles of reperfusion and the collateral circulation, Prog. Neurobiol. (2016). doi:10.1016/j.pneurobio.2016.09.002.

[48] Y. Shi, L. Zhang, H. Pu, L. Mao, X. Hu, X. Jiang, N. Xu, R.A. Stetler, F. Zhang, X. Liu, R.K. Leak, R.F. Keep, X. Ji, J. Chen, Rapid endothelial cytoskeletal reorganization enables early blood–brain barrier disruption and long-term ischaemic reperfusion brain injury, Nat. Commun. 7 (2016) 10523. doi:10.1038/ncomms10523.

[49] K. Hattori, H. Lee, P.D. Hurn, B.J. Crain, R.J. Traystman, A.C. DeVries, B.G. Lyeth, Cognitive Deficits After Focal Cerebral Ischemia in Mice Editorial Comment, Stroke. 31 (2000) 1939–1944. doi:10.1161/01.STR.31.8.1939.

[50] M. Muraoka, H. Hayakawa, A. Kagaya, T. Kojima, S. Yamawaki, Effects of carbon monoxide exposure on serotonergic neuronal systems in rat brain., Life Sci. 62 (1998) 2101–8. http://www.ncbi.nlm.nih.gov/pubmed/9627089.

[51] T. Nabeshima, A. Katoh, H. Ishimaru, Y. Yoneda, K. Ogita, K. Murase, H. Ohtsuka, K. Inari, T. Fukuta, T. Kameyama, Carbon monoxide-induced delayed amnesia, delayed neuronal death and change in acetylcholine concentration in mice., J. Pharmacol. Exp. Ther. 256 (1991) 378–84. http://www.ncbi.nlm.nih.gov/pubmed/1671097.

[52] D. Taskiran, T. Nesil, K. Alkan, Mitochondrial oxidative stress in female and male rat brain after ex vivo carbon monoxide treatment, Hum. & Exp. Toxicol. 26 (2007) 645–651. doi:10.1177/0960327107076882.

[53] J. Zhang, W. Ho, C. Reis, O. Akyol, G. Akyol, R. Applegate II, R. Martin, Pharmacological Management Options to Prevent and Reduce Ischemic Hemorrhagic Transformation, Curr. Drug Targets. 17 (2016) 1–1. doi:10.2174/1389450117666160818115850.

SUPPLEMENTARY DATA

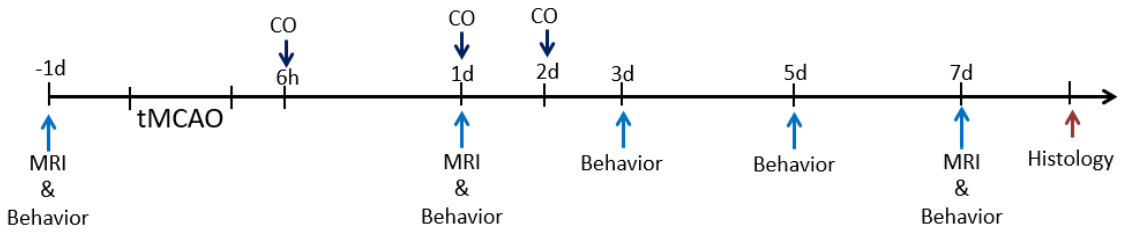

Figure S1 – Schematic representation of the experimental design. Doses of CO (3 mg / kg) were given i.p. at 6 h, 1 day and 2 days after injury. Baseline MRI and motor behavior data were collected. MRI was performed at day 1 and day 7 *post*-tMCAo. Behavior studies were performed every 2 days. Animals were euthanized at 7 days *post*-tMCAo. Brains were collected and analyzed, as described in the methods section.

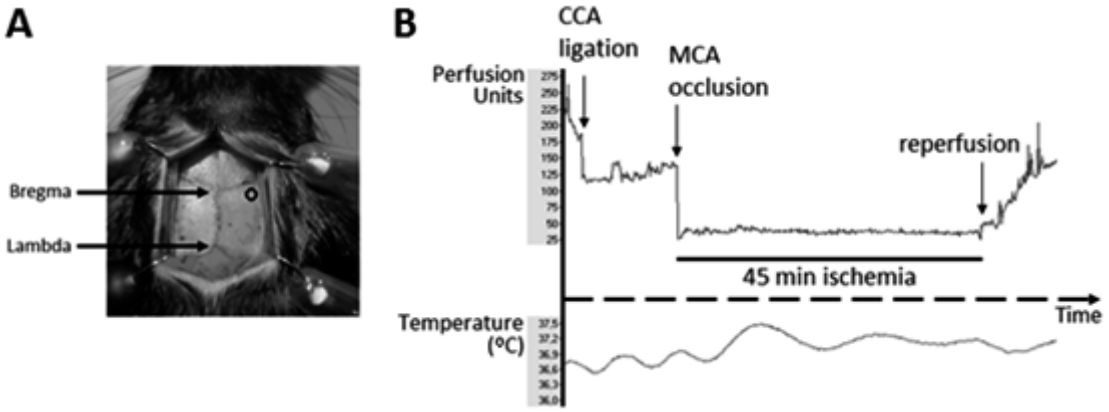

Figure S2 – Laser Doppler microtip placement and representative profile of laser doppler flux and changes in body temperature in a tMCAo experiment. (A) Illustration of the location where the microtip was glued (open circle), approximately 2 mm posterior and 6 mm lateral to the bregma. (B) Laser-doppler flux profile measured over the right lateral parietal cortex during 45 min of middle cerebral artery occlusion (MCAo). Body temperature was measured with a rectal probe.

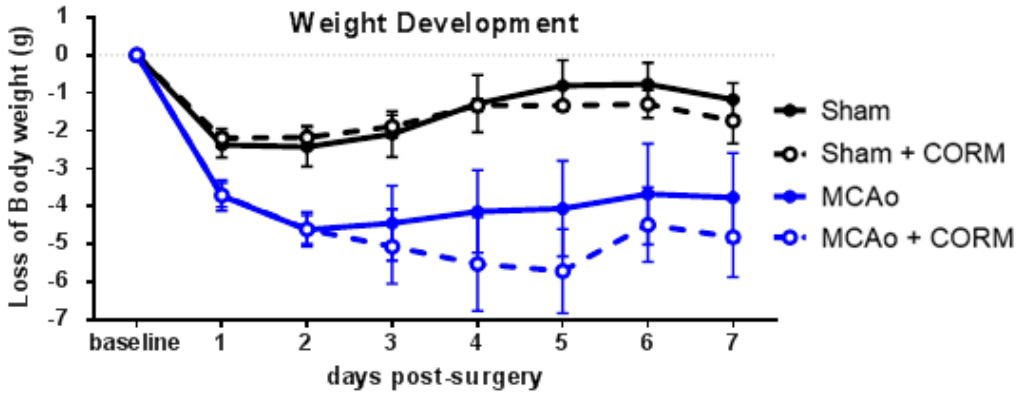

Figure S3 – Longitudinal body weight loss measurements. Black lines represent sham-operated mice and blue lines represent MCAO-operated mice. Full and dashed lines represent control and CO-treated mice, respectively. Values are expressed in grams (means ± SEM; n ≥ 5). Statistical analysis was performed using the two-way ANOVA followed by the Bonferroni *post*-test. No statistical difference was found between treated and untreated groups.

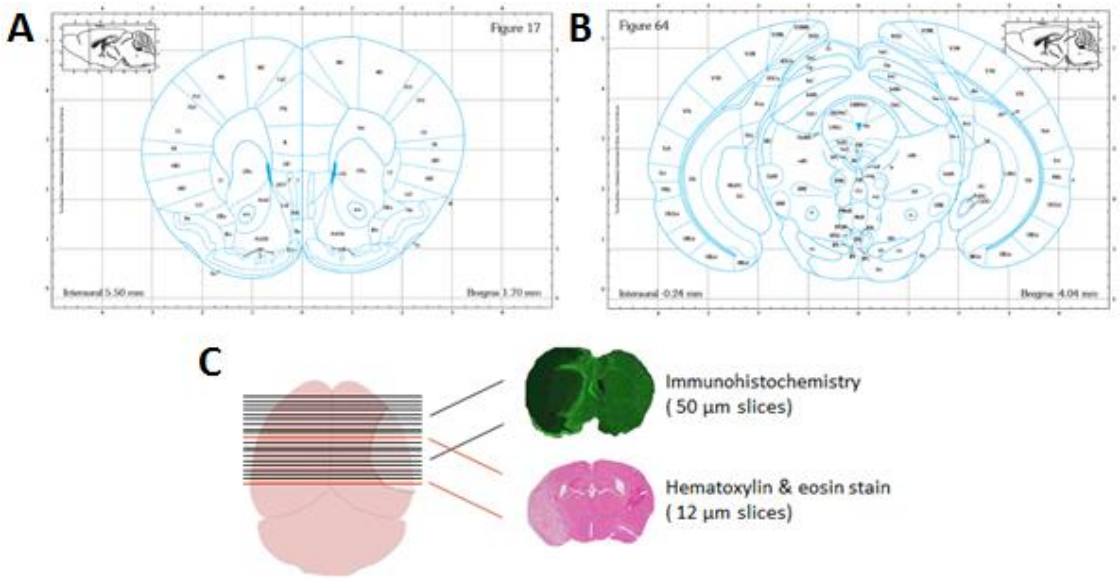

Figure S4 – Histological references and sampling scheme. Mouse Brain Atlas representation of the anterior (A) and the posterior (B) reference of slicing. (C) Scheme followed for histological sampling: 9 slices were cut for immunohistochemistry followed by one slice cut for H&E staining.

Chapter III

DISCUSSION AND CONCLUSIONS

INDEX

DISCUSSION

Stroke carries a huge social and economic burden and it is predicted to become even worse as ischemic stroke events are occurring to younger people and the population is aging [1]. Progress has been made regarding cytoprotective strategies and physiotherapy efficiency, but major improvements are still urgently needed. So far, tPA is the only approved drug against ischemic stroke, but this approach has critical limitations since it presents a therapeutic window of 4.5h maximum and it can only be administered to 4-7% of the stroke patients [2]. Concomitantly with tPA treatment, patients can still undergo endovascular mechanical thrombectomy. This procedure gives good results however is intrusive and carries the anesthesia risks and also present a short time window similar to tPA [3]. Both therapeutic options aim to promote reperfusion and do not target directly tissue protection.

Most commonly, stroke results in unilateral motor dysfunction and epilepsy [4]. As stroke patients suffer very limiting injuries, the urgency for novel therapies is massive.

Stroke is characterized by the involvement of many different players in its pathology, namely the vasculature, neuronal counterparts and inflammatory responsive cells. But the role of each contributor is still poorly known. Moreover, the timing at which neurons, astrocytes and other brain cells, as well as blood vessels critically act in cell fate decision is not fully described yet. Studying such a complex disease to discover efficient treatments able to tackle all the players is truly intricate and takes a very long time. Thus, a good alternative is to study compounds already known to have beneficial effects in many of the stroke contributors and evaluate their overall effect in the system. An example of these multifaceted compounds is carbon monoxide (CO), with proven therapeutic potential regarding neurons, astrocytes, vasculature and inflammation [5,6].

The current study helped in further understanding the cellular and systemic responses to a low dose of CO in a clinically relevant administration timing after the ischemic insult. As represented in Figure 13 (Chapter I), this thesis aimed at unveiling the CO effects at a cellular and systemic level, both in pathologic and physiologic contexts.

First, CO acts in a multitude of different pathways in a short time window (Chapter II.III). By performing RNASeq to study CO effect on astrocytes, we identified DEGs related to pathways as different as cell differentiation, cell communication, metabolic process, gene expression and transport among others. This observation confirms that CO, not only is able to act on different cell type, but also trigger different pathways within the same cell. Fine tuning the CO dose is key since it will determine the balance between all the pathways activated, resulting either in a beneficial or detrimental consequence.

Furthermore, it was investigated the putative role of FosB as a player in CO-induced astrocyte protection (Chapter II.III). Then, an animal model was used to scrutinize the vasomodulatory properties of CO (Chapter II.IV) and the therapeutic effect of CO against stroke (Chapter II.V). It is worthy of note that the timing of CO application in animal models were clinically relevant, since CO was administered after ischemic stroke and not before or during as most of the previously performed studies [7–9]. Furthermore, in a cerebral ischemia context, this work disclosed crucial information

regarding the contributions of some players, in particular the importance of therapeutically addressing the BBB for improved stroke outcome (Chapter II.V). In fact, CO was able to improve motor performance, accompanied by a reduction in the infarct lesion and metabolite load loss at an early phase. Using an integrated approach correlating data from MRI, and behavior and tissue analysis, allowed us to have a more complete awareness of the effects of CO and it has been a pioneer approach in CO's biology field. Importantly, the longitudinal characteristic of the study reinforced the importance of time window of CO treatment in stroke recovery.

In accordance with previous reports, in the present work we found that CO induces vasodilation in the cortical vasculature, using a non-invasive technique (Chapter IV). Nevertheless, this observation was strictly limited to male cortices. In addition, the other brain regions analyzed in males presented the opposite response to CO. Our study addressing non-cortical regions and gender dimorphism in the vasculature response to CO treatment highlights the importance of including region and sex variables in therapeutic studies. In CO research field these subjects have been largely neglected.

Moreover, we also concluded that CO presents a systemic therapeutic potential when administered in clinical relevant timing (Chapter V). In an integrative approach, a novelty in the CO field, behavior paradigms and MRI analysis were performed in tMCAo subjected mice to truly understand the complexity of CO effects. CO presented particularly protective results regarding BBB integrity maintenance and limb strength and coordination. This study also collected evidences of a transient metabolites preservation upon CO administration, nevertheless further studies are needed to better understand metabolites load management after an ischemic stroke.

Each section of the present study provided relevant contributions to the present knowledge regarding the potential use of CO as a therapeutic molecule in stroke treatment. The combined results raised new questions and opened new possibilities to fasten CO transition from bench to bedside. More integrative studies are needed to address CO effect, since a wide range of effects are known to occur due to this gasotransmitters administration.

FUTURE STEPS

This thesis confirmed that CO may induce very fast responses (as fast as 30 min, Chapter II.III) which can be maintained long after CO administration (as long as 7 days, Chapter II.V). This was observed both *in vitro* or *in vivo*, and several questions were answered in the present work. Nevertheless, the present work also raised several questions which can be addressed as follows:

- **CO target disclosure or molecular & cellular studies**
  a) Since a wide variety of potential CO target candidates were identified in this work (Chapter II.I and II.III), more functional validations are needed. It will be of interest to further investigate the putative role of groups of candidates related to different cellular functions, as there is a great potential of CO acting by regulating more than one target/pathway. This strategy would disclose which biological processes have a major role in CO-induced cytoprotection. Downregulating a number of target candidates (Chapters II.I and II.III) and/or inhibiting the activation of some of the most represented transcription factors among the identified DEGs (Chapter II.I) would be a great effort contributing to understanding of CO intracellular impact.
  b) With the finding that CO triggers different responses depending on brain region and gender, it will be important to characterize the molecular and cellular players responsible for the differential CO action in such contexts.
- **Systemic animal studies**
  a) In the case of validating a gene as a crucial effector of CO-induced cytoprotection *in vitro*, a pre-clinical study subjecting genetic modified mice to tMCAo would ultimately confirm the identified gene as a key player in CO axis.
  b) As gender modulates the effect of CO on neurovascular dilation (Chapter II.IV), a detailed evaluation needs to be performed. Synchronized and postmenopausal females, as well as dominant and submissive males should be tested to determine the influence of hormones in CO effects in the brain vasculature.
  c) Since grooming behavior was rescued upon CO administration in stroked mice (Chapter II.V), a comprehensive study of the effects of CO on grooming should be performed, including modulation of the stereotyped pattern, as well as initiation and duration of the self-grooming behavior.
  d) Different CO dosage conditions should be tested, including the number of CO doses and timing, with the aim of achieving full recovery or prolonging the benefits observed in some of the parameters evaluated at day 1 on CO treated mice (Chapter II.V).
  e) In the case of validating the therapeutic efficacy of CO administration 6h or longer after the ischemic event, a pre-clinical study subjecting mice to tMCAo would be required. First, determining the therapeutic concentration in plasma with a single dose would be necessary. Then administering multiple CO doses separated by increasing intervals and verify if a cumulative effect occurs.

CONCLUSIONS

The plethora of pathways modulated by CO is very diverse. Therefore, to fine tune the CO dosage in order to deviate the cell fate to survival is not trivial.

The current thesis contributed to strength the potential of CO as a therapeutic molecule. CO was found to activate an array of stress responses in astrocytes. Moreover, given systemically, CO enabled the BBB to better cope with an ischemic injury and time resolution of its action was characterized. Several motor benefits were described in a mouse model of ischemic stroke. The possible enlargement of the therapeutic window from the current 4.5 h to 6h is of critical importance, since timing is crucial in stroke treatment. For that to happen, several optimizations are still needed, such as specific CNS-targeting of CO releasers, CORMs with backbone structures easier to be eliminated or absorbed by the organism, amongst other properties.

In conclusion, the knowledge gathered contributed to further advance CO into clinical usage, in particular in stroke therapy.

REFERENCES

[1] Y. Béjot, H. Bailly, J. Durier, M. Giroud, Epidemiology of stroke in Europe and trends for the 21st century, Presse Med. (2016). doi:10.1016/j.lpm.2016.10.003.

[2] L.H. Schwamm, S.F. Ali, M.J. Reeves, E.E. Smith, J.L. Saver, S. Messe, D.L. Bhatt, M. V. Grau-Sepulveda, E.D. Peterson, G.C. Fonarow, Temporal Trends in Patient Characteristics and Treatment With Intravenous Thrombolysis Among Acute Ischemic Stroke Patients at Get With the Guidelines-Stroke Hospitals, Circ. Cardiovasc. Qual. Outcomes. 6 (2013) 543–549. doi:10.1161/CIRCOUTCOMES.111.000303.

[3] G. Tsivgoulis, A. Safouris, C. Krogias, A.S. Arthur, A. V Alexandrov, Endovascular reperfusion therapies for acute ischemic stroke : dissecting the evidence, Expert Rev. Neurother. 7175 (2016). doi:10.1586/14737175.2016.1168297.

[4] M. Dąbrowska-Bender, M. Milewska, A. Gołąbek, A. Duda-Zalewska, A. Staniszewska, The Impact of Ischemic Cerebral Stroke on the Quality of Life of Patients Based on Clinical, Social, and Psychoemotional Factors, J. Stroke Cerebrovasc. Dis. (2016). doi:10.1016/j.jstrokecerebrovasdis.2016.08.036.

[5] B. Olas, Carbon monoxide is not always a poison gas for human organism: Physiological and pharmacological features of CO, Chem. Biol. Interact. 222 (2014) 37–43. doi:10.1016/j.cbi.2014.08.005.

[6] K.A. Hanafy, J. Oh, L.E. Otterbein, Carbon Monoxide and the Brain: Time to Rethink the Dogma, Curr Pharm Des. 19 (2013) 2771–2775.

[7] C.S.F. Queiroga, S. Tomasi, M. Widerøe, P.M. Alves, A. Vercelli, H.L.A. Vieira, Preconditioning Triggered by Carbon Monoxide (CO) Provides Neuronal Protection Following Perinatal Hypoxia-Ischemia, PLoS One. 7 (2012) e42632. doi:10.1371/journal.pone.0042632.

[8] Y. Guo, A.B. Stein, W.J. Wu, W. Tan, X. Zhu, Q.H. Li, B. Dawn, R. Motterlini, R. Bolli, Administration of a CO-releasing molecule at the time of reperfusion reduces infarct size in vivo, Am J Physiol Hear. Circ Physiol. 286 (2004) H1649-53. doi:10.1152/ajpheart.00971.2003.

[9] J.E. Clark, P. Naughton, S. Shurey, C.J. Green, T.R. Johnson, B.E. Mann, R. Foresti, R. Motterlini, Cardioprotective actions by a water-soluble carbon monoxide-releasing molecule, Circ Res. 93 (2003).